General Disclaimer

One or more of the Following Statements may affect this Document

- This document has been reproduced from the best copy furnished by the organizational source. It is being released in the interest of making available as much information as possible.

- This document may contain data, which exceeds the sheet parameters. It was furnished in this condition by the organizational source and is the best copy available.

- This document may contain tone-on-tone or color graphs, charts and/or pictures, which have been reproduced in black and white.

- This document is paginated as submitted by the original source.

- Portions of this document are not fully legible due to the historical nature of some of the material. However, it is the best reproduction available from the original submission.

Produced by the NASA Center for Aerospace Information (CASI)

DOE/NASA/0037-79/1
NASA CR-159580

CONCEPTUAL DESIGN STUDY OF IMPROVED AUTOMOTIVE GAS TURBINE POWERTRAIN — FINAL REPORT

Engineering Staffs of Ford Motor Company and AiResearch Manufacturing Company of Arizona, Division of The Garrett Corporation



May 1979

Prepared for
NATIONAL AERONAUTICS AND SPACE ADMINISTRATION
Lewis Research Center
Under Contract DEN 3-37

For
U.S. DEPARTMENT OF ENERGY
Office of Conservation and Solar Applications
Division of Transportation Energy Conservation

(NASA-CR-159580) CONCEPTUAL DESIGN STUDY OF IMPROVED AUTOMOTIVES GAS TURBINE POWERTRAIN Final Report (Ford Motor Co.) 215 p
HC A10/MF A01 CSCL 13F
N79-31088
Unclas
G3/85 31868

NOTICE

This report was prepared to document work sponsored by the United States Government. Neither the United States nor its agent, the United States Energy Research and Development Administration (now Department of Energy), nor any Federal employees, nor any of their contractors, subcontractors or their employees, makes any warranty, express or implied, or assumes any legal liability or responsibility for the accuracy, completeness, or usefulness of any information, apparatus, product or process disclosed, or represents that its use would not infringe privately owned rights.

DOE/NASA/0037-79/1
NASA CR-159580

CONCEPTUAL DESIGN STUDY OF IMPROVED AUTOMOTIVE GAS TURBINE POWERTRAIN — FINAL REPORT

Engineering Staffs of Ford Motor Company and AiResearch Manufacturing Company of Arizona, Division of The Garrett Corporation

May 1979

Prepared for
NATIONAL AERONAUTICS AND SPACE ADMINISTRATION
Lewis Research Center
Cleveland, Ohio 44135
Under Contract DEN 3-37

For
U.S. DEPARTMENT OF ENERGY
Office of Conservation and Solar Applications
Division of Transportation Energy Conservation
Washington, D.C. 20545
Under Interagency Agreement EC-77-A-31-1040

FOREWORD

This report presents the results of a six month Conceptual Design Study of an Improved Gas Turbine Powertrain — Phase I for automotive application under NASA/DOE Contract No. DEN 3-37. The work was performed by the Turbine Research Department of Ford Motor Company and AiResearch Manufacturing Company, a Division of the Garrett Corporation, as a joint team effort.

The Principal Investigator for the program was Mr. B. T. Howes of Ford Motor Company, assisted by Mr. L. W. Norman and Dr. F. Suriano of AiResearch. Mr. Richard P. Geye was the Project Manager for NASA, from whom special thanks are due for his assistance in editing this report.

TABLE OF CONTENTS

Page

SUMMARY 1

INTRODUCTION 3

1.0 VEHICLE SPECIFICATION 5

2.0 ENGINE CONCEPTS ASSESSMENT AND SELECTION 8

2.1 Introduction and Summary 8

2.2 Candidate Engine Concepts 8

2.3 Method of Selection 9

2.4 Results 14

2.5 Recommendations and Discussion 16

3.0 ESTABLISHMENT OF TECHNOLOGY PROJECTIONS 16

3.1 Compressor 16

3.2 Turbines 18

3.2.1 Axial Turbines 18

3.2.2 Radial Turbines 20

3.3 Heat Exchanger 21

3.4 Combustor 22

3.5 Duct Pressure Losses 22

3.6 Engine Leakages and Cooling Flow Rates 25

3.7 Accessory and Auxiliary Power Requirements 25

3.8 Bearing Losses 27

3.9 Reduction Gearbox Losses 27

3.10 Material Strength Limitations 28

3.10.1 Ceramics 28

3.10.2 Metals 28

3.11 Transmission Concepts 30

3.11.1 Introduction and Summary 30

3.11.2 Concepts 30

3.11.3 Method of Selection 46

3.11.4 Results 51

3.11.5 Recommendations and Discussion 51

4.0 CYCLE ANALYSIS 52

TABLE OF CONTENTS

		Page
5.0	PRELIMINARY ENGINE SELECTION COMPARISON	54
5.1	Engine Performance	54
5.2	Vehicle Performance and Economy	59
5.3	Engine Layout Studies	63
5.4	Mechanical Design Analysis	64
5.5	Transmission Analysis	80
5.6	Powertrain Installation Studies	80
5.7	Sensitivity Analysis	97
5.8	Risk Analysis	99
5.9	Cost Comparison	102
5.10	Powertrain Selection	103
6.0	SELECTED ENGINE DESIGN	104
6.1	Component Aerothermo Designs	104
6.1.1	Compressor	104
6.1.2	Radial Turbine	108
6.1.3	Regenerator	115
6.1.4	Combustor	115
6.2	Mechanical Design	115
6.2.1	Introduction	115
6.2.2	Turbine Diffuser Mounting	123
6.2.3	Turbine Rotor — Shaft Attachment	123
6.2.4	Dynamic Analysis of the Main Rotor System	123
6.2.5	Regenerator Support	124
6.2.6	Reduction Gear	126
6.2.7	Bearing Housing and Compressor Shroud Deformation Analysis	127
6.2.8	Compressor Rotor Analysis	127
6.2.9	Oil Cooler	129
6.3	Thermal Analysis	129
6.3.1	Introduction	129
6.3.2	Thermal Map Approach	129
6.3.3	Discussion and Results	133
6.4	Control Systems Concept	134
6.4.1	Control System Overview	134
6.4.2	Control System Components	136
6.4.3	Fuel Metering Section	136

TABLE OF CONTENTS

Page

6.4.4 Inlet Guide Vane Control 136
6.4.5 Start Sequencing System 136
6.4.6 Failure Detector/Failure Mode Control 138
6.4.7 Combustor Geometry Control 138
6.4.8 Transmission Control 138
6.4.9 Variable Stator Torque Converter Control 139
6.4.10 Sensors/Actuators 140
6.4.11 Control System Design 141

7.0 COST ANALYSIS 144
7.1 Initial Vehicle Cost 144
7.2 Scheduled Maintenance and Repairs 144
7.3 Fuel Cost 144
7.4 Cost of Ownership Difference Comparison 145

8.0 POWERTRAIN DEVELOPMENT PLAN 145
8.1 Research and Development Program 145
8.1.1 Engine Design 148
8.1.2 Engine Development 149
8.1.3 Radial Turbine — Aerodynamic Development 150
8.1.4 Compressor Development 151
8.1.5 Ceramic Design Technology 151
8.1.6 Low Loss Ducting 152
8.1.7 Low Emissions Combustor 152
8.1.8 Air Bearings and Shaft Dynamics 153
8.1.9 Ceramic Stationary Components (Process) 153
8.1.10 Ceramic Component Development (Test) 154
8.1.11 Regenerator Flow Distribution 154
8.1.12 Regenerator Seal Leakage (2.5%) 155
8.1.13 Regenerator Temperature, 1100°C (2000°F) 155
8.1.14 Ceramic Radial Turbine Wheel (Process) 156
8.1.15 Ceramic Wheel Attachment 156
8.1.16 Turbine Nozzle Sealing 157
8.1.17 Control System Development 157
8.1.18 Combustion Temperature Sensor Development 157
8.1.19 Optimum Transmission Development 158
8.1.20 Non-Destructive Evaluation 159

TABLE OF CONTENTS

Page

8.1.21 Ceramic Materials Characterization 160
8.1.22 Vehicle Package Design 160
8.1.23 Inlet System Ducting 161
8.1.24 Exhaust System Ducting 161
8.1.25 Powder Metal Compressor Wheel 161
8.1.26 Die-Cast Compressor Wheel 162
8.1.27 Non-Metallic Cases 162
8.1.28 Turbine Wheel Casting 162
8.1.29 Ceramic Recuperator 163
8.2 Estimated Production Engineering Cost and Schedule 163

DISCUSSION OF RESULTS 166

CONCLUSIONS 172

APPENDIX I — Ranking Criteria for Engine Concepts Assessment 173

APPENDIX II — Transmission Concepts, Ranking Criteria 174

APPENDIX III — Transmission Concepts, Rating Determination 175

APPENDIX IV — List of Acronymns 177

APPENDIX V — List of Symbols 178

LIST OF REFERENCES 179

LIST OF ILLUSTRATIONS

Figure		Page
1.1	Generalized Rear Axle Efficiency for Economy Projections	6
1.2	Generalized Rear Axle Efficiency for Steady State Speed and Performance Projections	7
1.3	Estimated Bevel Gear Efficiency for Typical Front Wheel Drive Applications	7
2.1	Schematics of Cycle Configuration Concepts	10
2.2	Fuel Economy Rating	11
2.3	Engine Cost Rating	12
2.4	Engine Packageability Rating	12
2.5	Technical Risk Rating	12
2.6	Engine Response Time Rating	13
2.7	Engine Starting Time Rating	13
2.8	Idle Creep Torque Rating	13
2.9	Vehicle Heater Rating	14
2.10	Engine Power, Time Distribution Over the Federal Urban Driving Cycle	14
3.1	Single-Stage Centrifugal Compressor Efficiency Projections	17
3.2	Adiabatic Efficiency Correction Factor vs. Specific Speed for Single-Stage Centrifugal Compressor	17
3.3	Axial Turbine Stage Efficiency Projections	19
3.4	Radial Turbine Efficiency Projections	20
3.5	Typical Regenerator Effectiveness Variation	23
3.6	Typical Effect of Design Pressure Ratio on the Regenerator Core Pressure Losses at Different Percentage Engine Speeds	23
3.7	Typical Regenerator Seal Leakage Variation with Engine Design Pressure Ratio	24
3.8	Estimate of Spool Bearing Losses	27
3.9	Concept 1. Ford C-4 Transmission	34
3.9(a)	Efficiency of Concept 1 at 100% Input Power with Single-Shaft Turbine Engine	34
3.10	Concept 2. Variable Stator Torque Converter with C-4 Transmission	34
3.10(a)	Efficiency of Concept 2	35
3.11	Concept 3. Variable Stator Torque Converter with Modified Ford FIOD Transmission	35
3.11(a)	Efficiency of Concept 3	35
3.12	Concept 4. Split Power Variable Stator Torque Converter with Ford C-4 Transmission	36
3.12(a)	Efficiency of Concept 4	36
3.13	Concept 5. Differential Variable Stator Torque Converter and Ford C-4 Transmission W/O Torque Converter with Slip Clutch	36
3.13(a)	Efficiency of Concept 5	37
3.14	Concept 6. Differential Variable Stator Torque Converter with Ford FIOD Transmission w/o Torque Converter with Shaft Lock-up and Slip Clut	37
3.14(a)	Efficiency of Concept 6	37
3.15	Concept 7. Inline Variable Speed Traction Drive and Ford C-4 Transmission with Fixed Stator Torque Converter	38
3.15(a)	Efficiency of Concept 7	38
3.16	Concept 8. Regenerative Variable Speed Traction Drive with 3-Mode Transmission and Slip Clutch	38
3.16(a)	Efficiency of Concept 8	39
3.17	Concept 9. Differential Variable Speed Traction Drive with Ford C-4 Transmission and Fixed Stator Torque Converter	39

LIST OF ILLUSTRATIONS

Figure		Page
3.17(a)	Efficiency of Concept 9	39
3.18	Concept 10. Differential Variable Speed Traction Drive with Ford FIOD Transmission and Fixed Stator Torque Converter	40
3.18(a)	Efficiency of Concept 10	40
3.19	Concept 11. Differential Variable Speed Traction Drive with Ford FIOD Transmission W/O Torque Converter with Slip Clutch and Shaft Lock-Up	40
3.19(a)	Efficiency of Concept 11	41
3.20	Concept 12. Differential Variable Speed Traction Drive with 3-Mode Transmission	41
3.20(a)	Efficiency of Concept 12	41
3.21	Concept 13. Differential Variable Speed Traction Drive with 4-Mode Transmission	42
3.21(a)	Efficiency of Concept 13	42
3.22	Concept 14. 2-Mode Differential Variable Speed Traction Drive with 3-Mode Transmission i.e., 6-Mode	42
3.22(a)	Efficiency of Concept 14	43
3.23	Concept 15. Hydromechanical Tri-Mode Transmission	43
3.23(a)	Efficiency of Concept 15	43
3.24	Concept 16. Variable Belt Drive with Variable Stator Torque Converter and 2-Speed Transmission	44
3.24(a)	Efficiency of Concept 16	44
3.25	Concept 17. Free Power Turbine with Ford C-4 Transmission and Fixed Stator Torque Converter	44
3.26	Concept 18. Free Power Turbine with Ford C-4 Transmission W/O Torque Converter	45
3.26(a)	Efficiency of Concepts 17 and 18	45
3.27	Concept 19. Free Power Turbine with Ford FIOD Transmission and Fixed Stator Torque Converter	45
3.27(a)	Efficiency of Concept 19	46
4.1	Assumed Variation of Centrifugal Compressor Airflow Parameter with Speed for the Cycle Analysis	53
4.2	Specific Fuel Consumption (SFC) and Airflow vs. Engine Design Pressure Ratio	53
5.1	Schematics of Engine Configurations Including Station Numbers	55
5.2	Specific Fuel Consumption vs. Horsepower of Single-Shaft Engines with Radial Turbines	57
5.3	Specific Fuel Consumption vs. Horsepower of Single-Shaft Engines with Axial Turbines	57
5.4	Specific Fuel Consumption vs. Horsepower of Free Turbine Engines with Variable Power Turbine Nozzles	58
5.5	Inline Arrangement of Ford IGT Engine	65
5.6	Folded Drive Arrangement of Ford IGT Engine	67
5.7	Design Adaptation of IGT Engine to 9425 Rad/s (90,000 rpm) Spool Configuration	69
5.8	Design Adaptation of IGT Engine to 3-Stage Axial Turbine Configuration	71
5.9	Ceramic Radial Inflow Turbine at 1370°C (2500°F) and 12357 Rads/s (118,000 rpm)	72
5.10	Change of Temperature with Time at Full Power Acceleration from Low Fuel Idle for Ceramic Radial Turbine	73

LIST OF ILLUSTRATIONS

Figure		Page
5.11	Change of Maximum Principle Tensile Stress at Full Power Acceleration from Low Fuel Idle for Ceramic Radial Turbine	73
5.12	Uncooled Metallic Radial Inflow Turbine at 1200°C (2200°F) T.I.T. and 12357 Rads/s (118,000 rpm)	74
5.13	Temperature Distribution for the Cooled Metallic Radial Inflow Turbine at 1200°C (2200°F) T.I.T. and 12357 Rads/s (118,000 rpm) — (0.1% Coolant Flow)	74
5.14	First Stage Ceramic Axial Turbine Disk at 1370°C (2500°F) T.I.T. and 12357 Rads/s (118,000 rpm) — (Cooled Metallic Bolt)	75
5.15	First Stage Ceramic Axial Turbine Disk at 1370°C (2500°F) T.I.T. and 12357 Rads/s (118,000 rpm) — (Ceramic Bolt)	75
5.16	Second Stage Ceramic Axial Turbine Disk at 1370°C (2500°F) T.I.T. and 12357 Rads/s (118,000 rpm) — (Ceramic Bolt)	76
5.17	Third Stage Ceramic Axial Turbine Disk at 1370°C (2500°F) T.I.T. and 12357 Rads/s (118,000 rpm) — (Ceramic Bolt)	76
5.18	Strength Requirements for the Radial and Axial Ceramic Turbine Rotors as a Function of Weibull Slope for 99% Reliability	77
5.19	Radial Inflow Turbine Inner Diffuser Shell at Full Power Steady-State Loading (1370°C T.I.T.) (5 mm Thickness)	78
5.19(contd.)	Radial Inflow Turbine Inner Diffuser Shell Deformation at Full Power Steady-State Loading (1370°C T.I.T.) (5 mm Thickness)	79
5.20	Radial Inflow Turbine Inner Diffuser Shell at Full Power Steady-State Loading (1370°C T.I.T.) (10 mm in. Thickness)	79
5.20(contd.)	Radial Inflow Turbine Inner Diffuser Shell Deformation at Full Power Steady-State Loading (1370°C T.I.T.) (10 mm Thickness)	80
5.21(a)	Power Loss Characteristics of the Ford FIOD Transmission Without Torque Converter, Including Oil Pump. First Gear	84
5.21(b)	Power Loss Characteristics of the Ford FIOD Transmission Without Torque Converter, Including Oil Pump. Second Gear	84
5.21(c)	Power Loss Characteristics of the Ford FIOD Transmission Without Torque Converter, Including Oil Pump. Third Gear	85
5.21(d)	Power Loss Characteristics of the Ford FIOD Transmission Without Torque Converter, Including Oil Pump. Fourth Gear	85
5.22	Ford Variable Stator Torque Converter Test Results	86
5.23	Assumed Efficiency of Traction Drive Element (Reference 6)	86
5.24(a)	Rear Wheel Drive Installation of Ford IGT Engine (Side View)	87
5.24(b)	Rear Wheel Drive Installation of Ford IGT Engine (Front View)	89
5.24(c)	Rear Wheel Drive Installation of Ford IGT Engine (Plan View)	91
5.25(a)	Front Wheel Drive Installation of Ford IGT Engine (Side View)	93
5.25(b)	Front Wheel Drive Installation of Ford IGT Engine (Front View)	95
6.1	Centrifugal Compressor Rotor Meridional Cross-Section	105
6.2	Centrifugal Compressor First Stage Diffuser	106
6.3	Effect of Centrifugal Compressor Speed and Hub Diameter on the Relative Mach Number at Inducer Blade Tip	106
6.4	Effect of Centrifugal Compressor Speed and Hub Diameter on the Efficiency	107
6.5	Single-Stage Centrifugal Compressor Pressure Ratio and Airflow Characteristic Map	107
6.6	Single-Stage Centrifugal Compressor Efficiency Characteristic Map	108
6.7	Radial Turbine Rotor and Stator Meridional Cross-Section (Metallic Rotor)	109
6.8	Radial Turbine Rotor and Stator Meridional Cross-Section (Ceramic Rotor)	112
6.9	Radial Turbine Efficiency Characteristics — Metallic Rotor Tip Speed 722 m/s (2368 fps)	113

LIST OF ILLUSTRATIONS

Figure		Page
6.10	Radial Turbine Airflow Characteristics — Metallic Rotor Tip Speed 722 m/s (2368 fps)	113
6.11	Radial Turbine Efficiency Characteristics — Ceramic Rotor Tip Speed 758 m/s (2487 fps)	114
6.12	Radial Turbine Airflow Characteristics — Ceramic Rotor Tip Speed 758 m/s (2487 fps)	114
6.13	Detail Design Layout of Ford IGT Engine	117
6.14	Bill of Materials for Ford IGT Engine	119
6.15	Ford IGT Engine Parts List	121
6.16	Shaft Vibration Model	123
6.17	Critical Speed vs. Gas Bearing Spring Rate	124
6.18	Critical Speed vs. Gear Spring Rate Coefficient	125
6.19	Vibration Mode Shapes	125
6.20	Bearing Housing and Compressor Shroud Deformation	127
6.21	Compressor Rotor Radial Stresses (MPa)	128
6.22	Compressor Rotor Tangential Stresses (MPa)	128
6.23	Compressor Rotor Equivalent Stresses (MPa)	128
6.24	Compressor Rotor Thermal and Centrifugal Growths (mm), (Thermal only Growths in Parenthesis)	129
6.25	Flow Diagram for Thermal Analysis	130
6.26	Axi-symmetric Finite Element Model Showing Temperature Distribution at Full Power with Metal Turbine Rotor	131
6.27	Functional Schematic of Control System	135
6.28	Fuel Metering Section	137
6.29	Inlet Guide Vane Control	137
6.30	Variable Geometry Combustor Control	139
6.31	Variable Stator Torque Converter Control	140
6.32	Vehicle Control System Block Diagram	143
8.1	DOE/NASA Gas Turbine Engine Program — Timing Chart	147
8.2	Engine Test Schedule — Timing Chart	148
8.3	Ceramic Components Development — Timing Chart	155

LIST OF TABLES

Table		Page
1.1	Comparison of 1978 Fairmont with Baseline Vehicle	5
1.2	Roadload Power at the Wheels for the Baseline Vehicle	6
2.1	Candidate Engine Concepts	9
2.2	Engine Concept Ranking Matrix	11
2.3	Reasons for Eliminated Concepts	15
2.4	Concept Ranking Summary	15
3.1	Effect of VIGV's on Radial Compressor Characteristics	18
3.2	Regenerator Matrix F&J Data	21
3.3	Engine Duct Pressure Losses	24
3.4	Estimated Turbine Cooling Airflow Rates	25
3.5	Accessories and Auxiliaries — Power Absorbed	26
3.6	Ceramics Technology Projections — Material Strength	29
3.7	Metals Technology Projections — Material Strength	31
3.8	Transmission Concept Ranking Matrix	47
3.9	Transmission Relative Costs	48
4.1	Cycle Performance — Summary of Results	54
5.1	Engine Configurations Analyzed	56
5.2	Engine Leakages for Performance Analysis	56
5.3	Engine Ranking at 20 Percent Power, Based on SFC's	58
5.4	Vehicle Performance and Economy for Single-Shaft Engines with Radial Turbines	60
5.5	Effect of Transmission Type on Vehicle Performance and Economy with Single-Shaft Engines	61
5.6	Effect of Axial and Radial Turbines on Vehicle Performance and Economy with Single-Shaft Engines	62
5.7	Comparison of Vehicle Performance and Economy for Single-Shaft and Free Turbine Engines	63
5.8	Variable Stator Torque Converter Plus Ford FIOD Gearbox (concept 3, Section 3.11.2). Efficiency vs. Speed Ratio	81
5.9	Differential Split-Power Traction Drive Plus 4-Speed Transmission (concept 13, Section 3.11.2). Efficiency vs. Speed Ratio	82
5.10	Differential Split-Power Variable Stator Torque Converter Plus Ford FIOD Gearbox (concept 6, Section 3.11.2). Efficiency vs. Speed Ratio	83
5.11	Engine Parameters and Sensitivities	98
5.12	Effects of Technology Changes on Fuel Economy of Engine Configuration SS8	99
5.13	Estimates of 1983 Component Performance at 20 Percent Power	100
5.14	Specific Fuel Consumption from Cycle Analysis	101
5.15	CFDC Fuel Economy	101
5.16	Probability of Obtaining a Specified Minimum Percentage Improvement Over the Baseline Fuel Economy	101
5.17	Cost Comparisons	102
5.18	Powertrain Selection Matrix	104
6.1	Single Stage Centrifugal Compressor Design	105
6.2	Metal Radial Turbine Design Point	110
6.3	Ceramic Radial Turbine Design Point	112
6.4	Improved Gas Turbine Engine Parts List	116
6.5	Reduction Gearing Design Results	126
6.6	Compressor Clearance Changes Due to Thermal Growth	133
6.7	Turbine Clearance Changes Due to Thermal Growth	134
8.1	Overall Component Development Program	147
8.2	Production Facilitization Costs, $(Million)	165
8.3	Major Differences Between Turbine and Piston Engines Relative to Facility Cost Estimates	166
9.1	Conclusions — Performance and Fuel Economy	168
9.2	Effect on Ceramic Engine Fuel Economy — Current vs. 1983 Technology	169

SUMMARY

This report presents the results of an in-depth study for identifying an improved gas turbine for automotive applications. The study was performed by the Ford Motor Company and AiResearch Division of the Garrett Corporation under contract to DOE/NASA.

The principal specified objectives of this contract were:

- Fuel economy a minimum of 20 percent better than 8.3 km/l (19.6 mpg) for a 1542 kg (3400 lbs.) test weight baseline vehicle, when tested over the Combined Federal Driving Cycle at emissions objectives of .41 gm/mi HC, 3.4 gm/mi CO, and .4 gm/mi NO_X.
- Acceleration capability of 15 seconds from 0 to 96.5 km/hr. (0 to 60 mph).
- A design capable of reaching a level of development in 5 years (by the year 1983) such that a decision to start a production program could be considered.

Additionally, Ford requirements for the engine were:

- A fuel economy objective of 30 to 50 percent better than the baseline vehicle.
- A 4 second vehicle start-up distance of 19.5 m (64 ft.).

Investigations for an improved gas turbine system identified twenty-two candidate engine concepts. These were examined judgementally, based on the previous experience of both contracting Companies, and were ranked for fuel economy, cost packageability, risk of a long development program, and driveability feel. Double weight was assigned to the cost and fuel economy.

Three of the candidate concepts were selected for further study. The regenerated, single-shaft engine with a centrifugal compressor, variable inlet guide vanes and a radial turbine ranked first. The same configuration utilizing an axial turbine ranked second. The two-shaft (i.e., free power turbine) engines were not ranked near the top principally due to the higher cost and development risks associated with variable geometry ceramic nozzles. However, because of industry interest in this configuration, a two-shaft regenerative arrangement with centrifugal compressor, variable inlet guide vanes, radial gasifier turbine and an axial power turbine with variable nozzles was also studied.

Component efficiencies and material properties used in assessing the three-engine concepts were predicted based on extrapolations of current test data to the expected technological achievement within a 5-year period. In developing these predictions, key technical areas for development were identified. These areas include ceramics, aerodynamics, transmissions, low emissions combustors, and low cost production techniques, etc. Component development plans were constructed and integrated with the overall engine development program.

Selection criteria were established and used to evaluate the engine concepts. These criteria were weighted and included in order of rank, fuel economy, manufacturing cost, technical risks, installation considerations, and development and growth potential. The result was that the single shaft regenerative engine with a centrifugal compressor with variable inlet guide vanes and radial turbine appeared most favorable and it was selected for a more detailed engine design and vehicle installation study. The rotational speed of the engine was optimized at 12357 rads/s (118000 rpm) and the ceramic radial turbine tip speed was optimized at 759 m/s (2487 fps). The design output at 1370°C (2500°F) was 100 kW (134 HP) with a specific fuel consumption of 0.194 kg/kW-hr. (0.319 lbs./HP-hr.). At 20 percent power the specific fuel consumption of the engine was 0.197 kg/kW-hr. (0.324 lbs./HP-hr.) and a minimum specific fuel consumption of 0.182 kg/kW-hr. (0.300 lbs./HP-hr.) occurred at about 60 percent power.

Studies identified sixteen potential continuously variable transmissions for the single-shaft engine from which three were selected for a viable development program. The prime candidate transmission consisted of a differential split-power arrangement with a variable stator torque converter and a modified Ford FIOD gearbox. The preferred transmission, but with a greater risk attached to the development, involved replacement of the variable stator torque converter with a traction drive unit. As a backup to these transmissions, available components consisting of a Ford variable stator torque converter and a modified Ford FIOD gearbox in a non split-power configuration were recommended.

The optimized ceramic engine with the available continuously variable transmission had a calculated improvement of 56 percent in fuel economy over the baseline vehicle. With the prime candidate

transmission the fuel economy improvement increased to 76 percent and for the preferred transmission the improvement increased to 93 percent over the baseline vehicle.

A cost analysis study indicated that the initial cost of a vehicle with the single-shaft gas turbine engine would carry a premium of $560 to $1120. However, due to the savings in fuel costs, for a 160,934 km (100,000 miles) period, the total net cost of the gas turbine engined vehicle would show a savings of $156 to $1164, depending on the transmission used and assuming maintenance costs are the same as for a piston engine vehicle.

A powertrain development plan has been outlined to indicate the magnitude of effort necessary to attain the level of the technological predictions and to provide for the demonstration of a single-shaft gas turbine engine in a vehicle, so that, by the end of 1985, a decision can be made on the viability of a production program.

INTRODUCTION

This report covers the results of an Improved Gas Turbine Powertrain Conceptual Design Study, performed jointly by the Ford Motor Company as contractor and AiResearch Manufacturing Company of Arizona, a Division of the Garrett Corporation as subcontractor, under NASA/DOE Contract No. DEN 3-37.

The design study comprised four basic tasks, described below:

	Task	Description
I	Powertrain Definition	Specification and assessment of candidates
II	Powertrain Analysis	Analysis and comparison of the four best concepts
III	IGT Vehicle Characterization	Detailed preliminary design of selected baseline powertrain
IV	IGT Powertrain Development Plan	Identification and prioritization of long-lead items. Summary of development program and timing chart.

The principal objectives of this contract were:

- Fuel economy a minimum of 20% better than 8.3 km/l (19.6 mpg) for a 1542 kg (3400 lb.) test weight baseline veicle, when tested over the Combined Federal Driving Cycle at emissions objectives of .41 gm/mi HC, 3.4 gm/mi CO, and .4 gm/mi NO_x.
- Acceleration capability of 15 seconds from 0 to 96.5 km/hr. (0 to 60 mph).
- A design capable of reaching a level of development in 5 years (by the year 1983) such that a decision to start a production program could be considered.

In the original proposal to NASA/DOE, the Ford Motor Company proposed the need for a fuel economy objective of 30% to 50% better than the baseline vehicle if the engine is to be sufficiently better than other automotive powerplants which are likely to be available in the mid-1980's, and consequently this study addresses the higher fuel economy objective. In addition, although not a contract objective, the initial response time as measured by the distance traveled in the first 4 seconds is a matter of concern for a gas turbine engined vehicle. A comparable piston engine vehicle of 15 second, 0 to 96.5 km/hr. (0-60 mph) capability would have a 4 second start-up distance of 19.5 m (64 ft.). This was considered a desirable criteria.

Initial studies indicated that a 75 kW (100 HP) engine was required to meet the vehicle acceleration goal of 0 to 96.5 km/hr. (0 to 60 mph) in 15 seconds. In view of the probability of a long development time being necessary to realize a ceramic turbine rotor, it was decided to initially size the engine to provide 75 kW (100 HP) with a metal turbine rotor operating at a turbine inlet temperature of 1150°C (2100°F). It was envisaged that this interim metal rotor engine configuration would be developed in parallel to ensure that vehicle testing and system integration effort could proceed at the earliest possible date. When the ceramic turbine rotor is developed, and since it is of approximately the same size as the metal rotor, it could be readily substituted in the engine without changing rotational speeds or the compressor. Utilization of the higher turbine inlet temperature capability of the ceramic rotor, i.e. 1370°C (2500°F), would improve the thermal efficiency of the engine and increase the power output to 100 kW (134 HP). With the improved engine response time, vehicle performance level, and fuel economy derived from a ceramic turbine rotor engine, it is judged that such a configuration would be more likely to be a marketable product.

Initially, twenty-two configurations of gas turbine engines were considered. These were subjectively ranked, based on the previous experience of both Ford and AiResearch, according to weighted criteria, including fuel economy, cost, packageability, development risks and driveability. The outcome of this exercise was three engine concepts which were to be studied further.

To evaluate these concepts, component performance predictions were necessary and were based on current test data with projections from that base with consideration given to expected technological

development over a 5 year time frame. A cycle analysis study made for a 75 kW (100 HP) gas turbine engine at 100 percent and 20 percent power level, with a turbine inlet temperature of 1150°C (2100°F), was used to optimize the engine design airflow and pressure ratio. Ford evaluated two optimized single-shaft engine designs, one with a radial turbine and the other with an axial turbine. AiResearch evaluated a more conservatively stressed single-shaft engine with a radial turbine and also a two-shaft engine with a radial gas generator turbine and an axial power turbine with variable nozzles. The performance of each engine configuration was calculated using complete component characteristics over the whole operating range. Engine design layouts and vehicle installation studies were done to the extent necessary to define the system and to prepare a cost comparison. Risk and sensitivity studies were also completed for each concept. The four engine designs were evaluated and a selection made using weighted criteria, including fuel economy, cost, technical risk, installation considerations and growth potential. The best concept was then selected for more detailed design and analysis.

While the two-shaft engine was assumed to use a conventional automatic transmission, the single-shaft engine requires some form of continuously variable transmission. A total of 19 candidate transmission concepts (three for the two-shaft engine) were studied, compared, and ranked. Ford had previously developed a continuously variable transmission for use with the single shaft engine, but in the course of this study it was shown that other concepts of transmission would substantially improve performance and fuel economy of the vehicle. The three best concepts of transmissions for single-shaft engines were analyzed in greater detail and efficiency characteristics were derived for use in vehicle route studies.

This design study also included the recommended 5 year research and development plan to bring the preferred design to the point at which a decision to enter the production phase could be made. Each sub-project was addressed individually and the total predicted annualized cost, at 1978 economics, was derived.

1.0 VEHICLE SPECIFICATION

A 1978 Ford Fairmont, 4-door has been selected as the vehicle which closely represents the NASA baseline vehicle. The comparison is shown in Table 1.1 and it can be seen that the Fairmont dimensions agree quite closely with the baseline vehicle. The 5.0L piston engine with automatic transmission compares favorably in weight and fuel economy, but is four seconds faster in the 0-96.5 km/hr. (0-60 mph) acceleration. An optional 3.3L piston engine with automatic transmission has an acceleration time of 14.7 seconds and a fuel economy of 9.2 km/l (21.7 mpg) but it is lighter in test weight at 1466 kg (3233 lbs.).

The 1978 Fairmont was used in all packaging and installation studies of the Improved Gas Turbine engine. Engine compartment drawings, accessory and auxiliary component drawings, a front wheel drive concept drawing, and a rear wheel drive conventional layout drawing have been utilized for the installation studies.

For the purpose of performance and fuel economy studies, the characteristics of the baseline vehicle as specified by NASA and as shown in Table 1.1 were used. Additionally, the Fairmont drag coefficient of 0.52 was assumed for the baseline vehicle. Table 1.2 shows the roadload power calculated for the baseline vehicle. The difference between the chassis dynamometer powers for the "Front Drive" and "Rear Drive" is due to the weight differences on the pair of driving wheels, with adjustments such that the road loads are equal at 80.5 km/hr. (50 mph). The difference between the "Test Track" and "Chassis Dynamometer" road load at 80.5 km/hr. (50 mph) is due to a correction because of the different ambient conditions at which these tests are conducted. The column labeled "Test Track" shows the total road load horsepower at the wheels, as calculated for the baseline vehicle, for evaluating the performance of the vehicle for both front wheel drive and rear wheel drive configurations. The two columns under the "Chassis Dynamometer" heading show the power at the driving wheels (for front wheel drive or rear wheel drive) to be used in computing the fuel economy over the Combined Federal Driving Cycle (CFDC) routes.

TABLE 1.1

Comparison of 1976 Fairmont with Baseline Vehicle

	Baseline Vehicle	1978 Fairmont (5.0L)
Curb Weight	1406 kg (3100 lb.)	1432 kg (3156 lb.)
Test Weight	1542 kg (3400 lb.)	1568 kg (3456 lb.)
Frontal Area/Drag Coefficient	$2m^2$ ($21.5\ ft^2$)/Cd = .52*	$2m^2$ ($21.7\ ft^2$)/Cd = .52
Wheel Base	2.8m (109.5 in.)	2.7m (105.5 in.)
Axle Ratio	2.70:1	2.73:1
Tires	ER78-14	B,C,DR 78-14 (Avail. Opts.)
HP/WT Ratio	0.05 kW/kg (0.03 HP/lb)	0.07 kW/kg (0.04 HP/lb)
Transmissions (Auto. 3 Spd.)		
1st Ratio	2.5:1	2.46:1
2nd Ratio	1.5:1	1.46:1
3rd Ratio	1.0:1	1.00:1
0-96.5 km/hr. (0-60 mph) Accel.	15.0 sec.	11.1 sec.
Minimum range	483 km (300 mi.)	510 km (317 mi.)
Fuel Economy (CFDC)	8.3 km/l(19.6 MPG)	7.9 km/l (18.6 MPG)
Roominess Index	6.9m (273 ins.)	7.0m (275.8 ins.)
Hip Room	1.5m (57 ins.)	1.4mF/1.0mR (56.2 ins. F/53.7 ins. R)
Shoulder Room	1.4m (55 ins.)	1.4m (56.7 ins.)
Trunk Space	$0.45m^3$ ($16.0\ ft^3$)	$0.48m^3$ ($1.8\ ft^3$)

*Drag coefficient for baseline vehicle assumed the same as the 1978 Fairmont in order to compute road load.

TABLE 1.2

Road Load Power at the Wheels
For the Baseline Vehicle

Vehicle Speed km/hr. (mph)	Test Track kW (HP)	Chassis Dynamometer Front Drive kW (HP)	Chassis Dynamometer Rear Drive kW (HP)
16.1 (10)	0.8 (1.1)	1.0 (1.3)	0.7 (1.0)
32.2 (20)	1.9 (2.6)	2.3 (3.1)	1.9 (2.5)
48.3 (30)	3.7 (5.0)	4.1 (5.5)	3.7 (4.9)
64.4 (40)	6.5 (8.7)	6.7 (9.0)	6.4 (8.6)
80.5 (50)	10.5 (14.1)	10.4 (14.0)	10.4 (14.0)
96.6 (60)	16.2 (21.7)	15.5 (20.8)	16.1 (21.6)
112.7 (70)	23.8 (31.9)	22.2 (29.7)	23.7 (31.8)
128.7 (80)	33.7 (45.2)	30.7 (41.2)	33.6 (45.1)

The test track power for the baseline vehicle is the same for both front and rear wheel drive configurations.

Generalized axle efficiency curves used in the vehicle performance and economy calculations are shown in Figures 1.1 through 1.3. Figure 1.1 shows the rear wheel drive axle efficiency vs. axle input torque to be used in computing the CFDC fuel economy. Figure 1.2 shows rear wheel drive axle efficiency vs. axle input torque to be used in computing vehicle performance. Figure 1.3 shows two similar efficiency curves for a front wheel drive configuration. The axle efficiency data for the CFDC fuel economy projections is lower than that for the performance projections because of the cold start requirements of the CFDC test. The performance projections are assumed to be made with a fully warmed-up vehicle.

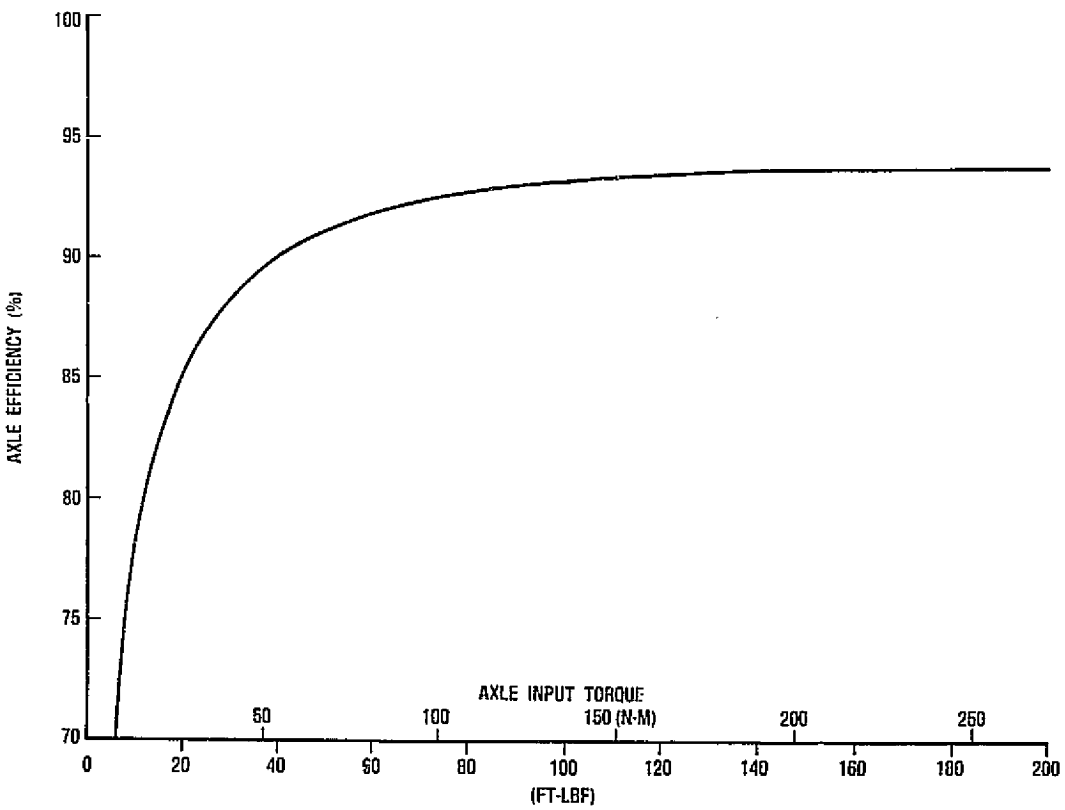


Figure 1.1 Generalized Rear Axle Efficiency for Economy Projections

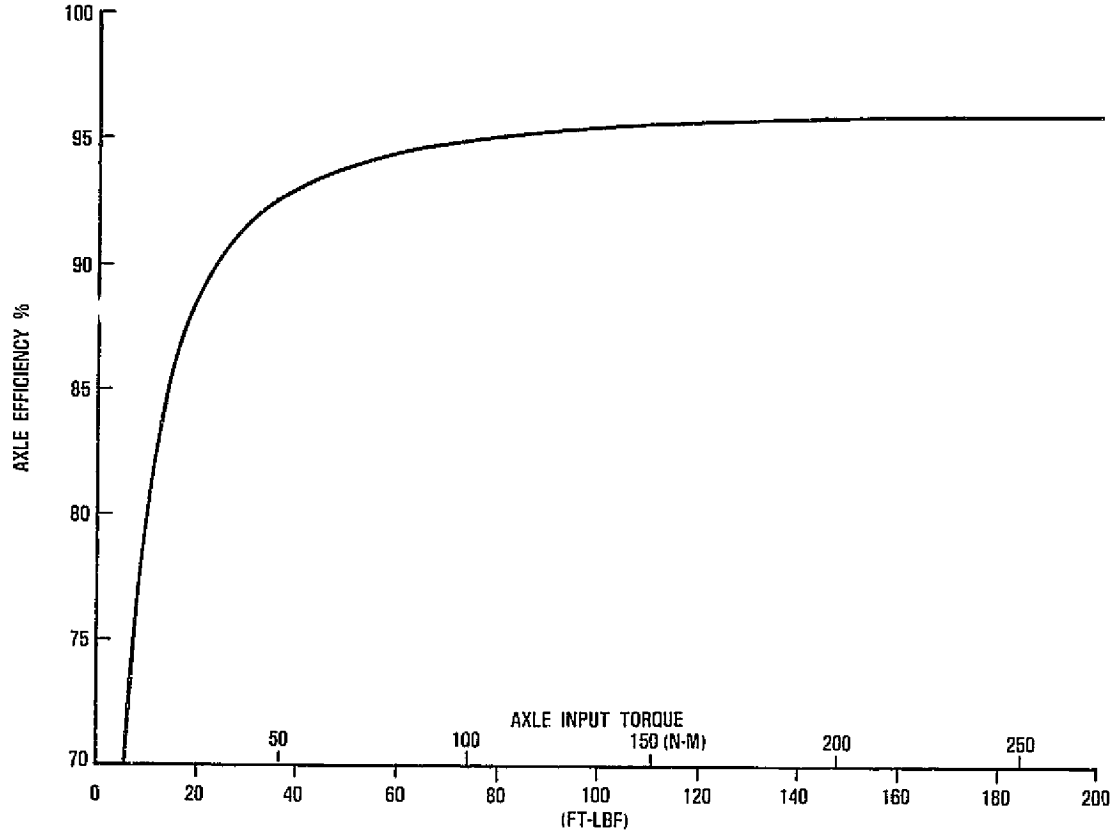


Figure 1.2 Generalized Rear Axle Efficiency for Steady State Speed and Performance Projections

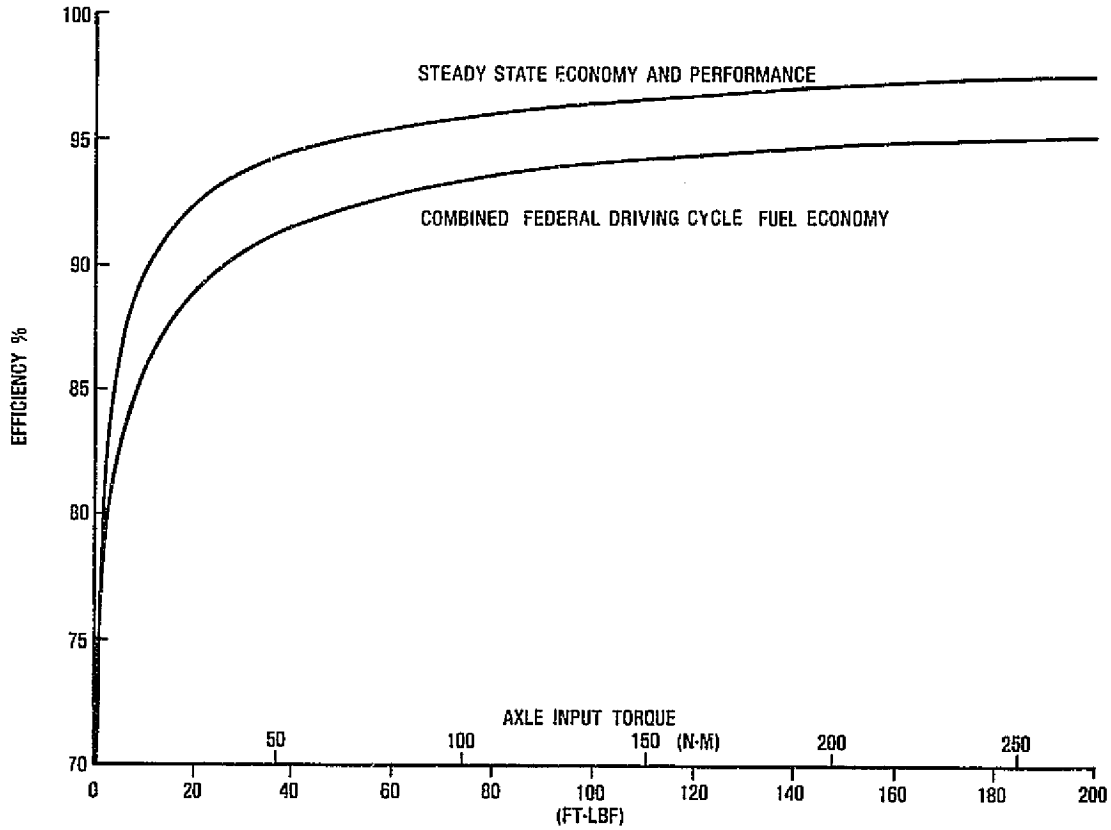


Figure 1.3 Estimated Bevel Gear Efficiency for Typical Front Wheel Drive Applications

2.0 ENGINE CONCEPTS ASSESSMENT AND SELECTION

2.1 Introduction and Summary

The objective of this task was to compare and rank a total of twenty-two candidate IGT concepts. The candidate concepts considered are presented schematically in Figure 2.1 and the ranking criteria of Appendix I were applied to all of the concepts through a Concept Ranking Matrix. The completed Concept Ranking Matrix is presented in Table 2.2 and summarized in Table 2.4.

The ranking of the candidate IGT concepts showed that single-shaft, regenerated engines with variable inlet guide vanes are the first two choices (Concepts 1.5 and 3.5).

2.2 Candidate Engine Concepts

Table 2.1 gives a brief description of each engine concept evaluated and Figure 2.1 presents schematic diagrams of the candidates. Candidates 1.5, 3.5, 4.5, 7.5, 8.5, 10.5 and 14.5 were created by adding compressor variable inlet guide vanes (VIGV) to concepts 1.0, 3.0, 4.0, 7.0, 8.0, 10.0 and 14.0, respectively. The latter concepts are briefly explained below:

Concept 1.0 is a single-shaft engine with a centrifugal compressor, a radial turbine, and a single rotary regenerator.

Concept 3.0 is the same as concept 1.0 except that a 3-stage axial turbine replaces the radial turbine.

Concept 4.0 is the same as concept 3.0 except that a 2-stage axial turbine is used.

Concept 5.0 is the same as concept 1.0 except that two stages of radial turbine are used.

Concept 6.0 is the same as concept 1.0 except that two radial stages of compression and expansion are used.

Concept 7.0 is the same as concept 1.0 except that the single regenerator core is replaced by dual cores.

Concept 8.0 is the same as concept 1.0 except that a fixed geometry recuperator replaces the rotary regenerator.

Concept 9.0 is the same as concept 1.0 except that the engine is nonrecuperative. To be competitive in part load fuel consumption, this engine will have to be designed for a much higher pressure ratio than concepts 1.0 through 8.0.

Concept 10.0, called a free turbine, consists of a radial compressor and axial turbine forming the gas generator spool, and another axial stage with variable nozzles for the power turbine. The engine as defined would have a single rotary regenerator. Accessories would be driven from the gas generator spool.

Concept 11.0 is the same as concept 10.0 except that the power turbine has fixed geometry nozzles and a modulated slipping clutch connects the power turbine shaft with the gas generator shaft.

Concept 12.0 is somewhat similar to concept 10.0 except that three axial stages of turbine are used. The first stage of turbine is typically directly coupled to the compressor forming the gas generator spool. The other two stages of turbine may be differentially connected between the output shaft and the gas generator spool. Variable turbine nozzles are also used on one turbine stage.

Concept 13.0 is the same as concept 10.0 except that the accessories for the engine and vehicle are driven from the power turbine shaft.

Concept 14.0 is the same as concept 10.0 except that the gas generator turbine is a radial stage.

Concept 15.0 consists of two gas generator spools and a free power turbine. The compressors are arranged in series to provide a high engine pressure ratio.

Concept 16.0 is the same as concept 15.0 except that intercooling is used between the compression stages, and reheat is used after the first turbine stage.

TABLE 2.1

Candidate Engine Concepts

CONCEPT	TYPE	COMP/TURB	HEAT EXCH	VIGV	OTHER
1	Single Shaft	CEN/RAD	Regen	No	
1.5	Single Shaft	CEN/RAD	Regen	Yes	
3	Single Shaft	CEN/3 AX	Regen	No	
3.5	Single Shaft	CEN/3 AX	Regen	Yes	
4	Single Shaft	CEN/2 AX	Regen	No	
4.5	Single Shaft	CEN/2 AX	Regen	Yes	
5	Single Shaft	CEN/2 RAD	Regen	No	
6	Single Shaft	2 CEN/2 RAD	Regen	No	
7	Single Shaft	CEN/RAD	Dual Regen	No	
7.5	Single Shaft	CEN/RAD	Dual Regen	Yes	
8	Single Shaft	CEN/RAD	Recup	No	
8.5	Single Shaft	CEN/RAD	Recup	Yes	
9	Single Shaft	CEN/RAD	No	No	
10	Free Turbine	CEN/AX/AX	Regen	No	Variable Turbine Nozzle
10.5	Free Turbine	CEN/AX/AX	Regen	Yes	Variable Turbine Nozzle
11	Free Turbine	CEN/AX/AX	Regen	No	Power Transfer
12	3-Shaft Free Turbine	CEN/AX/AX/AX	Regen	No	Variable Nozzle at Aux. Turb, Aux. Turb Supplements GGT or Power Turbine
13	Free Turbine	CEN/AX/AX*	Regen	No	Variable Turbine Nozzle
14	Free Turbine	CEN/RAD/AX	Regen	No	Variable Turbine Nozzle
14.5	Free Turbine	CEN/RAD/AX	Regen	Yes	Variable Turbine Nozzle
15	2-Shaft with Free Turbine	High & Low Spd CEN/High & Low Speed RAD/AX	Regen	No	Accessories Driven from High Speed GGT
16.5	2-Shaft with Free Turbine	High & Low Spd CEN/High & Low Speed RAD/AX	Regen	No	Accessories Driven from High Speed GGT, Reheat, Intercooling

*Accessories driven by power turbine (otherwise GGT).

2.3 Method of Selection

Ranking criteria from Appendix I are presented graphically in Figures 2.2 through 2.9. Each figure is for a separate criterion. Table 2.2 presents the Concept Ranking with the concepts as rows and the ranking criteria as columns. The rating factors are shown at the top for each ranking criterion. The purpose of the rating factors was to assign a certain "weight" to each of the criteria. Note that all four driveability criteria were assigned the same weight.

Based on experience, available data from (Reference 1), and judgment, each concept was ranked on a 1 to 10 scale using the rating charts (Figures 2.2 through 2.9) and the rating value entered in its appropriate block in the Concept Ranking Matrix. After assigning an appropriate value to each criterion for each concept, an overall total measure of effectiveness was computed for each concept. The overall measure of effectiveness is the sum of the products of the rating values and the corresponding rating factors. The concept with the highest measure of effectiveness was ranked No. 1 and the next highest No. 2, and so on.

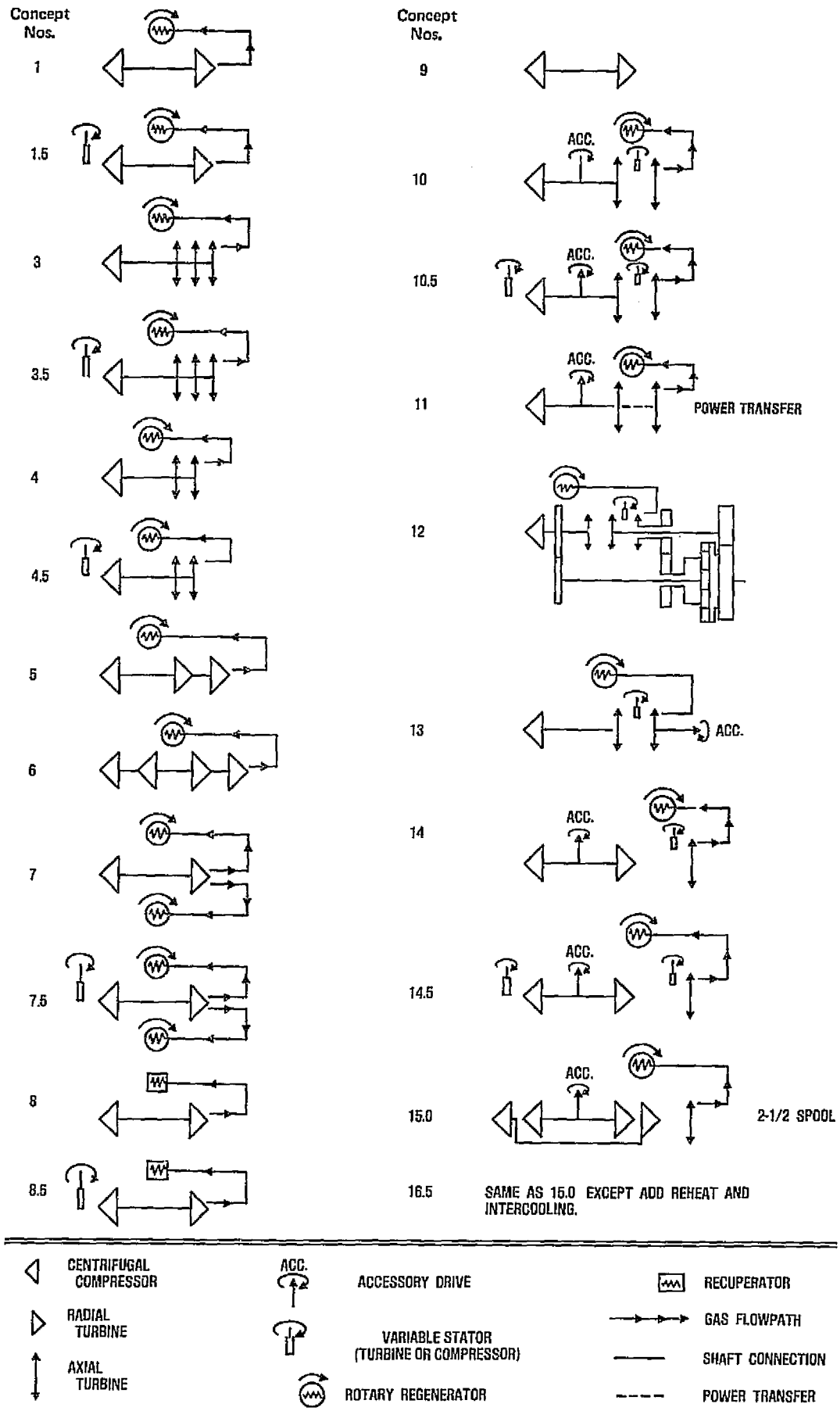


Figure 2.1 Schematics of Cycle Configuration Concepts

The ranking criteria (Figures 2.2-2.9) have minimum "no-go" values. Concepts which did not meet a "no-go" condition for at least one of the criteria were eliminated from the overall ranking. A zero entry for that criterion in the Table 2.2 matrix indicates a failed "no-go" condition; a zero also appears under "measure of effectiveness" for that concept.

The estimation of compressor VIGV benefits in rating the fuel economy criterion was done as follows: An off-design computer model was run subject to a 2000°F regenerator inlet temperature limit at idle speed, with and without VIGVs. This data was then applied to the urban driving cycle time distribution shown in Figure 2.10 to estimate the percentage improvement in fuel economy attributable to compressor VIGVs. This benefit was then reduced by 50 percent, since the urban driving cycle represents about one-half of the total driving time on the Combined Federal Driving Cycle, see References 2 and 3.

TABLE 2.2

Engine Concept Ranking Matrix

Concept No.	Compressor	Turbine (1)	Turbine (2)	Heat Exchanger	Economy	Cost	Package-ability	Technical Risk	Driveability: Response Time	Driveability: Start Time	Driveability: Idle Creep	Driveability: Heater BTU	Overall Measure of Effectiveness	
		Rating Factor			2	2	1	1	1/4	1/4	1/4	1/4		Rank
1	CEN	RAD	—	Regen	4.4	6.4	7.0	4.0	7.3	6.25	9.0	5.5	39.61	5
1.5	VIGV+CEN	RAD	—	Regen	6.1	6.0	7.0	4.0	7.3	5.6	9.0	5.5	42.05	1
3	CEN	AX+AX+AX	—	Regen	4.8	4.7	7.0	5.5	7.3	6.25	9.0	5.5	30.51	6
3.5	VIGV+CEN	AX+AX+AX	—	Regen	6.9	4.25	7.0	5.5	7.3	5.6	9.0	5.5	41.65	2
4	CEN	AX+AX	—	Regen	3.7	5.5	7.0	5.5	8.2	8.6	9.0	5.5	32.23	8
4.5	VIGV+CEN	AX+AX	—	Regen	5.4	5.0	7.0	5.5	8.2	5.9	9.0	5.5	40.45	4
5	CEN	RAD+RAD	—	Regen	—	—	—	0.0	—	—	—	—	0.0	
6	CEN+CEN	RAD+RAD	—	Regen	—	—	—	0.0	—	—	—	—	0.0	
7	CEN	RAD	—	Regen+Regen	4.2	6.0	7.0	4.0	7.3	6.25	9.0	5.5	38.41	7
7.5	VIGV+CEN	RAD	—	Regen+Regen	6.0	5.5	7.0	4.0	7.3	5.6	9.0	5.5	40.85	3
8	CEN	RAD	—	Recup	2.9	6.9	5.0	2.5	5.5	4.5	9.0	6.0	33.35	13
8.5	VIGV+CEN	RAD	—	Recup	4.7	6.4	5.0	2.5	5.5	4.1	9.0	6.0	35.85	9
9	CEN	RAD	—	—	0.0	—	—	—	—	—	—	—	0.0	
10	CEN	AX (ACC)	VPTN+AX	Regen	5.1	4.6	5.0	3.0	1.0	5.6	9.0	7.0	33.05	14
10.5	VIGV+CEN	AX (ACC)	VPTN+AX	Regen	5.2	4.25	5.0	3.0	5.5	4.9	9.0	7.0	33.50	12
11	CEN	AX (ACC)	AX	Regen	—	—	—	—	0.0	—	—	—	0.0	
12	CEN	AX+AX+AX		Regen	—	—	—	0.0	—	—	—	—	0.0	
13	CEN	AX VPTN+AX (ACC)		Regen	5.4	4.6	5.0	3.0	1.5	5.9	9.0	7.0	33.85	11
14	CEN	RAD (ACC)	VPTN+AX	Regen	—	—	—	—	0.0	—	—	—	0.0	
14.5	VIGV+CEN	RAD (ACC)	VPTN+AX	Regen	5.9	4.25	5.0	2.5	5.0	4.5	9.0	7.0	34.18	10
15	CEN	RAD (ACC)	AX	Regen	—	0.0	—	—	—	—	—	—	0.0	
16	CEN	RAD (ACC)	AX	I/C-R/H-Regen	—	0.0	—	—	—	—	—	—	0.0	

NOTE: See Appendix I for discussion of Ranking Criteria.

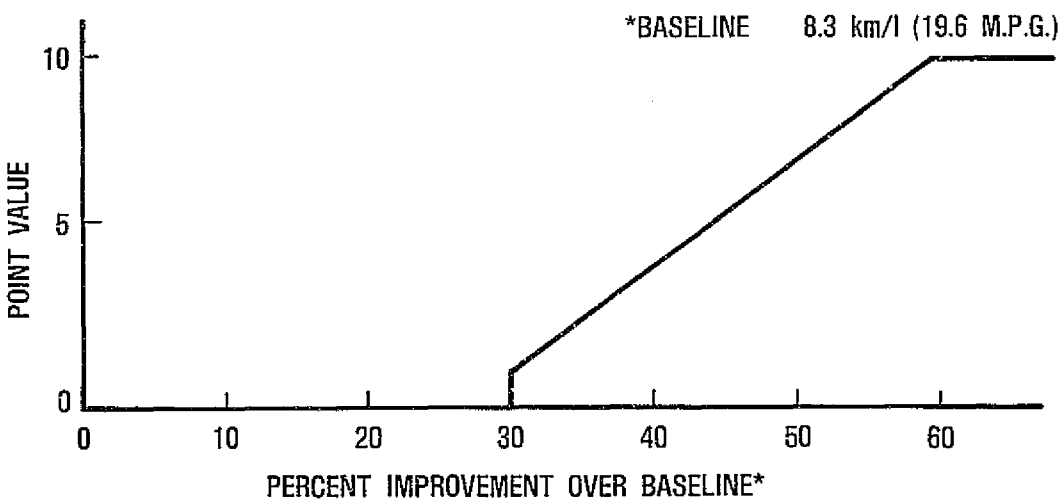


Figure 2.2 Fuel Economy Rating

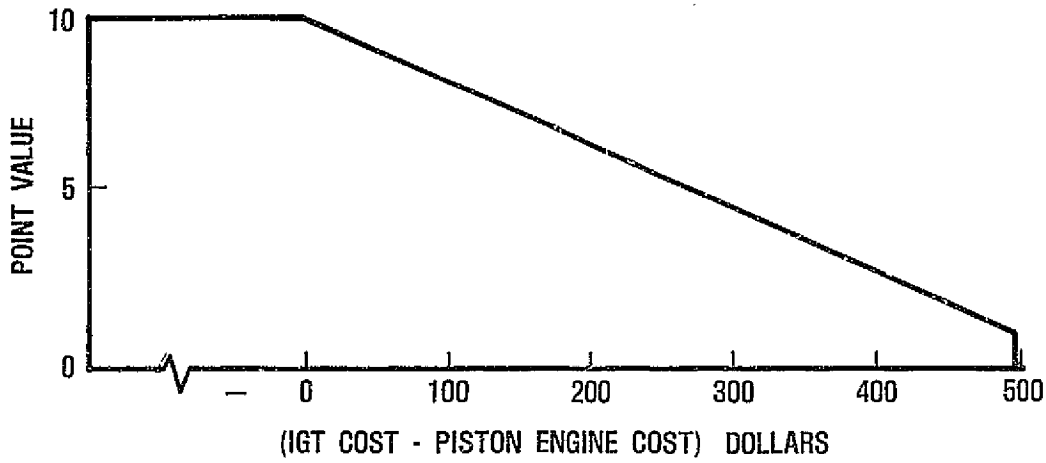


Figure 2.3 Engine Cost Rating

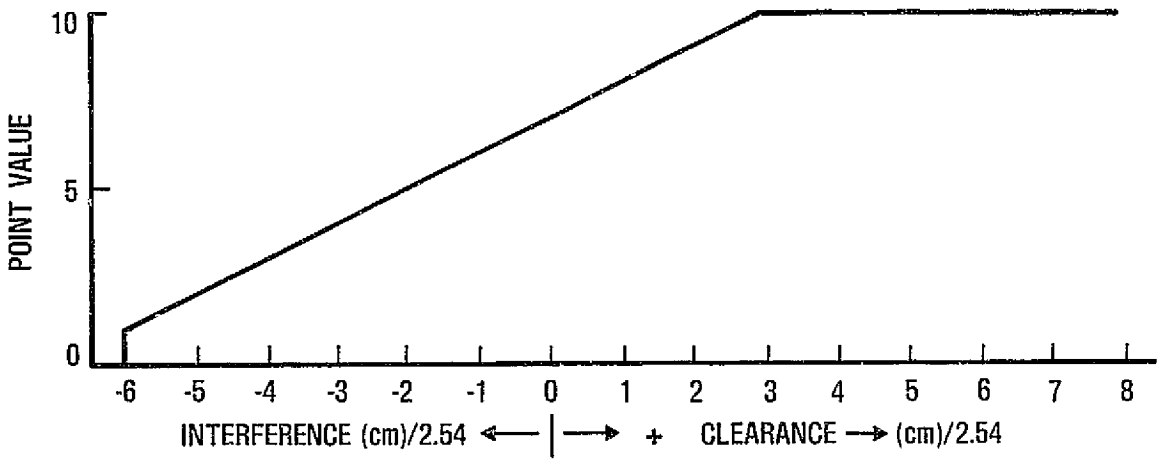


Figure 2.4 Engine Packageability Rating

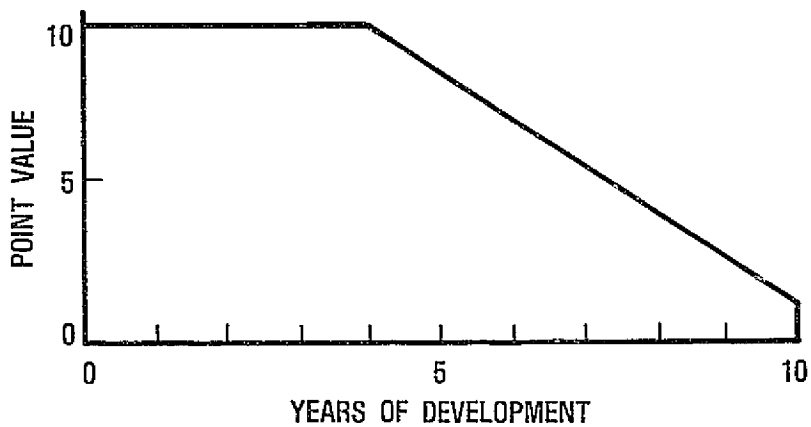


Figure 2.5 Technical Risk Rating

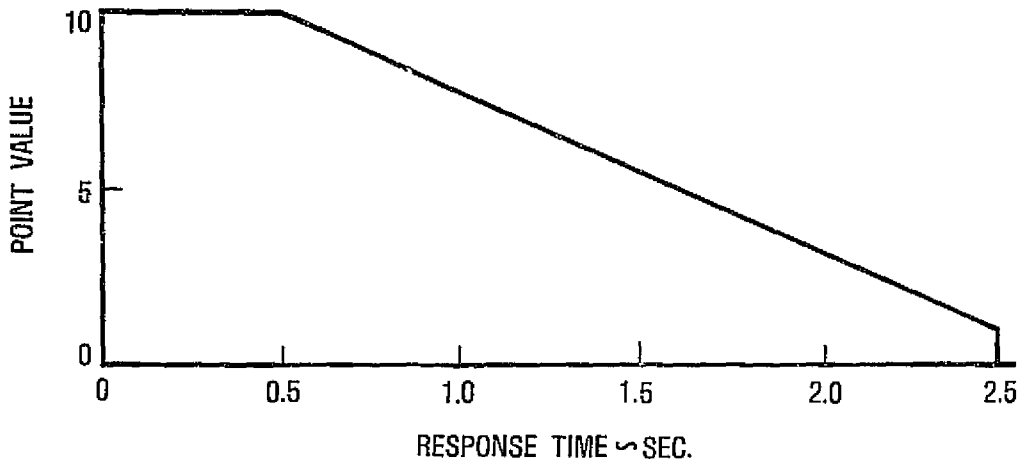


Figure 2.6 Engine Response Time Rating

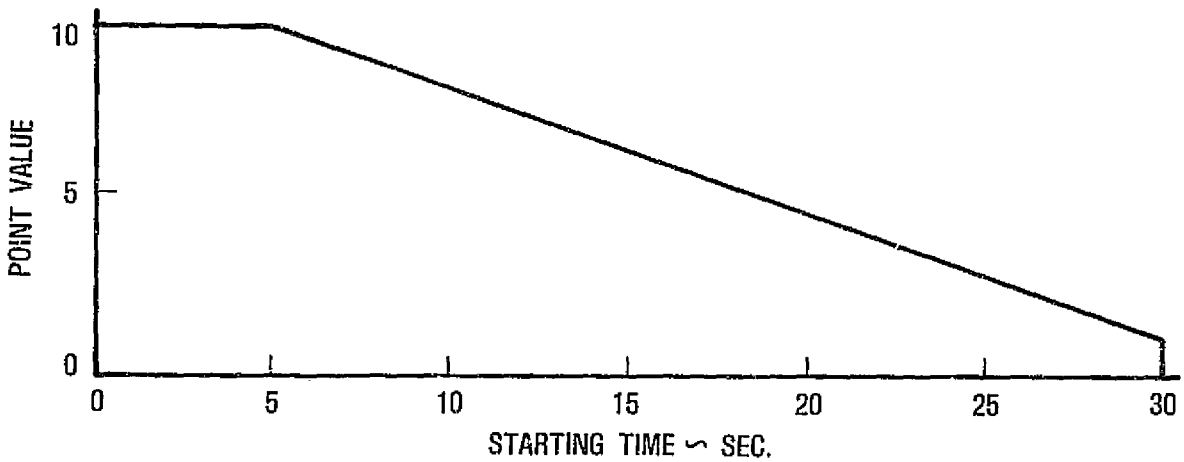


Figure 2.7 Engine Starting Time Rating

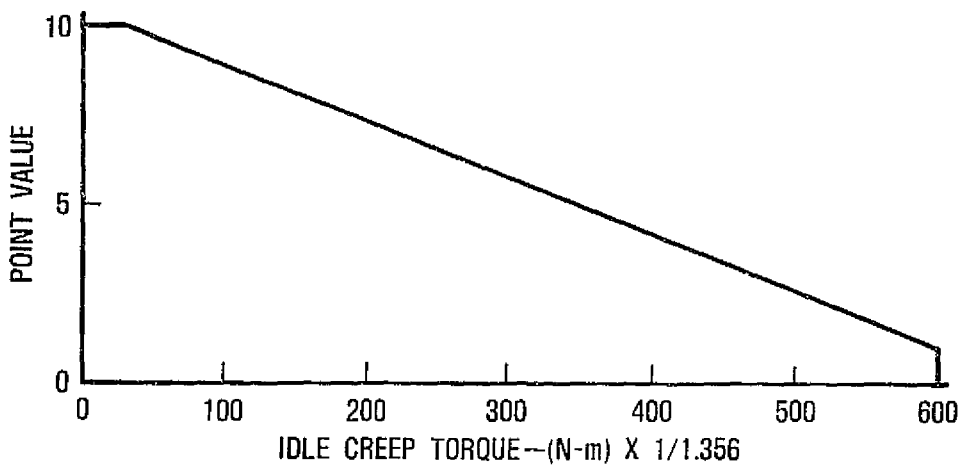


Figure 2.8 Idle Creep Torque Rating

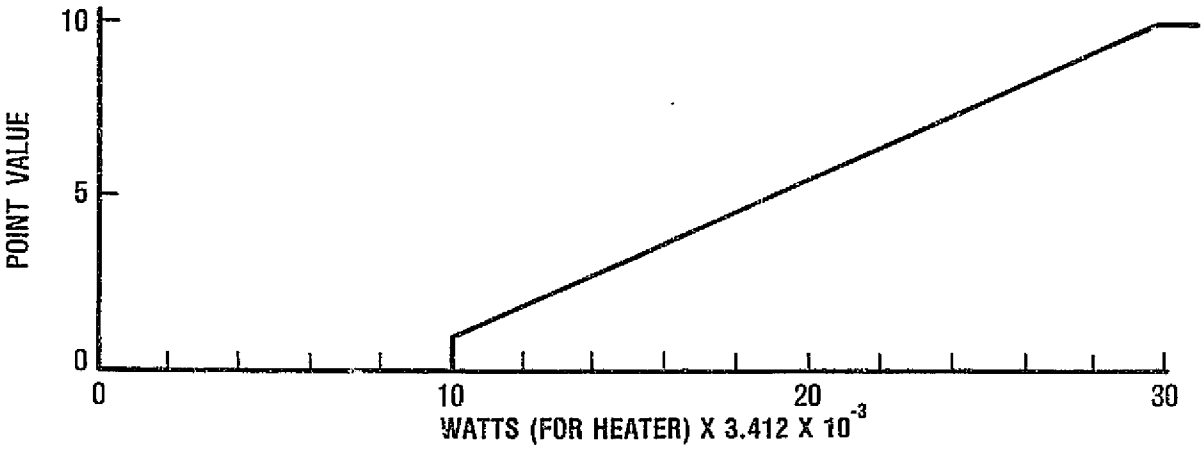


Figure 2.9 Vehicle Heater Rating

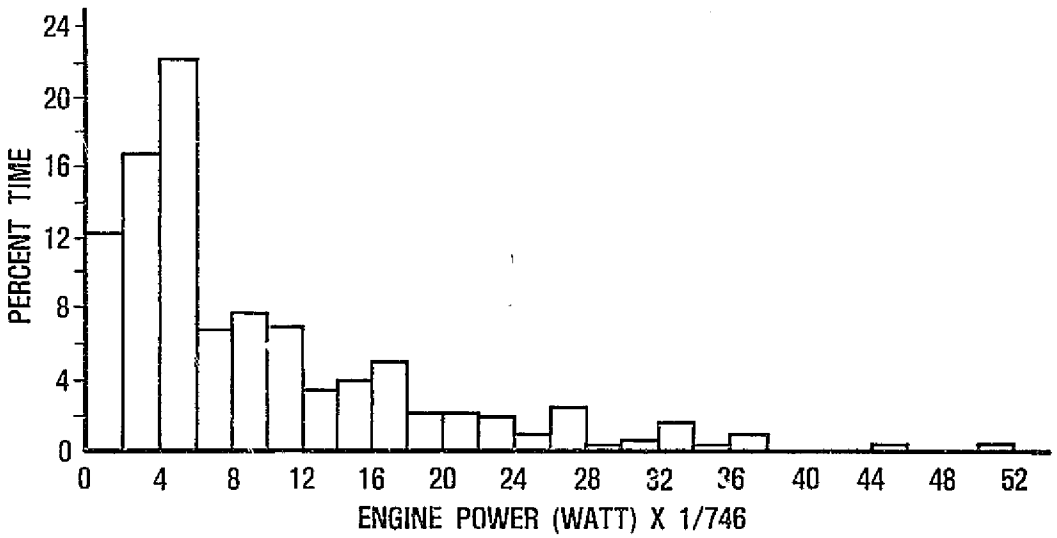


Figure 2.10 Engine Power, Time Distribution Over the Federal Urban Driving Cycle

2.4 Results

Table 2.2 presented the completed Concept Ranking Matrix, showing the criteria values assigned for all of the engine concepts and the resulting computed overall measure of effectiveness. Note that Concepts 5, 6, 9, 11, 12, 14, 15, and 16 were eliminated because of "no-go" entries for at least one ranking criterion. The concepts eliminated and the specific failed criteria are listed below in Table 2.3.

Concepts 5 and 6 failed because of the technical risks associated with the 2-stage radial turbine. This configuration would probably require a bearing between the stages of turbine, which would result in a complex structure to maintain that bearing.

Concept 9 would not provide the fuel economy required at low engine loads due to elimination of the heat exchanger.

Concept 11 would not have the capability of utilizing power available from the free turbine to accelerate the gas generator spool, consequently the gas generator response would suffer.

Concept 12 failed due to the technical risk and complexity of the system.

Concept 14 failed due to the high inertia of the gas generator radial turbine which would result in a poor engine response time.

Concepts 15 and 16 failed because the complexity of the engines would result in an expectedly high cost.

TABLE 2.3

Reasons for Eliminated Concepts

Concept No.	Criterion Failed	Reason
5	Risk	Questionable hot-end
6	Risk	Questionable hot-end
9	Economy	No heat recovery
11	Response	Free turbine lag
12	Risk	Complexity
14	Response	Free turbine lag
15	Cost	Complexity
16	Cost	Complexity

Table 2.4 presents the ranking of the concepts for clarity. The first nine concepts are single-shaft engines. The first four concepts are regenerated cycles with variable engine inlet guide vanes. It is interesting to note that the concepts ranked 5, 6, 7 and 8 are identical to those ranked 1, 2, 3, 4 except for the compressor VIGVs. Based on preliminary calculations, VIGVs on single-shaft concepts were credited with a substantial improvement in fuel economy over the Combined Federal Driving Cycle. This obviously was a factor in favor of VIGVs in rating the single-shaft concepts for economy. Compressor VIGVs on free turbines were not credited with a significant improvement in economy. These were, however, credited with an improvement in free turbine response times, as were variable power turbine nozzles (VPTN). Free turbines with axial gas generator turbines were rated with better response times than those with radial gas generator turbines.

TABLE 2.4

Concept Ranking Summary

Rank	Overall Measure of Effectiveness	Concept No.	Type	Comp/Turb	Heat Exch.	Engine Inlet VIGV
1	42.05	1.5	Single Shaft	CEN/RAD	Regen	Yes
2	41.65	3.5	Single Shaft	CEN/3 AX	Regen	Yes
3	40.85	7.5	Single Shaft	CEN/RAD	Dual Regen	Yes
4	40.45	4.5	Single Shaft	CEN/2 AX	Regen	Yes
5	39.61	1.0	Single Shaft	CEN/RAD	Regen	No
6	38.51	3.0	Single Shaft	CEN/3 AX	Regen	No
7	38.41	7.0	Single Shaft	CEN/RAD	Dual Regen	No
8	38.23	4.0	Single Shaft	CEN/2 AX	Regen	No
9	35.85	8.5	Single Shaft	CEN/RAD	Recup	Yes
10	34.18	14.5	Free Turbine	CEN/RAD/AX*	Regen	Yes
11	33.85	13.0	Free Turbine	CEN/AX/AX*†	Regen	No
12	33.5	10.5	Free Turbine	CEN/AX/AX*	Regen	Yes
13	33.35	8.0	Single Shaft	CEN/RAD	Recup	No
14	33.05	10.0	Free Turbine	CEN/AX/AX*	Regen	No

*VPTN on power turbine
†Accessories on power turbine (otherwise GGT)

2.5 Recommendations and Discussion

It was recommended that the following IGT engine concepts be carried forward: 1.5, 3.5, and 14.5.

The selection of Concepts 1.5 and 3.5 is obvious, since they rank first and second in Table 2.4. Concept 1.0 and 1.5 differ only by the deletion of compressor VIGVs. Since Reference 1 indicates that the complexity and cost of VIGVs may not be warranted if turbine inlet temperature is high enough, a thorough analysis of compressor VIGVs and their utility is recommended. It is also recommended that free-turbine concept 14.5 be "carried along" since: 1) this will provide a direct comparison with single-shaft concepts, and 2) it was the highest ranking free-turbine concepts in Table 2.4. The free-turbine concepts with variable turbine nozzles ranked high in fuel economy in all cases. These concepts were down-graded on cost, packageability and, in some cases, technical risk.

An option being left open at this time is the examination of recuperated concepts (8.0 and 8.5) should it be estimated that the ceramic recuperator risk can be decreased.

3.0 ESTABLISHMENT OF TECHNOLOGY PROJECTIONS

In order to accurately predict the performance of a future generation automobile, it is first necessary to predict the performance expected in the time frame of interest of each of the components within the powertrain. Performance predictions are based on current test data and extrapolations from that base using the designer's knowledge of probable technology improvements that will occur, such as, advanced computer modeling programs and new test and manufacturing techniques. By using these predictions in a cycle analysis it is possible to choose an optimum engine design for the desired time frame, in this case 1983.

3.1 Compressor

Shown in Figure 3.1 are predictions of the "design point," total-total, efficiencies of single stage centrifugal compressors for state-of-the-art cast and machined impellers. The state-of-the-art curves represent mean lines drawn through the data of test results of several existing designs, including production units. Also shown in Figure 3.1 are the 1983 performance predictions which reflect "expert opinion" regarding technology improvements that will be achieved in the next five years. The 1983 projection indicates that about 1.5 percentage point efficiency improvement is expected to be achieved at a pressure ratio of 5:1. These projections are basically for a 0.7 kg/s (1.5 pps) compressor size at optimum specific speed but, for the purposes of this study, the efficiency level was assumed to apply over an airflow range from 0.3 to 0.9 kg/s (0.7 to 2 pps.) However, it is recognized that the compressor losses would be expected to increase as the compressor size is reduced, consequently, for airflow rates lower than 0.7 kg/s (1.5 pps) the compressor efficiency may be somewhat optimistic. The effect on compressor efficiency of departure from the optimum specific speed is shown by the curve in Figure 3.2.

It is expected that compressor variable inlet guide vanes (VIGV) will only be used at engine idle speed i.e., when the power level is less than about 10 percent. Assuming properly designed VIGV's are located in a relatively low velocity region of the compressor inlet, no losses have been attributed to the VIGV's at the zero angle setting, at VIGV angles other than zero, the modifying effect on the compressor characteristics, based on test data, is given in Table 3.1.

Successful achievement of the 1983 technology level in compressors is predicated on an adequately funded R & D program which will explore new techniques, currently being developed and used by the aerodynamicist, to better understand the flow conditions within the centrifugal compressor. Isolation of losses within the flow field will lead to better designs of increased efficiency. Two important new tools that the aerodynamicist will have to analyze and test new designs are 3-D viscous flow computer models and the LDV (Laser Doppler Velocimeter) measurement system. Also, it is believed that with an adequate investment in high quantity production tooling, impellers may be manufactured from either casting or powdered metal processes of a quality equal to today's machined impellers.

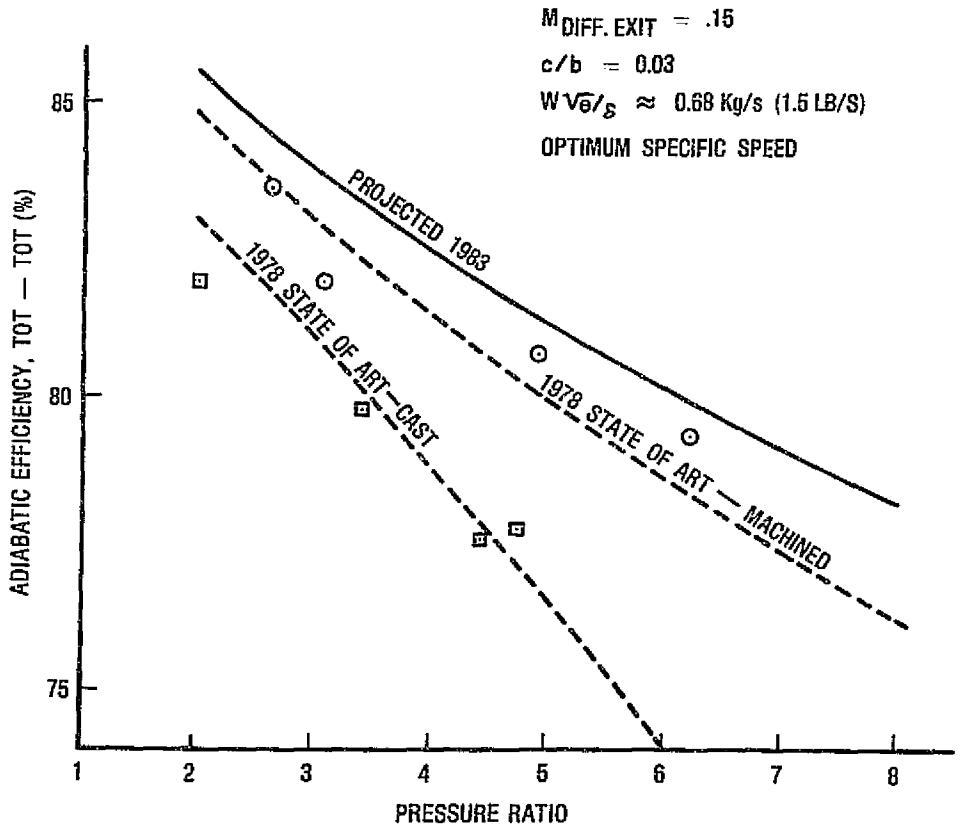


Figure 3.1 Single-Stage Centrifugal Compressor Efficiency Projections

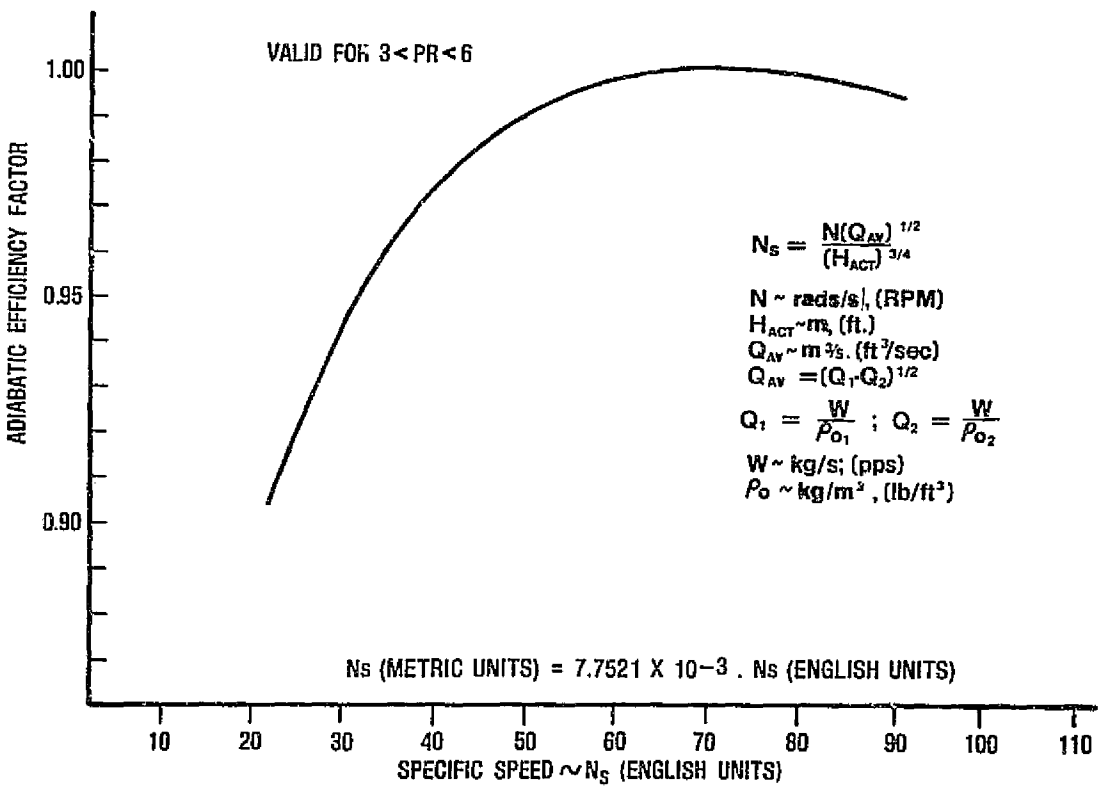


Figure 3.2 Adiabatic Efficiency Correction Factor vs. Specific Speed for Single-Stage Centrifugal Compressor

TABLE 3.1

Effect of VIGV's on Radial Compressor Characteristics

VIGV Angle β (Degs.)	Airflow Ratio $\frac{W_\beta}{W_{\beta o}}$	Pressure Ratio $\frac{R_\beta}{R_{\beta o}}$	Efficiency Ratio $\frac{\eta_\beta}{\eta_{\beta o}}$
−13	1.10	1.08	0.99
0	1.00	1.00	1.00
20	0.89	0.91	0.97
40	0.81	0.84	0.93
60	0.68	0.73	0.84
80	0.44	0.42	0.51
90	0.26	0.07	0.15

3.2 Turbines

The projections of radial and axial turbine, total-total, efficiencies for 1983 represent an optimistic look forward. However, a degree of optimism is justified because new analytical and test techniques are rapidly being developed and these new tools will give the turbine designer greater ability to understand the flow processes within a given turbine design and to optimize the design. The performance projections have in all cases been made starting with a firm base of actual test data from existing designs including production units.

3.2.1 AXIAL TURBINES

Figure 3.3 presents a correlation of axial turbine stage efficiency, on a total-to-total basis, as a function of the mean work coefficient. The 1978 technology curve is the maximum envelope of current test data from AiResearch turbines. Rating stations are from the stator inlet to the rotor exit. The efficiencies of the turbine are extrapolated to a zero rotor tip clearance condition and are representative of a machine Reynold's number of 4.23×10^5. The mean work coefficient is defined by the following equation:

$$\lambda_m = \frac{g \int \Delta H}{U_m^2 \; Z}$$

where ΔH = the actual enthalpy drop through the turbine
U_m = the mean rotor blade tip speed
Z = the number of stages

Corrections for other than zero tip clearance are made with the equation:

$$\eta_T = \eta_{TO} \left[1 - k \left(\frac{c}{h}\right) \frac{R_t}{R_m}\right]$$

where η_T = turbine efficiency with clearance

η_{TO} = turbine efficiency at zero clearance

k = 1 for shrouded blades

k = 2 for unshrouded blades

c = radial tip clearance

h = blade height

R_t = blade tip radius

R_m = blade mean radius

The effect of Reynold's number changes is estimated from the following relationship:

$$\frac{1 - \eta_T}{1 - \eta_{T_{REF}}} = 0.4 + 0.6 \left(\frac{Re}{Re_{REF}} \right)^{-0.18}$$

where

$\eta_{T_{REF}}$ = turbine efficiency at reference Reynold's number

Re = Reynold's number, defined as $\frac{W}{\mu R_m}$

Re_{REF} = reference Reynold's number, 4.23×10^5

W = flow rate

μ = dynamic viscosity

The 1983 technology projections were based on the demonstrated advanced technology AiResearch LART turbine program test results, see reference 4. An improvement in efficiency of about 1.3 percentage points over that obtained in the LART program was considered possible by 1983 through the application of the following techniques:

- Improved rotor design programs now being developed.
- Improved understanding of blade row interaction effects.
- Better understanding of the flow conditions at the blade tip clearance through advanced analytical tools for analyzing flow in that region.
- LDV (Laser Doppler Velocimeter) measurements during testing.

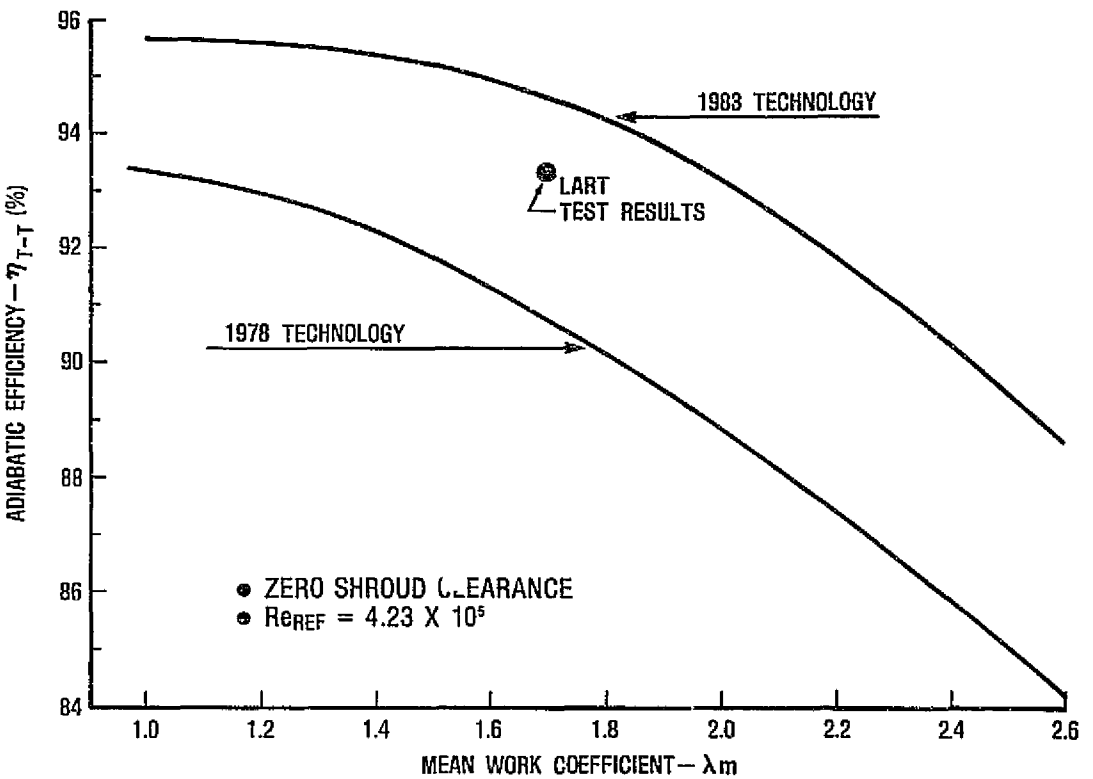


Figure 3.3 Axial Turbine Stage Efficiency Projections

Extrapolation of the 1983 technology curve of efficiency for work coefficients less than those of the LART turbine was accomplished by assuming a similar trend as that obtained from a plot of the peak efficiencies obtained from the commonly used Smith correlation of reference 5. At work coefficients greater than those of the LART turbine, the slope of the curve was made somewhat greater than that of the Smith correlation to reflect a more pronounced secondary flow effect.

A decrement of 3 points in efficiency was assigned to ceramic axial turbine projections to account for an estimated increased trailing edge blockage effect, which may be unavoidable, due to the likely requirement of more robust ceramic blades.

In the case of the free turbine engines, to account for the losses due to interstage ducting and variable geometry power turbine nozzles, a total pressure loss of 2 percent was assumed, see Table 3.3. For engine off-design performance calculations, complete characteristic maps of turbine performance were generated for a complete range of nozzle angles. Interpolation was done, as necessary, to match the desired turbine inlet temperature schedule.

3.2.2 RADIAL TURBINES

A correlation of stage work coefficient with efficiency for a radial turbine is presented in Figure 3.4. The stage work coefficient is defined by the equation:

$$\lambda_S = \frac{g\,J\,\Delta H}{U_T^2}$$

where:

U_T = turbine tip speed

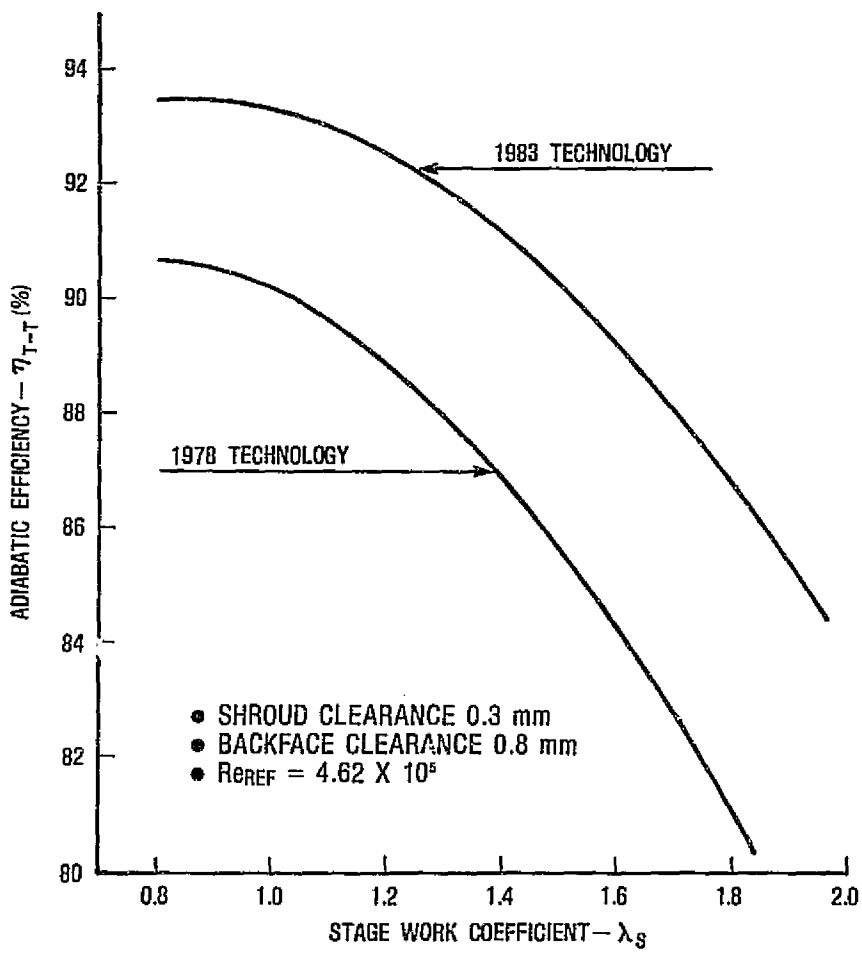


Figure 3.4 Radial Turbine Efficiency Projections

The efficiencies of the radial turbine are presented for a backface clearance of 0.8mm (0.030 in.) and 0.3mm (0.010 in.) clearance between the blade and shroud. The projection assumed that 14 full blades would be a sufficient quantity for the loading criteria. In the cycle analysis study the blade number was reduced to 11 for stress reasons; some proprietary data indicated that an across-the-board efficiency reduction of 1/4 percentage point was then necessary. The base Reynold's number for the efficiency projections of Figure 3.4 was 4.62×10^5 and Reynold's number corrections were estimated from the following relationship:

$$\frac{1 - \eta_T}{1 - \eta_{T_{REF}}} = 0.4 + 0.6\left(\frac{Re}{Re_{REF}}\right)^{-0.2}$$

where:

Re_{REF} = reference Reynold's number, 4.62×10^5

For radial turbines, the projections of efficiency at the 1983 technology level have been derived from an analytical loss model with inputs of predicted advancements in the areas of:

- reduced incidence losses through the use of advanced blading designs.
- reduced stator secondary flow losses due to endwall contouring.
- reduced shroud and backface clearances due to seal treatment.
- analytical and experimental techniques currently being developed, as described for axial turbines.

3.3 Heat Exchanger

A rotary ceramic regenerator is the heat exchanger system which was considered for this design study based on the concepts assessment analysis. The heat transfer and pressure drop through the core was calculated using the F & J (Fanning friction factor and Colburn Number for heat transfer) data shown in Table 3.2. This table shows two levels of technology for a ceramic core. State-of-the-art

TABLE 3.2

Regenerator Matrix F & J Data

Definition	Current Technology Level*	1983 Technology Level**
No. of Fins per Row per cm.	15.0	21.6
No. of Rows per cm.	13.6	12.0
No. of Openings per cm^2	203	259
Fin Thickness, mm.	0.061	0.089
Plate Thickness, mm.	0.061	0.089
Open Area Ratio	0.787	0.680
Hydraulic Diameter, mm.	0.58	0.46
Heat Transfer Surface Area per Unit, m^2/m^3	5423	5951
Fanning Friction Factor Constant, C_1	16.1	10.9
Reynold's No. Exponent for Fanning Friction Factor	−1.0	−1.0
Colburn No. Constant, C_2	3.94	3.93
Reynold's No. Exponent for the Colburn No.	−1.0	−1.0
Type of Fin [1=Triangle; 2=Rect]	1	1

* Corning, 2 sheet triangular matrix.
** Extruded triangular matrix.

technology, which is a wrapped, 2 sheet, triangular matrix configuration manufactured by Corning Glass Works, while the 1983 technology is projected to be an extruded triangular matrix of 0.089 mm (0.0035 ins.) wall thickness. The current technology core material would be typically an aluminum silicate (AS) or magnesium aluminum silicate (MAS) material which has been proven for many thousands of hours at 1000°C (1840°F) gas inlet temperature on engine test rigs. It is projected that the MAS material can be further developed to satisfactorily withstand gas inlet temperatures of 1100°C (2000°F) and this would be the material to be used for 1983 technology cores. Applying the F & J data and operating temperature limits to an engine, typical of the size expected from this design study, resulted in effectiveness and pressure loss characteristics as shown by Figure 3.5 and 3.6. These characteristics were used only for the preliminary cycle analysis and selection phase of the study. For detailed engine performance analysis, after the engine airflow and pressure ratio had been selected, the F & J data was used directly in the computer program to project off-design engine performance.

The probable trend of regenerator core seal leakage with engine design pressure ratio and airflow was calculated from the equation below. It was assumed that for an engine of typical expected size, a single regenerator core would be used and the ratio of airflow to core area would be constant and the same as that used in the effectiveness calculations above. Also, assumed in the equation is that leakage is basically due to flow underneath the seal and that the gap and seal width would remain constant.

$$\frac{W_L}{W} = K\sqrt{\frac{R.\,[R-1]}{W}}$$

where:

W_L = leakage flow

W = engine airflow

R = engine pressure ratio

K = constant

The constant K was derived for state-of-the-art seal technology, on the basis that 5 percent leakage in a 4 to 1 pressure ratio engine of design airflow equal to 0.45 kg/s (1 pps) per core was determined for the Ford 707 gas turbine engine. For 1983 seal technology it was assumed that this leakage can be reduced by half, based on some preliminary static rig test data.

The variation of seal leakage with design airflow and pressure ratio (see Figure 3.7.) was used only for the cycle analysis study. After selection of the engine, the total regenerator seal leakage was assumed to be a constant percentage over the range of engine operating speeds; this assumption is based on a correlation of engine test data with leakage estimates from a computer model.

3.4 Combustor

The combustor for the Improved Gas Turbine has to be a concept which will be capable of meeting the 0.41 HC gm/mile, 3.4 CO gm/mile, 0.4 NOX gm/mile Federal Emission Standards. Previous experience at Ford has indicated that a premix/prevaporizing, variable geometry type of combustor will be capable of meeting the emissions standards. Overall efficiency of a low emissions combustor was estimated to be 99.7%. The total pressure loss $\left(\frac{\Delta P}{P}\right)$, from the combustor plenum inlet to the turbine stator inlet, was estimated to be 3 percent. Both of these estimates were further assumed to be constant over the engine operating range, due to the variable geometry combustor characteristics, as demonstrated from some limited test data.

3.5 Duct Pressure Losses

The total pressure losses assumed through the engine ducting at the maximum horsepower ratings are tabulated below in Table 3.3 as percentages of the component inlet total pressure. For off-design calculations, it was assumed that these duct pressure losses vary according to the local flow parameter, $\left(\frac{W\sqrt{T}}{P}\right)^2$.

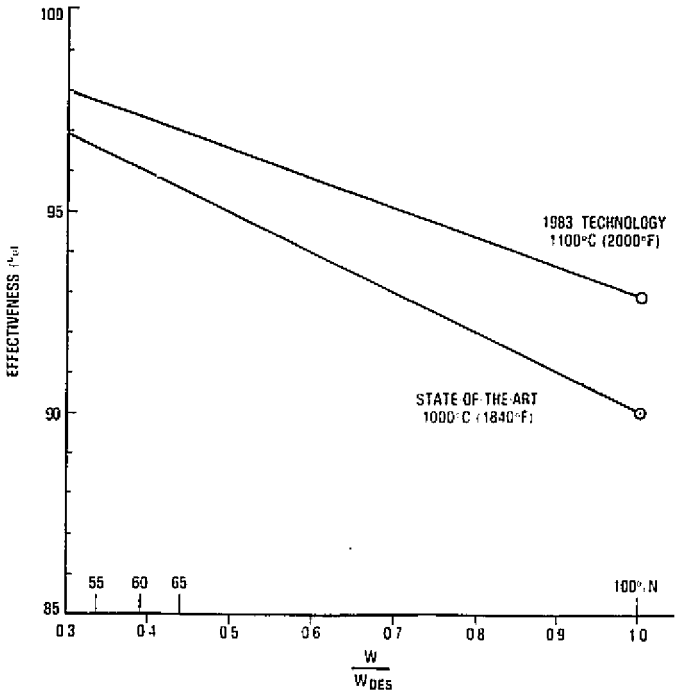


Figure 3.5 Typical Regenerator Effectiveness Variation

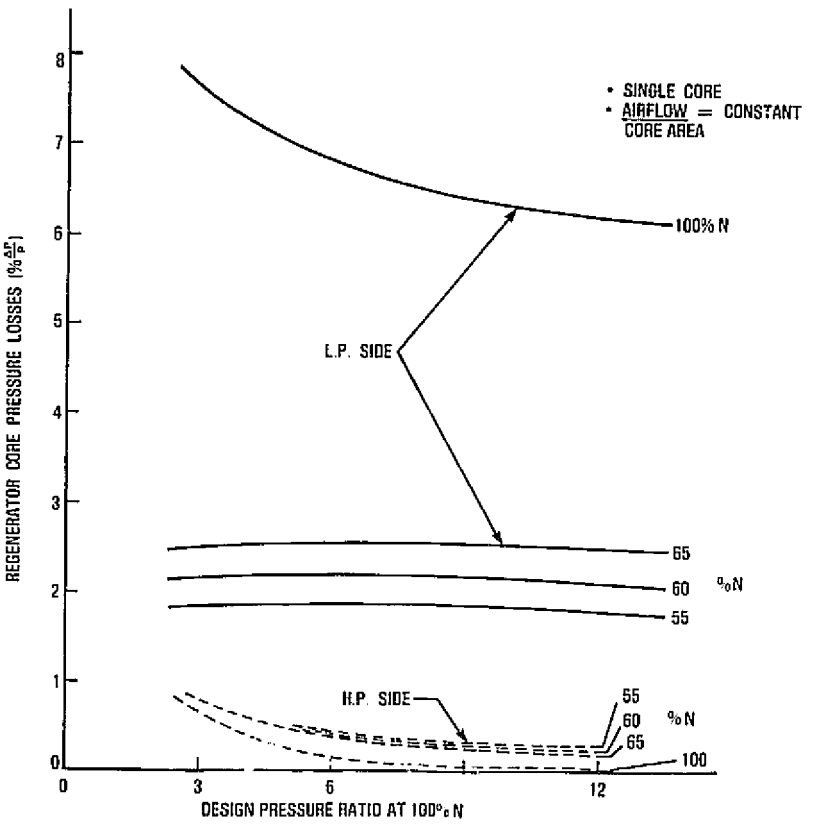


Figure 3.6 Typical Effect of Design Pressure Ratio on the Regenerator Core Pressure Losses at Different Percentage Engine Speeds

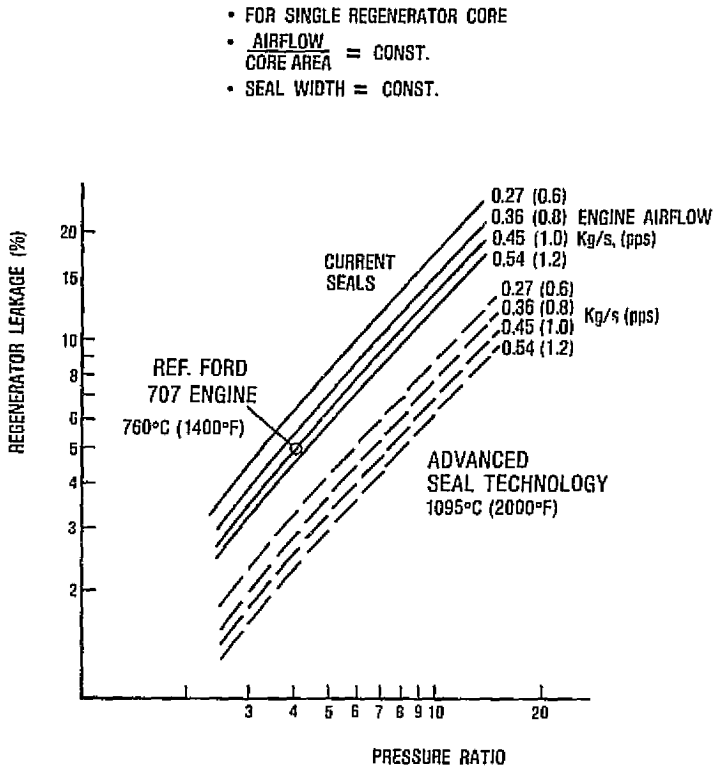


Figure 3.7 Typical Regenerator Seal Leakage Variation with Engine Design Pressure Ratio

TABLE 3.3

Engine Duct Pressure Losses

Component	Percentage Pressure Loss
Inlet Filter & Duct	1.0
Compressor Diffuser Discharge Loss	100% of the dynamic head, assuming Mach. no. of 0.15 at 100%N
Turbine Inlet Scroll (If Used)	1.0
Inter-turbine Duct, Incl. Variable Nozzle for Free Turbine Engine	2.0
Turbine Diffuser and Discharge Collector	36% of the dynamic head leaving the turbine rotor, assuming a Mach no. of 0.4 at 100%N
Exhaust Duct	2.0

3.6 Engine Leakages and Cooling Flow Rates

A total leakage to atmosphere of one percent of the compressor discharge air was assumed to take place at flanges, regenerator drive seals, labyrinth seals, etc. Additionally, half of one percent of the compressor discharge air was assumed to supply and cool the air bearing(s) assembly. The air bearing discharge was assumed to pass to the atmosphere.

It was assumed that metal radial turbines would be adaptable to low cost, simple cooling schemes and consequently they could be operated at temperature levels higher than for uncooled turbines. For obvious reasons, it is unlikely that an effective low cost cooling scheme could be derived for an axial metal turbine. No cooling air was considered necessary for ceramic axial or radial turbines. Table 3.4 below lists the assumed turbine cooling air rates and the associated maximum turbine inlet temperature. Note that significantly higher cooling air rates have been estimated for the free turbine machine with metal turbines due to the lower expansion ratio over the gasifier turbine.

TABLE 3.4

Estimated Turbine Cooling Airflow Rates

Configuration	Max. Turb. Inlet Temp. °C, (°F)	Cooling Airflow as Percent of Comp. Discharge Air
S.S. Engine		
• Metal Radial Turbine	1150, (2100) 1205, (2200)	1.25 2.00
• Metal Axial Turbine	1065, (1950)	0
• Ceramic Radial Turbine	1370, (2500)	0
• Ceramic Axial Turbine	1370, (2500)	0
F.T. Engine		
Metal Rad/Ax. Turbines	1205, (2200)	5
Ceramic Rad/Ax. Turbines	1370, (2500)	0

3.7 Accessory and Auxiliary Power Requirements

Auxiliaries are defined as the necessary requirements for operation of an installed engine such as, oil and fuel pumps, regenerator drive, alternator and an oil cooling fan. For performance and economy projections, the alternator is assumed to operate at half load. Table 3.5 lists the power absorbed by the auxiliaries as a function of engine speed and for reference purposes the alternator power at full load is also shown.

Accessories are defined as customer added requirements such as power steering and air conditioning. Accessories are assumed to be engine driven and the power absorbed is a function only of engine speed (or gas generator speed in the case of a multi-shaft machine). For performance and economy projections, the power steering is assumed to be set in the straight-ahead position and the air conditioner is switched off. Table 3.5 lists the power absorbed by the accessories and for reference purposes the air conditioner power at maximum load.

The total power absorbed by the combined accessories and auxiliaries, is also listed in Table 3.5, and this total has been used in the cycle performance analysis and all performance and economy projections.

TABLE 3.5

Accessories & Auxiliaries — Power Absorbed (kW)

	% N_E	100	90	80	70	60	50
Oil Pump (Engine Only)		0.19	0.16	0.13	0.10	0.07	0.05
Fuel Pump		0.15	0.13	0.12	0.10	0.09	0.07
Regenerator Drive		0.38	0.33	0.27	0.21	0.16	0.10
Alternator (40A-1/2 Load)		0.60	0.57	0.55	0.52	0.48	0.45
Oil Cooling Fan		0.11	0.09	0.07	0.05	0.04	0.03
Total		1.43	1.28	1.14	0.98	0.84	0.70
Alternator (40A-Full)		1.33	1.22	1.10	0.98	0.86	0.73
II. ACCESSORIES							
Power Str. (Str. Ahead)		0.32	0.29	0.25	0.22	0.19	0.15
A/C (Declutched)		0.19	0.17	0.15	0.13	0.11	0.10
Total		0.51	0.46	0.40	0.35	0.30	0.25
A/C (Full Load)		2.45	2.30	2.13	1.96	1.79	1.60
FOR PERFORMANCE & ECONOMY PROJECTIONS							
Total Accessories & Auxiliaries		1.94	1.74	1.54	1.33	1.14	0.95

Accessories & Auxiliaries — Power Absorbed (HP)

	% N_E	100	90	80	70	60	50
I. AUXILIARIES							
Oil Pump (Engine Only)		0.25	0.21	0.18	0.14	0.10	0.07
Fuel Pump		0.20	0.18	0.16	0.14	0.12	0.10
Regenerator Drive		0.51	0.44	0.36	0.28	0.21	0.13
Alternator (40A-1/2 Load)		0.80	0.77	0.74	0.70	0.65	0.60
Oil Cooling Fan		0.15	0.12	0.10	0.07	0.05	0.04
Total		1.91	1.72	1.54	1.33	1.13	0.94
Alternator (40A-Full)		1.78	1.63	1.48	1.32	1.15	0.98
II. ACCESSORIES							
Power Str. (Str. Ahead)		0.43	0.39	0.34	0.29	0.25	0.20
A/C (Declutched)		0.25	0.23	0.20	0.18	0.15	0.13
Total		0.68	0.62	0.54	0.47	0.40	0.33
A/C (Full Load)		3.29	3.08	2.86	2.63	2.40	2.15
FOR PERFORMANCE & ECONOMY PROJECTIONS							
Total Accessories & Auxiliaries		2.59	2.34	2.08	1.80	1.53	1.27

3.8 Bearing Losses

In order to estimate the bearing losses for the rotor of a single shaft engine, a particular bearing system was assumed.

The rotor was supported on a single full cylindrical gas bearing between turbine and compressor with the gear end located by the planet gears of a planetary gear unit.

Rotor thrust was taken by a tapered land oil lubricated thrust bearing with the thrust load minimized by balancing gas loading against helical gear thrust.

The assumed spool bearing losses are shown in Figure 3.8 for a no-load and design (or maximum) load condition. The losses at any given speed and load are found by interpolation.

3.9 Reduction Gearbox Losses

The reduction gear losses were expressed as power loss as a function of horsepower transmitted at a percentage of design speed (N) by the following equation.

$$HP_{loss} = \frac{HP}{HP_{max}} + 1.75 - \left[1 - \left(\frac{\%N}{100}\right)\right]$$

This corresponds to a maximum efficiency of 97.25 percent for a 75 kW (100 HP) unit, and assumes two to three gear meshes at a mesh loss of .75 to 1.12 percent and a total bearing loss of .5 percent at 100 percent power.

The equation permits the calculation of power loss at any reasonable combination of input power and speed.

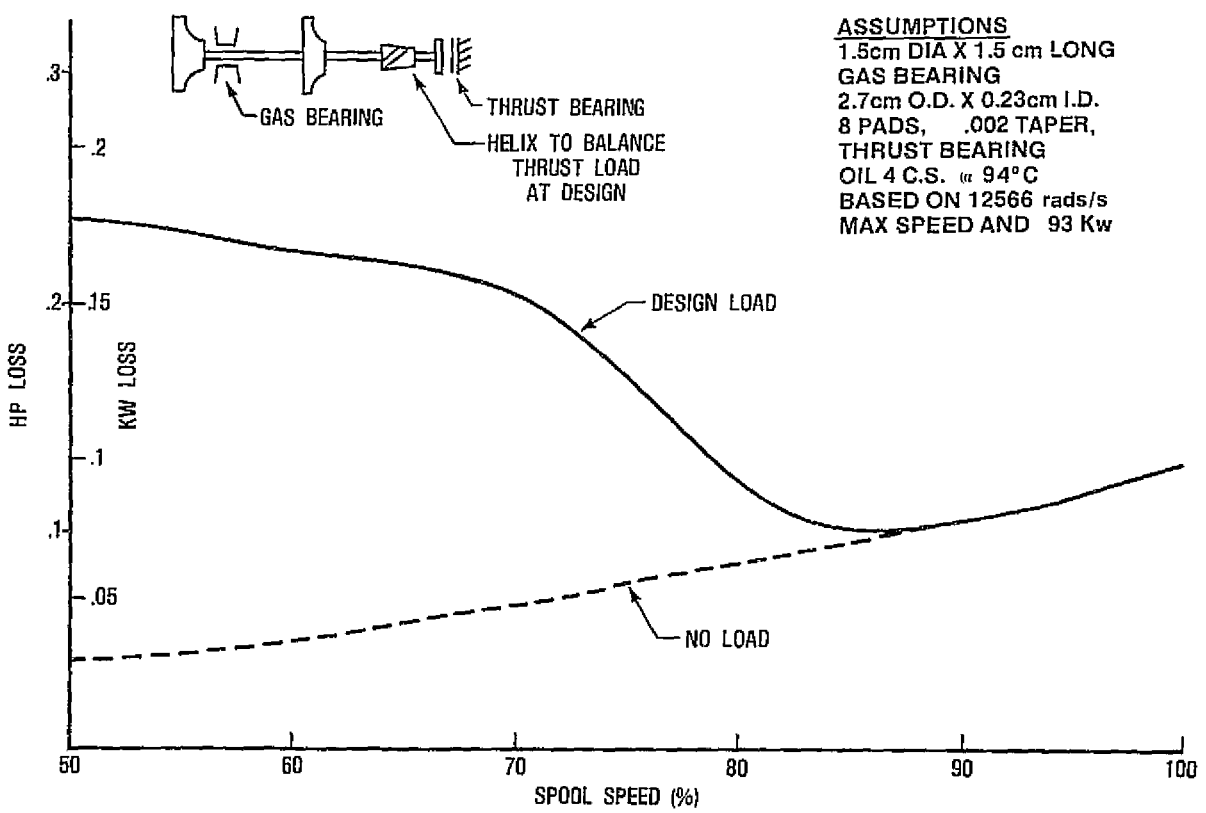


Figure 3.8 Estimate of Spool Bearing Losses

3.10 Material Strength Limitations

3.10.1 CERAMICS

The IGT engine is projected to operate at turbine inlet temperatures of 1370°C (2500°F) and higher. Since air cooling of components is undersirable, on account of penalties in efficiency and cost, the entire hot flow-path of the engine will be constructed of refractory ceramics. Silicon Carbide (SiC) and Silicon Nitride (Si_3N_4) ceramics are considered prime candidates for turbine rotors and stationary structures that will be exposed to peak cycle temperature. Both of these materials in their various forms have seen considerable development in rig or engine testing. For structures, which will operate at somewhat lower temperatures 1000-1100°C (1840-2000°F) but will require insulating properties, to minimize heat losses, Lithium Aluminum Silicate (LAS) and Magnesium Aluminum Silicate (MAS) oxide ceramics will be considered.

Strength of ceramics is customarily presented in terms of statistical Weibull parameters: the characteristic strength (S_θ) which corresponds to a failure rate of 63.7% and the shape parameter or the slope (m) which is a measure of scatter in strength properties. Because strength of ceramics is dependent on size and, as in the case of hot pressed Si_3N_4 (HPSN) at elevated temperatures, on the stress-rate, the strength levels are referenced to the geometry and loading mode of the test specimen and to the rate at which the specimen was loaded to fracture. The values quoted in this report, unless otherwise stated, are point estimates (50% confidence level) based on a 3.2 x 6.4 x 19mm Modulus of Rupture (MOR) test bar in 4-point bending, 1/4-point loading (inner span of 9.5mm) and were obtained at a standard crosshead speed of 0.5 mm/min. (approx. 2200 MPa/min.).

Strength data for ceramic materials that are candidate for the IGT engine are summarized in Table 3.6 along with the data source. Two levels of Weibull strength parameters (S_θ and m) are shown: the current, 1978 levels as reported by the various sources and the 1983 technology levels projected by the same sources as being attainable with adaquate R & D funding.

The differences in the 1978 strength levels reported by Ford and AiResearch for Norton Company's HPSN (NC-132) lie in specimen preparation. AiResearch specimens were ground transversely and were oxidized prior to test, while Ford specimen were ground longitudinally and were tested in the virgin state. It is projected that NC-132 will not be the optimum material by 1983 and that a material with thermal and physical properties similar to NC-132 but with improved strength parameters, as quoted in Table 3.6, and net shape capability by a hot isostatic pressing (HIP) process will be available.

The values shown represent statistical strength levels attainable in MOR bars. It is projected that with appropriate quality control and R & D funding these levels will be attained by 1983 in finished engine components and are, therefore, assumed in this study to represent design limits of strength for the candidate ceramic materials.

3.10.2 METALS

It is well recognized that the development of a ceramic turbine rotor to the levels of cost and quality required of mass produced automotive components, is still a few years away. Considerable rig and engine development can, however, be accomplished in the interim with a metallic rotor operating at lower inlet temperature. Also, prior studies conducted at Ford have shown that an engine operating at turbine inlet temperatures of 1150-1205°C (2100-2200°F) represents an attractive interim IGT candidate and that these temperatures were attainable with moderately cooled radial inflow rotors. For this reason candidate materials for the metallic version are included in the projections. Table 3.7 shows strength limits of superalloys that are currently available and for those projected to be available in 1983. The average values (failure rate of 50%) of 100 hr. stress rupture (S_R), ultimate strength (S_U) and the 0.2% offset yield (S_Y) and elongation (EL) are shown in Table 3.7 as a function of temperature. Because of funding and time limitations, the evaluation of the mechanical integrity of critical engine components will be limited in this study to steady state loadings in which case the yield and stress rupture or creep criteria suffice. The average life of an automotive engine is estimated at approximately 3000 hrs. Since less than 3% of this life will be spent at near full power condition, a 100 hrs.

TABLE 3.6

Ceramics Technology Projections — Material Strength

Assumptions: 1983 Projections assume an adquate R & D funding. All values of Weibull parameters are point estimates, i.e. 50% confidence limits obtained at standard crosshead speed of 0.5 mm/min. which corresponds to a stress rate of approx. 2200 MPa/min. Test specimen: MOR bar 3.20 mm x 6.40 mm x 19.00 mm in 4-point, 1/4 point loading (inner span 9.50 mm).

Material	Source	Temp. (°C)	1978 Techn. S_θ (MPa)	1978 Techn. m	1983 Techn. S_θ (MPa)	1983 Techn. m
Hot Pressed Silicon Nitride	(Ford)	RT	876	11.4	—	—
		850	720	16.9	—	—
		1200	710	23.0	—	—
		1370	372	25.8	—	—
	(AiResearch)	RT	669	12	938	15
		600	662	—	—	—
		800	648	—	938	
		1100	517	—	724	
		1200	441	16	—	—
		1370	—	—	579	—
Reaction Bonded Silicon Nitride	(Ford 2.8 g/cc)	RT-1370	310	8	345	10-12
	(Ford 2.9 g/cc)	RT-1370	—	—	414	10-12
	(AiResearch)	RT	276	6-8	331-372	10
		600	345	—	407	—
		1000	373	—	427	—
		1200	407	—	441	—
		1370	427	—	41	—
Pressureless Sintered Silicon Nitride	(Ford)	RT-1370	—	—	552-621	10-12
	(GTE)	RT	552	—	—	—
	(MOR 6.40 m x 3.20 mm x 38.10 mm)	1100	483	—	—	—
		1300	358	—	—	—
	(AiResearch)	RT	448	—	690	—
	(MOR 6.40 mm x 3.20 mm x 38.10 mm)	1150	—	—	621	—
		1250	238	—	550	—
		1370	—	—	483	—
Reaction Bonded Silicon Carbide	(Ford)	RT-1200	345	6	690	12
		1370	207	—	345-414	—
Sintered Silicon Carbide	(Carborundum)	RT	455	8-12	621	15
		1000	—	—	636	—
		1200	>455	—	—	—
		1370	—	—	690	—
Lithium-Aluminum Silicate	(Corning)	RT-980	87	11.5	—	—

stress rupture criterion at full power condition is deemed to represent a realistic goal for the IGT engine components.

The data in Table 3.7 has been supplemented for future reference with limited LCF data expressed as total strain, elastic plus plastic, ϵ_T. The LCF data will be used in the follow-up design phase of the program in evaluating mechanical integrity of components under transient loading conditions.

Included also in Table 3.7 are three aluminum alloys that are being considered for the compressor rotor, the only heavily stressed metallic component besides the turbine rotor.

3.11 Transmission Concepts

3.11.1 INTRODUCTION

The results of transmission concepts analysis are presented in this section. A total of 19 candidate transmission concepts were compared and ranked as an objective of this study. Three of the concepts were for use with two shaft engines and the remaining sixteen were for single shaft engine use.

The candidate concepts are illustrated schematically in Figures 3.9 through 3.27 and the full power efficiency characteristics across the transmission speed ratio range for each concept are represented by Figures 3.9(a) through 3.27(a). The efficiency calculations for the fixed and variable stator torque converters, the automatic transmissions, and gear mesh losses were based on known Ford test data. Data for the traction drive roller elements was based on information in reference 6. Hydrostatic pump and motor characteristics were based on information in reference 7. The characteristics for variable belt drive units was obtained from reference 1.

The ranking criteria of Appendix II were applied to all the concepts by the rating determination factors of Appendix III to form a Decision Matrix, shown completed in Table 3.8.

3.11.2 CONCEPTS

The transmission concepts are briefly described and discussed in this section. Full power average transmission efficiencies are shown beneath each concept number and this measure of efficiency has been used as an approximation for preliminary screening of the concepts. As can be seen from the Transmission Concept Ranking Matrix of Table 3.8, the full power average efficiency accounts for a maximum of 20 percent of the total rating points.

At 100 percent engine power input to the transmission full power average efficiency is best defined by the equation below:

$$\overline{\eta} = \frac{\int_{\left(\frac{N_O}{N_I}\right)_{MIN}}^{\left(\frac{N_O}{N_I}\right)_{MAX}} \eta \cdot d\left(\frac{N_O}{N_I}\right)}{\left[\left(\frac{N_O}{N_I}\right)_{MAX} - \left(\frac{N_O}{N_I}\right)_{MIN}\right]}$$

Concept 1 Figure 3.9 (49.8%)

Ford C4 Transmission with Ford Fixed Stator Torque Converter (3 speed production automatic transmission). In Figure 3.9(a) the efficiency at 100% power is defined as available output power from this transmission and single shaft engine combination, divided by the maximum horsepower capability of the engine. The transmission is actually more efficient than this power ratio efficiency, however, due to the fixed capacity of the fixed stator torque converter at various speed ratios, the converter cannot transmit maximum engine power for more than one converter speed ratio.

The solid line on the inset in Figure 3.9(a), represents engine power as a function of engine speed. The dotted lines represent converter capacity at various speed ratios as a

TABLE 3.7

Metals Technology Projections — Material Strength
Data Shown Are Estimated Average Values

1978 Technology

Material (Source)	T (°C)	(S_R) 100 Hr. (MPa)	(S_Y) (MPa)	(S_U) (MPa)	% EL	LCF — ϵ_T Cycles 500	1,000	10,000
Aluminum Alloy	RT	—	393	434	5.6	1.65	1.35	0.70
206-T7	50	—	388	419	7.0	—	—	—
(AiResearch)	100	—	372	394	11.3	—	—	—
	150	345	345	360	13.5	—	—	—
	200	186	300	318	12.6	—	—	—
	300	97	190	264	12.8	—	—	—
Aluminum Alloy	RT	—	203	225	4.0	0.61	0.50	0.26
356-T6	50	—	200	225	4.0	—	—	—
(AiResearch)	100	—	194	224	4.0	—	—	—
	150	79	162	207	4.0	—	—	—
	200	61	138	184	4.0	—	—	—
	300	44	83	107	8.0	—	—	—
Superalloy	RT	—	807	883	5.5	1.6	1.1	.71
MAR-M-247	450	—	756	868	7.2	1.3	0.9	0.69
Equiaxed	600	—	706	796	6.9	1.2	0.8	.57
(AiResearch)	750	703	—	—	—	—	—	—
	850	577	—	—	—	—	—	—
	1000	126	—	—	—	—	—	—
Superalloy	RT		848	1014	9.0	—	—	—
IN-100	750	669	877	1099	6.5	—	—	—
(In't.	800	503	814	993	6.0	—	—	—
Nickel)	950	217	495	732	6.0	—	—	—
	1000	129	—	—	—	—	—	—
	1050	91	277	435	6.0	—	—	—

1983 Technology

Aluminum Alloy	RT	—	503	586	15.3	—	—	—
PM AL	150	—	441	483	36.9	—	—	—
MA 87	200	—	386	434	34.4	—	—	—
(AiResearch)	250	248	—	—	—	—	—	—
	300	—	241	359	35.0	—	—	—
	350	110	—	—	—	—	—	—
		Single Crystal MAR-M-247 (Blades)	Powdered Metal Astroloy (Hub)					
Dual Alloy	RT	—	1034	1455	21.0	1.4	1.3	0.9
Turbine Rotor	750	703	878	1054	12.0	—	—	—
(AiResearch)	850	577	—	—	—	—	—	—
	1000	126	—	—	—	—	—	—

function of engine speed or converter input speed. The end point on the solid maximum engine temperature line at the right, represents the maximum engine power point. The converter speed ratio lines pass through this point at only a speed ratio of zero or the converter stall point. At other converter speed ratios the engine power must be reduced to match the converter input power capability. This is essentially the reason why a variable stator or variable capacity torque converter is required as opposed to a fixed capacity converter.

For this analysis it was decided to express efficiency as a power ratio for this concept, to indicate that only a relatively small percentage of engine power is available due to the lack of a variable capacity converter.

Concept 2 Figure 3.10 (71.6%) Ford C4 Transmission with Ford Variable Stator Torque Converter (3 speed production automatic fitted with a new VSTC). Figure 3.10(a) indicates that this is a relatively efficient transmission and is used as the base transmission for these efficiency comparisons.

Concept 3 Figure 3.11 (76%) Ford FIOD Transmission modified with a Ford Variable Stator Torque Converter (4 speed production automatic fitted with a new VSTC). This transmission is 4.4% more efficient than the base and provides 15% more power for acceleration at low gear ratios due to the presence of the fourth gear, refer to Figure 3.11(a).

Concept 4 Figure 3.12 (74.6%) Split Power using a Ford Variable Stator Torque Converter with Ford C4 Transmission. As shown in Figure 3.12(a), this transmission has peak efficiencies 7% higher than the base but requires an additional gear change following the converter to obtain sufficient ratio overlap. A slip clutch is also required.

Concept 5 Figure 3.13 (70.9%) Differential Split Power using a Ford Variable Stator Torque Converter and Ford C4 Transmission W/O Torque Converter but with Slip Clutch. This transmission utilizes a differential reduction gear to minimize the power going through the torque converter. Although peak efficiencies are 8% higher than the base, the rapid fall off in efficiency illustrated in Fig. 3.13(a) results in a net loss in average efficiency of .7%.

Concept 6 Figure 3.14 (76.1%) Differential Split Power using a Ford Variable Stator Torque Converter and Ford FIOD Transmission W/O Torque Converter with Shaft Lock-Up and Slip Clutch. This transmission utilizes a differential reduction gear to minimize power going through the torque converter. Peak efficiencies 10% higher than the base are obtained as illustrated in Figure 3.14(a). The use of both a reversing bevel set after the differential reduction gear and a slip clutch reduces the attractiveness of this transmission.

Concept 7 Figure 3.15 (72.7%) Inline Variable Speed Traction Drive and Ford C4 Transmission with Fixed Stator Torque Converter. This concept is not viable since the variable speed traction unit must handle 100% engine power. Also, although the average efficiency is 1% higher than the base due to a large ratio range, the peak efficiencies are 3% lower than the base, due to the traction drive and torque converter being in series, refer to Figure 3.15(a).

Concept 8 Figure 3.16 (82%) Regenerative Variable Speed Traction Drive with 3 Mode Transmission and Slip Clutch. Although the average efficiency of this transmission is 10.4% greater than the base, refer to Figure 3.16(a), the concept loses its attractiveness when it is realized that the variable traction unit regenerates up to 100% of the engine power, which indicates a relatively large traction unit.

Concept 9 Figure 3.17 (79.3%) Differential Split Power using a Variable Speed Traction Drive with a Ford C4 Transmission and a Ford Fixed Stator Torque Converter. See concept 10.

Concept 10 Figure 3.18 (84.2%) Differential Split Power using a Variable Speed Traction Drive with a Ford FIOD Transmission and a Ford Fixed Stator Torque Converter. Both these concepts (9 and 10) use a differential reduction gear to limit the power going through the variable traction unit

from 17% to 33% of the maximum engine power. This results in a relatively small high efficiency traction unit. The use of this unique combined reduction gear and traction unit permits the use of production automatic fixed stator torque converter transmissions with single shaft turbine engines. The unproven durability of even a small variable speed traction drive is the main drawback to these concepts.

Concept 11 Figure 3.19 (84.2%) Differential Split Power using a Variable Speed Traction Drive with a Ford FIOD Transmission without Torque Converter, with Slip Clutch and Shaft Lock-Up. This transmission has peak efficiencies 11% higher than the base and has 21% more power available for acceleration at low gear ratios, refer to Figure 3.19(a). Non-optimum gear ratios and the use of a slip clutch remain negative factors. Although this concept may be ideal for evaluating the differential traction device.

Concept 12 Figure 3.20 (84.9%) Differential Split Power using a Variable Speed Traction Drive with a Three Mode Transmission. See concept 13.

Concept 13 Figure 3.21 (88.5%) Differential Split Power using a Variable Speed Traction Drive with a Four Mode Transmission. Both concepts (12 and 13) use the combined reduction gear and small variable traction differential unit in combination with three or four mode optimum ratio gear boxes and a slip clutch for vehicle startup. The four mode transmission which has an average efficiency 17% higher than the base, refer to Figure 3.21(a) and 52% more power available for acceleration at low speeds, probably represents the best transmission for a single shaft engine, if a small 31 kW (40 HP) traction drive can be developed and proven reliable.

Concept 14 Figure 3.22 (91.2%) Two Mode Differential Split Power using a Variable Speed Traction Drive with a Three Mode Transmission i.e. Six Mode. This transmission should operate at close to 22% efficiency at full power and represents close to an ideal transmission for a single shaft engine, refer to Figure 3.22(a). It is complicated due to a two-mode or shift provision in the differential traction unit. This is a completely new transmission concept and requires at least a 10 year program to determine production feasibility, durability, and reliability.

Concept 15 Figure 3.23 (86.1%) Hydromechanical Tri-Mode Transmission. This is a split power hydro-mechanical transmission which although of high efficiency, 14.5% higher than base, see Figure 3.23(a), is risky due to suspected durability and noise problems.

Concept 16 Figure 3.24 (84.6%) Variable Belt Drive with Variable Stator Torque Converter and 2 Speed Transmission. Relatively high efficiency transmission, 13% higher than base, refer to Figure 3.24(a), appears very costly, and requires belt drive that can handle 100% engine power.

Transmissions for two-shaft engines, i.e. free power turbine with variable power turbine nozzles, were considered next in the study. The power turbine section was considered part of the transmission with a fixed loss of 4.8% at 100% power and a 2:1 stall torque ratio for efficiency purposes.

Concept 17 Figure 3.25 (76.5%) and Concept 18 Figure 3.26 (74.5%) Free Power Turbine with Ford C4 Transmission and with (Concept 17) and without (Concept 18) a Ford Fixed Stator Torque Converter. The combination without torque converter was 6.7% higher in average efficiency than the base, but the combination with torque converter provided 10% more power for acceleration at low speeds than the non-torque converter, refer to Figure 3.26(a). Both of these combinations have been used extensively for passenger car turbine development.

Concept 19 Figure 3.27 (78.6%) Free Power Turbine with Ford FIOD Transmission and Fixed Stator Ford Torque Converter. Average 7% more efficient than base and 24% more power available for acceleration due to presence of fourth gear, refer to Figure 3.27(a).

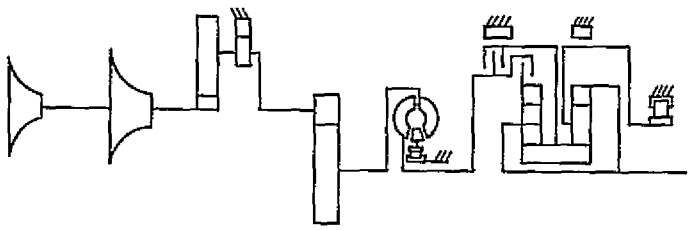


Figure 3.9 Concept 1. Ford C-4 Transmission

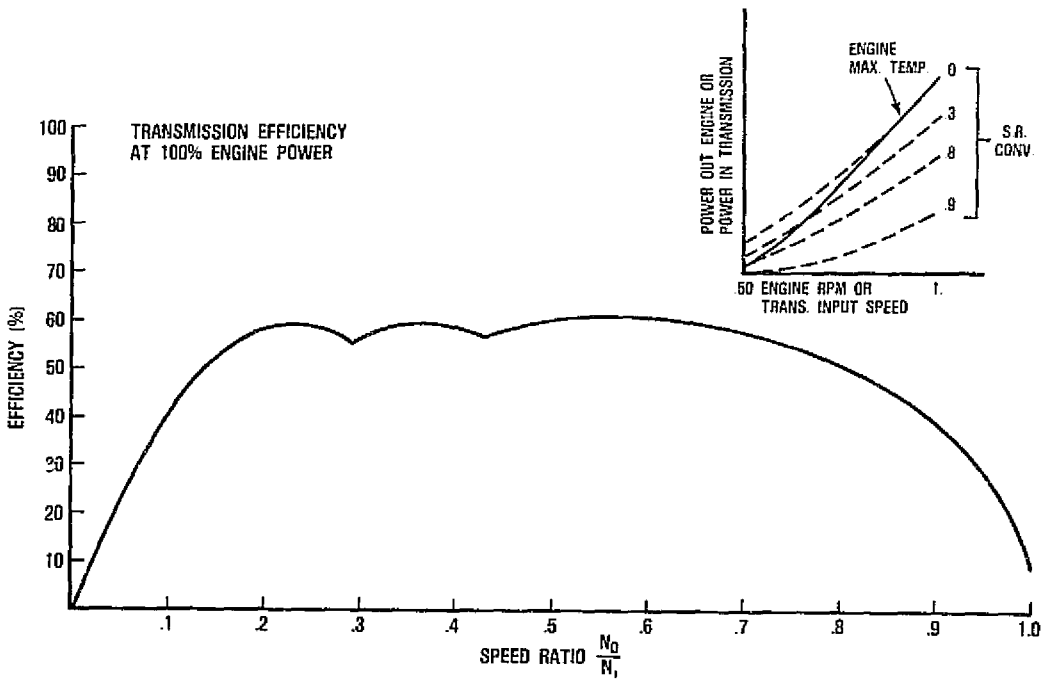


Figure 3.9(a) Efficiency of Concept 1 at 100% Input Power with Single-Shaft Turbine Engine

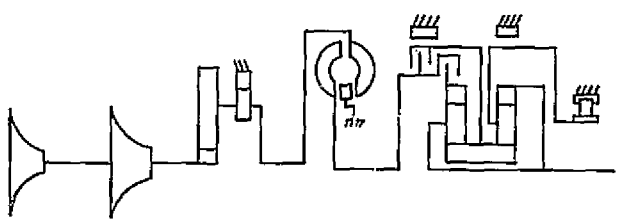


Figure 3.10 Concept 2. Variable Stator Torque Converter with C-4 Transmission

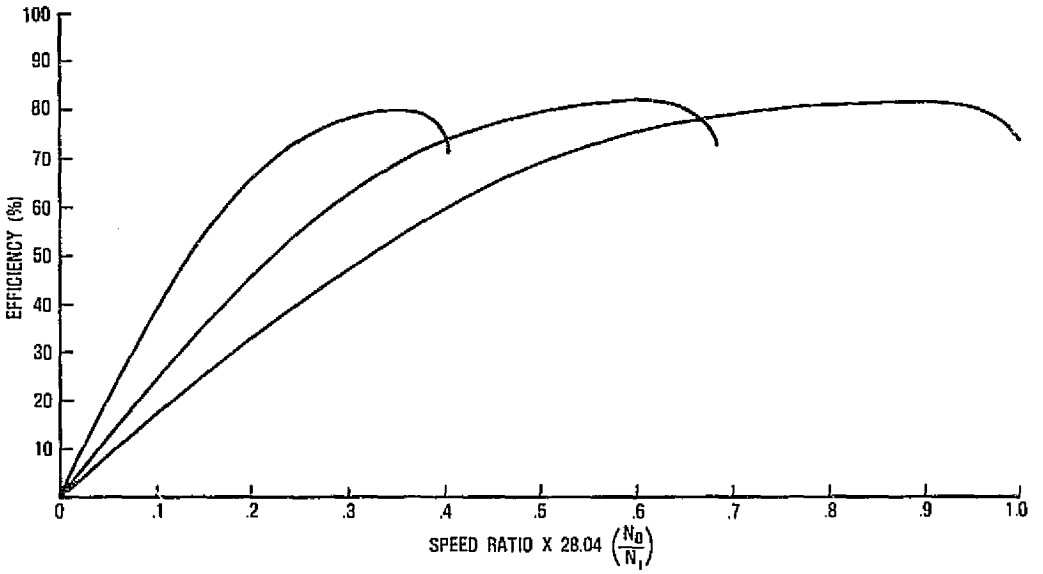


Figure 3.10(a) Efficiency of Concept 2

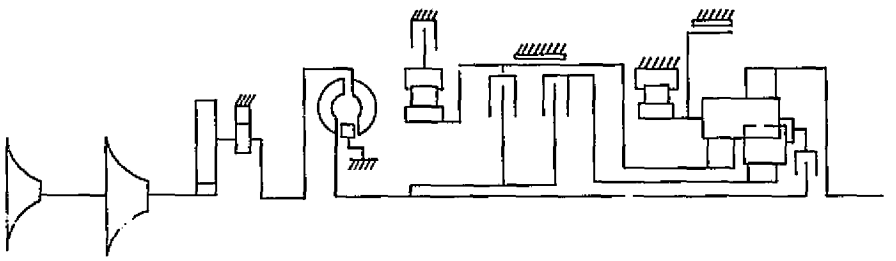


Figure 3.11 Concept 3. Variable Stator Torque Converter with Modified Ford FIOD Transmission

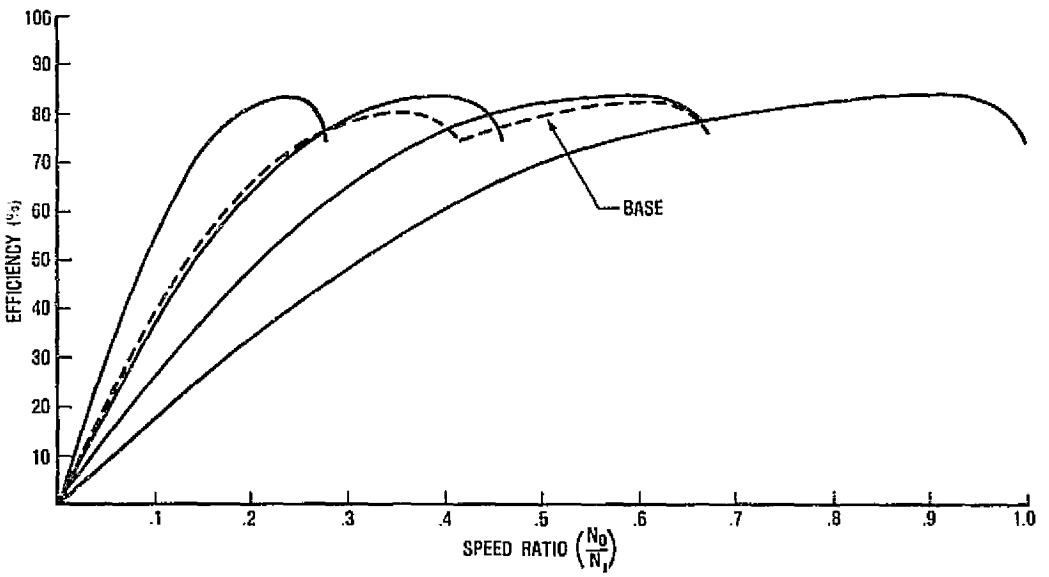


Figure 3.11(a) Efficiency of Concept 3

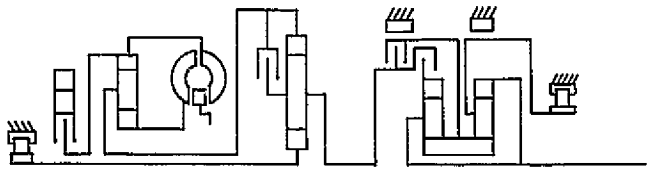


Figure 3.12 Concept 4. Split Power Variable Stator Torque Converter with Ford C-4 Transmission

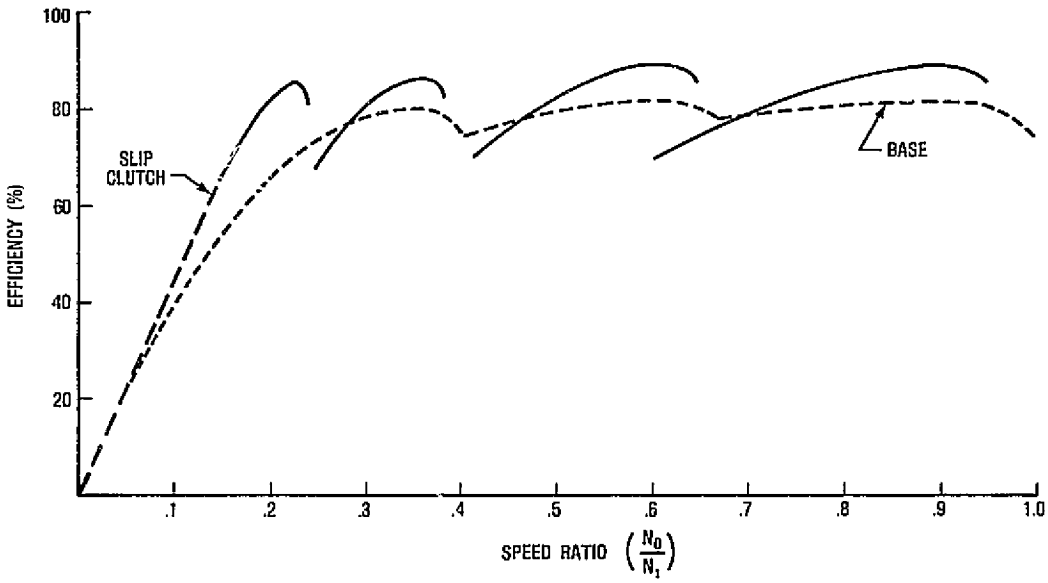


Figure 3.12(a) Efficiency of Concept 4

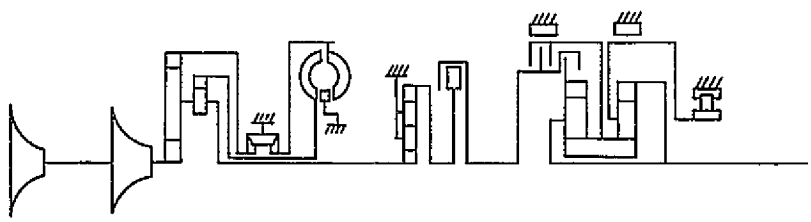


Figure 3.13 Concept 5. Differential Variable Stator Torque Converter and Ford C-4Transmission W/O Torque Converter with Slip Clutch

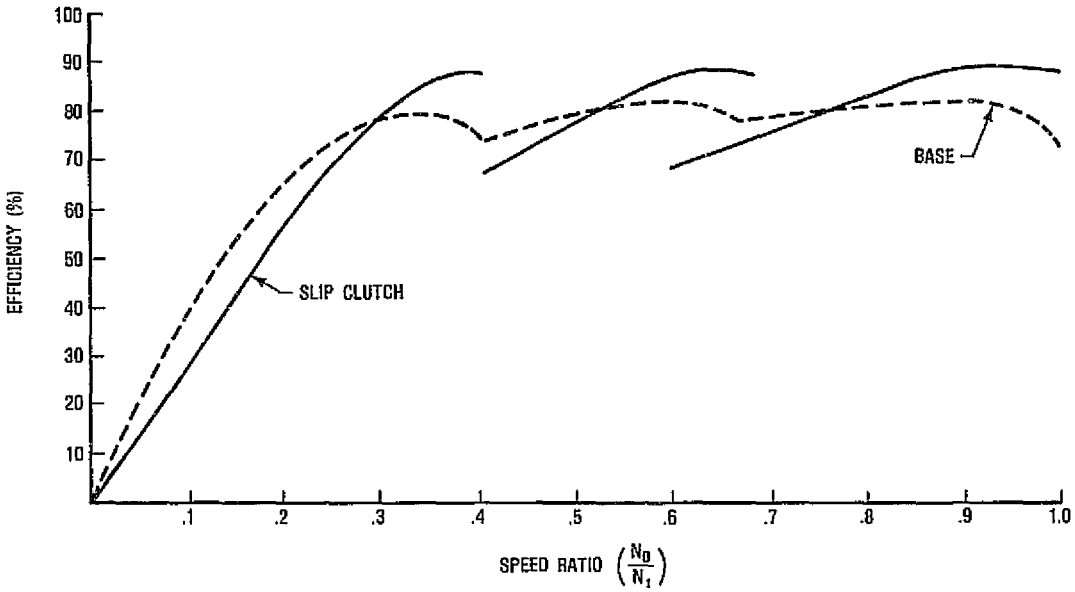


Figure 3.13(a) Efficiency of Concept 5

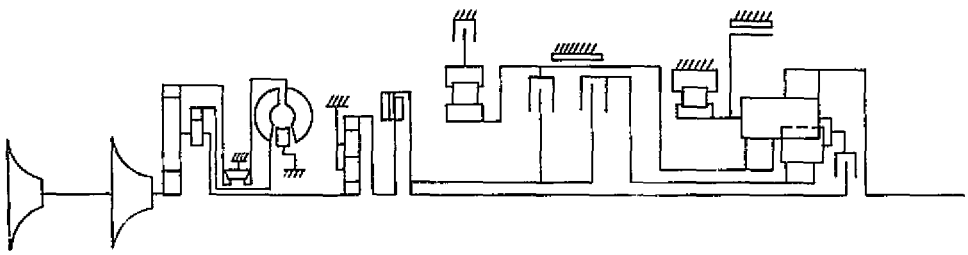


Figure 3.14 Concept 6. Differential Variable Stator Torque Converter with Ford FIOD Transmission w/o Torque Converter with Shaft Lock-up and Slip Clutch

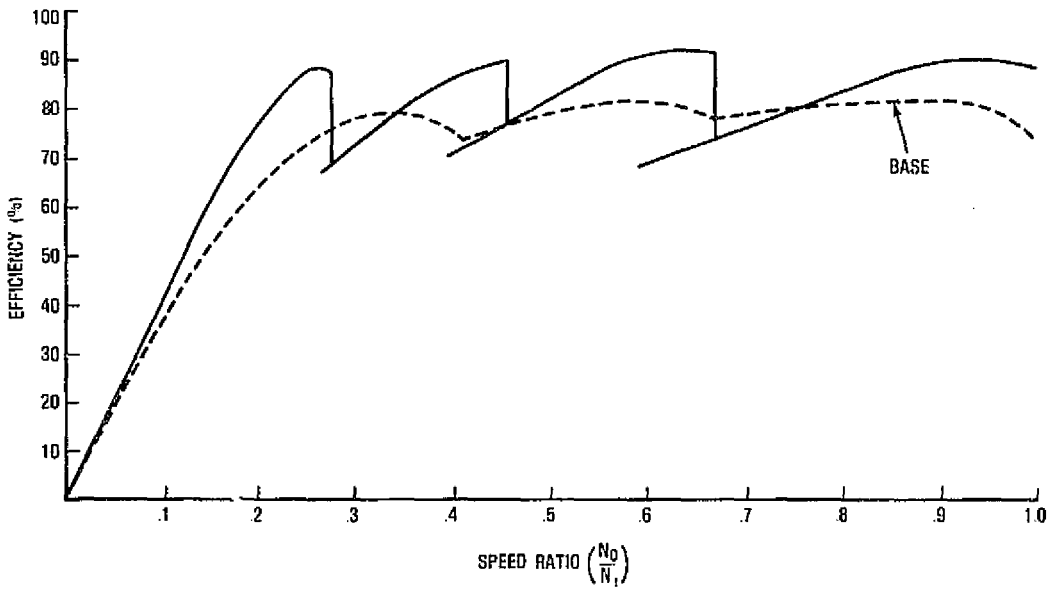


Figure 3.14(a) Efficiency of Concept 6

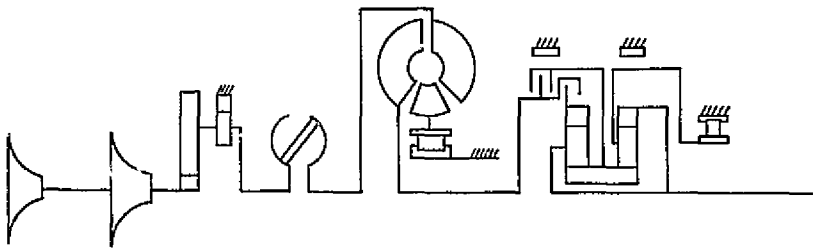


Figure 3.15 Concept 7. Inline Variable Speed Traction Drive and Ford C-4 Transmission with Fixed Stator Torque Converter

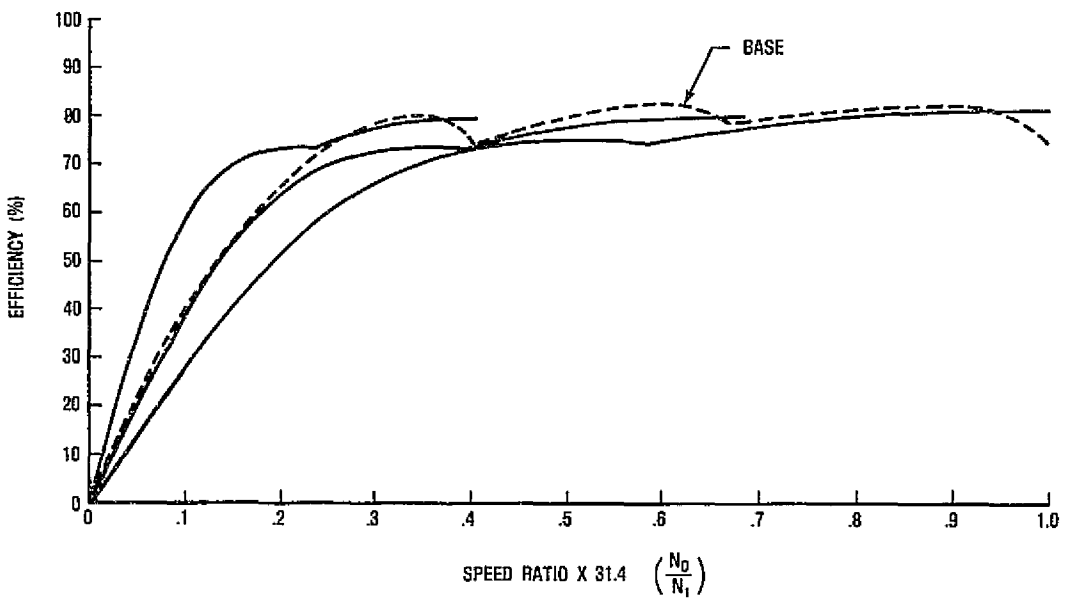


Figure 3.15(a) Efficiency of Concept 7

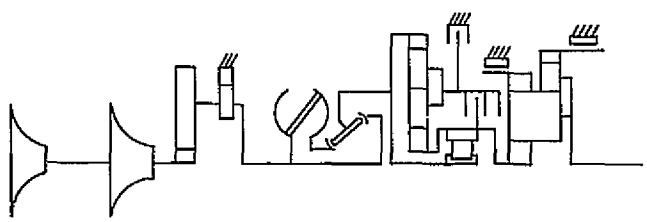


Figure 3.16 Concept 8. Regenerative Variable Speed Traction Drive with 3-Mode Transmission and Slip Clutch

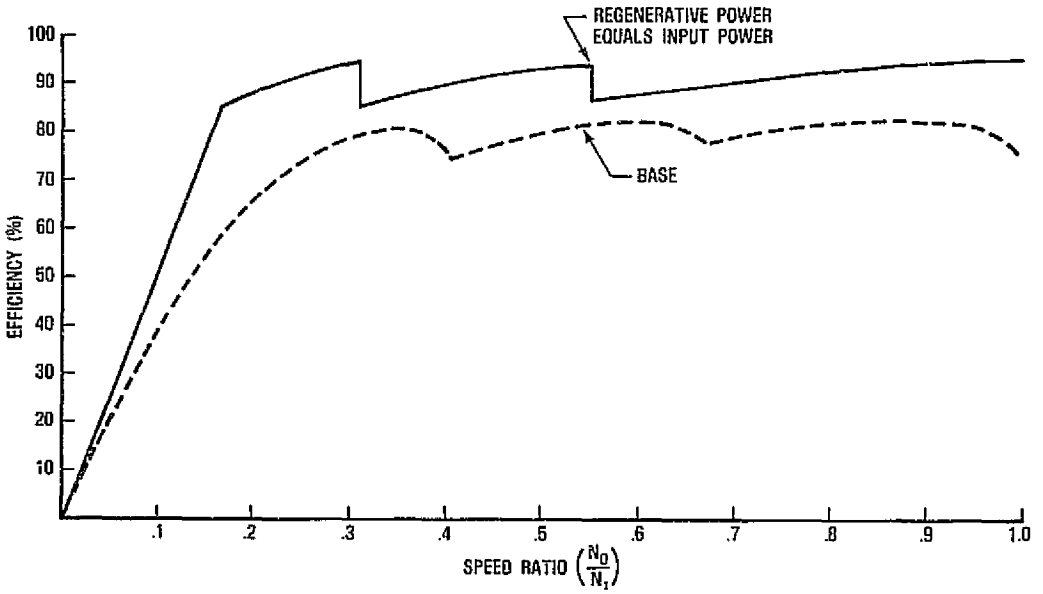


Figure 3.16(a) Efficiency of Concept 8

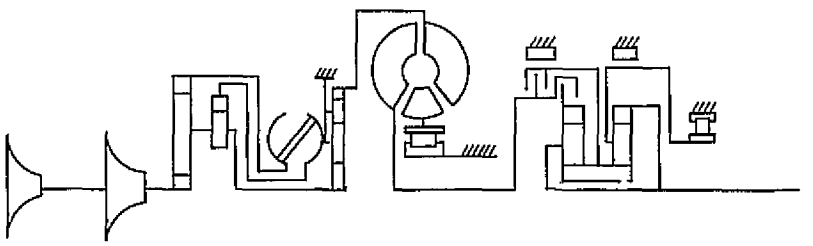


Figure 3.17 Concept 9. Differential Variable Speed Traction Drive with Ford C-4 Transmission and Fixed Stator Torque Converter

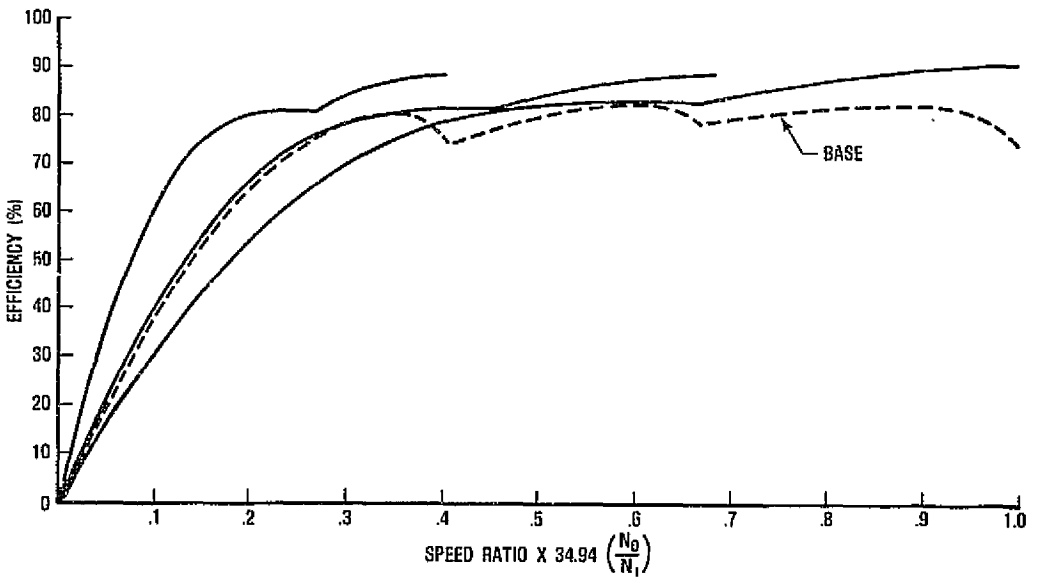


Figure 3.17(a) Efficiency of Concept 9

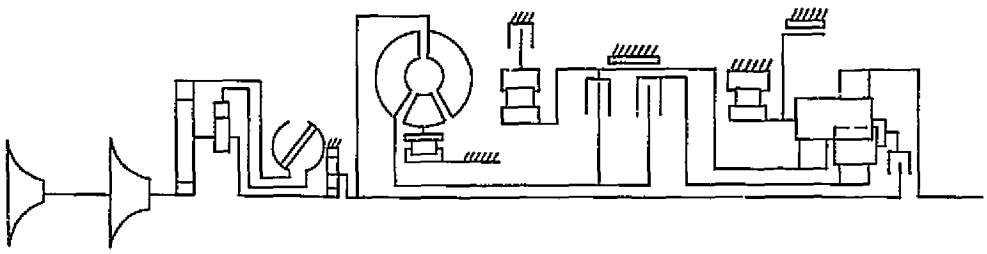


Figure 3.18 Concept 10. Differential Variable Speed Traction Drive with Ford FIOD Transmission and Fixed Stator Torque Converter

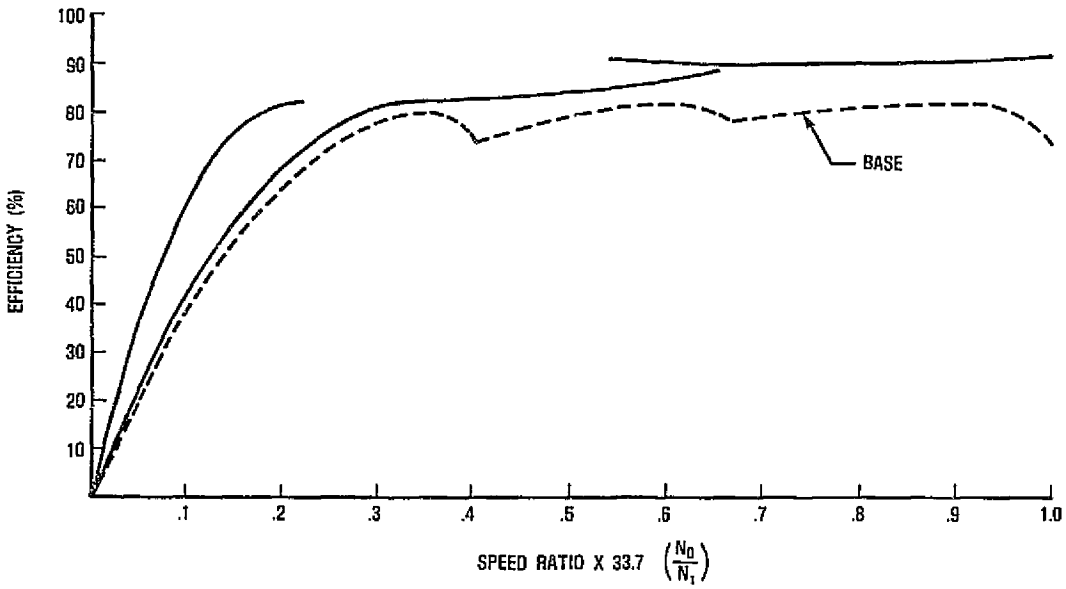


Figure 3.18(a) Efficiency of Concept 10

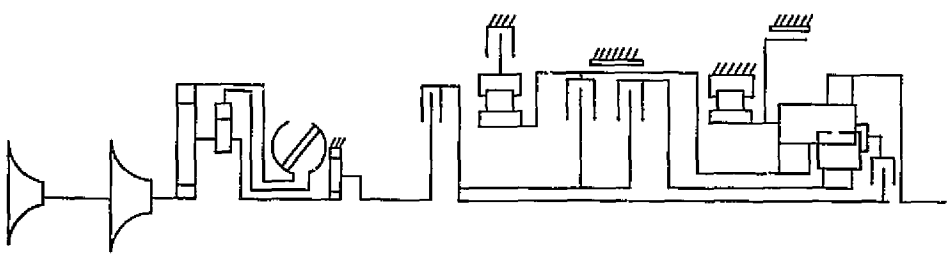


Figure 3.19 Concept 11. Differential Variable Speed Traction Drive with Ford FIOD Transmission W/O Torque Converter with Slip Clutch and Shaft Lock-Up

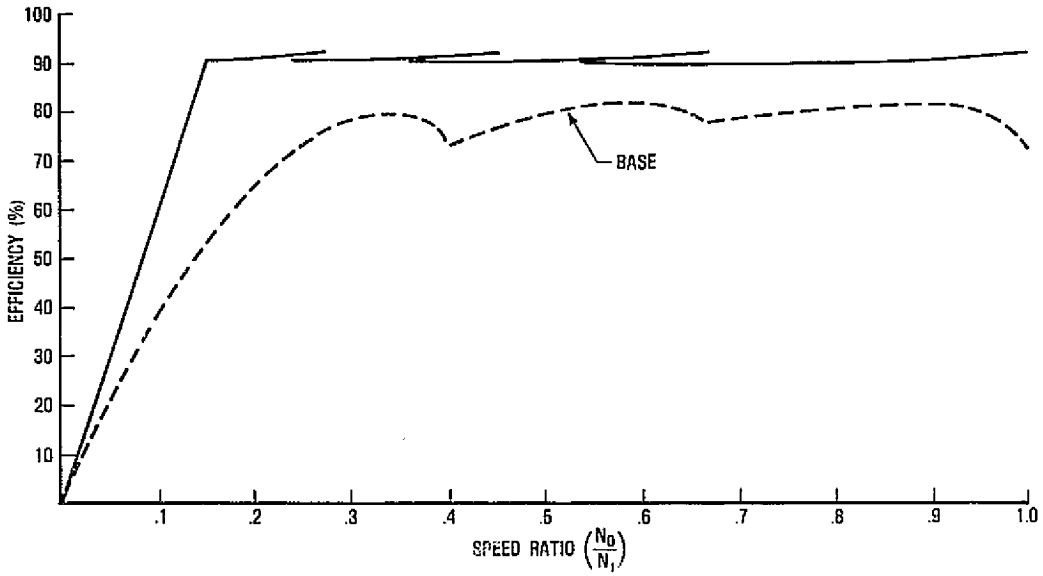


Figure 3.19(a) Efficiency of Concept 11

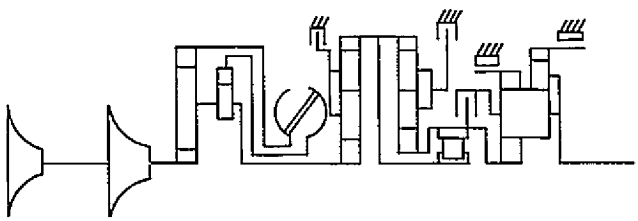


Figure 3.20 Concept 12. Differential Variable Speed Traction Drive with 3-Mode Transmission

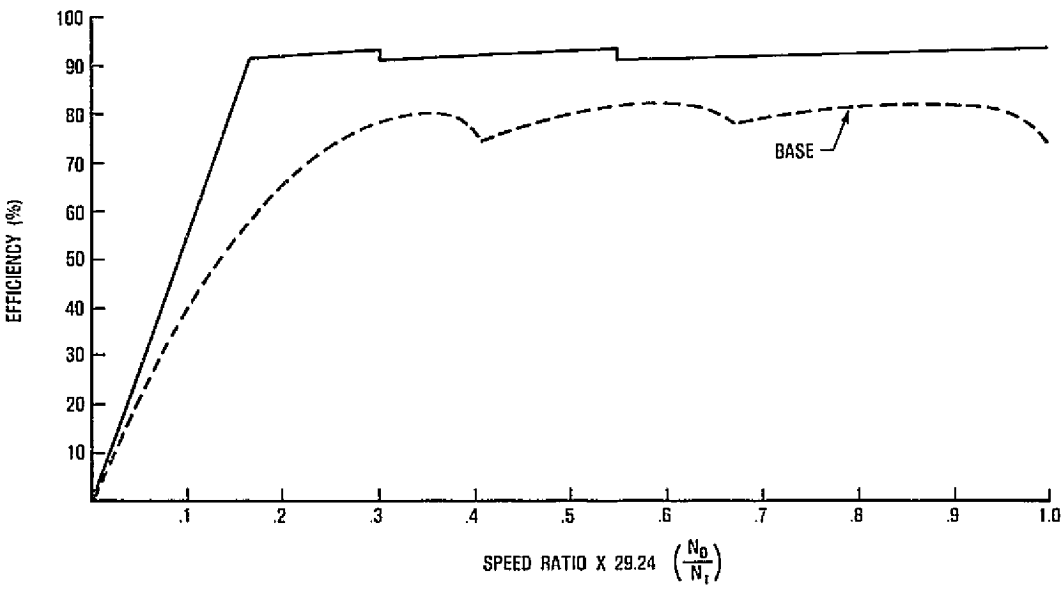


Figure 3.20(a) Efficiency of Concept 12

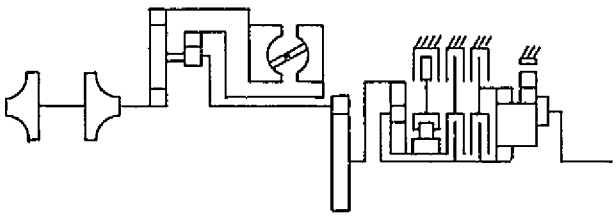


Figure 3.21 Concept 13. Differential Variable Speed Traction Drive with 4-Mode Transmission

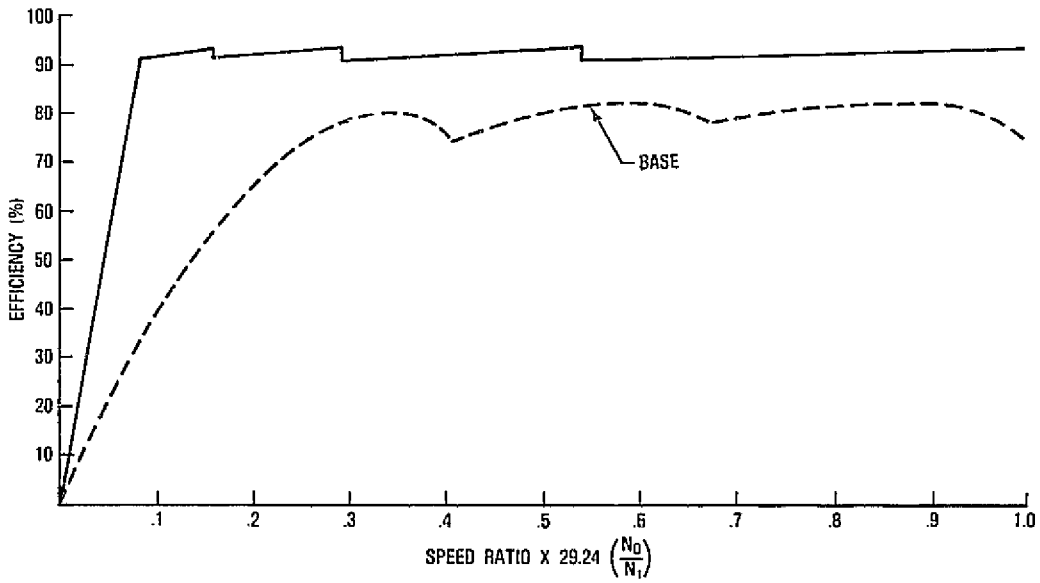


Figure 3.21(a) Efficiency of Concept 13

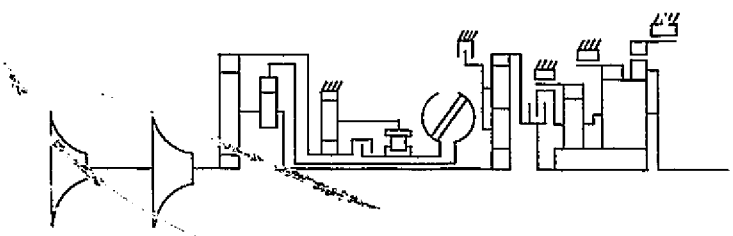


Figure 3.22 Concept 14. 2-Mode Differential Variable Speed Traction Drive with 3-Mode Transmission i.e., 6-Mode

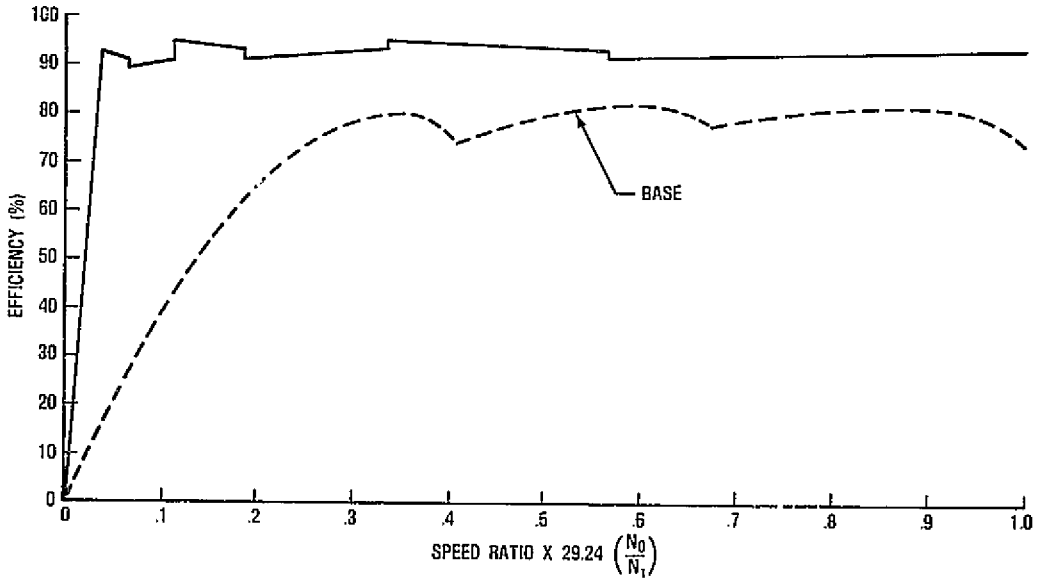


Figure 3.22(a) Efficiency of Concept 14

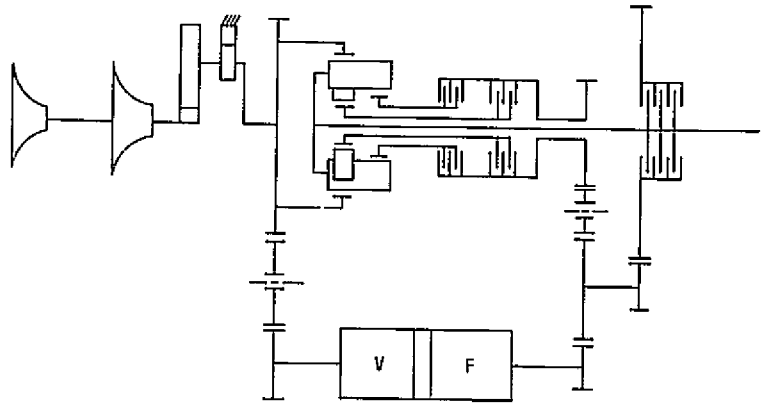


Figure 3.23 Concept 15. Hydromechanical Tri-Mode Transmission

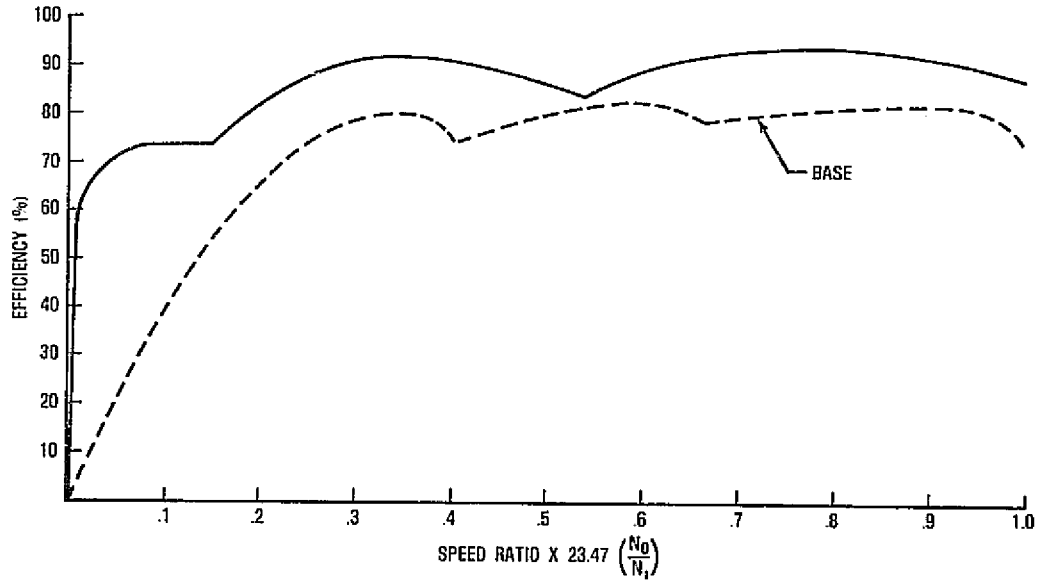


Figure 3.23(a) Efficiency of Concept 15

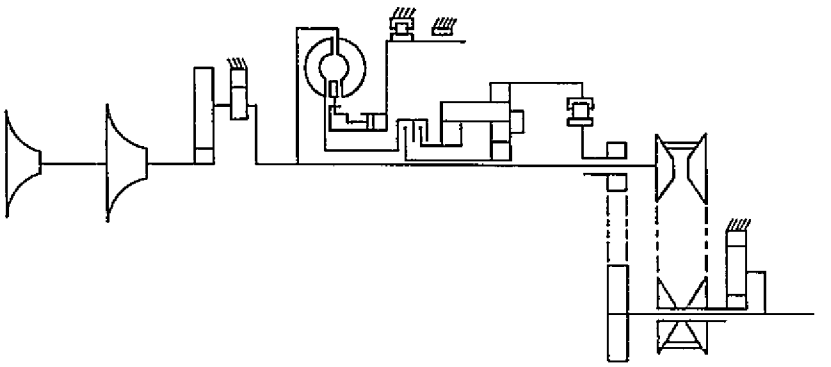


Figure 3.24 Concept 16. Variable Belt Drive with Variable Stator Torque Converter and 2-Speed Transmission

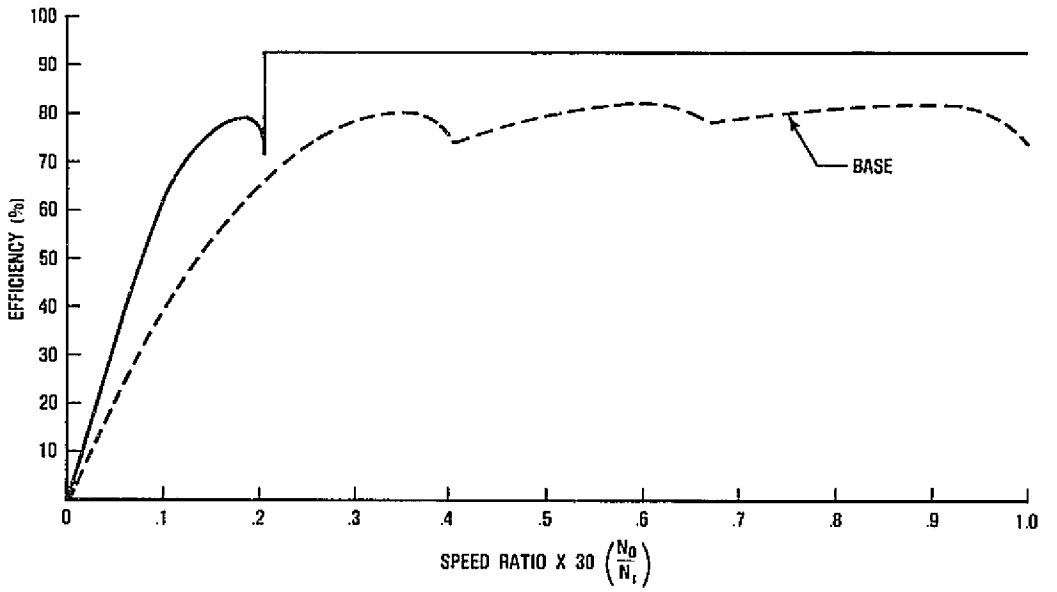


Figure 3.24(a) Efficiency of Concept 16

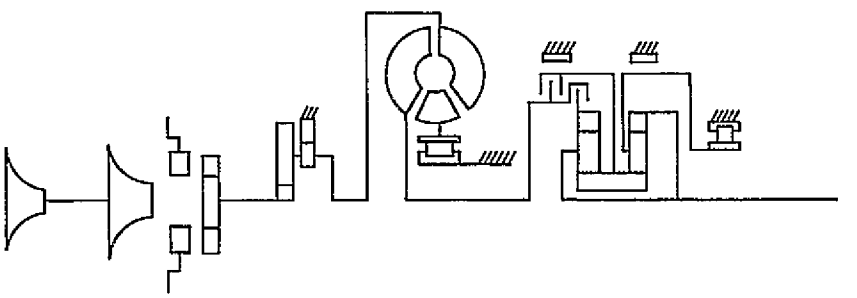


Figure 3.25 Concept 17. Free Power Turbine with Ford C-4 Transmission and Fixed Stator Torque Converter

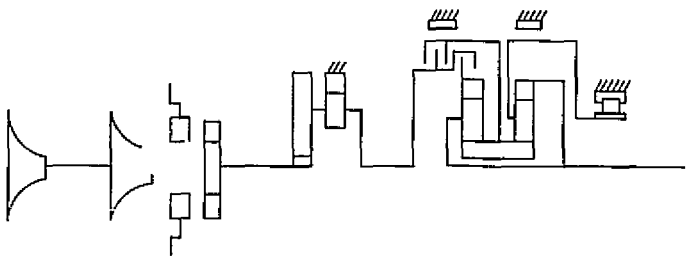


Figure 3.26 Concept 18. Free Power Turbine with Ford C-4 Transmission W/O Torque Converter

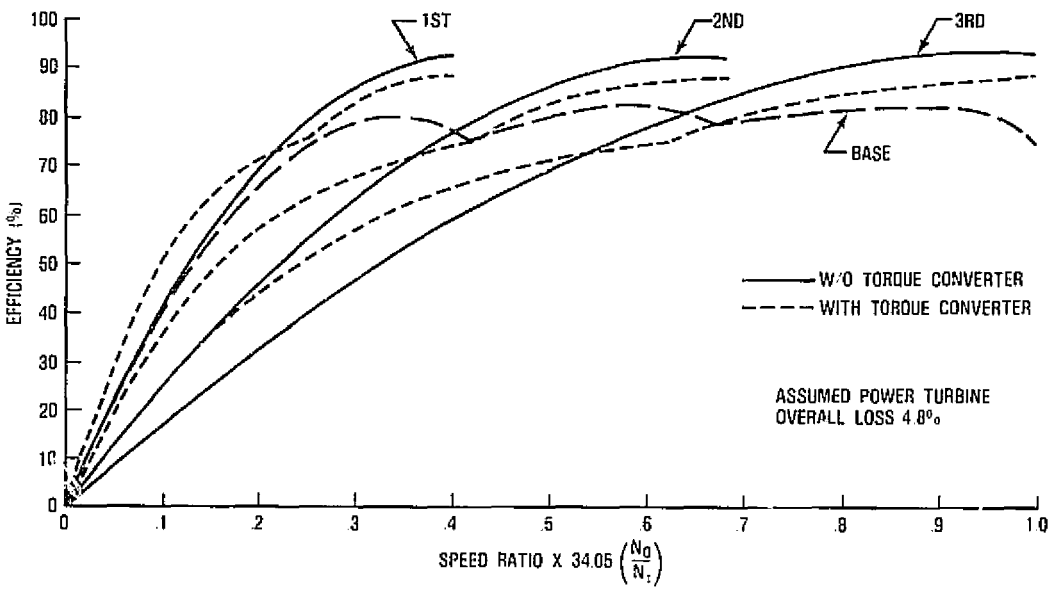


Figure 3.26(a) Efficiency of Concepts 17 and 18

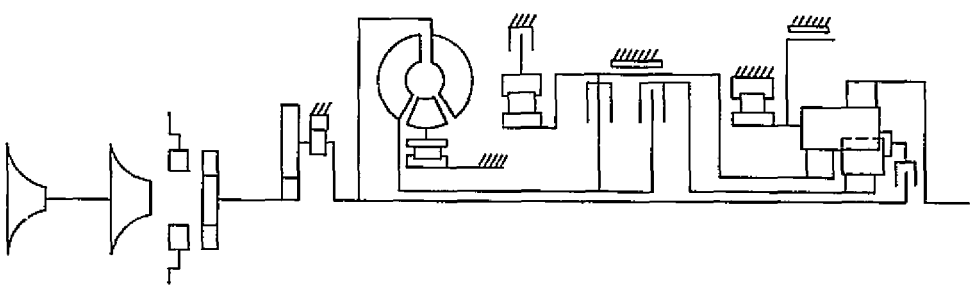


Figure 3.27 Concept 19. Free Power Turbine with Ford FIOD Transmission and Fixed Stator Torque Converter

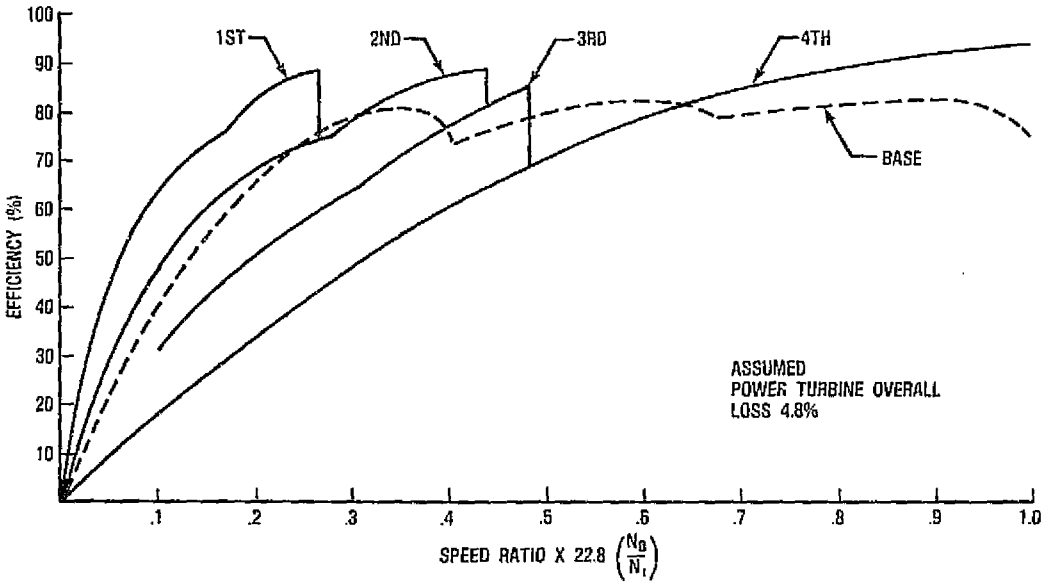


Figure 3.27(a) Efficiency of Concept 19

3.11.3 METHOD OF SELECTION

The ranking criteria of Appendix II and the rating determination factors of Appendix III were applied and the results are tabulated in Table 3.8 which ranks all the transmission concepts in descending order of merit. Following are the definitions of the rating determination factors of Appendix III:

Efficiency — This is the full power average efficiency as defined in Section 3.11.2.

Cost — As illustrated in Table 3.9, cost was determined relative to a production three-speed auto matic, Ford C4, and also includes the reduction gear. For two-shaft engines the cost of the power turbine and variable nozzle were included in transmission cost.

Two Second Distance — Estimated based on an idle start and assumption that the spool reaches maximum speed in two seconds as a measure of power split. It was further assumed that the spool is capable of accelerating from idle to full speed in 1 second using 100% of the available power.

Packageability — It was assumed that a production three-speed automatic transmission with a fixed stator torque could be packaged with no interference in the vehicle, other transmission packaging was estimated by speculating on component size.

Development Risk — It was assumed that a production three-speed automatic had less than a year's development time to adapt to a single shaft or two shaft turbine.

Those transmissions using a variable stator torque converter would require at least three years to develop a converter and the control system.

All other concepts, variable belt traction, or hydromechanical would require 6 to 10 years development time before they could be risked in a production program.

Noise — Defined as propulsion system noise in dBA at drivers ear when cruising at 80 km/h (50 mph). For turbine vehicle using free power turbine and three-speed gear box, reference 8.

	Turbine	V-8 Piston Engine
48 km/h (30 mph)	61 dBA	59 dBA
96 km/h (60 mph)	68 dBA	72 dBA
Estimated 80 km/h (50 mph)	65 dBA	67 dBA

For a hydromechanical transmission, reference 9, the passenger compartment sound pressure level at 80 km/h (50 mph) cruise is 71.7 dBA. Therefore a maximum allowable value of 72 dBA was selected for this study.

TABLE 3.8

Transmission Concept Ranking Matrix

Rank	Concept / Criteria (Value Range)	Efficiency (70 to 100%)	Cost (1X to 3X)	2 Sec. Dist. (0 to 3.4 m)	Package (−.15m. to +.08 m)	Risk (4Y to 10Y)	Noise (60 to 72dBA)	No. of Shifts (3 to 10)	Shift Quality (3 Sp. Auto Feel)	Idle Creep (0 to 29 km/h)	Total (Rating)	Concept No.
	Ideal Transmission	20	20	20	10	10	10	2	4	4	100	
1	Differential Traction-6 Mode	14.2 (91.2)	14.3 (1.57X)	12.4 (2.0)	7.8 (+.03)	0 (10Y)	9.56 (62dBA)	1.14 (6)	2.0 (5F)	3.6 (6.0)	65	14
2	Differential Traction-4 Mode	12.4 (83.5)	15.5 (1.45X)	11.0 (1.8)	8.0 (+.03)	0 (10Y)	9.56 (62dBA)	1.71 (4)	2.0 (5F)	2.9 (10.5)	63.1	13
3	VSTC and Ford FIOD	4.06 (76)	17.4 (1.26X)	8.2 (1.4)	5.6 (−.03)	10 (4Y)	8.26 (65dBA)	1.71 (4)	3.2 (8F)	1.8 (18)	60.2	3
4	Differential Traction + C4	6.25 (79.3)	15.2 (1.48X)	8.6 (1.4)	6.7 (0)	10 (4Y)	8.26 (65dBA)	2 (3)	3.2 (8F)	0 (29)	60.2	9
5	Differential Traction + FIOD	9.5 (84.2)	14.9 (1.51X)	9.0 (1.5)	5.6 (−1)	0 (10Y)	9.56 (62dBA)	1.71 (4)	2.0 (5F)	1.8 (18)	60	10
6	Differential Traction-3Mode	10.0 (84.9)	16 (1.4X)	8 (1.3)	8.3 (+.04)	0 (10Y)	9.56 (62dBA)	2 (3)	2.0 (5F)	2.52 (12.7)	58.4	12
7	Inline Traction + C4	1.87 (72.7)	16 (1.4X)	7.4 (1.3)	5.6 (−.03)	10 (4Y)	8.88 (64dBA)	1.71 (4)	2.4 (6F)	3.27 (1.88)	57.1	7
8	VSTC + C4	1.13 (71.6)	18.6 (1.14X)	6.4 (1.1)	7.2 (+0.1)	10 (3Y)	8.26 (65dBA)	2 (3)	3.2 (8F)	0 (29)	56.8	2
9	Differential VSTC + FIOD	4.15 (76.1)	15.2 (1.48X)	6.2 (1.1)	5.6 (−.03)	10 (4Y)	8.26 (65dBA)	1.7 (4)	3.2 (8F)	1.8 (18)	56.1	6
10	Split Power VSTC + C4	3.13 (74.6)	16.1 (1.39X)	6.4 (1.1)	5.6 (−.03)	10 (3Y)	8.26 (65dBA)	1.71 (4)	2.8 (7F)	1.7 (18)	55.7	4
11	Regenerative Traction + 3 Mode	8.07 (82.0)	16.5 (1.39X)	7.4 (1.2)	6.7 (0)	0 (10Y)	9.56 (62dBA)	2 (3)	2.0 (5F)	2.3 (14)	54.6	8
12	Diff. Traction & FIOD W/O TC	9.6 (84.2)	14.9 (1.51X)	9.1 (1.5)	5.6 (−.03)	0 (10Y)	9.56 (62dBA)	1.71 (4)	2 (5F)	1.8 (18)	54.3	11
13	Hydro-Mechanical Tri-Mode	10.8 (86.1)	16.4 (1.35X)	10.7 (1.8)	5.6 (−.03)	3.33 (8Y)	0 (72dBA)	1.43 (5)	2.0 (5F)	4 (0)	54.3	15
14	Differential VSTC + C4	.67 (70.9)	16.5 (1.35X)	4.4 (.7)	6.7 (0)	10 (4Y)	8.26 (65dBA)	2 (3)	2 (5F)	0 (29)	50.5	5
15	Variable Belt + VSTC & 2 Spd.	9.8 (84.6)	13.1 (1.69X)	8 (1.3)	5.6 (−.03)	0 (10Y)	5.55 (68dBA)	2 (2)	2.4 (6F)	3.2 (8.4)	49.7	16
16	Two Shaft + C4 W/O Conv.	5.60 (79.3)	12.8 (1.72X)	5.6 (.9)	3.33 (−.08)	3.33 (8Y)	8.26 (65dBA)	2 (3)	4 (10F)	0 (29)	44.9	18
17	C4	−13.4 (49.8)	20 (1X)	5.2 (9)	6.7 (0)	10 (0)	8.26 (65dBA)	2 (3)	4 (10F)	0 (29)	42.8	1
18	Two Shaft + FIOD with TC	5.80 (78.6)	10.1 (1.53X)	4.13 (1.4)	0 (−.15)	3.33 (8Y)	8.26 (65dBA)	1.71 (4)	3.2 (8F)	1.8 (18)	42.5	19
19	Two Shaft + C4 with TC	4.40 (76.5)	11.3 (1.87X)	7.0 (2.7)	0 (−.15)	3.33 (8Y)	8.26 (65dBA)	2 (3)	4 (10F)	0 (29)	40.3	17

NOTE: Transmission ranking criteria and rating factors are give in Appendices II and III.

Driveability — Number of Shifts is obvious and is listed in the ranking chart. This item is included since shift feel, shift time, and shift response are all compounded by the number of shifts required.

Shift Quality is judgmental, but certainly the C4 transmission with fixed stator torque converter has an acceptable shift feel. The addition of a variable stator torque converter may affect shift quality as the stators move, therefore a slight loss in shift quality rating seems reasonable. Both the hydromechanical tri-mode and the six mode traction have untried or unproven shift characteristics, therefore, shift quality is considered to be only 50% of a C4 transmission until proven otherwise.

TABLE 3.9

Transmission Relative Costs

	Baseline-Ford C4 3 Sp. Auto with Torque Converter	Variable Stator Torque Converter & Ford C4 Gearbox	Split Power VSTC & Ford C4 Gearbox	Differential Traction with Ford C4 Transmission	Differential Traction with Ford FIOD Transmission	Hydro Mechanical Tri-Mode
Planetary Gear Sets	18.0	18.0	27.0	24.0	24.0	18.0
Shafting	6.0	6.0	8.0	7.0	7.0	8.5
Transfer Gears	—	—	—	—	—	20.0
Clutches & Bands	21.0	21.0	31.5	21.0	31.5	10.5
Control System	7.0	12.0	12.0	12.0	12.0	12.0
Housings	14.0	14.0	16.0	16.0	16.0	16.0
Anti-Friction Bearings	1.0	1.0	1.0	1.0	1.0	3.5
Misc.	2.0	2.5	3.0	2.5	2.5	3.0
Assy. & Test	12.0	13.0	13.0	13.0	13.0	14.0
Hydraulic Unit	—	—	—	—	—	22.8
Torque Converter	14.0	21.0	21.0	14.0	14.0	—
Traction Unit	—	—	—	30.0	30.0	—
Units Total Mfg. Cost	95.0	108.5	132.5	140.5	151.0	128.3

Idle Creep — Both the fixed stator and variable stator torque converter versions of the C4 transmission require power at idle to drive the converter pump. It is estimated that vehicles equipped with these converters and C4 gear box will creep at 19 km/h (12 mph) when in a drive configuration. This means the stators are not completely closed in the variable stator torque converter.

The six mode transmission will idle at about 4.02 km/h (2.5 mph), due to the approximate 25 to 1 low gear range, if it is assumed that top speed is 161 km/h (100 mph), and that a single shaft turbine idles at 50% spool speed.

The hydromechanical tri-mode may have a neutral position that provides zero creep speed built into the operating mode. Although this has to be proven, for this analysis a zero speed is assumed.

TABLE 3.9 (Continued)

	Regenerative Traction Drive and 3 Mode Transmission	Differential VSTC and Ford FIOD	Diff. VSTC and Ford C4 W/O Conv.	VSTC and Ford FIOD	Diff. Tract. Ford FIOD W/O Conv.	Diff. Tract. 4 Mode
Planetary Gear Sets	30.0	30.0	30.0	18.0	24.0	30.0
Shafting	7.0	7.0	7.0	6.0	7.0	6.0
Transfer Gears	—	—	—	—	—	—
Clutches & Bands	17.0	37.8	25.2	29.4	37.8	28.0
Control System	12.0	12.0	12.0	12.0	12.0	12.0
Housings	15.0	15.0	15.0	15.0	15.0	15.0
Anti-Friction Bearings	2.0	2.0	2.0	2.0	2.0	1.7
Misc.	2.5	3.0	3.0	3.0	3.0	2.2
Assy. & Test	13.0	13.0	13.0	13.0	13.0	13.0
Hydraulic Unit	—	—	—	—	—	—
Torque Converter	—	21.0	21.0	21.0	—	—
Traction Unit	30.0	—	—	—	30.0	30.0
Units Total Mfg. Cost	128.5	140.8	128.2	119.4	143.8	137.9

TABLE 3.9 (Continued)

	Differential Traction Six Mode	Differential Traction Three Mode	Variable Belt with VSTC & 2 Speed Transmission	Inline Variable Speed Traction & Ford C4	Two Shaft IGT & Ford FIOD	Two Shaft IGT & Ford C-4
Planetary Gear Sets	36.0	30.0	24.0	18.0	18.0	18.0
Shafting	10.0	8.0	8.0	6.0	7.0	6.0
Transfer Gears	—		6.0	—	—	
Clutches & Bands	28.0	21.0	17.50	21.0	31.5	21.0
Control System	12.0	12.0	16.00	12.0	12.0	12.0
Housings	16.0	15.0	18.00	15.0	30.0[2]	30.0[2]
Anti-Friction Bearings	2.0	1.5	2.00	1.5	1.0	1.0
Misc.	2.5	2.5	3.00	2.5	3.5	3.5
Assy. & Test	13.0	13.0	15.00	13.0	16.0	16.0
Hydraulic Unit	—	—	—	—	—	
Torque Converter	—	—	21.0	14.0	14.0	14[3] 0[4]
Traction Unit	30.0	30.0	30.0 [1]	30.0	56.0[2]	56.0[2]
Units Total Mfg. Cost	149.5	133.0	160.5	133.0	189.0	177.5[3] 163.5[4]

(1) Variable Belt Drive
(2) Free Power Turbine Plus Variable Nozzle
(3) With Converter
(4) Without Converter

3.11.4 RESULTS

Table 3.8 presents the completed Ranking Matrix and includes the maximum rating for each criteria and the rating for each concept for each criteria. The chart also includes the absolute value for each criteria for purpose of comparison.

The first nine rankings are:

Rank	Concept No.	
1	14	Differential Traction — 6 Mode
2	13	Differential Traction — 4 Mode
3	3	VSTC and Ford FIOD
4	9	Differential Traction and Ford C4
5	10	Differential Traction and Ford FIOD
6	12	Differential Traction — 3 Mode
7	7	Inline Traction and Ford C4
8	2	VSTC and Ford C4
9	6	Differential VSTC + FIOD

Traction units are involved in six of the nine concepts. The Ford Motor Company has no experience in the high volume, 500,000 units per year, manufacture of traction drive, and therefore cannot now commit to a program using traction drives. Therefore, concepts 14, 13, 9, 10, 12 and 7 remain open issues.

The three remaining concepts all involve the use of a variable stator torque converter. Concept 2 and concept 6 are essentially of the same ranking, 56.8 and 56.1 points respectively. However, concept 6 has an overall efficiency of 76.1 as compared to 71.6 for concept 2. In the interest of fuel economy, the edge is with concept 6, and concept 2 will be eliminated.

Therefore, concepts 3 and 6 which have approximately equal average efficiencies, remain for evaluation. If another look is taken at the efficiency curves of these two concepts, it becomes apparent that concept 6 is significantly more efficient at the higher output speed end of the speed ratio range where most of the vehicle operation will occur. It is estimated that concept 6, due to these efficiency peaks, will provide significantly better fuel economy than concept 3, and is, therefore, the prime candidate transmission design.

3.11.5 RECOMMENDATIONS AND DISCUSSION

1. It is recommended that transmission development efforts for the IGT be concentrated on the differential variable stator with FIOD transmission gearbox (concept 6) in the following areas:

   a) Improve efficiency of present VSTC design.
   b) Develop shift pattern and control.
   c) Investigate and/or develop converter operation throughout the speed ratio range.

2. It is recommended that a separate but parallel program to the IGT be activated to develop the differential traction unit for eventual replacement of the differential VSTC (concept 10), as follows:

   a) Use FIOD with traction in initial studies.
   b) Develop optimum four speed gear box for use with traction unit.
   c) Improve average efficiency at full power by 12.5%.
   d) Improves available horsepower at 10% vehicle maximum speed by 30%.

3. As a backup to recommendations one and two, it is recommended that an inline VSTC and FIOD gearbox (concept 3) be continued in the IGT engine program.

4.0 CYCLE ANALYSIS

The study contract calls for a 1542 kg,(3400 lb.) vehicle to accelerate from 0-96.5km/h, (0-60 mph) in 15 secs. Based on past experience and prior performance calculations a nominal 75kW, (100 HP) engine is required. The strategy involved in this analysis was to perform a design point optimization study for a single shaft engine configuration of 75kW, (100 HP), at 1150°C, (2100°F) turbine inlet temperature with a cooled metal radial turbine as the preferred "near term" engine. The differences between a single-shaft and two-shaft engine as they affect a cycle optimization study were considered minor and were therefore neglected. As ceramic turbine rotors become available, the engine will be uprated to 1370°C, (2500°F) which will result in improved performance and economy. The effect of uprating the engine and also of using axial turbines in the place of radial turbines was evaluated. No effects of transmission efficiency were included in the cycle analysis.

Previous experience has indicated that the trend of specific fuel consumption (sfc) at 20 percent of the engine design power is approximately representative of the trend in vehicle fuel economy over the Combined Federal Driving Cycle (CFDC). Therefore comparing sfc's at 20 percent power was used as one of the criteria for selecting the optimum engine pressure ratio.

The design point pressure ratio optimatization study was performed for both 100 percent (design point) and 20 percent power operation. Basic design point parameters including compressor, turbine and combustor efficiency, pressure losses, regenerator effectiveness, cooling and leakage flows, parasitic losses and accessory loads were as established in section 3.0 for 1983 technology levels. Optimum compressor specific speed and optimum turbine tip speed were selected with appropriate corrections for Reynold's number and blade number being made for the turbine. For the investigation at 20 percent power, some simplifications were adopted for the purpose of the cycle analysis. Compressor, turbine, and combustor efficiency, and leakage flows were held constant and equal to their values at design speed. Regenerator effectiveness, pressure losses, accessory and parasitic losses were varied with speed and assumed to be as shown in Section 3.0. All the cooling and leakage flows were assumed to by-pass the turbine and dump to the atmosphere. Compressor work was assumed to vary as a function of rotor speed squared and compressor airflow was assumed to vary as shown in Figure 4.1. The 20 percent power point was determined by means of iteration on the engine speed. The turbine inlet temperature schedule was held constant as speed reduced until the regenerator inlet temperature limit of 1095°C, (2000°F) was reached, at which point regenerator inlet temperature was held constant and the turbine inlet temperature was reduced.

The results of the cycle analysis are shown in Figure 4.2. At 100 percent power a minimum sfc occurs for a design pressure ratio of 4. However, at 20 percent power a minimum sfc occurs with an engine designed for a pressure ratio of 6 to 7 at 100 percent speed. Minimum engine airflow (i.e. engine size) is seen to occur for engine design pressure ratios of 6 to 7.

From this analysis a compromise pressure ratio selection of 5 was chosen which resulted in an airflow rate of 0.39 kg/s, (0.85 pps) for a nominal 75 kW, (100 HP) engine. The advantage to be gained in sfc and airflow from selecting a higher pressure ratio was judged to be negligible. Also, the pressure ratio selected was considered to be the limit for use with an aluminum compressor impeller and a ceramic regenerator core even at 1983 technology levels.

A summary of the engine design point parameters, including the heat exchanger dimensions, is given in Table 4.1. The regenerator dimensions were based upon prior preliminary studies, considering packaging requirements and trade-offs of effectiveness and presure losses. This engine size was then used to compare other configurations of engines as follows:

- 2500°F uncooled ceramic radial turbine,
- 1950°F uncooled metal 3-stage axial turbine,
- 2500°F uncooled ceramic 3-stage axial turbine.

The results of this comparison are also shown in Table 4.1. As can be seen, and as would be expected, the effect of increasing temperature increases the maximum power from the engine and lowers the sfc. With an axial turbine replacing the radial turbine, the power and sfc are not so favorable due to the lower axial turbine efficiencies (and lower turbine inlet temperature in the case of the metal turbine) in engines of this airflow size.

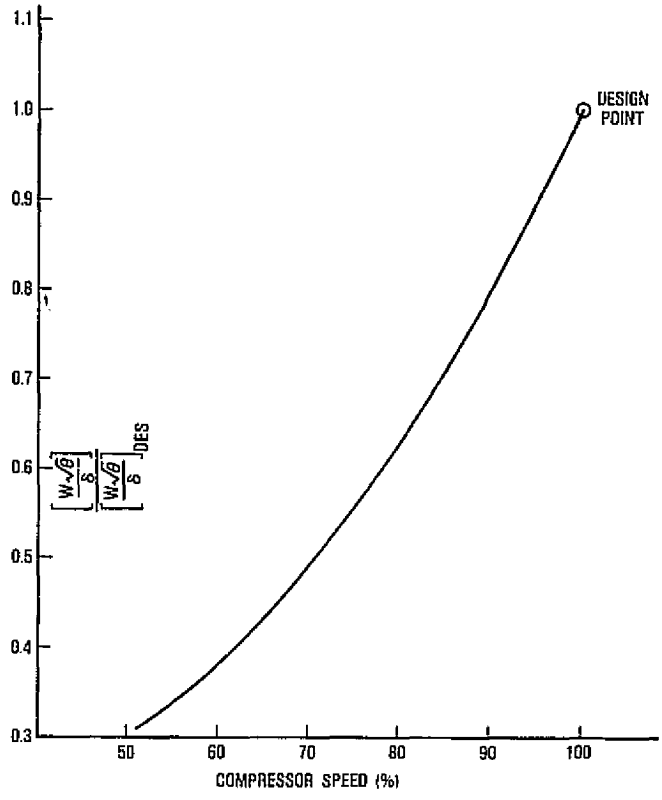


Figure 4.1 Assumed Variation of Centrifugal Compressor Airflow Parameter with Speed for the Cycle Analysis

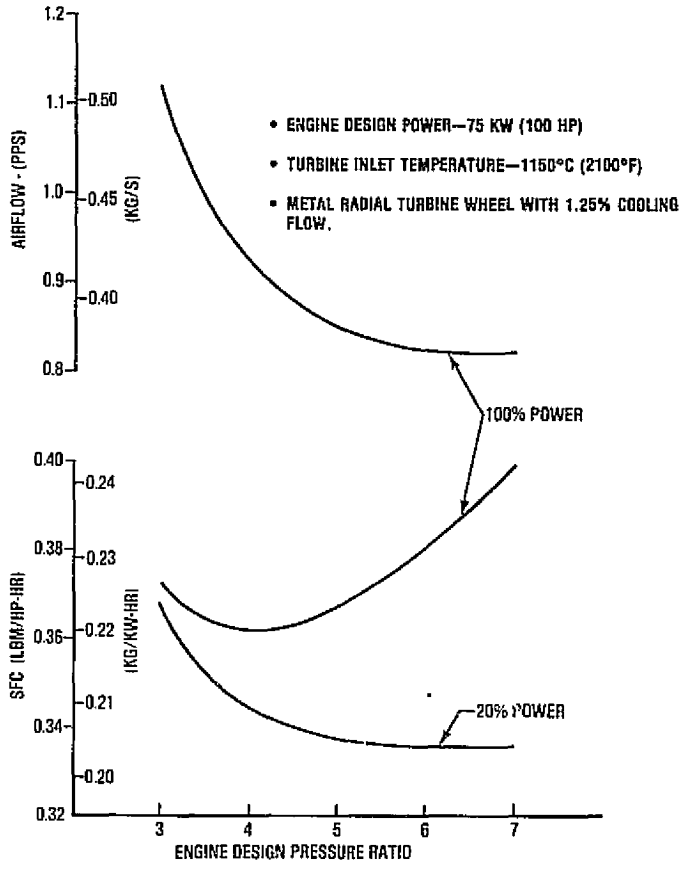


Figure 4.2 Specific Fuel Consumption (SFC) and Airflow vs. Engine Design Pressure Ratio

TABLE 4.1

Cycle Performance — Summary of Results

Design Point
Engine Air Flow 0.39 kg/s (0.85 pps)
Engine Pressure Ratio 5
Engine Speed 12357 rad/s (118,000 rpm)
Single Ceramic Core Heat Exchanger
0.37 m (14.5 ins) outer diameter
0.05 m (2.0 ins) inner diameter
0.07 m (2.8 ins) thick

	100% POWER				20% POWER			
CONFIGURATION	POWER	SFC	TIT	RIT	%N	SFC	TIT	RIT
Metal Radial Turbine (Cooled)	77(103)	0.218(0.358)	1149(2100)	767(1412)	61	0.206(0.338)	1149(2100)	972(1782)
Ceramic Radial Turbine (Uncooled)	106(142)	0.193(0.317)	1371(2500)	937(1719)	63	0.190(0.312)	1297(2367)	1093(2000)
Metal Axial Turbine (Uncooled)	67(90)	0.232(0.381)	1066(1950)	707(1305)	60	0.216(0.355)	1066(1950)	901(1654)
Ceramic Axial Turbine (Uncooled)	97(130)	0.202(0.333)	1371(2500)	956(1753)	63	0.198(0.326)	1288(2351)	1093(2000)

POWER = kW, (HP)
SFC = Specific Fuel Consumption kg/kW/h, (lb/hp-hr)
TIT = Turbine Inlet Temperature °C(°F)
RIT = Regenerator Inlet Temperature °C(°F) < 1095°C (2000°F)

5.0 PRELIMINARY ENGINE SELECTION COMPARISON

With the engine airflow and design pressure ratio selected, off-design analysis of two basic engine configurations were performed. Off-design analysis means determination of the fuel flow and net power, etc., at speeds from idle to maximum along a prescribed turbine inlet temperature schedule, with stated limits imposed on the regenerator inlet temperature and surge margin by using a complete computerized model of the engine. The basic engine configurations analysed were the single shaft and free turbine machines, schematics of the configurations and the station numbering system are shown in figure 5.1. Different versions of these engines were evaluated including both metal and ceramic, radial and axial turbines. Engine performance data in conjunction with several transmission types and the baseline vehicle characteristics were used to compute the performance 0-96.5km/hr, (0-60 mph) and fuel economy over the Combined Federal Driving Cycle (CFDC).

The selection of the powertrain for further detailed design and study was based on the results from a decision matrix involving not only the performance and fuel economy, but an evaluation of cost comparisions, risks and sensitivity analyses and judgmental evaluation of several vehicle installation studies.

5.1 Engine Performance

The single shaft engine (SS) was modeled in ten different versions and the free turbine engine (FT) was modeled in four different versions as shown in Table 5.1. For the single shaft engine, two compressor speeds were selected, a non-optimum, but conservative 9425 rads/s (90,000 rpm) and for

the optimum specific speed case, 12357 rads/s (118,000 rpm). For the free turbine engine a compressor speed of 9425 rads/s (90,000 rpm) was selected for comparison purposes. A radial turbine tip speed limit of 610 m/s (2000 fps) was conservatively selected for the 9425 rads/s (90,000 rpm) engines.For the 12357 rads/s (118,000 rpm) engines, the radial turbine tip speed was selected on the basis of optimum turbine efficiency, so that for engine types SS5 and SS6 the optimum radial turbine tip speed was calculated to be 722 m/s (2370 fps) and for types SS7 and SS8 a tip speed of 759 m/s (2490 fps) was calculated. For the axial turbine versions of the single shaft engine, cases SS9 and SS10, mean blade speeds for a 3 stage axial turbine were set to the projected 1983 limits of 396 m/s (1300 fps) for metal rotors and 457 m/s (1500 fps) for integrally bladed ceramic rotors. Idle speeds were generally set at 50%, however, speeds other than this were investigated. The effect of using variable inlet guide vanes at idle speed to reduce power while maintaining the highest possible turbine inlet temperature, and hence reduce the idle fuel flow to improve the fuel economy, was also investigated.

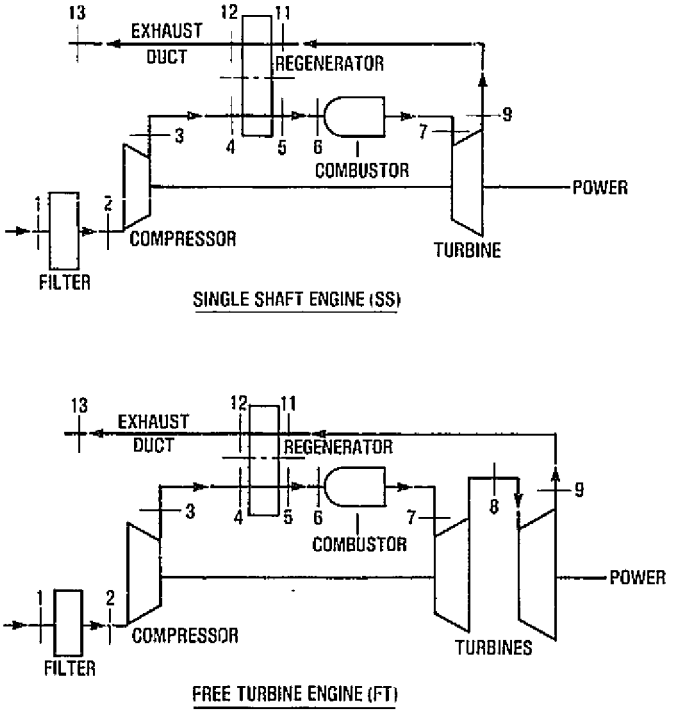


Figure 5.1 Schematics of Engine Configurations Including Station Numbers

The simplifying assumptions used in parts of the cycle analysis were dropped. Complete predicted compressor and turbine characteristics, which were based upon either realistic maps or derived from analytical loss models, with the design point efficiencies adjusted to match the 1983 technology levels were used in the engine computer program. The modifying effects of variable inlet guide vanes (VIGV's) on the compressor characteristics were as described in Table 3.1. Characteristics of the axial power turbines with variable nozzles, as used for the free power turbine engine analyses, were operated for a range of nozzle settings, as described in Section 3.2.1. Heat exchanger data was input as the F & J information of Table 3.2. Pressure losses were calculated in the program as a fixed percentage of the local dynamic head, except for the combustor (see Section 3.4) and the heat exchanger. Engine cooling air flows and leakages were handled differently than those in the cycle analysis study. The source and destination of the leakage flows is shown in Table 5.2. Wherever the leakage flow re-enters the main stream, the temperature after mixing is determined from an enthalpy balance. Mechanical, accessory and auxiliary power losses were calculated according to the projections of Section 3.0.

Matching of the engine was accomplished at 100 percent compressor speed by adjusting the turbine nozzle area so that an airflow of 0.39 kg/sec (0.85 pps) and a pressure ratio of 5.0 resulted. At off design speeds the turbine inlet temperature was held to the maximum design value so long as the regenerator inlet temperature was less than or equal to 1093°C (2000°F), or, so long as the compressor surge margin was not less than about 3.5%.

TABLE 5.1

Engine Configurations Analyzed

Configuration Ident.	Turbine(s)	Turbine Inlet Temperature °C, (°F)	Compressor Speed rads/s (RPM)	Maximum Turbine Tip Speed m/s (fps)	Variable Inlet Guide Vanes	Turbine Rotor Material
SS 1	Radial	1205 (2200)	9425 (90000)	610 (2000)	No	Metal
SS 2	Radial	1205 (2200)	9425 (90000)	610 (2000)	Yes	Metal
SS 3	Radial	1370 (2500)	9425 (90000)	610 (2000)	No	Ceramic
SS 4	Radial	1370 (2500)	9425 (90000)	610 (2000)	Yes	Ceramic
SS 5	Radial	1150 (2100)	12357 (118000)	722 (2370)	No	Metal
SS 6	Radial	1150 (2100)	12357 (118000)	722 (2370)	Yes	Metal
SS 7	Radial	1370 (2500)	12357 (118000)	759 (2490)	No	Ceramic
SS 8	Radial	1370 (2500)	12357 (118000)	759 (2490)	Yes	Ceramic
SS 9	Axial	1065 (1950)	12357 (118000)	396 (1300)	Yes	Metal
SS 10	Axial	1370 (2500)	12357 (118000)	457 (1500)	Yes	Ceramic
FT 1	Rad/Ax	1205 (2200)	9425 (90000)	528 (1733)	No	Metal
FT 2	Rad/Ax	1205 (2200)	9425 (90000)	528 (1733)	Yes	Metal
FT 3	Rad/Ax	1370 (2500)	9425 (90000)	522 (1712)	No	Ceramic
FT 4	Rad/Ax	1370 (2500)	9425 (90000)	522 (1712)	Yes	Ceramic

TABLE 5.2

Engine Leakages for Performance Analysis

Leakage Path Description	Percentage of Inlet Airflow	From Station*	To Station*
Flange and Seals (Misc.)	1	3	Atmos.
Air Bearing Coolant	0.5	3	Atmos.
Turbine Rotor Coolant	0-5**	3	9(SS) 8(FT)
Regenerator			
"D" Seal	1.188	3	12
"0" Seal	0.792	3	11
Cross-Arm Seal	1.620	5	11
Total	3.600		

* Station Reference Numbers are shown in Figure 5.1.
** Refer to Table 3.4 for actual leakage rates.

The results of the off-design calculations, expressed as specific fuel consumption (sfc) vs power, are shown in Figure 5.2 for single shaft engines with radial turbines, Figure 5.3 for single shaft engines with axial turbines, and Figure 5.4 for free turbine engines. The power and sfc results are net of auxiliary and accessory power loads and reduction gearbox losses, but exclude any transmission losses. Note that the effect of VIGV's is not discernible on the sfc graph since they are only used at power levels less than about 10 percent.

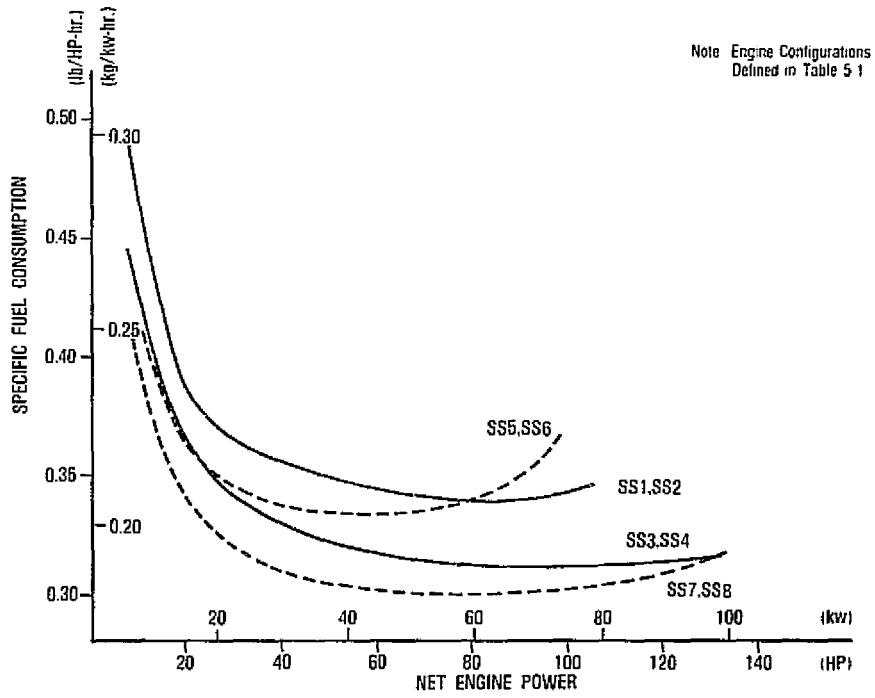


Figure 5.2 Specific Fuel Consumption vs. Horsepower of Single-Shaft Engines with Radial Turbines

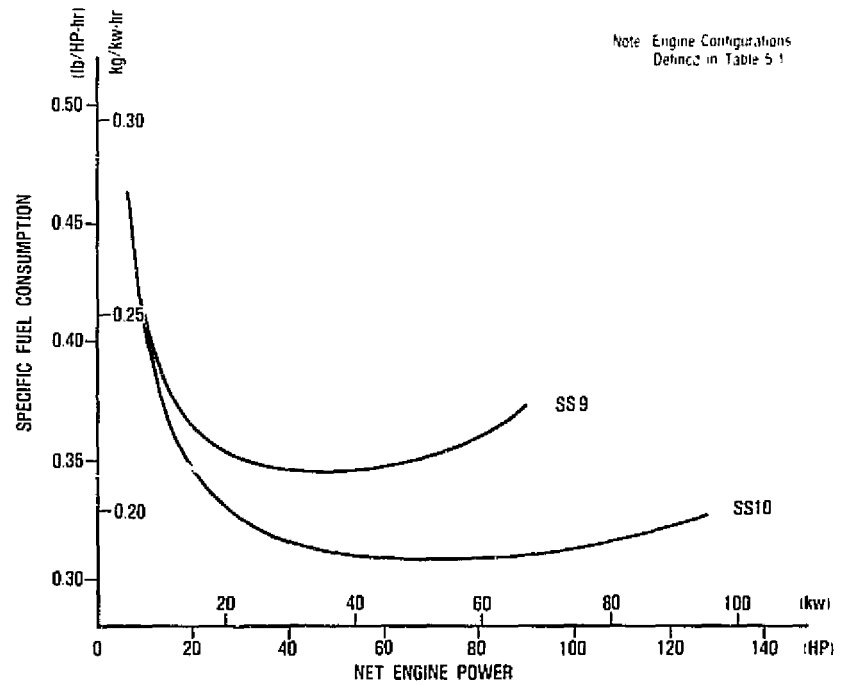


Figure 5.3 Specific Fuel Consumption vs. Horsepower of Single-Shaft Engines with Axial Turbines

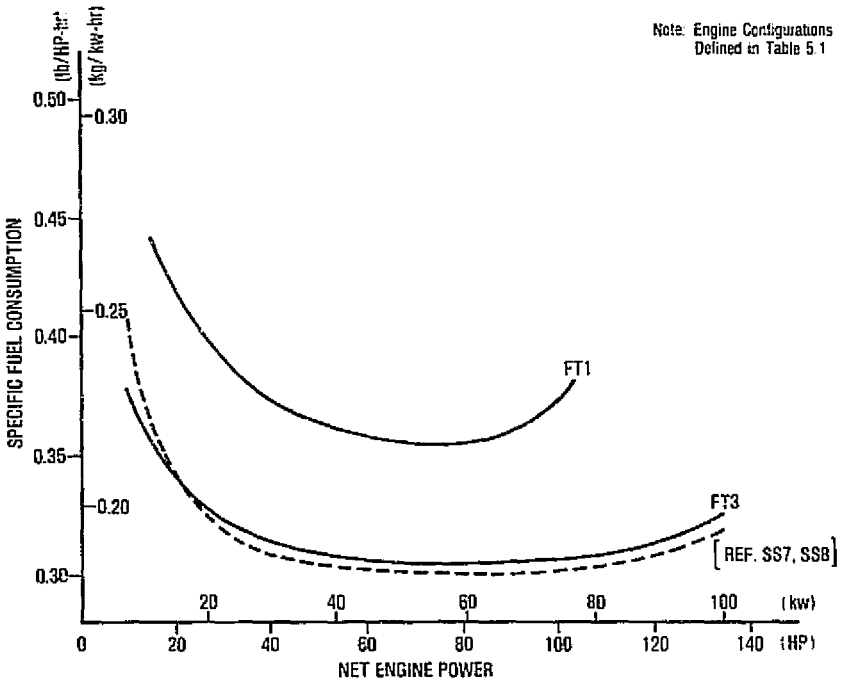


Figure 5.4 Specific Fuel Consumption vs. Horsepower of Free Turbine Engines with Variable Power Turbine Nozzles

Of interest in the comparison of single shaft machines with radial turbines, see Figure 5.2, is the effect of limiting the radial turbine tip speed. Comparing cases SS3-SS4 with SS7-SS8, it is seen that at the design speed, the maximum power and sfc is similar, but at part load the engines with the optimum turbine tip speed, SS7-SS8, have a lower sfc. This is attributable to the turbine efficiency of the limited tip speed rotor being significantly lower than that for the optimum tip speed design due to the higher inlet blading incidences at the lower speeds.

Figure 5.4 shows the sfc curve for the two free turbine engines without variable inlet guide vanes, FT1 and FT3, and for reference purposes the single-shaft, 2500°F engines SS7 and SS8 are also shown. It is seen that these engines are about comparable in performance indicating that the additional free turbine losses due to variable power turbine nozzles and the interstage ducting are not of great significance in a highly regenerative engine, see the sensitivity analysis in Section 5.6.

Table 5.3 shows the comparison of these eight engines as ranked by the sfc at 20 percent of the design power. Sfc's at 100 percent power and the minimum sfc are also included in the table.

TABLE 5.3

Engine Ranking at 20% Power, Based on SFC's

Engine Configuration*	Specific Fuel Consumption, kg/kW-hr; (lb/HP-hr) 20% Power	100% Power	Minimum sfc
SS7, SS8	0.197, (0.324)	0.194, (0.319)	0.182, (0.300)
FT3	0.198, (0.326)	0.199, (0.327)	0.185, (0.305)
SS10	0.202, (0.333)	0.199, (0.327)	0.188, (0.309)
SS3, SS4	0.211, (0.347)	0.193, (0.317)	0.189, (0.311)
SS5, SS6	0.222, (0.365)	0.223, (0.366)	0.203, (0.334)
SS9	0.223, (0.367)	0.227, (0.374)	0.210, (0.345)
SS1, SS2	0.232, (0.382)	0.211, (0.347)	0.206, (0.339)
FT1	0.253, (0.416)	0.232, (0.381)	0.216, (0.355)

* Engine configurations are defined in Table 5.1.

5.2 Vehicle Performance and Economy

Several driving simulation computer models, developed prior to the study, have been utilized to evaluate single shaft and two-shaft gas turbine engined vehicles for performance and fuel economy. Basically, the EPA urban and highway driving routes were simulated as a series of segments of constant speeds, constant accelerations, constant decelerations and idling conditions. The route economy program matches engine characteristics to the route profile with due consideration for vehicle and engine dynamic characteristics, variable ratio transmission efficiency, and other constraints specified by the user to accomplish the route requirements. Variables, such as transmission type, rear axle ratio, engine idle speed can be systematically varied to determine the best compromise between performance and economy. A different transmission and torque converter logic was required for the free turbine engine and the necessary changes were incorporated in a separate free turbine route analysis program. A total of fourteen different gas turbine engines, see Table 5.1, were evaluated in the vehicle simulation studies. For the single shaft machines the transmissions used were the variable stator torque converter with a Ford FIOD four speed gearbox (Concept 3, Section 3.11.2) and two others consisting of a differential split power arrangement utilizing either a traction drive unit (Concept 13, Section 3.11.2) or a variable stator torque converter (Concept 6, Section 3.11.2) as the variator. Transmission concept number 13 was preferred over the recommended concept number 10, see Section 3.11.5, since it scored higher and has the better potential. Additionally, the effects of changes in engine idle speed and a front wheel drive installation were evaluated. The transmission for the free turbine engines consisted of a fixed geometry, standard automotive torque converter and the Ford FIOD transmission, Concept 19, Section 3.11.2.

Fuel economy over the Combined Federal Driving Cycle (CFDC) is calculated from the expression:

$$CFDC = \frac{1}{\frac{0.55}{UDC\ (C - H)} + \frac{0.45}{HDC}} \quad km/l,\ (mpg)$$

where:

UDC (C − H) = average of a cold and hot start for the EPA Urban Driving Cycle (UDC), fuel economy, km/l, (mpg).

HDC = EPA Highway Driving Cycle, fuel economy, km/l, (mpg).

The computer program does not differentiate between a cold start and a hot start for the UDC driving cycle. Therefore, UDC (C − H) is calculated by making an allowance based on a piston engine correlation, as follows:

$$UDC\ (C - H) = (0.93)\ X\ UDC$$

Vehicle performance is represented by three criteria,

- engine response time in accelerating from idle speed to maximum speed with an average accessory load and the normal transmission drag, (depends upon type of transmission and mode of operation)
- 4 second distance, which is the distance the vehicle travels starting from rest with the engine at idle, then assuming instantaneous application of wide open throttle.
- 0-96.5 km/hr (0-60 mph) acceleration time, assuming the same initial conditions as the 4 second distance case.

The performance results that are presented assume that for the single shaft engine, accelerations are accomplished by first accelerating the engine to 100% speed and then accelerating the vehicle. This is probably the optimum method for minimizing the 0-96.5 km/hr (0-60 mph) time but it would no doubt result in an unsatisfactory vehicle for the normal accelerations encountered in urban driving. More likely to be suitable is some degree of power splitting to partially accelerate the vehicle with the engine. This would result in a greater 0-96.5 km/hr (0-60 mph) time but the "feel" of the vehicle may be improved. The vehicle simulation computer program can be used to evaluate different degrees of power splitting, however, limitations on time did not permit including this in the study.

Table 5.4 shows the relative performance and economy of two single shaft engine designs. SS1 through SS4 represents the conservative approach which was a 9425 rads/s (90,000 rpm) engine with a

limited radial turbine tip speed. SS5 through SS8 represents an optimized design at 12357 rads/s (118,000 rpm) and a radial turbine tip speed selected for maximum turbine efficiency.

TABLE 5.4

Vehicle Performance and Economy for Single Shaft Engines with Radial Turbines

Transmission: T1; Variable Stator Torque Converter and
4-speed Ford FIOD Transmission (Concept 3, Section 3.11.2)
Vehicle Test Weight: 1542 kg, (3400 lb.)
Fuel: 3.15×10^4 MJ/m^3 (113,000 BTU/gal.)

Engine Config.**	Engine Inertia kg-m-sec^2† (lb-ft-sec^2)	Idle Speed (%)	Engine Response Time (secs)	4 Second Distance m, (ft)	Acceleration Time For 0-96.5 km/hr (0-60 mph) (secs)	CFDC Fuel Economy km/l (mpg)	CFDC Fuel Economy Improvement (%)*
SS1	0.1005, (0.727)	50	4.1	0.9, (3)	15.9	10.7, (25.1)	28
SS2	0.1005, (0.727)	50	4.1	0.9, (3)	15.9	10.8, (25.4)	30
SS1	0.1005, (0.727)	60	2.4	7.9, (26)	14.2	9.4, (22.2)	13
SS2	0.1005, (0.727)	60	2.4	7.9, (26)	14.2	10.0, (23.6)	20
SS3	0.0492, (0.356)	50	1.6	14.9, (49)	12.0	11.7, (27.5)	40
SS4	0.0492, (0.356)	50	1.6	14.6, (48)	12.1	11.9, (28.0)	43
SS5	0.0618, (0.447)	50	2.4	7.6, (25)	15.2	11.7, (27.5)	40
SS6	0.0618. (0.447)	50	2.4	7.6, (25)	15.2	12.0, (28.3)	44
SS7	0.0422, (0.305)	50	1.2	19.5, (64)	11.6	12.4, (29.2)	49
SS8	0.0422, (0.305)	50	1.2	19.5, (64)	11.6	13.0, (30.5)	56

* Improvements over the NASA piston engine baseline economy of 8.3 km/l, (19.6 mpg).

† Includes accessories, auxiliaries, gears, etc. reflected to 419 rads/sec. (4000 rpm) driveshaft input speed at 100% engine speed.

** Engine configurations are defined in Table 5.1.

Comparing the engines with metal radial turbines and with a 50 percent idle speed, the optimized designs SS5 and SS6 are significantly better than the conservative designs, SS1 and SS2, in both performance and economy. For the 4 second distance, a target of 19.5 km (64 feet) is considered acceptable and comparable to that of a piston engined vehicle which typically achieves 0-96.5 km/hr (0-60 mph) in 15 seconds. Neither of the metal turbine engines achieve this distance although they do approach the 15 second time for acceleration from 0-96.5 km/hr (0-60 mph). The fuel economy of these engines does exceed the baseline improvement goal of 20%. Increasing the idle speed of the conservative engine designs, SS1 and SS2, from 50% to 60% improves the vehicle performance but still does not provide a satisfactory 4 second distance. The associated penalty in fuel economy makes the achievement of the 20% goal marginal for the engine with inlet guide vanes, SS2, and unacceptable for the engine without inlet guide vanes, SS1.

With the ceramic rotor engines, of course, the power is significantly greater than that for the metal turbines. Consequently the performance results are much improved, however, the non-optimized designs SS3 and SS4, still fall short of meeting the goal for the 4 second distance. The optimized designs, SS7 and SS8, achieve the 19.5 km (64 feet) 4 second distance target and, are well below the 15 second acceleration time to 96.5 km/hr (60 mph) and the fuel economy improvement exceeds the target of 20 percent. It is possible that for the ceramic rotor designs SS3 and SS4, trade-offs between the fuel economy and the 4 second distance may be considered whereby the 4 second distance is increased by setting the engine to an idle speed higher than 50 percent.

The effect of different transmissions for the single shaft engine are shown in Table 5.5 for the metal and ceramic engine configurations. For the prime candidate transmission (differential split power with a 4-speed Ford FIOD gearbox and a variable stator torque converter — T2) and the optimized ceramic engine SS8, a 76 percent improvement in fuel economy over the baseline was calculated. Using the optimum transmission, (a differential split-power with a 4-speed gearbox and a variable traction drive unit — T3) an improvement in fuel economy of 93 percent was calculated for engine configuration SS8. For the transmission consisting of the 4-speed Ford FIOD gearbox and the variable stator torque converter, configuration T1, with engine SS8, the fuel economy improvement is calculated to be 56 percent and also exceeds the highest objective, which was an improvement of 50 percent. The 4 second start-up distances with transmissions T2 and T3 well exceed the requirement of 19.5 km (64 ft.), and with transmission T1 the requirement is just met.

With the transmissions T2 and T3 the improvements in fuel economy are attributed to the higher overall transmission efficiencies, especially at the lower vehicle speeds, and the capability of declutching at idle. Declutching at idle reduces the drag on the engine and hence lowers the idle fuel flow.

For the optimized metal engine SS6, transmission T1 was considered to be unacceptable. With transmission T3, the idle speed of the engine SS6 would have to be raised to improve the 4 second start-up distance, which would result in a trade-off with the fuel economy. It is anticipated that a satisfactory trade-off could be accomplished for engine SS6 with transmission T3 to meet the objectives. No calculations were made for engine SS6 with transmission T2 because it was not considered likely to meet the objectives, based on a comparison with engine SS8.

TABLE 5.5

Effect of Transmission Type on Vehicle Performance and Economy with Single Shaft Engines

Engine Config.**	Transmission Type	Engine Response Time (Secs.)	4 Second Distance m (ft.)	Accel. Time 0-96.5 km/hr (0-60 mph) (Secs.)	CFDC Fuel Economy km/l, (mpg)	CFDC Fuel Economy Improvement (%)*
SS6	T1	2.4	7.6, (25)	15.2	12.0, (28.3)	44
SS6	T3	2.0	16.2, (53)	12.6	14.8, (34.9)	78
SS8	T1	1.2	19.5, (64)	11.6	13.0, (30.5)	56
SS8	T2	1.3	21.0, (69)	10.1	14.7, (34.5)	76
SS8	T3	1.1	25.6, (84)	9.1	16.1, (37.9)	93

where:

T1 = Variable Stator Torque Converter with 4 speed Ford FIOD Transmission (concept 3, Section 3.11.2).

T2 = Differential Split-power, 4-Speed Ford FIOD with Variable Stator Torque Convertor (Concept 6, Section 3.11.2).

T3 = Differential Split-power, 4-Speed Transmission with Variable Ratio Traction Drive Unit (Concept 13, Section 3.11.2).

* Improvement over the NASA piston engine baseline economy of 8.33 km/l, (19.6 mpg).

** Engine configurations are defined in Table 5.1.

Table 5.6 shows the effect of using axial instead of radial turbines. The most significant improvement that is noted from this comparison is in the short time performance results, i.e. response time and 4 second distance. This is mainly attributable to the reduced inertia of a 3 stage axial turbine compared

to the equivalent radial turbine. The reason that the 0-96.5 km/hr (0-60 mph) acceleration time does not reflect the initial performance advantage is due to the lower power of the axial machines. In the case of the metal machines, SS6 (radial) and SS9 (axial), the uncooled axial turbine is limited to 1065°C (1950°F) turbine inlet temperature compared to 1150°C (2100°F) for the cooled radial turbine. This results in the maximum power of the axial machine being 7.4 percent lower. In the case of ceramic machines, SS8 (radial) and SS10 (axial), the axial turbine efficiency is 2.3 percentage points lower due to allowances which had to be made for blade trailing edge blockages. This resulted in the maximum power of the axial machine being 4.8 percent lower.

TABLE 5.6

Effect of Axial and Radial Turbines on Vehicle Performance and Economy with Single Shaft Engines

Transmission: T1; Variable Stator Torque Converter and 4-Speed Ford FIOD Transmission

Engine Config.**	Engine Inertia† kg-m-sec² (lb-ft-sec²)	Engine Response Time (Sec.)	4 Second Distance m (ft.)	Accel. Time 0-96.5 km/hr (0-60 mph) (Secs.)	CFDC Fuel Economy km/l (mpg)	CFDC Fuel Economy Improvement*(%)
SS6 (Radial)	0.0618, (0.447)	2.4	7.6, (25)	15.2	12.0, (28.3)	44
SS9 (Axial)	0.0377, (0.273)	1.7	12.2, (40)	15.5	12.1, (28.5)	45
SS8 (Radial)	0.0422, (0.305)	1.2	19.5, (64)	11.6	13.0, (30.5)	56
SS10 (Axial)	0.0308, (0.223)	0.9	21.9, (72)	11.6	12.6, (29.6)	51

* Improvement over the NASA piston engine baseline economy of 8.3 km/l, (19.6 mpg).

† Includes accessories, auxiliaries, gears, etc. reflected to 419 rads/sec (4000 rpm) driveshaft input speed at 100% engine speed.

** Engine configurations are defined in Table 5.1.

Comparison of the fuel economy figures of Table 5.6 reveals that the ceramic axial turbine engine SS10, is somewhat worse than the ceramic radial turbine engine, SS8. This is due to the lower efficiency of the axial turbine as explained above.

The difference between a front wheel drive and rear wheel drive installation is almost insignificant. Due to the greater weight on the driving wheels, the front wheel drive vehicle had an advantage of about 2 percent in the 4 second distance and 0-96.5 km/hr (0-60 mph) time.

The performance and fuel economy comparison between single shaft and free turbine engines was made by adjusting the idle speed of the free turbine engine to approximately match the 4 second distance and 0-96.5 km/hr, (0-60 mph) time criteria of four of the single shaft engine/transmission configurations. Table 5.7 shows that comparison. Comparing the ceramic free turbine configuration, FT4, with the ceramic single shaft engine, SS8, and the advanced T3 transmission, shows that for almost equal performance the single shaft configuration is about 23 percent better in fuel economy. This difference is mainly attributable to the higher idle speed (60 percent) required for the free turbine engine compared to the single shaft engine (50 percent) in order to match the vehicle performance. As can be seen from Figure 5.4 the specific fuel consumption of these two engines is about the same.

The best fuel economy for the free turbine engines (FT1 and FT3) was obtained without the use of the variable inlet guide vanes. This was attributable to the, consequently, lower idle speed, and hence idle fuel flow, of the gas generator. However, as a consequence of the lower idle speed some loss in performance was incurred. No further work was done in comparing the free turbine engine due to the other disadvantages of this configuration, see the cost comparisons in Table 5.17, and also because of the time limitations of the study.

TABLE 5.7

Comparison of Vehicle Performance and Economy for Single Shaft and Free Turbine Engines

Engine Config.**	Transmission Type	Idle Speed (%)	4 Second Distance m, (ft.)	Accel. Time 0-96.5 km/hr (0-60 mph) (secs.)	CFDC Fuel Economy km/l, (mpg)	CFDC Fuel Economy Improvement* (%)
FT1	T4	49	7.9, (26)	14.4	11.9, (27.9)	42
SS5	T1	50	7.6, (25)	15.2	11.7, (27.5)	40
FT2	T4	60	15.2, (50)	12.7	10.1, (23.7)	21
SS6	T3	50	16.2, (53)	12.6	14.8, (34.9)	78
FT3	T4	56	21.6, (71)	9.5	14.6, (34.3)	75
SS7	T1	50	19.5, (64)	11.6	12.4, (29.2)	49
FT4	T4	60	25.6, (84)	9.1	13.1, (30.8)	57
SS8	T3	50	25.6, (84)	9.1	16.1, (37.9)	93

where:

T4 = Fixed Geometry Torque Converter with 4-speed Ford FIOD transmission. (Concept 19, Section 3.11.2.)

* Improvement over the NASA piston engine baseline economy of 8.3 km/l, (19.6 mpg).

** Engine configurations are defined in Table 5.1.

5.3 Engine Layout Studies

Powertrain configuration studies were conducted on three engine concepts of the Improved Gas Turbine (IGT) which were described in section 5.1, namely:

1. Two versions of a single-shaft turbine each with both a ceramic and metallic radial inflow turbine rotor.
   - 12357 rads/s, (118,000) rpm shaft speed and 722-759 m/s (2370-2490 fps) turbine tip speed, and
   - 9425 rads/s, (90000 rpm) shaft speed and 610 m/s (2000 fps) turbine tip speed.

2. Single-shaft turbine with a 3-stage ceramic axial turbine rotor, 12357 rads/s, (118,000 RPM) shaft speed and 457 m/s (1500 fps) mean turbine blade speed, and

3. A two-shaft free turbine concept with a radial inflow gasifier turbine and a variable geometry axial power turbine stage, both either ceramic or metallic.

The 12357 rads/s (118,000 RPM) version of a single shaft turbine with a high tip speed radial rotor represents an optimum aerodynamic design for the compressor and turbine rotors resulting in an optimum specific speed for the compressor and an optimum efficiency for the turbine rotor. The high tip speed design will require maximum utilization of material, and thus imposes very stringent demands on strength and quality control in the turbine rotor. The 9425 rads/s, (90000 RPM) version with a 610 m/sec tip speed represents a more conservative approach to material strength requirements and as such was originally selected as a more practical starting point for engine development even though it entailed a loss in fuel economy. Later studies have shown, however, that the increased spool inertia of the lower speed engine version resulted in an unacceptable compromise in performance. This loss in performance combined with the loss in overall efficiency swayed the decision in favor of the higher speed version of the engine.

Preliminary design layouts of three (3) engine concepts were generated in sufficient detail to describe the concept and perform system cost comparisons. Time and funding did not permit to do a

comparable design study of a variable geometry power turbine stator assembly for the free turbine engine suitable for both ceramic and metallic construction. Consequently, this aspect of the free turbine engine concept was evaluated on the basis of Ford's past experience with metallic versions of variable geometry for larger vehicular engines.

Although preliminary layouts were generated for all engine concepts, only the optimum speed version of the single-shaft radial wheel concept and its adaptation to a 3-stage axial turbine rotor configuration are shown in this report. These two concepts have been studied for considerable time at Ford Motor Company prior to this contract and their design has reached a fairly advanced stage as far as conceptual studies are concerned.

The outstanding feature of this Ford IGT engine, the cross section of which is shown in Figure 5.5, is its mechanical and thermal symmetry which favors ceramics, allows use of lighter structures and results in a very lightweight engine. Preliminary calculations estimate the weight of engine proper without the speed reducer at 68 kg (150 lb) or 90-105 kg (200-230 lb) with the speed reducer and accessory drive. Compressor inlet separates the hot section of the engine from the oil lubricated mechanical drive unit that is comprised of speed reducer, accessory drive, variable stator torque converter and the transmission. The combustor, a scaled ceramic version of Ford's variable geometry, low emissions combustor, and the regenerator are arranged coaxially with the main spool which is supported at the turbine end by an air lubricated foil bearing. The other support of the spool is provided by the planetary gear arrangement. Spool thrust is taken up by an oil lubricated spiral groove (Whipple type) thrust bearing located at the gear end of the spool. The entire hot flowpath is ceramic. Because of rotational symmetry of the flowpath its components are composed of shapes simple to fabricate by a variety of ceramic processes. The hot flowpath is amply insulated from relatively cool compressor discharge air which shrouds the entire engine. The configuration offers great flexibility for development as it is easily adaptable to an axial turbine arrangement, a stationary heat exchanger of annular, doughnut configuration and to variable compressor and turbine geometries.

Two basic configurations of the powertrain-drive utilizing the above engine concept were studied.

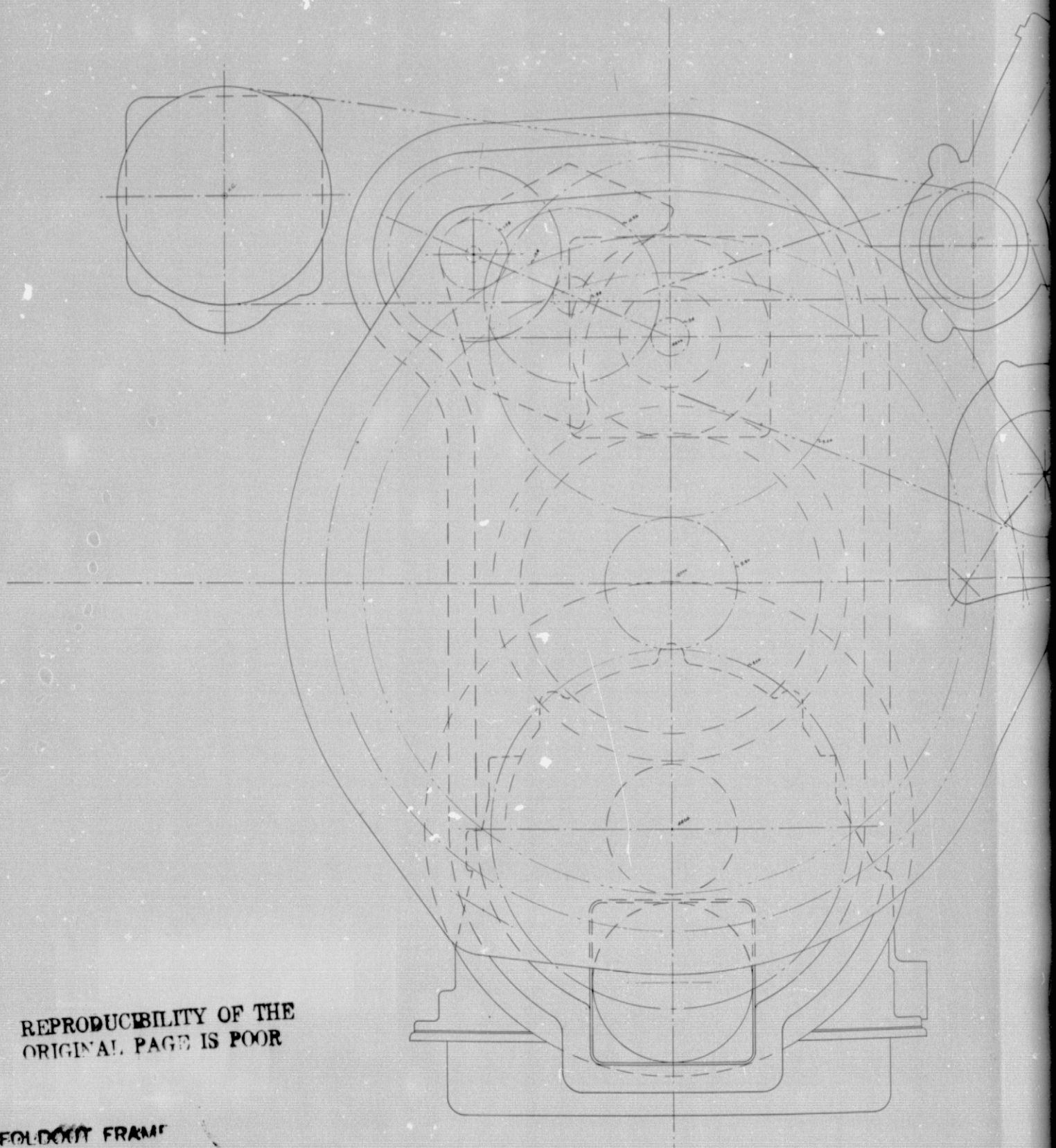
a. An in-line arrangement shown in Figure 5.5, with the transmission offset by way of speed-reducer drop-box to facilitate conventional rear wheel drive installation, and
b. a folded drive arrangement shown in Figure 5.6, with the transmission arranged parallel to engine centerline. This arrangement offers more installation flexibility as it readily adapts to a front wheel drive configuration with only minor modifications to the existing Ford C4 transmission.

Figure 5.7 shows a design adaptation of the engine to the lower speed 9425 rads/s, (90000 RPM) spool configuration discussed earlier, while Figure 5.8 is an adaptation of the same engine to a 3-stage axial turbine rotor configuration. The inherent flexibility of the Ford engine concept is clearly demonstrated in the ease with which it adapts to a completely different rotor and flowpath configurations with no change to the outside engine envelope and only minor modifications to few ceramic structural components.

5.4 Mechanical Design Analysis

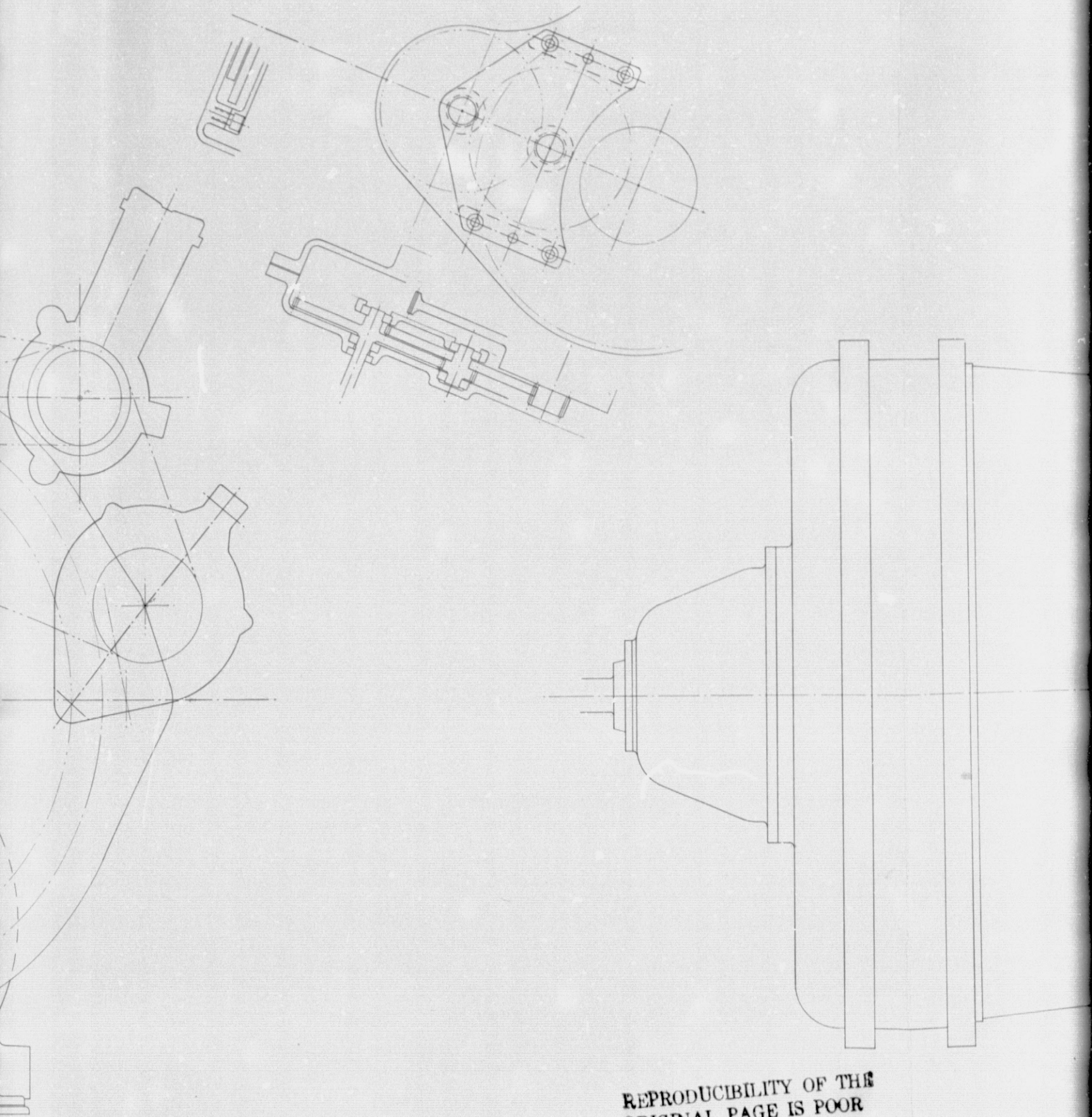
In the course of engine design, preliminary analyses were conducted on key engine components to define their geometry and/or verify their theoretical feasibility from the mechanical integrity stand point.

Over the past few years Ford Motor Company has been conducting detailed mechanical design studies of advanced high tip-speed (760 m/s) radial inflow turbine rotors in both ceramic and metallic configurations. These studies, made within the design constraints of Ford's IGT engine concept, and therefore relevant to the current program, have shown 760 m/s tip-speed turbine rotors to be mechanically feasible insofar as the stresses generated within the rotor at the full power point steady state operation were found to be within the strength capabilities of existing materials, ceramics as well as superalloys,which was the controlling criterion at this stage of the study. An implicit assumption was being made in these studies that with appropriate R&D these strength levels, measured in test coupons, were realizable in fabricated to shape rotors.



REPRODUCIBILITY OF THE
ORIGINAL PAGE IS POOR

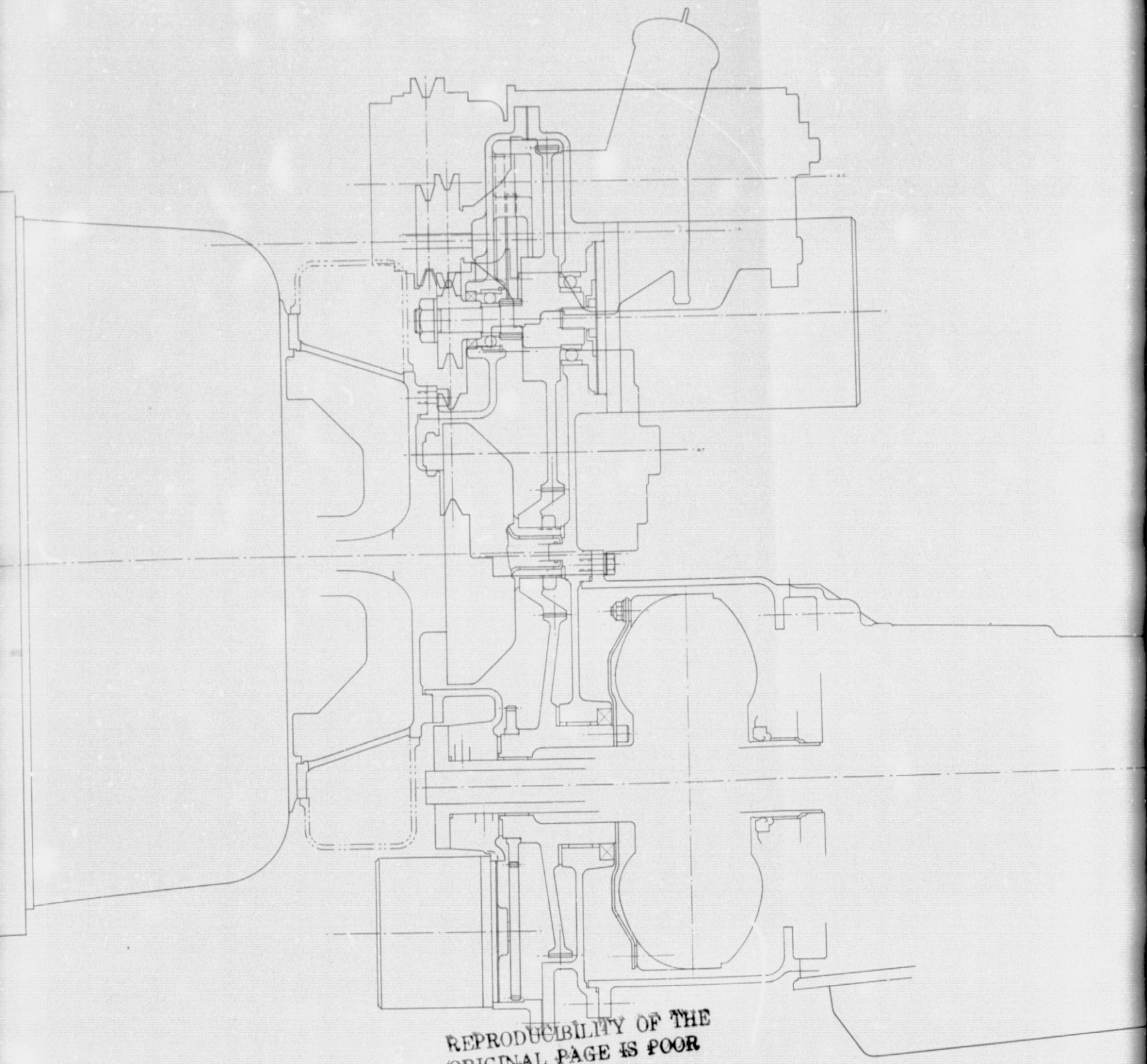
FOLDOUT FRAME



REPRODUCIBILITY OF THE
ORIGINAL PAGE IS POOR

2 FOLDOUT FRAME

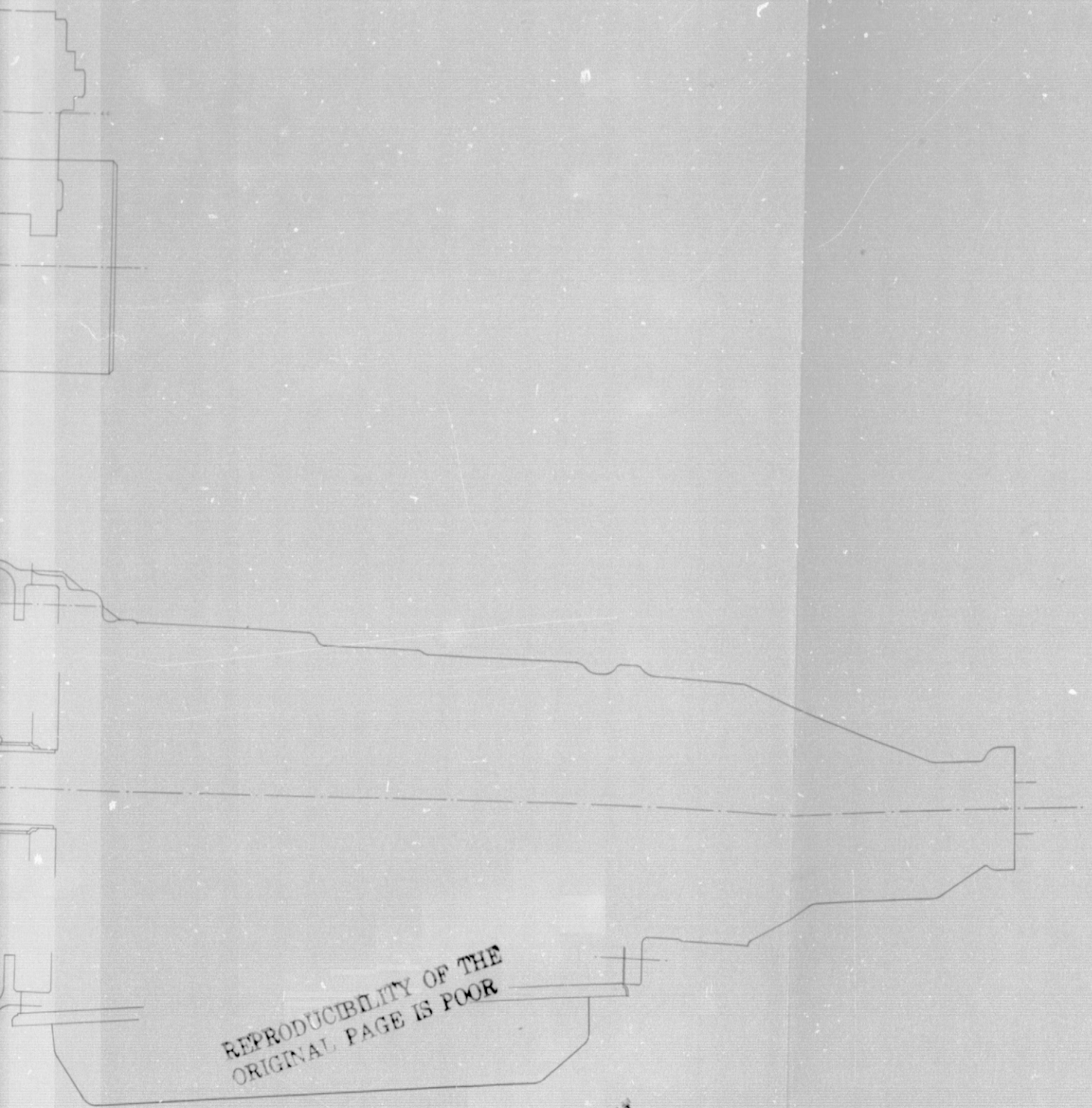
Figure 5.5 Inline Arrangement of Ford IGT Engine



REPRODUCIBILITY OF THE
ORIGINAL PAGE IS POOR

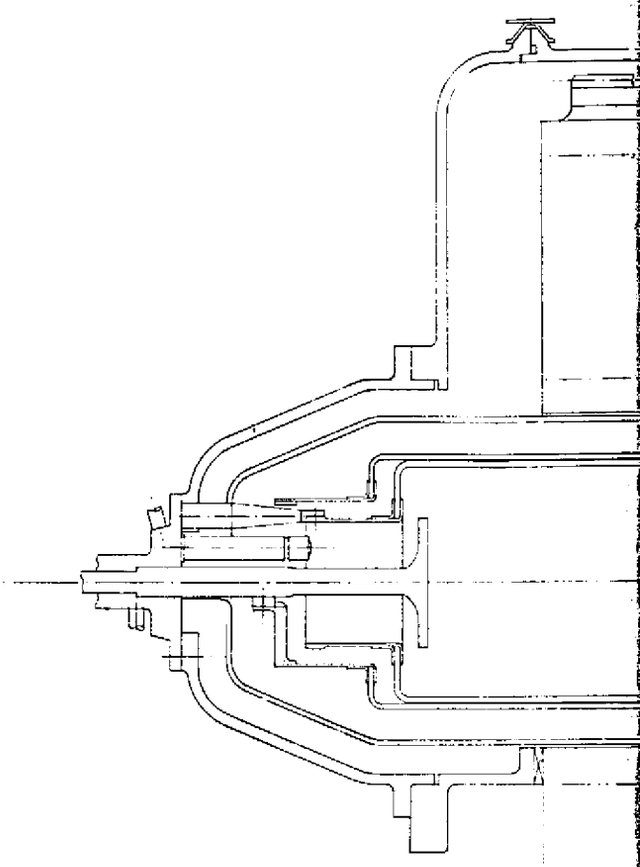
3

FOLDOUT FRAME



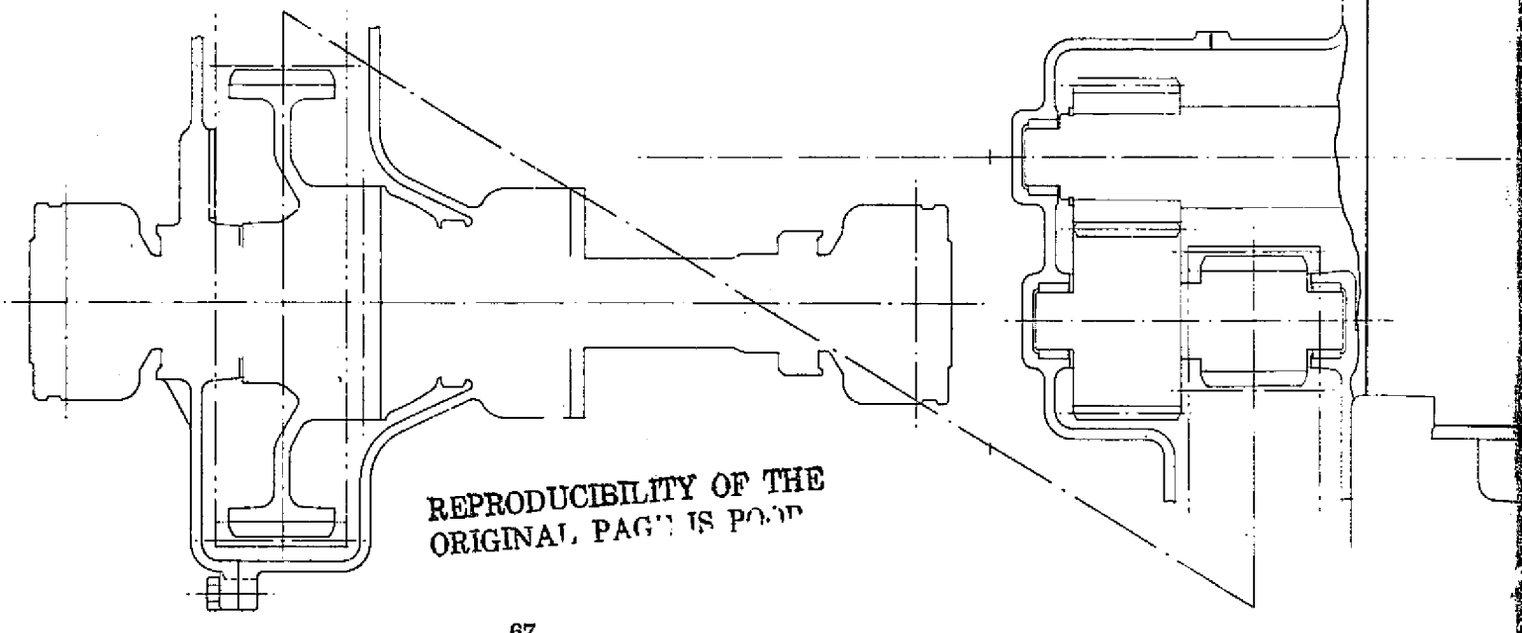
REPRODUCIBILITY OF THE
ORIGINAL PAGE IS POOR

FOLDOUT FRAME 4



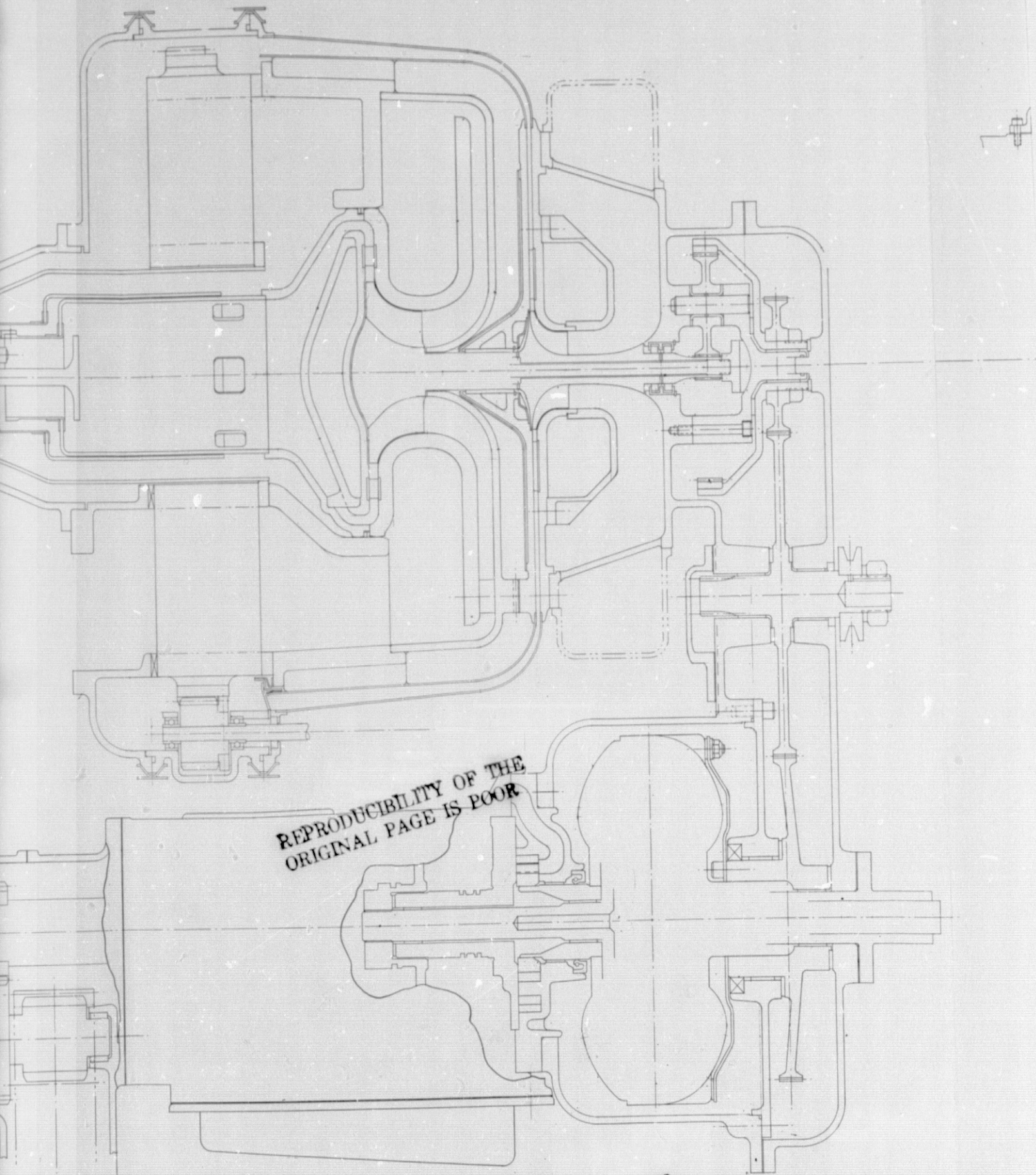
PRECEDING PAGE BLANK NOT FILMED

PRECEDING PAGE BLANK NOT FILMED



REPRODUCIBILITY OF THE
ORIGINAL PAGE IS POOR

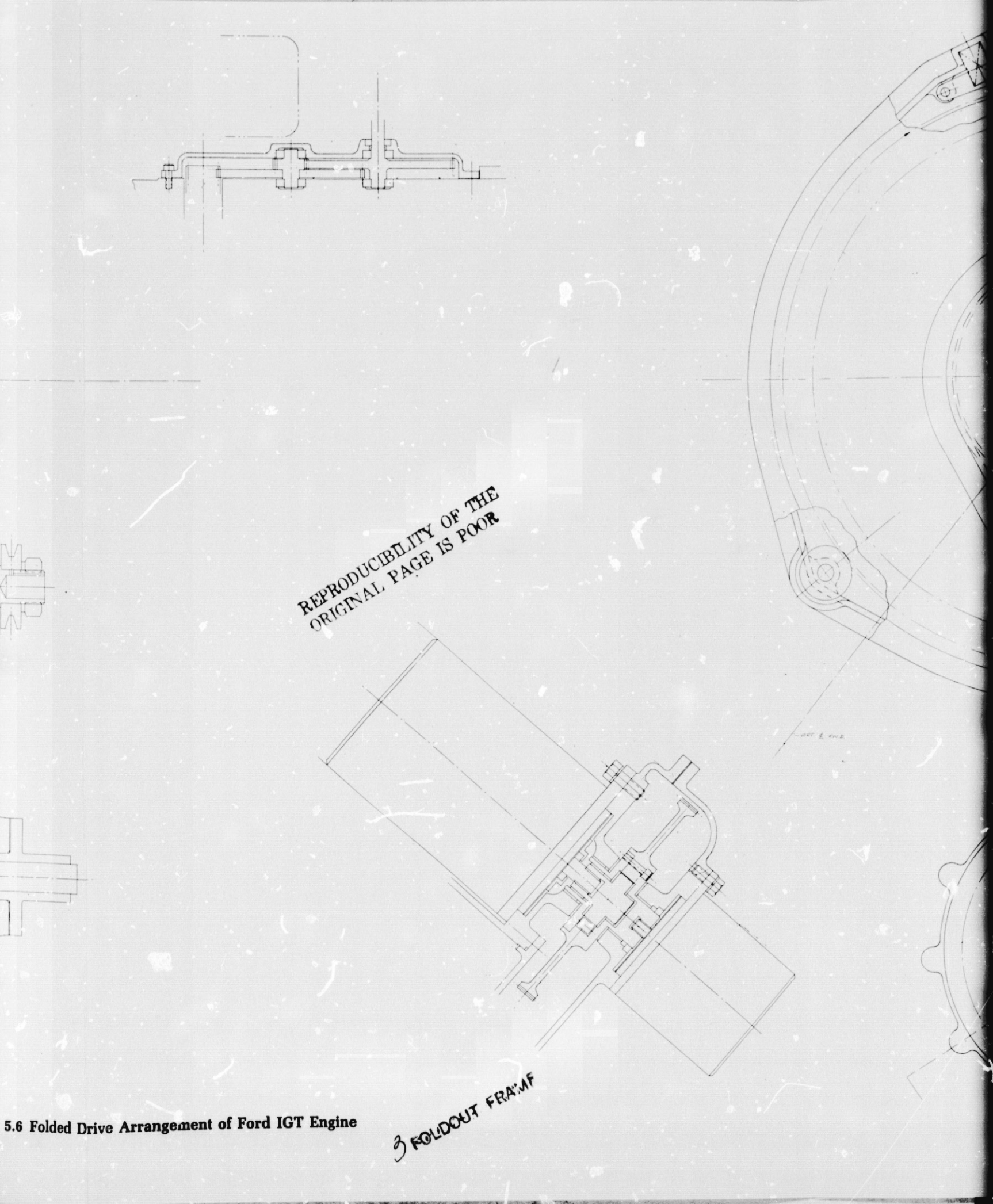
FOLDOUT FRAME



REPRODUCIBILITY OF THE
ORIGINAL PAGE IS POOR

FOLDOUT FRAME 2

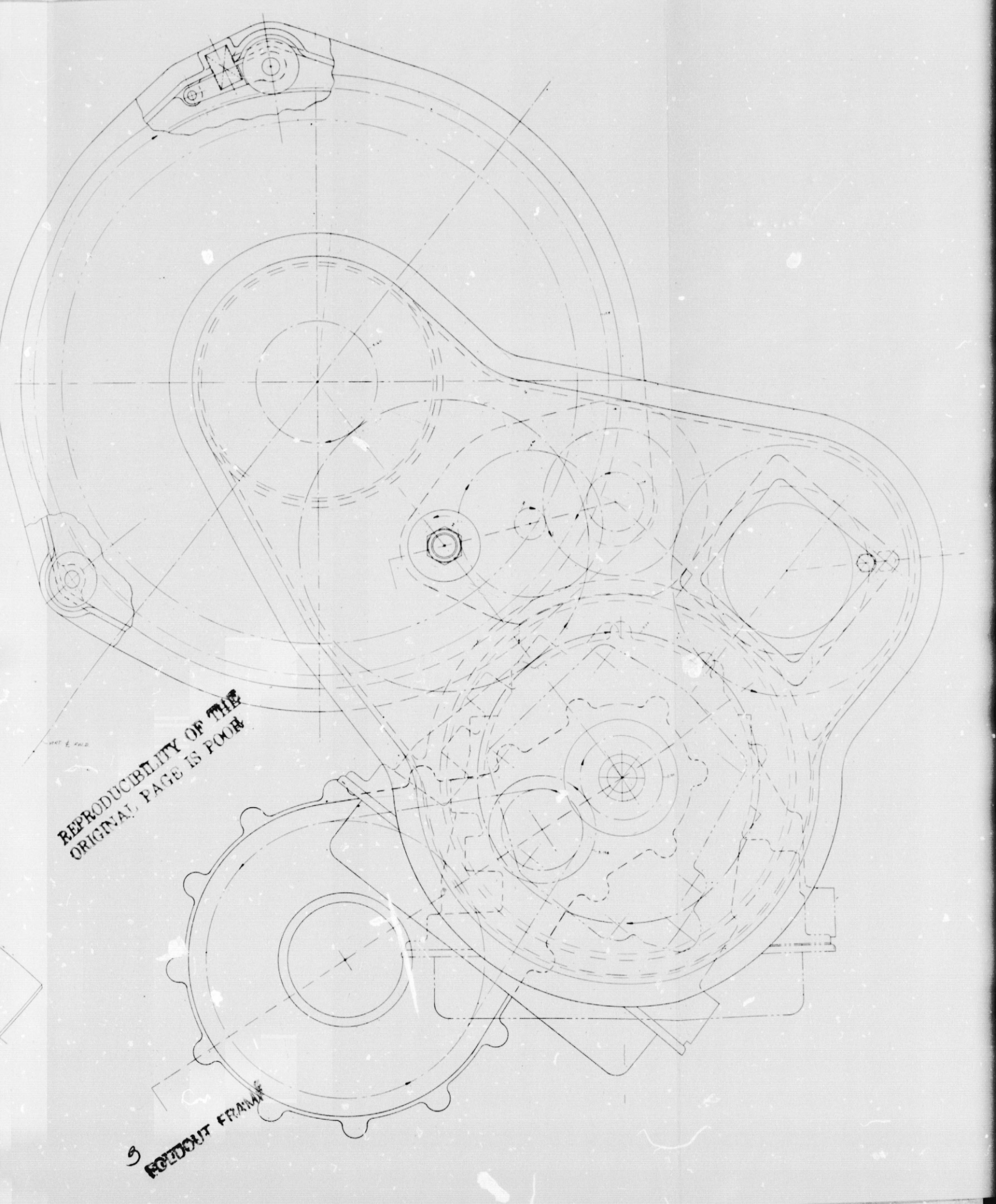
Figure 5.6 Folded Drive Arrangeme



REPRODUCIBILITY OF THE
ORIGINAL PAGE IS POOR

5.6 Folded Drive Arrangement of Ford IGT Engine

3 FOLDOUT FRAME



REPRODUCIBILITY OF THE
ORIGINAL PAGE IS POOR

3 FOLDOUT FRAME

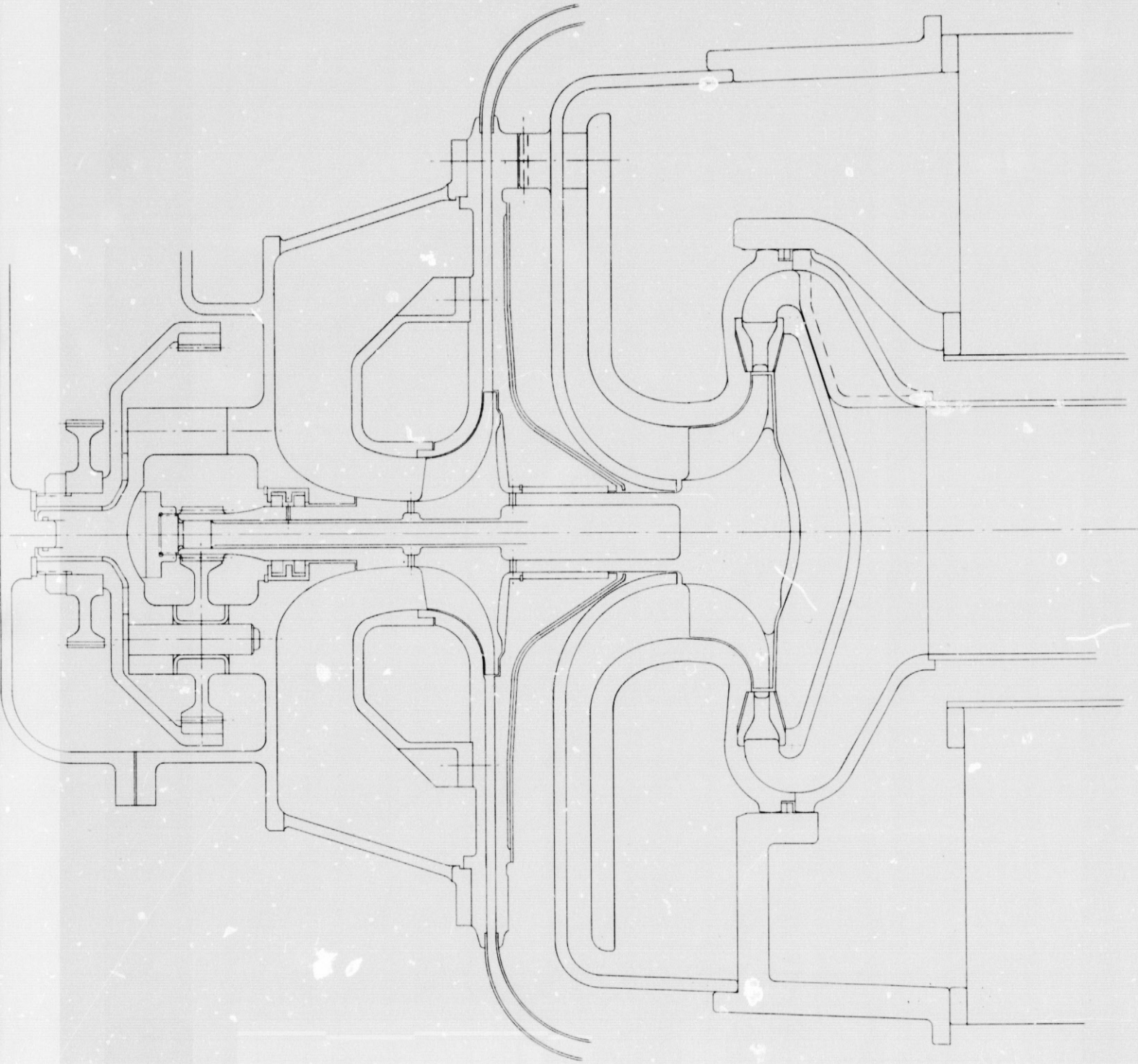


Figure 5.7 Design Adaptation of IGT Engine to 9425 Rad/s (90,000 rpm) Spool Configuration

PRECEDING PAGE BLANK NOT FILMED

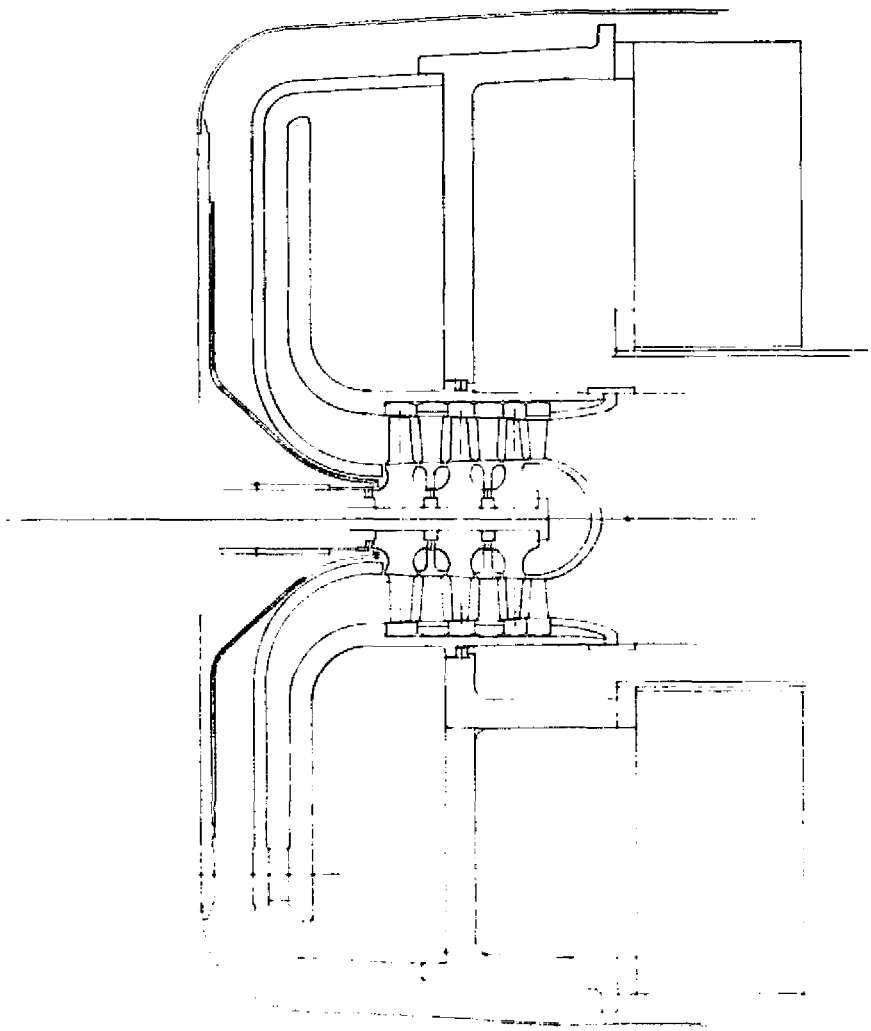


Figure 5.8 Design Adaptation of IGT Engine to 3-Stage Axial Turbine Configuration

During the initial phase of the conceptual study program concern was expressed as to the mechanical integrity of the rotor, ceramic in particular, under transient conditions that prevail in a vehicular application. AiResearch experience with radial inflow turbine rotors in aerospace applications does indicate the transients to be the most common cause of rotor failures. Consequently a transient loading considered to represent the most severe case likely in an automotive application was defined and a transient analysis performed on a ceramic version of the rotor to check its mechanical integrity.

The results of this transient analysis along with the steady state results obtained earlier for ceramic and metallic rotor concepts are shown in Figures 5.9 to 5.13. Figure 5.9 shows steady state temperature and stress contour maps for an eleven-vaned, 760 m/s (2495 fps) tip speed, ceramic radial turbine rotor at full power operation, 1370°C (2500°F) TIT and 12357 rads/s (118,000 rpm). Physical properties used in the analysis were those of NC-132 hot pressed Si_3N_4. Because of the way the hot flowpath components are arranged in the Ford IGT engine concept, thermal stresses in the rotor are minimized, so that the rotor configuration is governed primarily by centrifugal loading. For this reason it is anticipated that in a SiC-version of the same rotor, with the theoretical density of these two materials being equal, the steady state stress levels will be not much different than for the hot pressed Si_3N_4 rotor and consequently the conclusions as regards strength requirements will be same for both materials.

Results of transient analysis for a hot pressed Si_3N_4 radial rotor are shown in Figures 5.10 and 5.11. The transient considered consisted of a step acceleration from low fuel flow idle 570°C (1050°F) TIT and 6177 rads/s (59,000 rpm) to full power 1370°C (2500°F) TIT and 12357 rads/s (118,000 rpm) and

held for 11 sec., when the vehicle supposedly has reached 96.5 km/hr (60 mph) followed by a step deceleration to 1220°C (2225°F) TIT and 8030 rads/s (76,700 rpm). Effects of prolonged full power acceleration were also studied and are depicted by dotted lines. Figures 5.10 and 5.11 show respectively changes of temperatures and stress with time in the critical areas of the rotor identified in Figure 5.9. The maximum transient stresses in the two critical areas of the hub, i.e. near the axis of rotation (point 1) and at the vane fillet (point 6) are shown to increase 15 to 25% over the steady state values respectively. Using Ford test data on NC-132, probabilities of failure were estimated for steady state at $3x10^{-5}$ and for the peak transient case at $2x10^{-4}$ both of which are well within the assumed allowable of $1x10^{-2}$.

As mentioned in previous Sections, a metallic rotor operating at TIT between 1150-1205°C (2100-2200°F) provides an attractive intermediate solution. To check the mechanical feasibility of such a concept the design study was extended to metallic rotors. Figure 5.12 shows temperature and stress distributions for a ten-vaned, 722 m/s. (2370 fps) tip speed, uncooled metallic rotor at 1205°C (2200°F) TIT. Indicated below the isotherm values are the corresponding average limits for 100 hr. stress rupture (S_T) and 100 hr. 1% creep (S_C) for IN-100 alloy. These two criteria provide a measure of the mechanical strength and integrity of the rotor under steady state operation. Superposition of stress and strength distributions reveals that either the stresses or the temperatures in the rotor at full power loading are too high for the IN-100 alloy. Consequently, an uncooled 1150°C (2100°F) TIT and a cooled, 1205°C (2200°F) TIT versions were studied. The temperature/strength distributions for these are shown in Figure 5.13. As mentioned earlier, because of the way the turbine rotor is mounted in the Ford engine concept, the stresses in the rotor are predominantly centrifugal. Indeed the stresses for the uncooled 1150°C (2100°F) TIT case were found to be not much different than for the uncooled 1205°C (2200°F) case shown in Figure 5.12. It became, therefore, evident that in order for a metallic rotor to be a viable candidate for 1150-1205°C (2100-2200°F) TIT operation, it will need to be air cooled. As shown in Figure 5.13, a simple cooling scheme consisting of a circular conduit under each vane flowing 0.1% of compressor discharge air, does lower the temperature adequately to make the concept mechanically feasible. The effects of localized stress concentrations around the conduits could not be evaluated in this study for lack of adequate low cycle fatigue (LCF) data. Although peak stresses fall below .2% offset yield strength, the LCF is a more appropriate criterion to be used in this case in view of the transient nature of rotor operation (starts and accelerations).

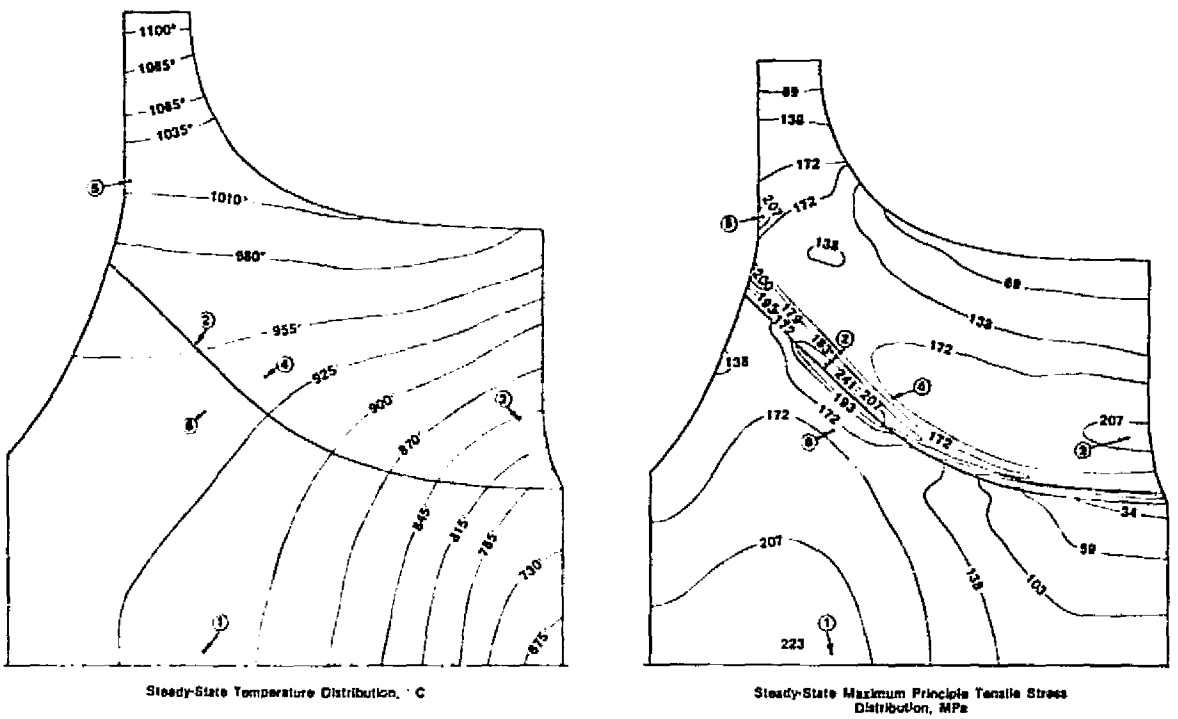


Figure 5.9 Ceramic Radial Inflow Turbine at 1370°C (2500°F) and 12357 Rads/s (118,000 rpm)

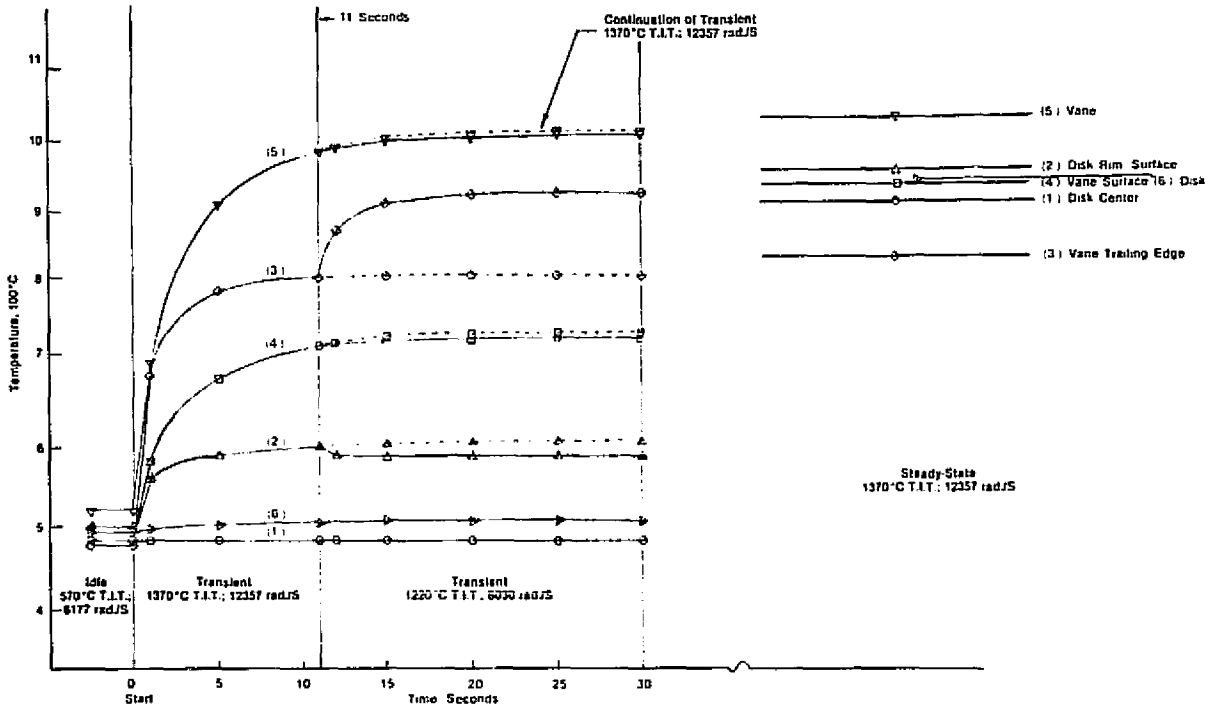


Figure 5.10 Change of Temperature with Time at Full Power Acceleration from Low Fuel Idle for Ceramic Radial Turbine

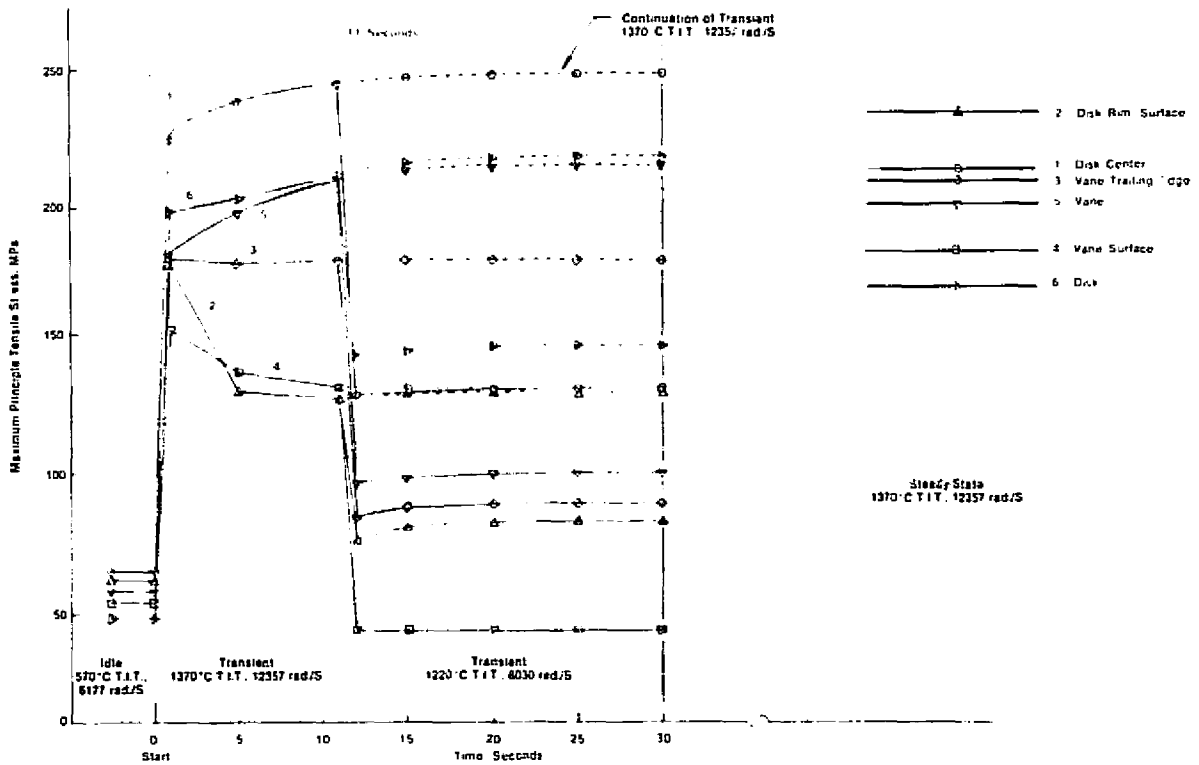


Figure 5.11 Change of Maximum Principle Tensile Stress at Full Power Acceleration from Low Fuel Idle for Ceramic Radial Turbine

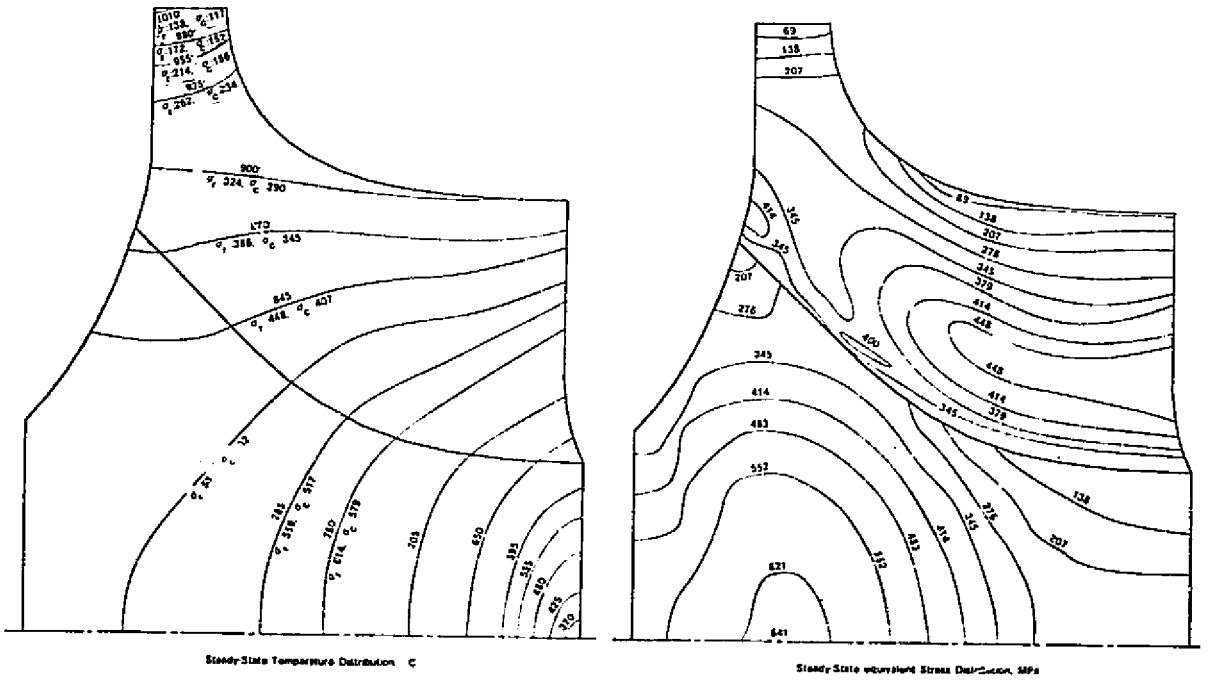


Figure 5.12 Uncooled Metallic Radial Inflow Turbine at 1200°C (2200°F) T.I.T. and 12357 Rads/s (118,000 rpm)

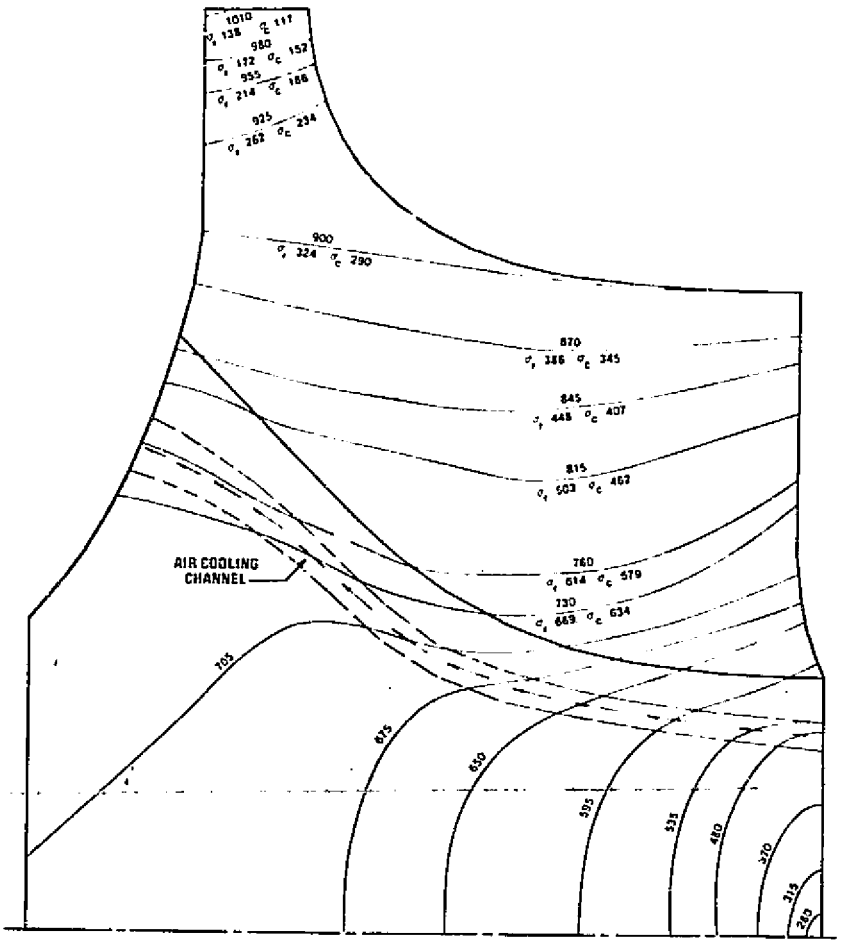


Figure 5.13 Temperature Distribution for the Cooled Metallic Radial InflowTurbine at 1200°C (2200°F) T.I.T. and 12357 Rads/s (118,000 rpm) — (0.1% Coolant Flow)

The transient analysis of the metallic rotor was outside the scope and funding of the current program. It is anticipated that as a result of LCF and transient studies both the cooling conduit geometry and its location may require modification as no attempt was made in the current studies at optimizing these.

As an alternate concept to a single stage radial inflow turbine rotor a three-stage, ceramic axial rotor was sized and analyzed. Again no attempt was made in the current study at optimizing its configuration. The results of this analysis are presented in Figures 5.14 through 5.17 which show the temperature and stress distributions at full power, 1370°C (2500°F) TIT and 12357 rads/s (118000 rpm), for each of the rotor stages respectively. The disk configurations presented are of a duo-density concept, deemed the more appropriate for axial rotors, where a monolithic blade ring made of reaction bonded Si_3N_4 is chemically attached to a hot pressed Si_3N_4 disk. Physical properties used in the study for the hot

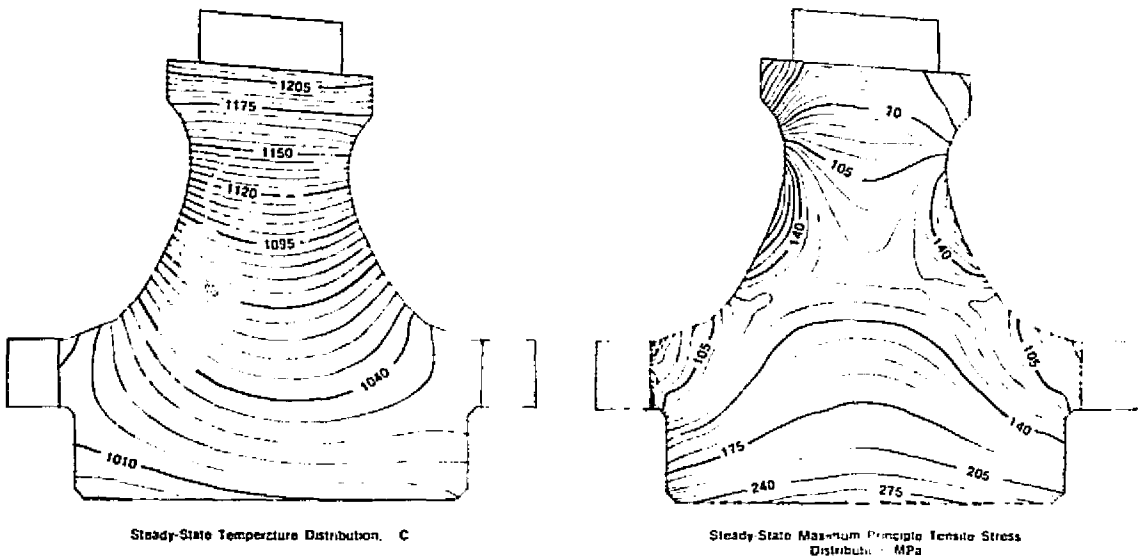
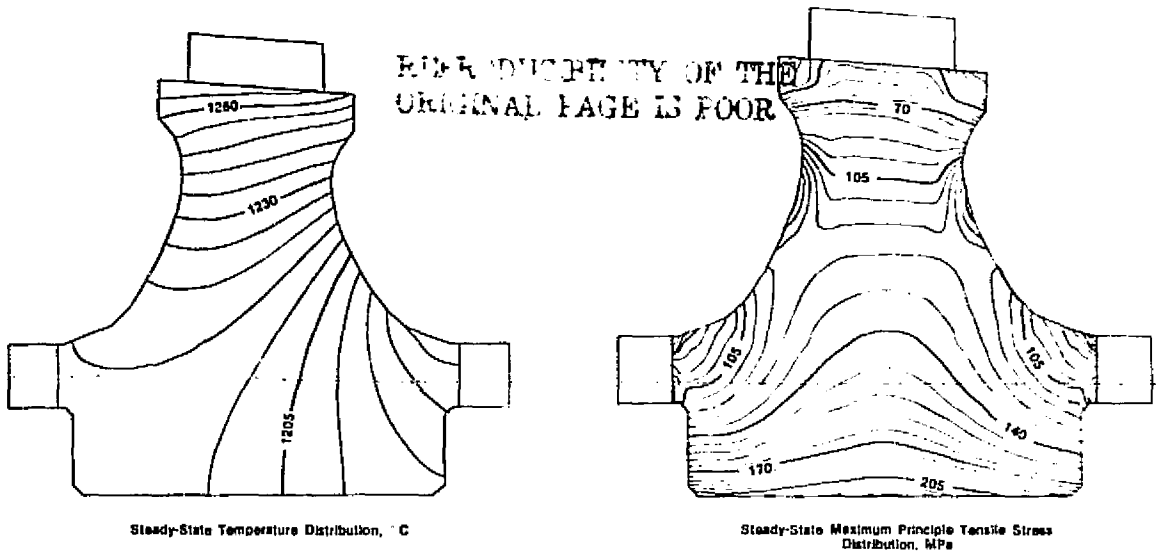


Figure 5.14 First Stage Ceramic Axial Turbine Disk at 1370°C (2500°F) T.I.T. and 12357 Rads/s (118,000 rpm) — (Cooled Metallic Bolt)



BEST QUALITY OF THE ORIGINAL PAGE IS POOR

Figure 5.15 First Stage Ceramic Axial Turbine Disk at 1370°C (2500°F) T.I.T. and 12357 Rads/s (118,000 rpm) — (Ceramic Bolt)

pressed Si_3N_4 were those of NC-132. Two bolting concepts were studied; a more conventional concept with a cooled metallic bolt (Figure 5.14) and an alternate concept with an uncooled ceramic attachment, the analytical results for which are shown in Figure 5.15 through 5.17. Elimination of bolt cooling reduces drastically the radial temperature gradients and the resulting stresses. It does, however, increase the material temperature, particularly in the first stage, to a point where time-dependent phenomena such as subcritical crack growth must be considered in defining strength requirements or the reliability of the rotor.

In defining the strength requirements for ceramic rotors, a reliability goal of 99% at 100 hrs. of full power operation was selected. A probabilistic strength analysis was conducted using stress distributions shown in previous Figures and making the assumption that all ceramic materials considered in this study can be represented by a Weibull statistical model of brittle strengths. In the Weibull analysis the strength of material is expressed by means of two parameters: the characteristic strength (S_θ) referenced to a specific test coupon and a Weibull slope or shape parameter (m). As indicated earlier in the report, the test coupon referenced to in this study is a 3.2 x 6.4 x 19mm MOR-bar in four-point bending, quarter-point loading (inner span 9.5mm).

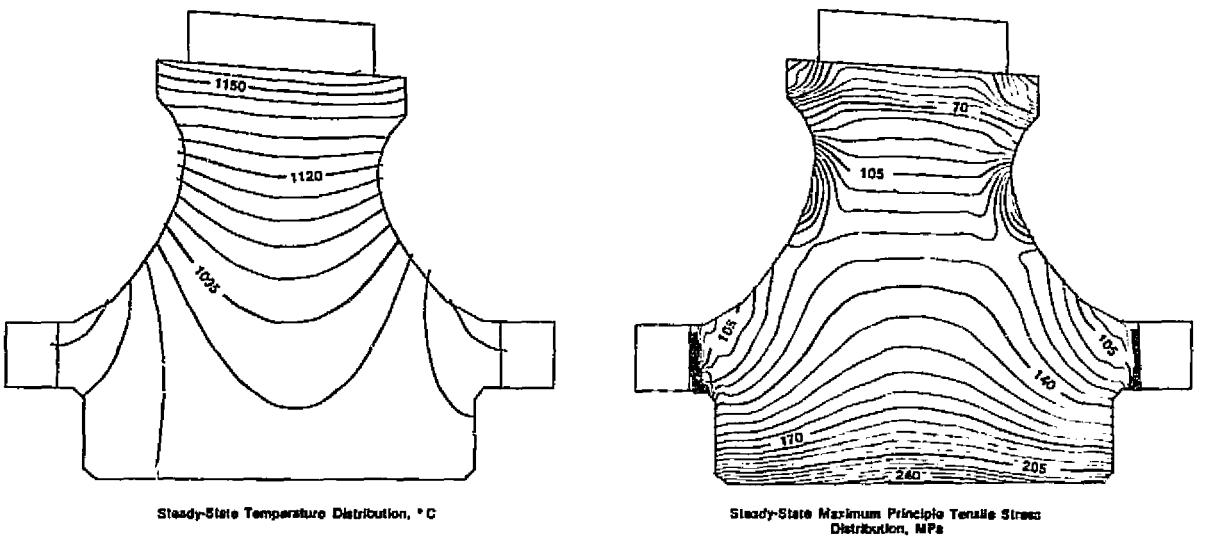


Figure 5.16 Second Stage Ceramic Axial Turbine Disk at 1370°C (2500°F) T.I.T. and 12357 Rads/s (118,000 rpm) — (Ceramic Bolt)

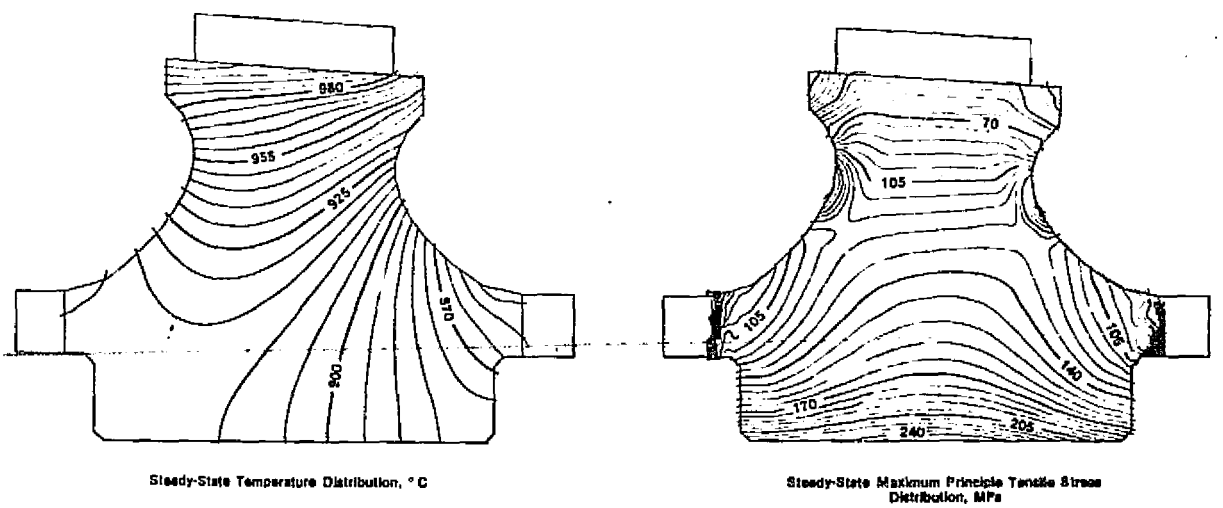


Figure 5.17 Third Stage Ceramic Axial Turbine Disk at 1370°C (2500°F) T.I.T. and 12357 Rads/s (118,000 rpm) — (Ceramic Bolt)

The results of the strength analysis are presented in Figure 5.18 where the characteristic, inert (fast fracture) strength requirements (S_θ) averaged over the rotor volume and temperature as described on page 6 of reference 10, are plotted as function of Weibull slope (m) for the ceramic turbine rotors studied. Any combination of characteristic strength and the corresponding slope will satisfy the assumed reliability goal of 99 percent. Superimposed on the strength requirement curves are points indicating current and predicted early 1980's technology strength levels of various materials.

In a cooled bolt version of a first stage axial rotor only the disk was evaluated for strength requirements. From past Ford experience (References 11 and 12) the first stage disk was found to be the critical one. The curve furthest to the left represents inert strength requirements for the first stage disk with bolt cooling eliminated, i.e. a ceramic attachment, without consideration of time dependent failure modes such as due to subcritical crack growth (SCG). Also shown is a curve for the uncooled third stage. The second stage curve would fall between the first and third stage. The curve furthest to the right represents inert strength requirements for the first stage disk but with consideration of SCG. It was generated for 99% survival probability at 100 hrs. of full power operation (static fatigue goal) using a crack propagation exponent of n = 17.0, which is representative of hot pressed Si_3N_4 and for a stress rate of 1317 MPa/hr. The dramatic increase in strength requirements necessary to compensate for strength degradation resulting from SCG suggests the uncooled bolting concept to be more suitable for the reaction sintered SiC or pressureless sintered Si_3N_4 which are not expected to be susceptible to subcritical crack growth at the temperature levels these rotors will see in service (max. 1270°C). Strength projections for either of these materials exceed the requirements, as shown in Figure 5.18.

The cooled bolt concept with higher disk stresses but considerably lower temperatures appears, on the other hand, to favor hot pressed Si_3N_4 in either a monolithic or duo-density configuration. Again the strength requirements in this case are within the projected values for that material.

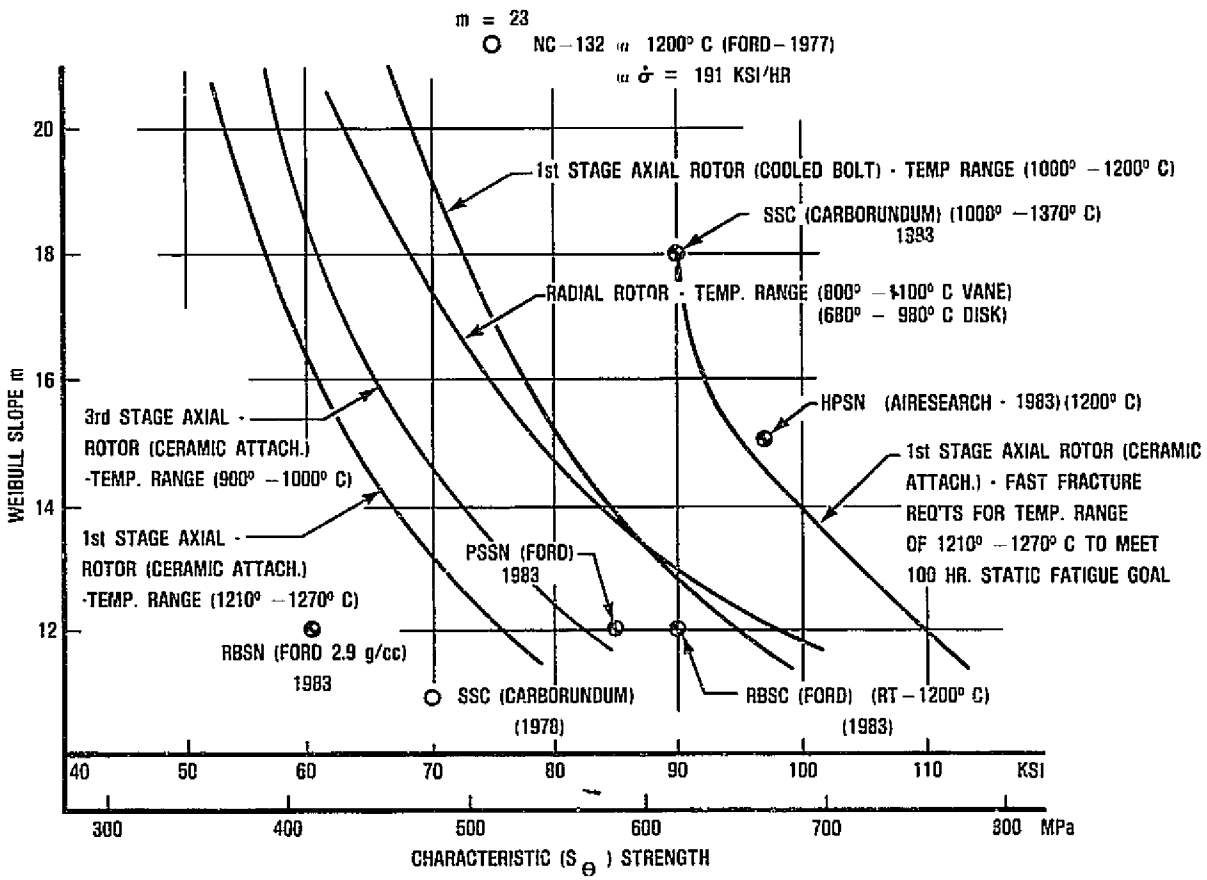
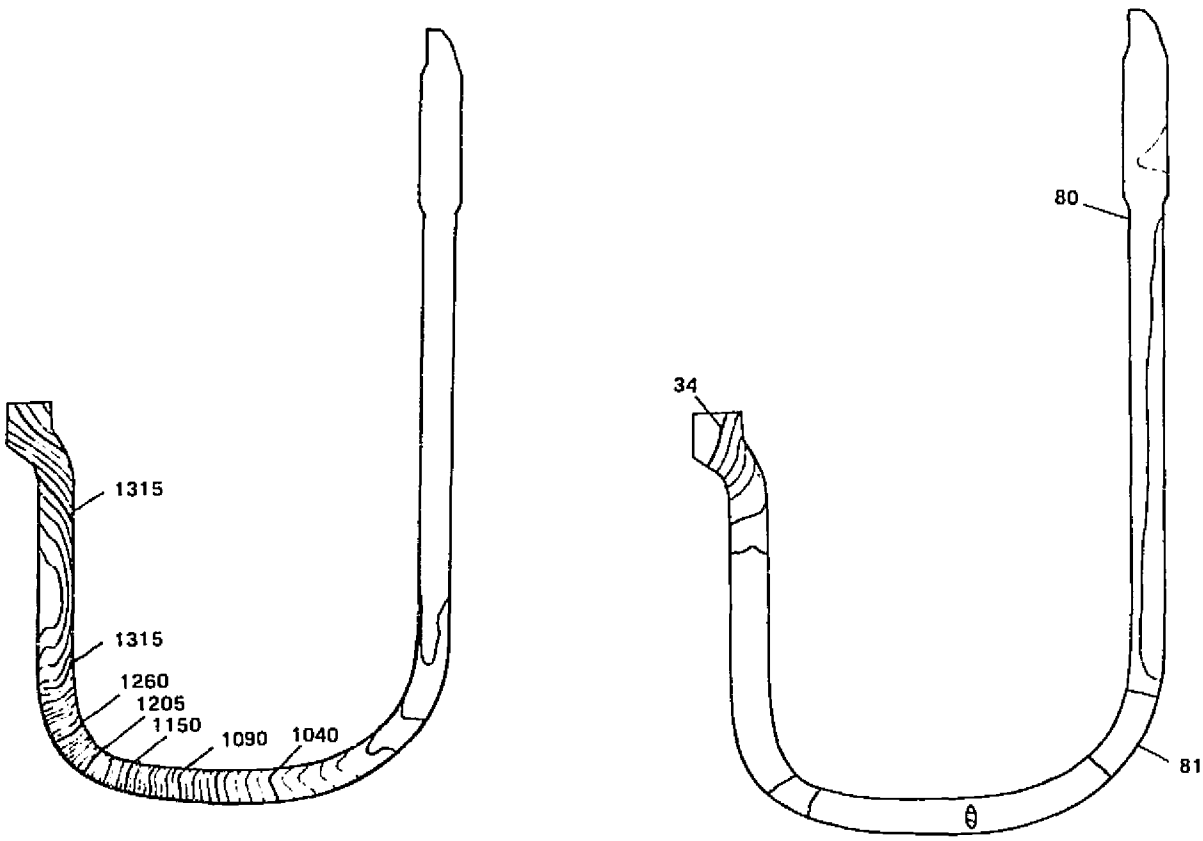


Figure 5.18 Strength Requirements for the Radial and Axial Ceramic Turbine Rotors as a Function of Weibull Slope for 99% Reliability

The last of the components investigated was the shroud-diffuser structure for the radial turbine rotor. It consists of two axisymmetric shells mounted at the diffuser exit to the main bearing housing by means of a face spline — a modified curvic coupling. The inner shell of the structure serves a dual role of a shroud for the turbine rotor and a radial diffuser wall. The shroud portion of the shell is subjected to full pressure drop of 395 kPa (57 psi) and a temperature gradient from 1330°C (2425°F) to 1000°C (1840°F). The outer shell forming the other wall of the radial diffuser being insulated from the compressor diffuser by a thick refractory blanket operates at uniform temperature and is virtually unloaded.

The dominating design criterion for the inner diffuser shell, besides its mechanical integrity, is the requirement that its axial deformation be minimized so that an effective control over the very critical axial clearances in the expeller portion of the rotor is maintained over the operating range of the engine. Furthermore, to maximize diffuser effectiveness all flow obstructions such as the struts carrying the mounting bolts must be located as remotely from the turbine rotor exit as possible. This remote location of the mounting points increases flexibility of the shell and makes control of rotor clearances difficult. This is evidenced in Figure 5.19 in which temperature and stress distributions at full power loading are presented along with the corresponding deformations for the original, thin-wailed, i.e., 5mm (0.2 ins.) shroud/diffuser shell. The stresses are quite reasonable, 81 MPa (11,750 psi) for either reaction bonded or reaction sintered Si_3N_4 or SiC. The axial deformations at the tip of the rotor are, however, excessive, .28 mm (0.011 ins.) at turbine inlet as compared to the running clearance of .25 mm (0.010 ins.) and in the direction of increasing running clearance. The excessive deformations were traced to the mechanical loading. Doubling the wall thickness to 10 mm (0.394 ins.), Figure 5.20, not only decreased the magnitude of deformation to .11 mm (0.004 ins.) but reversed its direction causing the clearance to close. The stresses in the modified shell have been also drastically reduced to 28 MPa (4060 psi) maximum which is well within the capabilities of current ceramic materials.



Steady-State Temperature Distribution. C

Steady-State Maximum Principle Tensile Stress Distribution, MPa

Figure 5.19 Radial Inflow Turbine Inner Diffuser Shell at Full Power Steady-State Loading (1370°C T.I.T.) (5 mm Thickness)

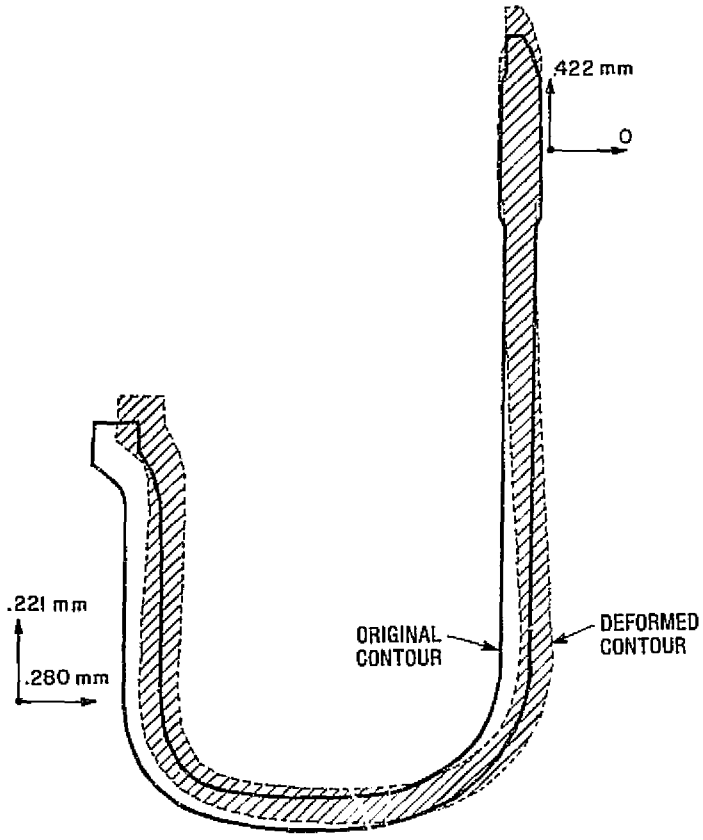


Figure 5.19(contd.) Radial Inflow Turbine Inner Diffuser Shell Deformation at Full Power Steady-State Loading (1370°C T.I.T.) (5 mm Thickness)

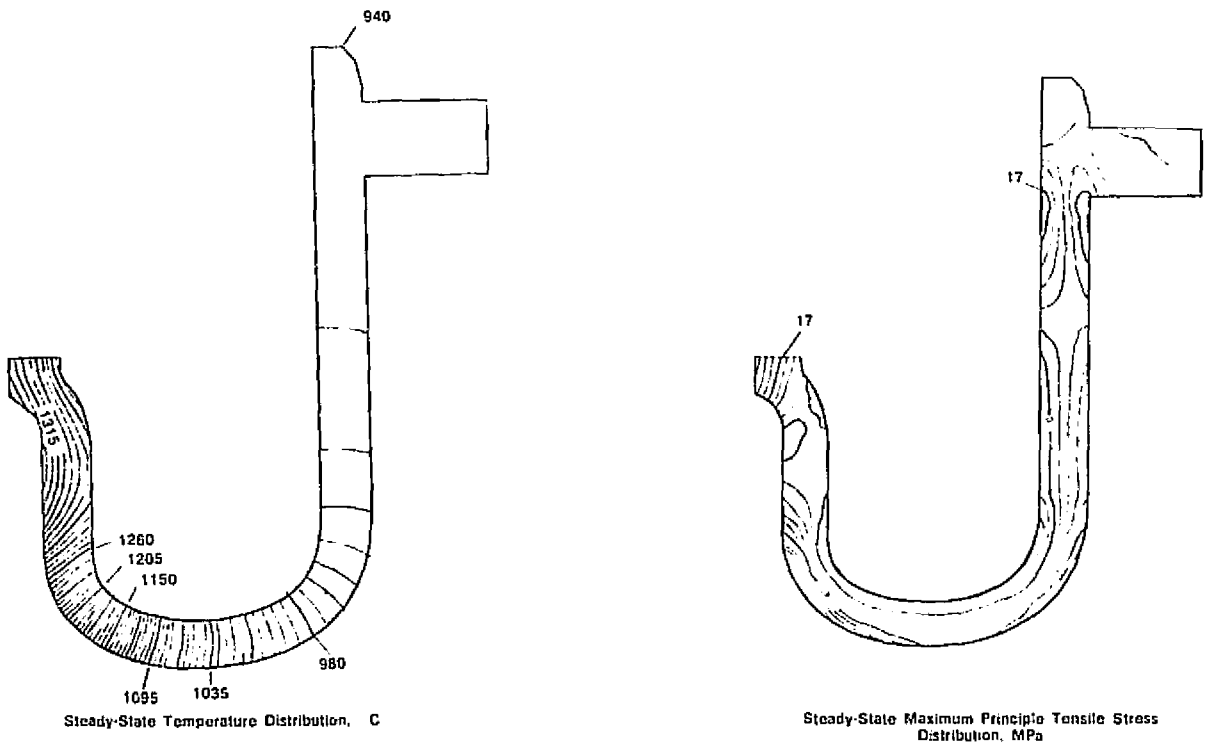


Figure 5.20 Radial Inflow Turbine Inner Diffuser Shell at Full Power Steady-State Loading (1370°C T.I.T.) (10 mm in. Thickness)

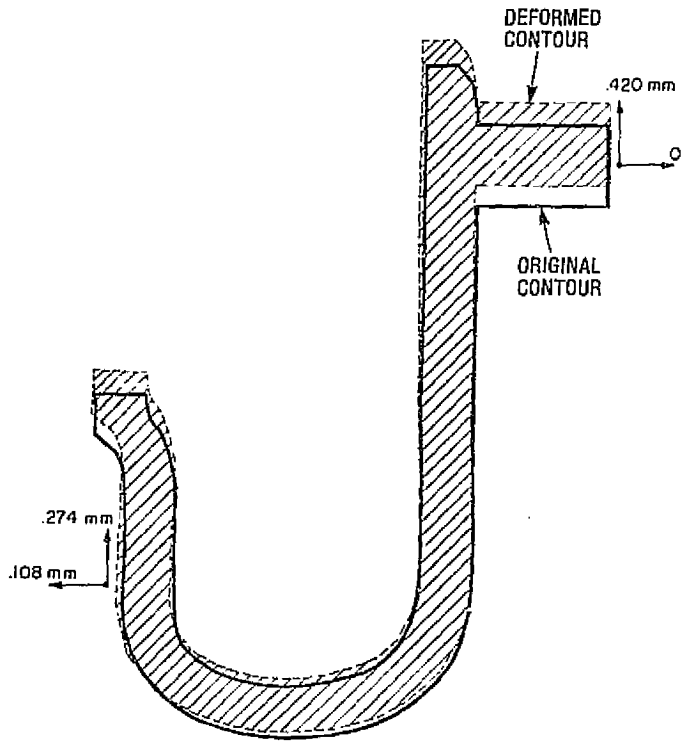


Figure 5.20(contd.) Radial Inflow Turbine Inner Diffuser Shell Deformation at Full Power Steady-State Loading (1370°C T.I.T.) (10 mm Thickness)

5.5 Transmission Analysis

An efficiency analysis was made on three of the single shaft engine transmission concepts investigated in Section 3.11 of this report.

Efficiencies were developed for 100%, 50%, and 20% power levels in various gear ratios and are shown in Tables 5.8 through 5.10 for various overall transmission speed ratios. Speed ratio is defined as the transmission output shaft speed (vehicle driveshaft) divided by the transmission input speed. Since the reduction gear ratio will depend upon the type of transmission used it has been included in the overall transmission gear ratio. Therefore, the transmission input speed, for these tabulations, is the same as the gas turbine spool speed (i.e. 12357 rads/s (118,000 rpm) at 100 percent speed). Efficiencies at other power levels can be obtained by interpolation or extrapolation.

Loss curves for the Ford FIOD gear-box referred to in the tables, and efficiency data for the Ford variable stator torque converter and traction drive components are shown in Figures 5.21 (a) through (d) and Figures 5.22 and 5.23 respectively.

5.6 Powertrain Installation Studies

Installation studies were conducted in a Ford Fairmont vehicle of the two IGT powertrain configurations described in Section 5.3:

- a conventional rear wheel drive installation using the inline engine-transmission configuration shown in Figure 5.24(a), (b) and (c).
- a front wheel drive installation using the folded drive arrangement shown in Figure 5.25(a) and (b).

The studies involved defining of packaging envelopes for the various powertrain configurations, sizing and layout of exhaust and air inlet ducts including the air inlet filter and silencer and the sizing of an oil cooler matrix and fan for the variable geometry torque converter.

TABLE 5.8

Variable Stator Torque Converter Plus Ford FIOD Gear Box
(Concept 3, Section 3.11.2)
EFFICIENCY (η) VS. SPEED RATIO (No/Ni)

1ST GEAR (2.4:1)				3RD GEAR (1:1)			
No/Ni	100% Input Power	50% Input Power	20% Input Power	No/Ni	100% Input Power	50% Input Power	20% Input Power
.01327	—	—	.6117	.03186	—	—	.5792
.01313	—	—	.7641	.03151	—	—	.7459
.01292	.6899	.6932	—	.03103	.7373	.7187	—
.01239	.7517	.7555	.7672	.02976	.8093	.7831	.7723
.01166	.7599	.7637	.7794	.02801	.8226	.8178	.7396
.01021	.7434	.7473	.7631	.02450	.8062	.8035	.7824
.00875	.7177	.7208	.7286	.02100	.7805	.7810	.7631
.00729	.6632	.6667	.6514	.01750	.7229	.7238	.6991
.00583	.5810	.5840	.5650	.01400	.6334	.6340	.6127
.00438	.4751	.4747	.4522	.01050	.5203	.5176	.4939
.00292	.3424	.3369	.3201	.00700	.3743	.3716	.3516
.00149	.1830	.1807	.1666	.00350	.1974	.1991	.1860
0	0	0	0	0	0	0	0

2ND GEAR (1.47:1)				4TH GEAR (.67:1)			
No/Ni	100% Input Power	50% Input Power	20% Input Power	No/Ni	100% Input Power	50% Input Power	20% Input Power
.02167	—	—	.6077	.04755	—	—	.6138
.02144	—	—	.7692	.04704	—	—	.7723
.02110	.7548	.7340	—	.04630	.7167	.7259	—
.02024	.8216	.8014	.7733	.04440	.7918	.7912	.7916
.01905	.8298	.8106	.7835	.04191	.8072	.8065	.8109
.01667	.8123	.7943	.7906	.03658	.7938	.7922	.7835
.01429	.7835	.7667	.7266	.03135	.7712	.7739	.7631
.01191	.7198	.7044	.6463	.02612	.7198	.7198	.7133
.00953	.6283	.6115	.5457	.02090	.6303	.6309	.6199
.00714	.5090	.4911	.4207	.01568	.5141	.5125	.4989
.00476	.3589	.3522	.2866	.01045	.3712	.3686	.3546
.00238	.1902	.1879	.1392	.00523	.1985	.1960	.1880
0	0	0	0	0	0	0	0

Where:

No = Transmission Output Speed
Ni = Transmission Input Speed
η = $\frac{\text{Trans. Output Power}}{\text{Power @ Engine Shaft}}$

Power @ engine shaft is engine power less accessory power.

Includes:

- Reduction gear power loss including any transfer drives if required
- Variable stator torque converter (Ford Data)
- Ford FIOD Transmission (Ford Data)
- Transmission oil pump losses.

Figures 5.24(a), (b) and (c) show respectively the side, front and plan views of the rear wheel drive installation of the inline engine-transmission concept, while Figures 5.25(a) and (b) show respectively the side and front views of the front wheel drive installation of the folded powertrain concept.

The rear wheel drive installation accommodates easily Ford's largest production model, 4-speed FIOD transmission, modified as required for the in-line variable stator torque converter, (concept 3, Section 3.11.2). Preliminary layout studies have also indicated that this installation will accommodate equally well the differential split-power transmissions (concepts 6 and 13, Section 3.11.2) as discussed in the preceding section.

TABLE 5.9

Differential Split-Power Traction Drive Plus Four Speed Transmission
(Concept 13, Section 3.11.2)
EFFICIENCY (η) VS. SPEED RATIO (No/Ni)

No/Ni	100% Input Power	50% Input Power	20% Input Power	Gear Range
.03419	.9205	.9065	.8359	
.03165	.9185	.9035	.8399	
.02644	.9175	.8925	.8519	
.02330	.9195	.8955	.8689	4TH
.02120	.9195	.8985	.8729	
.01965	.9215	.9015	.8729	
.01850	.9253	.9065	.8643	
.01712	.9285	.8985	.8539	
.01431	.9215	.8895	.8429	
.01261	.9215	.8865	.8379	3RD
.01147	.9215	.8855	.8369	
.01063	.9215	.8835	.8349	
.01001	.9247	.8902	.8459	
.00926	.9285	.8985	.8593	
.00774	.9215	.8895	.8429	
.00682	.9215	.8865	.8379	2ND
.00620	.9215	.8855	.8369	
.00575	.9215	.8835	.8349	
.00541	.8884	.8670	.8363	
.00501	.8495	.8475	.8379	
.00419	.8435	.8375	.8269	1ST
.00369	.8435	.8365	.8229	
.00336	.8425	.8345	.8219	
.00311	.8425	.8335	.8219	
.00293	.8425	.8335	.8219	
.00234	.6740	.6668	.6575	
.00176	.5055	.5001	.4931	
.00117	.3370	.3334	.3288	CLUTCH
.00059	.1685	.1667	.1644	SLIP
.00029	.0843	.0834	.0822	
.00015	.0421	.0417	.0411	
.00003	.0084	.0083	.0082	
0	0	0	0	

Includes:

- Differential reduction gear loss including any transfer drives if required.
- Traction loss from reference 11.
- Transmission loss from Ford FIOD Data

C-2

The front wheel drive installation because of the limited width of engine compartment required use of a small, 3-speed Ford C4 transmission, (concept 2, Section 3.11.2), also a production model, to which a chain driven transaxle was added. Because of limited time, and since no plans exist to install the IGT engine as a front wheel drive application, no effort was made to investigate in detail front wheel suspension concepts for this engine installation.

At this stage of investigation it appears that except for minor changes to the front crossmember no major modification to the engine compartment are foreseen for either of the above installations.

Air inlet is located in both installations at the front sharing the space vacated by the radiator with an oil cooler heat exchanger matrix and a modified A/C condenser mounted in series with the oil cooler. A commercially available, electrically driven fan was selected to provide the required air flow for the two heat exchangers. It is located at the bottom directly behind the exchangers. The volume of inlet filter-silencer package was set at 9450 cm^3 and the inlet and exhaust ducts were sized for minimum pressure drop at 329 and 310 cm^2 cross-sectional area respectively.

TABLE 5.10

Differential Split-Power Variable Stator Torque Converter Plus Ford FIOD Gearbox (Concept 6, Section 3.11.2) EFFICIENCY (η) VS. SPEED RATIO (No/Ni)

1ST GEAR (2.4:1)

No/Ni	100% Input Power	50% Input Power	20% Input Power
.00840	.7836	.7843	.7891
.00824	.8151	.8154	.7987
.00789	.8196	.8185	.7946
.00749	.8160	.8158	.7863
.00706	.7968	.7935	.7550
.00638	.7584	.7568	.7142
.00585	.7058	.7017	.6562
.00549	.6870	.6808	.6383
.00515	.6683	.6635	.5985
.00412	.5346	.5308	.4790
.00309	.4010	.3981	.3593
.00206	.2673	.2654	.2395
.00103	.1337	.1327	.1198
.00052	.0668	.0664	.0605
.00026	.0334	.0332	.0302
.00005	.0067	.0066	.0058
0	0	0	0

2ND GEAR (1.47:1)

No/Ni	100% Input Power	50% Input Power	20% Input Power
.01372	.8584	.8328	.7936
.01345	.8929	.8656	.8032
.01286	.8978	.8691	.7990
.01223	.8939	.8663	.7907
.01152	.8729	.8426	.7593
.01041	8309	.8035	.7183
.00956	.7732	.7450	.6599
.00897	.7505	.7242	.6419
.00840	.7290	.7045	—

3RD GEAR (1:1)

No/Ni	100% Input Power	50% Input Power	20% Input Power
.02018	.8540	.8505	.8340
.01978	.8883	.8842	.8441
.01893	.8932	.8875	.8397
.01798	.8893	.8846	.8309
.01694	.8684	.8604	.7979
.01530	.8266	.8205	.7548
.01405	.7693	.7608	.6935
.01318	.7467	.7396	.6746
.01235	.7253	.7194	—

4TH GEAR (.67:1)

No/Ni	100% Input Power	50% Input Power	20% Input Power
.03011	.8496	.8416	.8250
.02951	.8837	.8750	.8350
.02826	.8886	.8783	.8307
.02682	.8847	.8754	.8220
.02529	.8640	.8515	.7893
.02284	.8224	.8120	.7467
.02097	.7653	.7529	.6860
.01968	.7428	.7319	.6673
.01845	.7215	.7120	—

Includes:

- Differential reduction gear loss including transfer drives if required.
- VSTC and FIOD gearbox efficiencies (Ford Data)

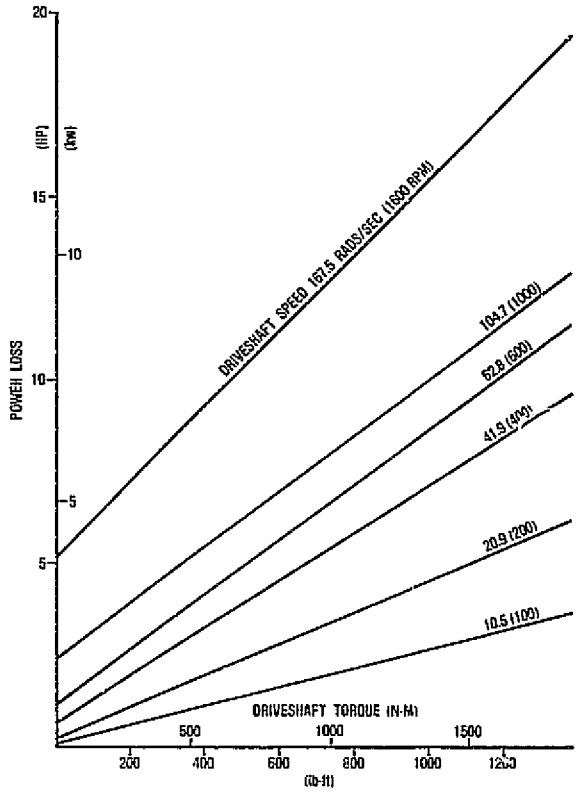


Figure 5.21(a) Power Loss Characteristics of the Ford FIOD Transmission Without Torque Converter, Including Oil Pump. First Gear

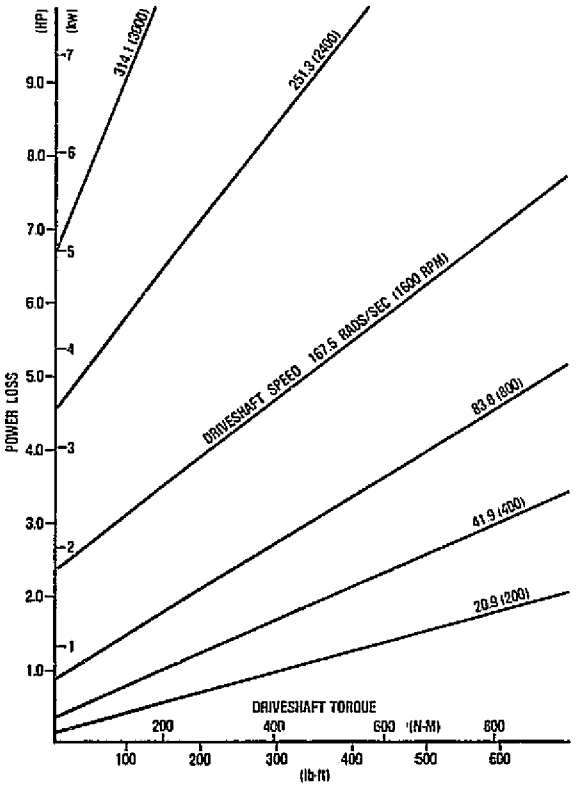


Figure 5.21(b) Power Loss Characteristics of the Ford FIOD Transmission Without Torque Converter, Including Oil Pump. Second Gear

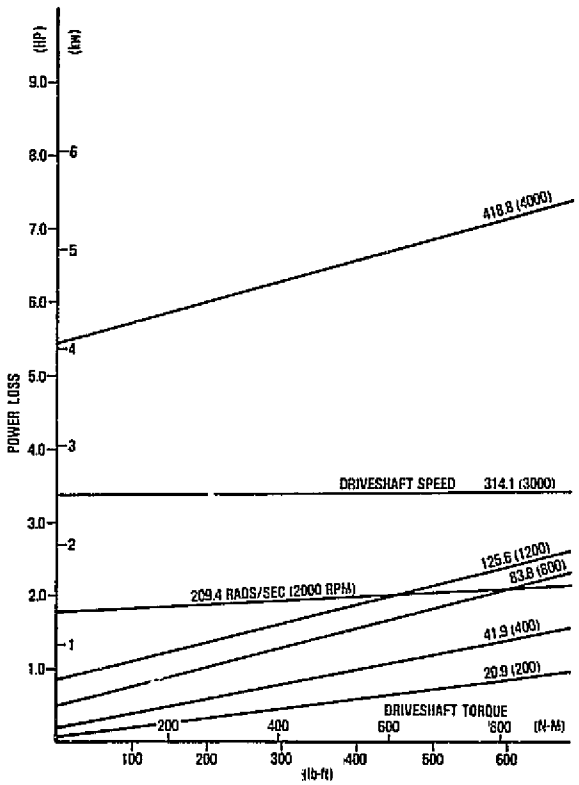


Figure 5.21(c) Power Loss Characteristics of the Ford FIOD Transmission Without Torque Converter, Including Oil Pump. Third Gear

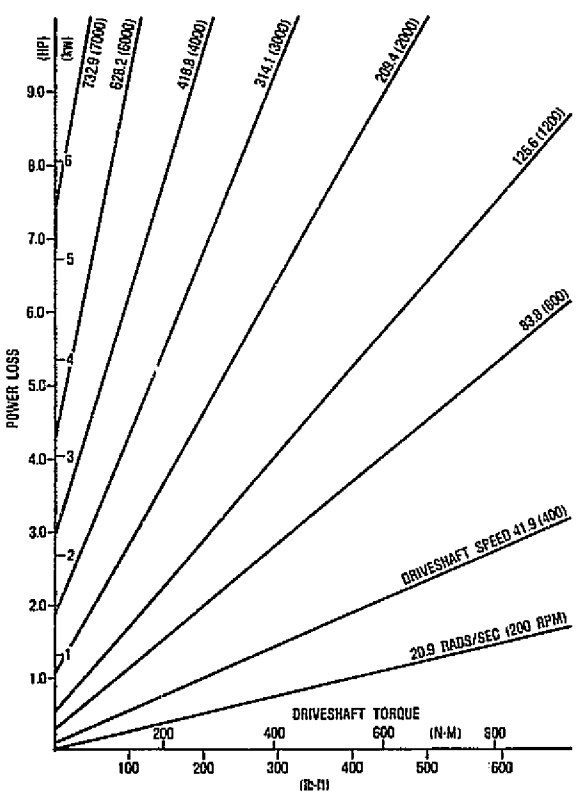


Figure 5.21(d) Power Loss Characteristics of the Ford FIOD Transmission Without Torque Converter, Including Oil Pump. Fourth Gear

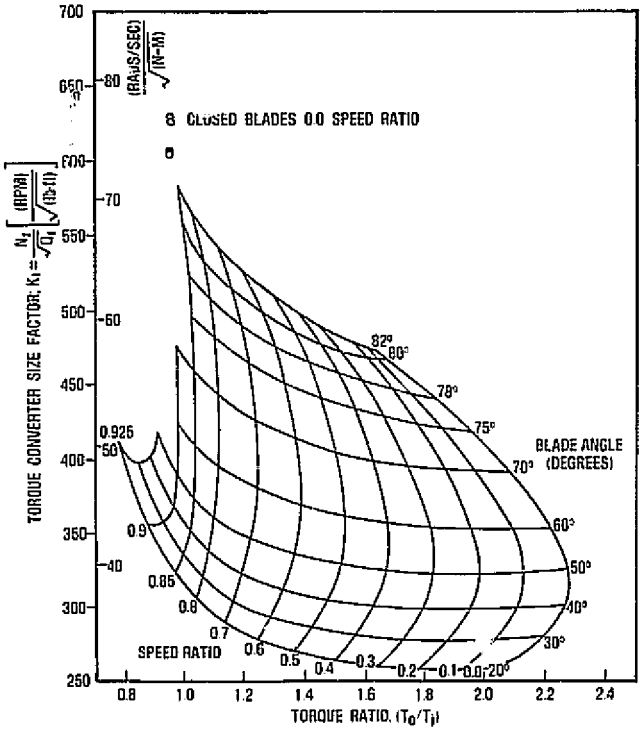


Figure 5.22 Ford Variable Stator Torque Converter Test Results

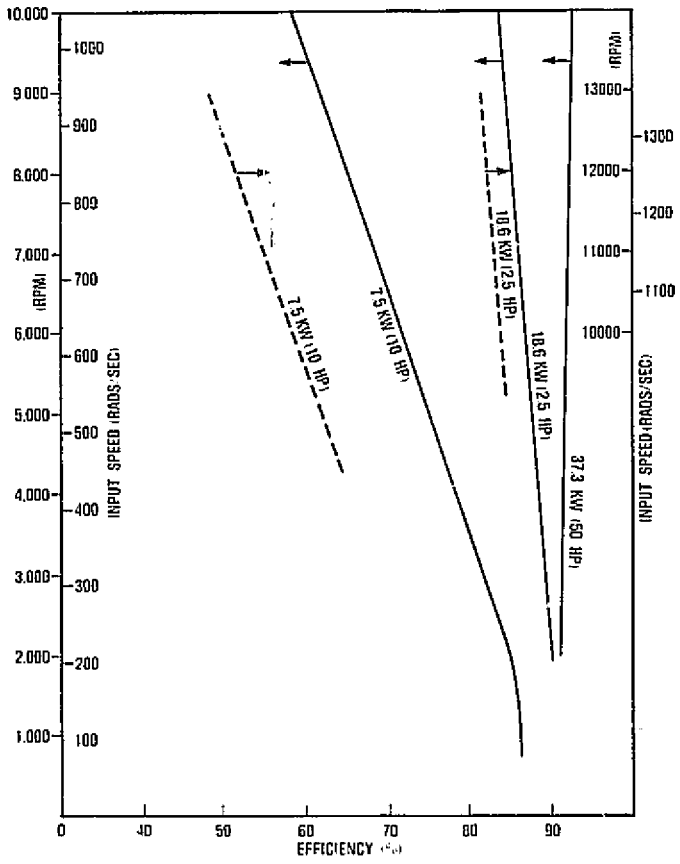
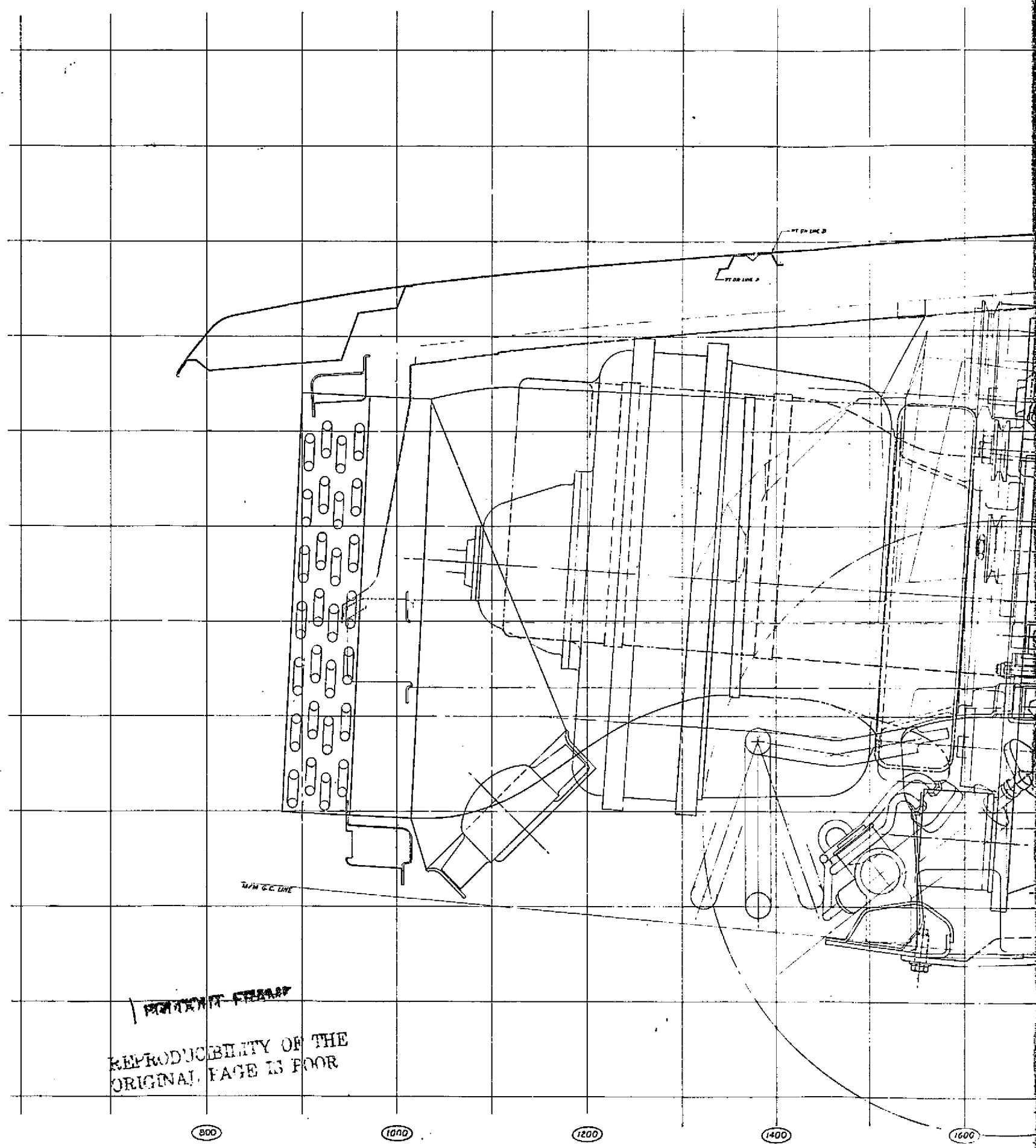


Figure 5.23 Assumed Efficiency of Traction Drive Element (Reference 6)



REPRODUCIBILITY OF THE
ORIGINAL PAGE IS POOR

Figure

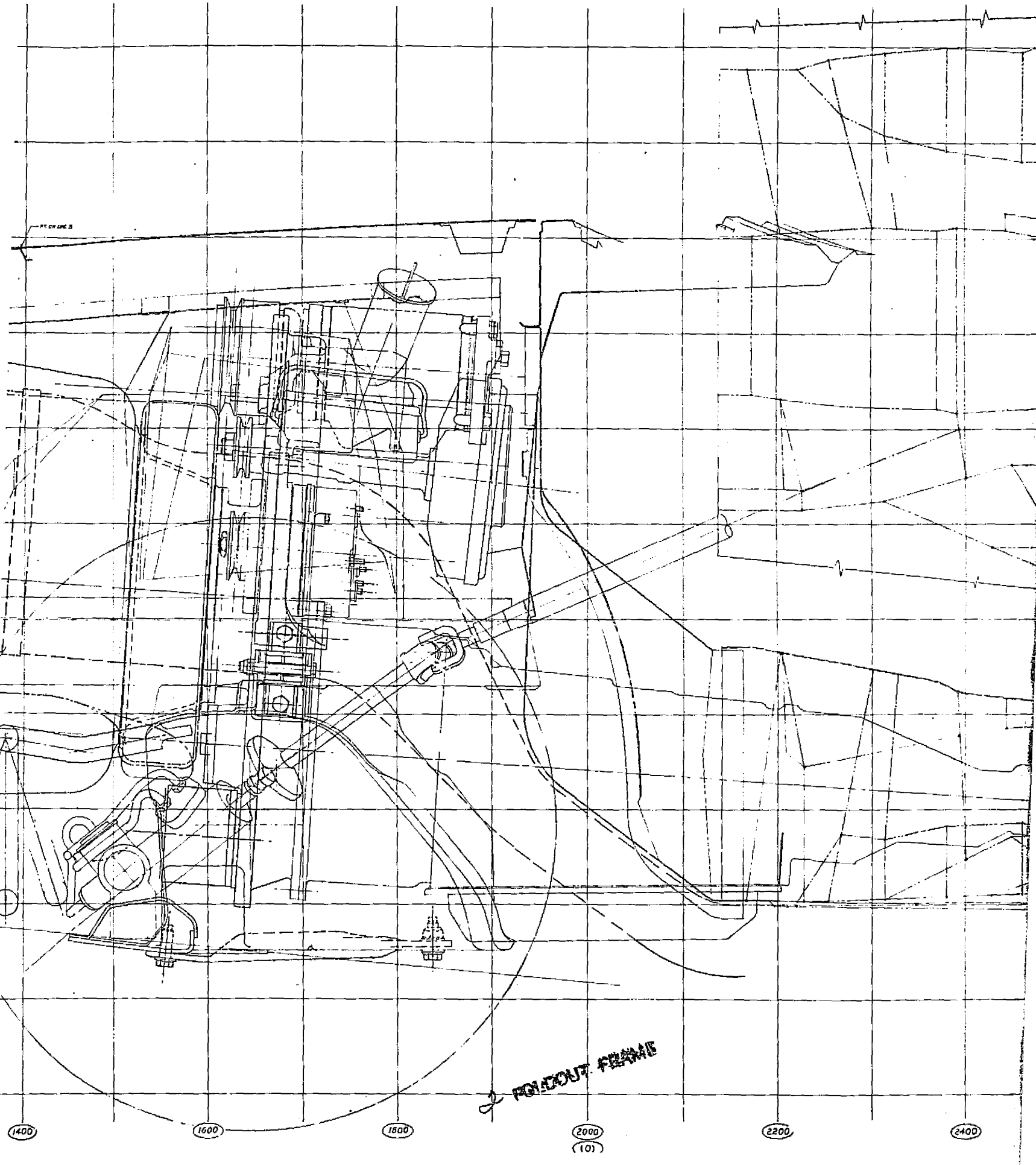
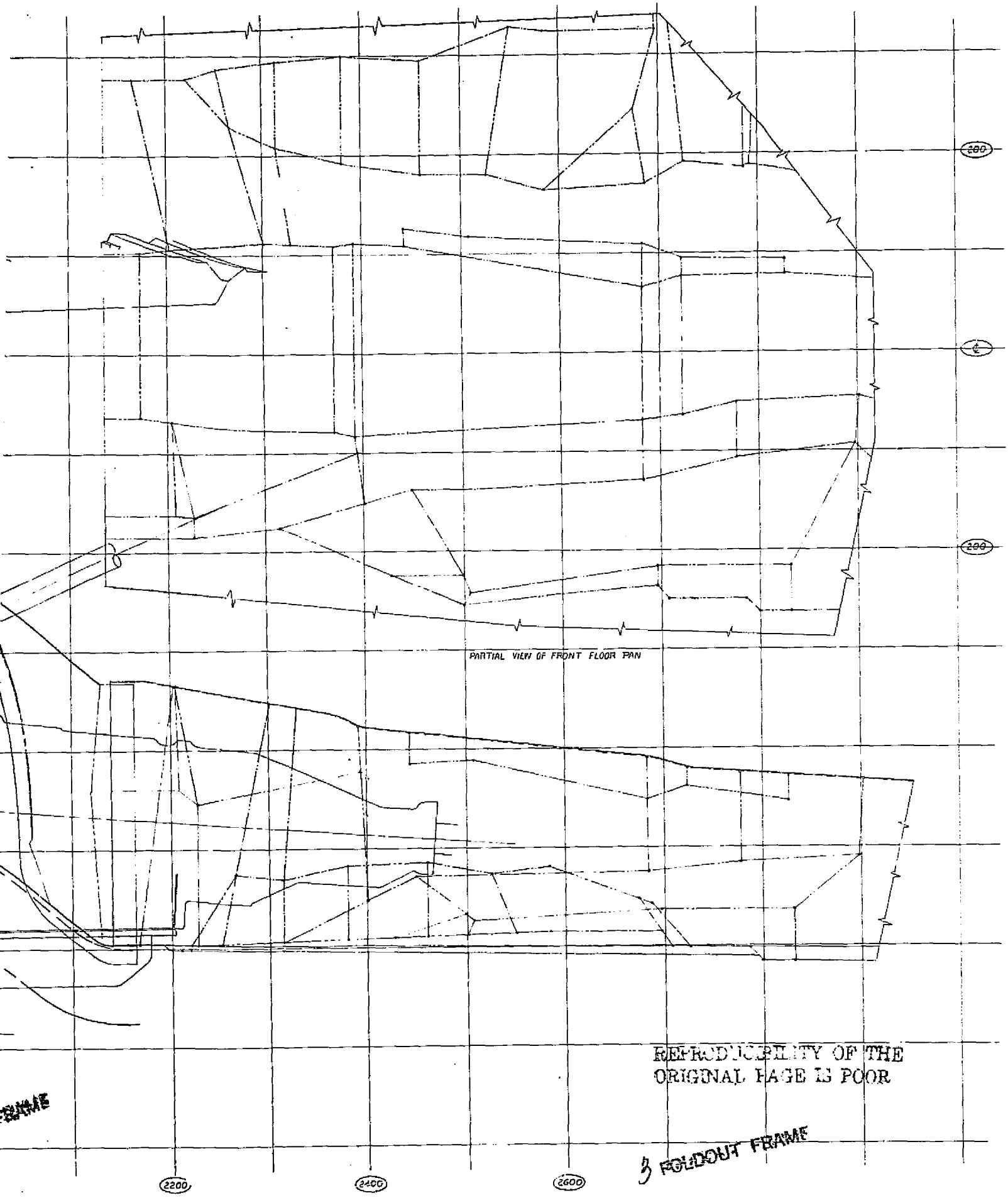


Figure 5.24(a) Rear Wheel Drive Installation of Ford IGT Engine (Side View)



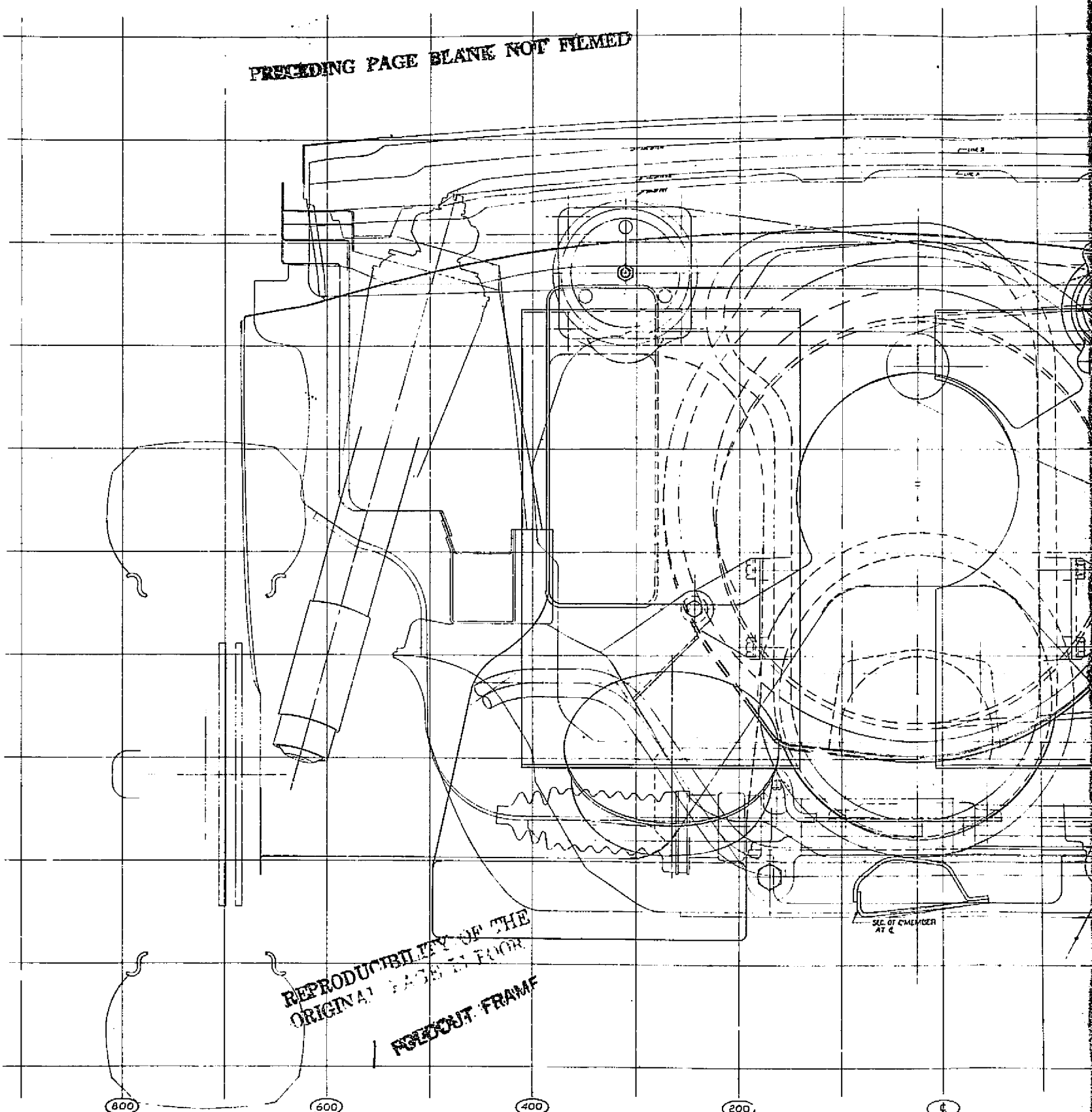
PARTIAL VIEW OF FRONT FLOOR PAN

REPRODUCIBILITY OF THE
ORIGINAL PAGE IS POOR

3 FOLDOUT FRAME

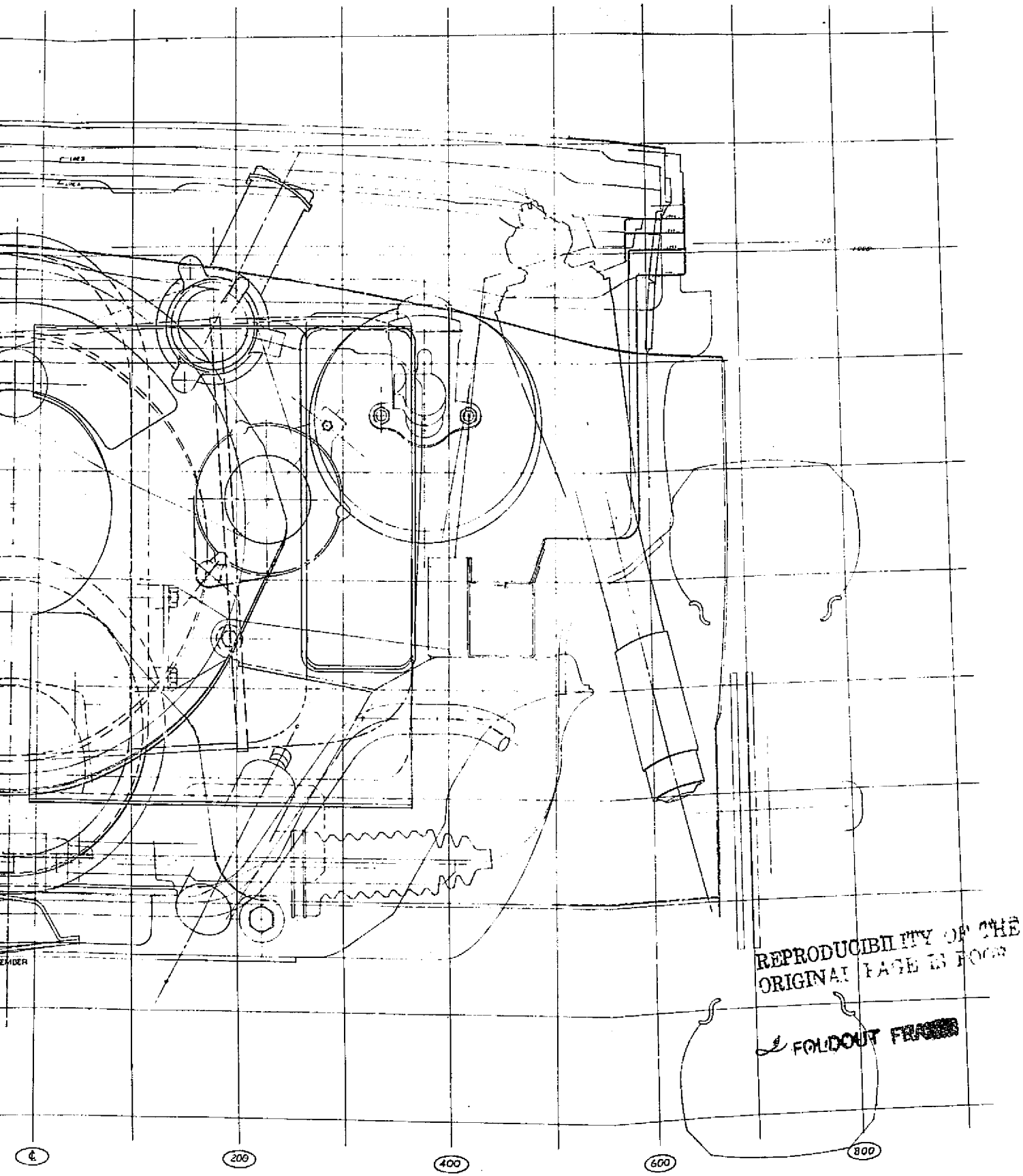
d IGT Engine (Side View)

PRECEDING PAGE BLANK NOT FILMED



REPRODUCIBILITY OF THE
ORIGINAL PAGE IS POOR

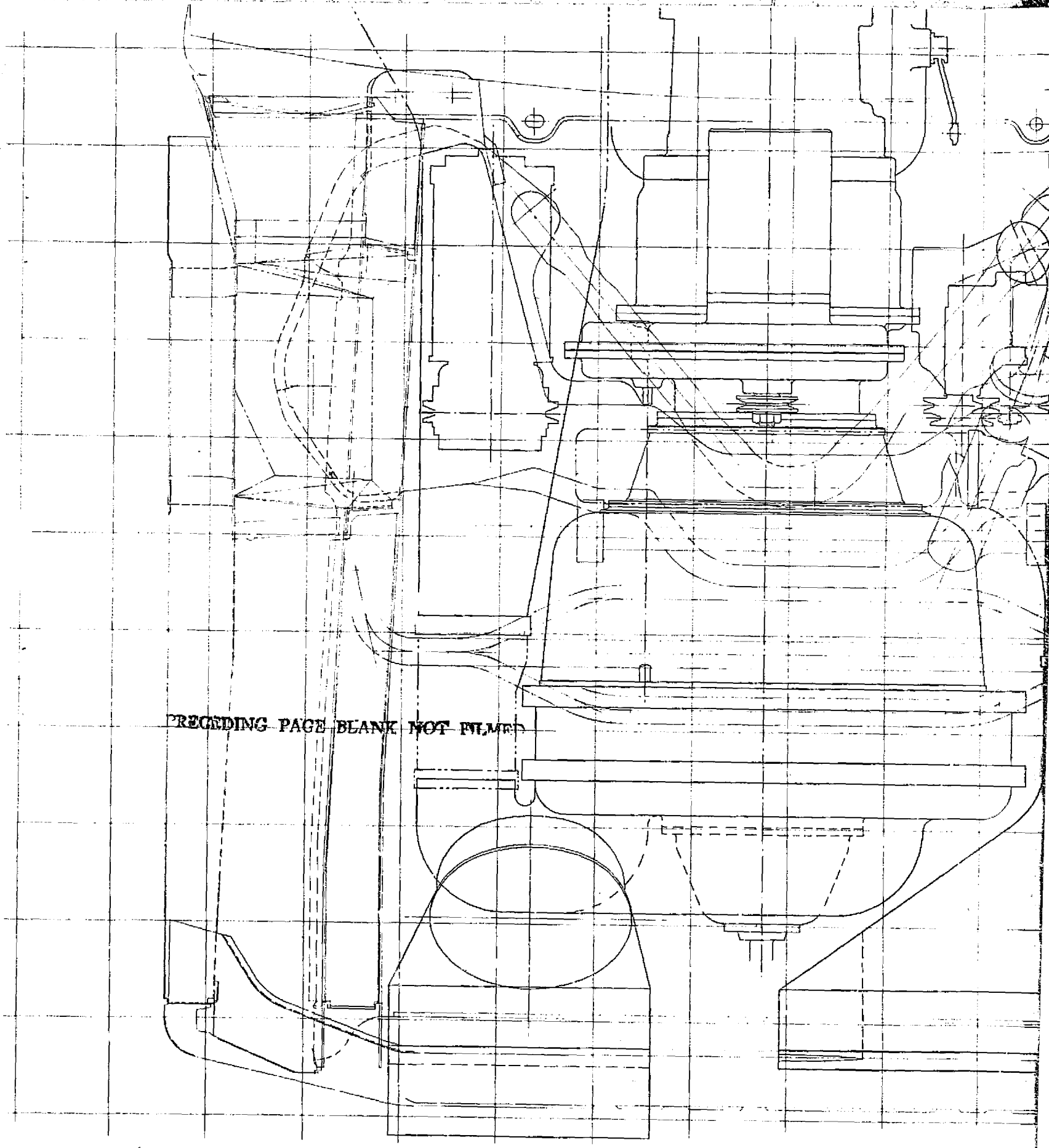
Figure 5.24(b) Rear Wheel Drive Installation of Ford IGT



REPRODUCIBILITY OF THE
ORIGINAL PAGE IS POOR

FOLDOUT FRAME

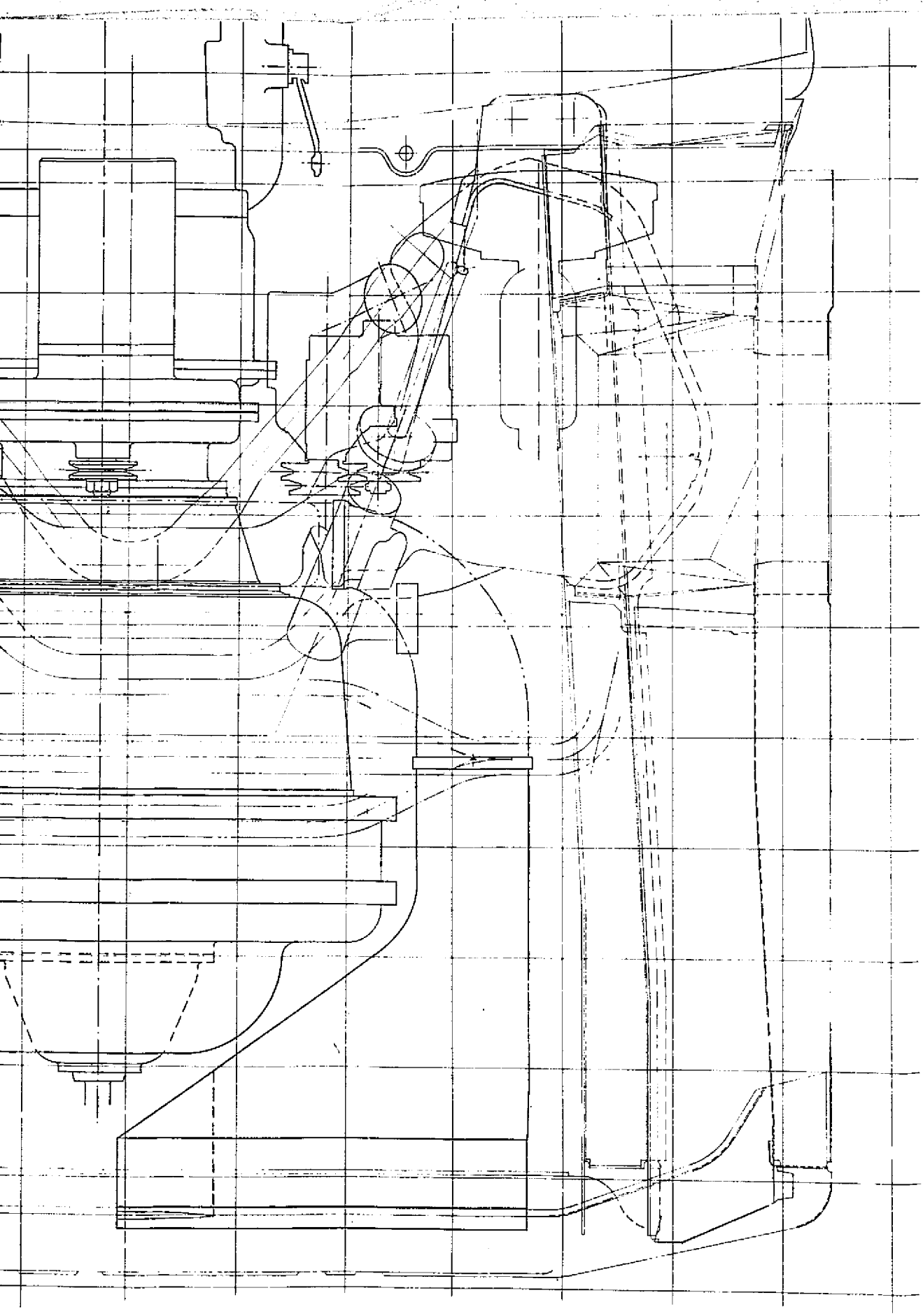
stallation of Ford IGT Engine (Front View)



PRECEDING PAGE BLANK NOT FILMED

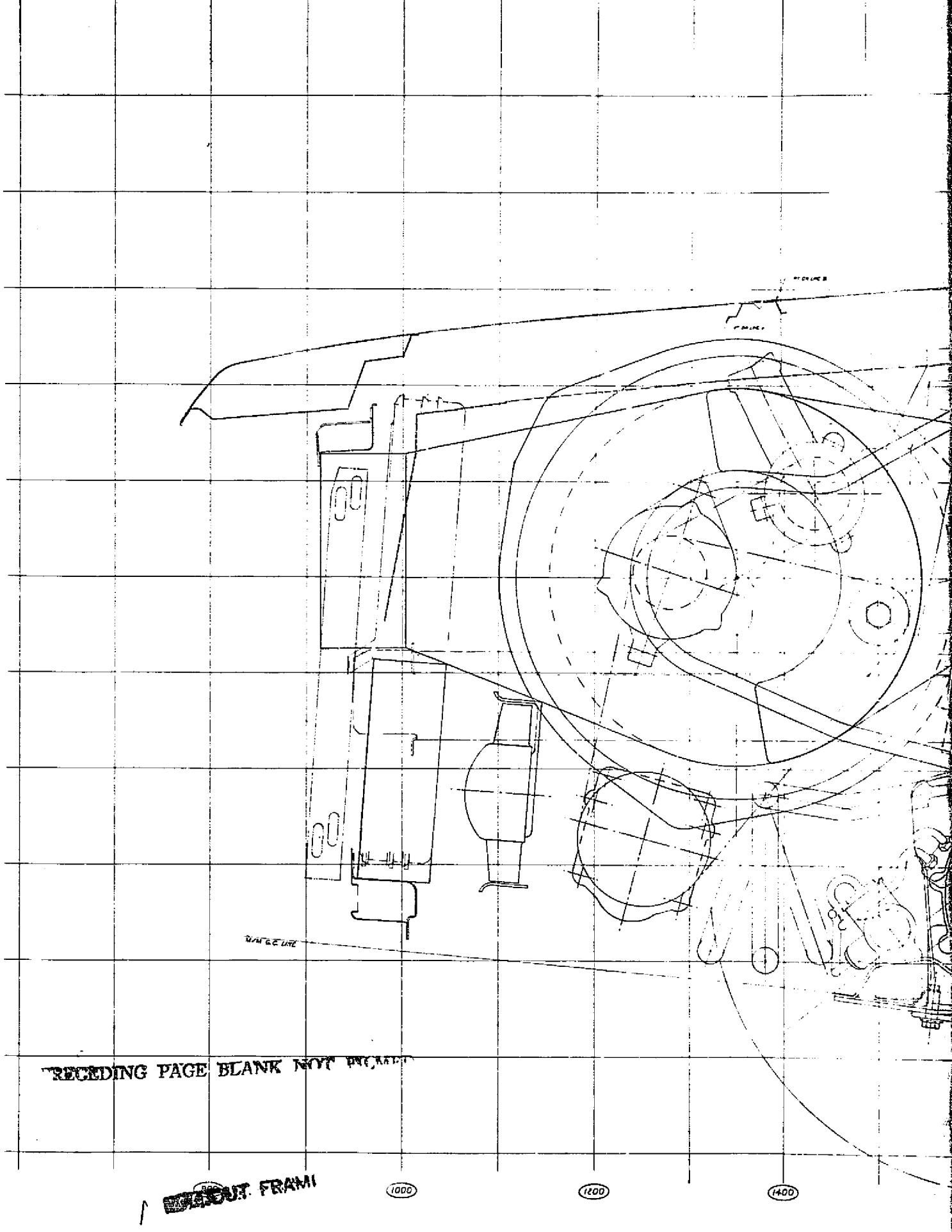
FOLDOUT FRAME

Figure 5.24(c) Rear Wheel Drive Installation of Ford IGT Engine (Plan



eel Drive Installation of Ford IGT Engine (Plan View)

2 FOLDOUT FRAME



PRECEDING PAGE BLANK NOT FILMED

BLACK AND WHITE PHOTOGRAPH

Figur

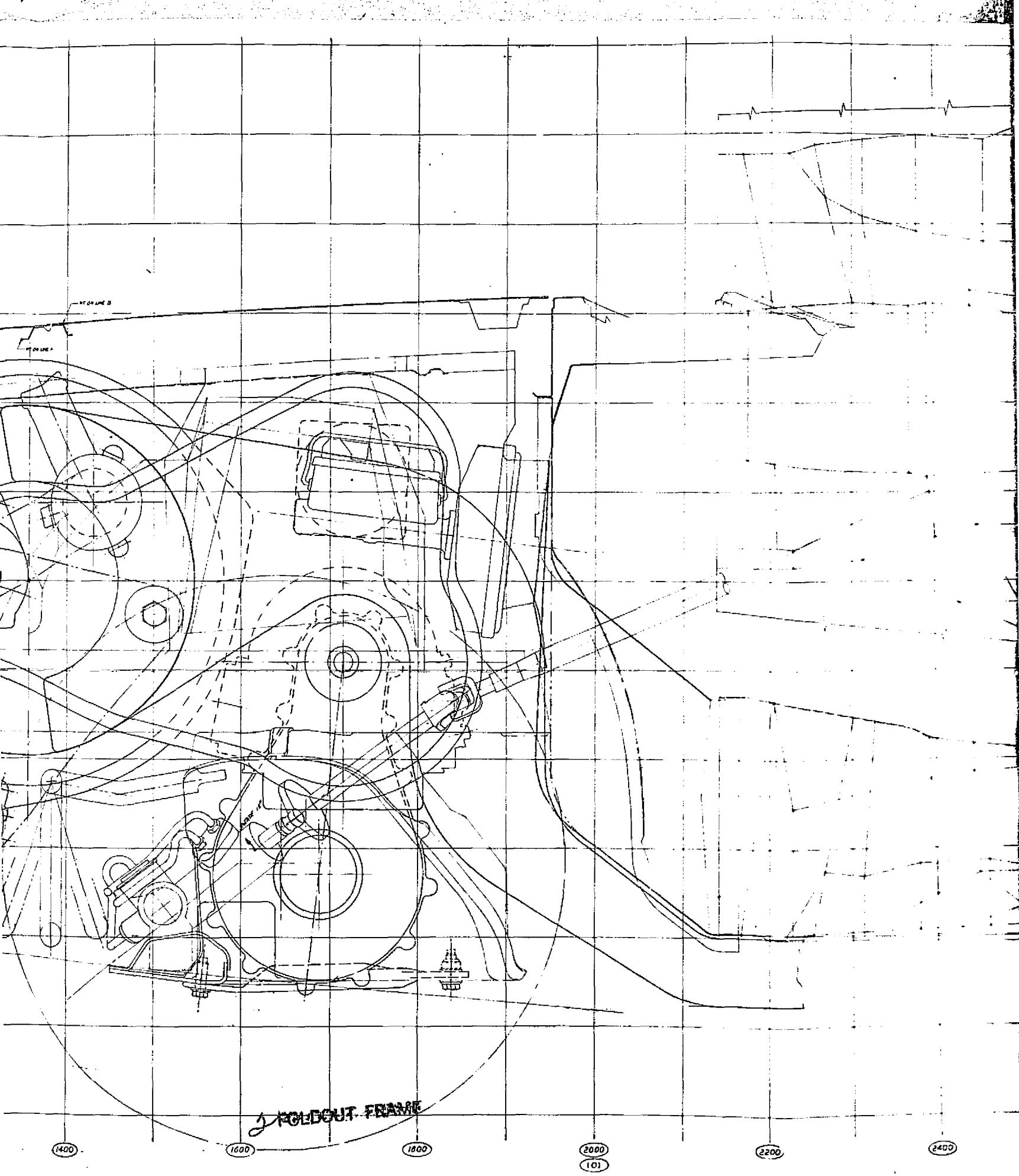
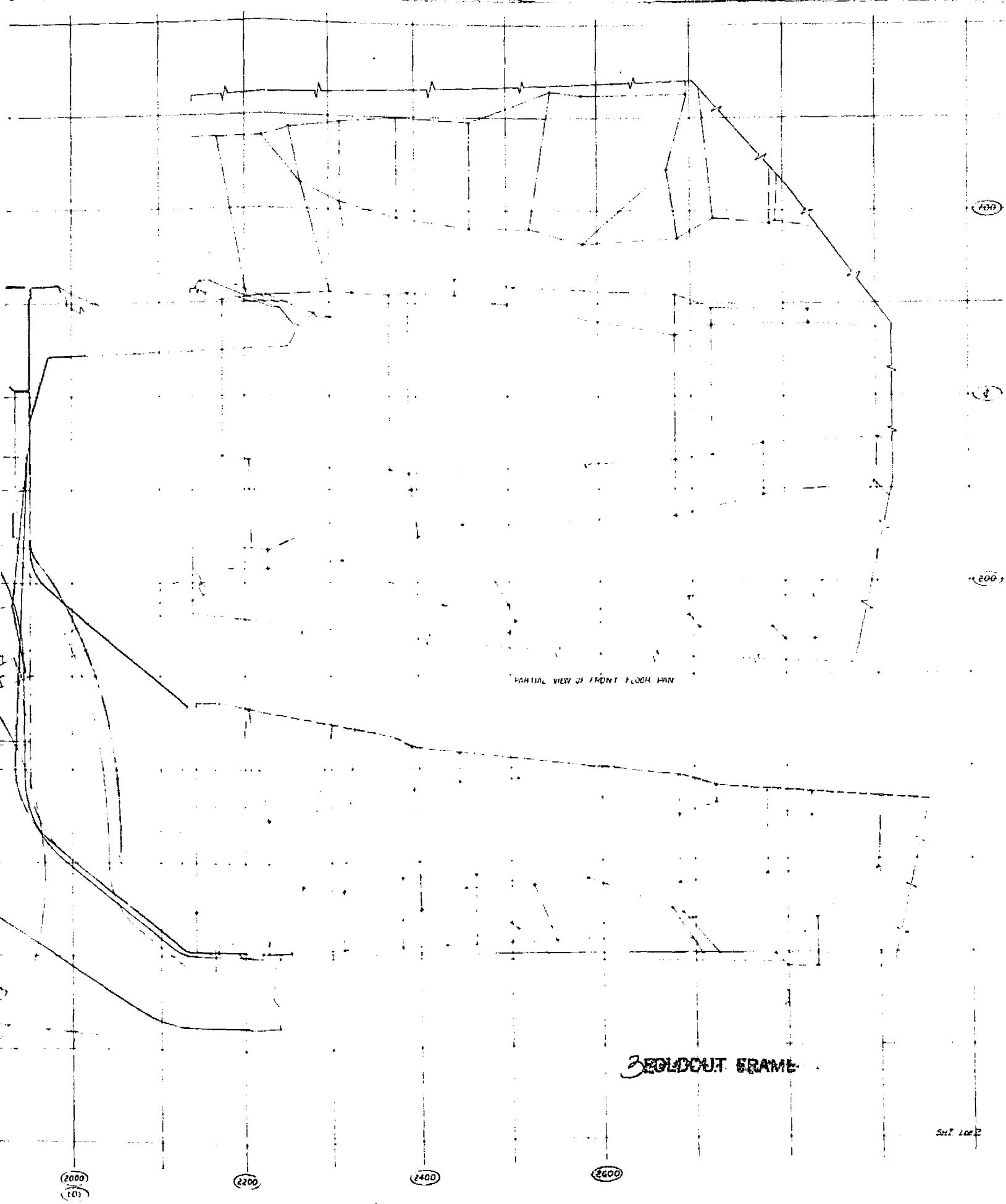
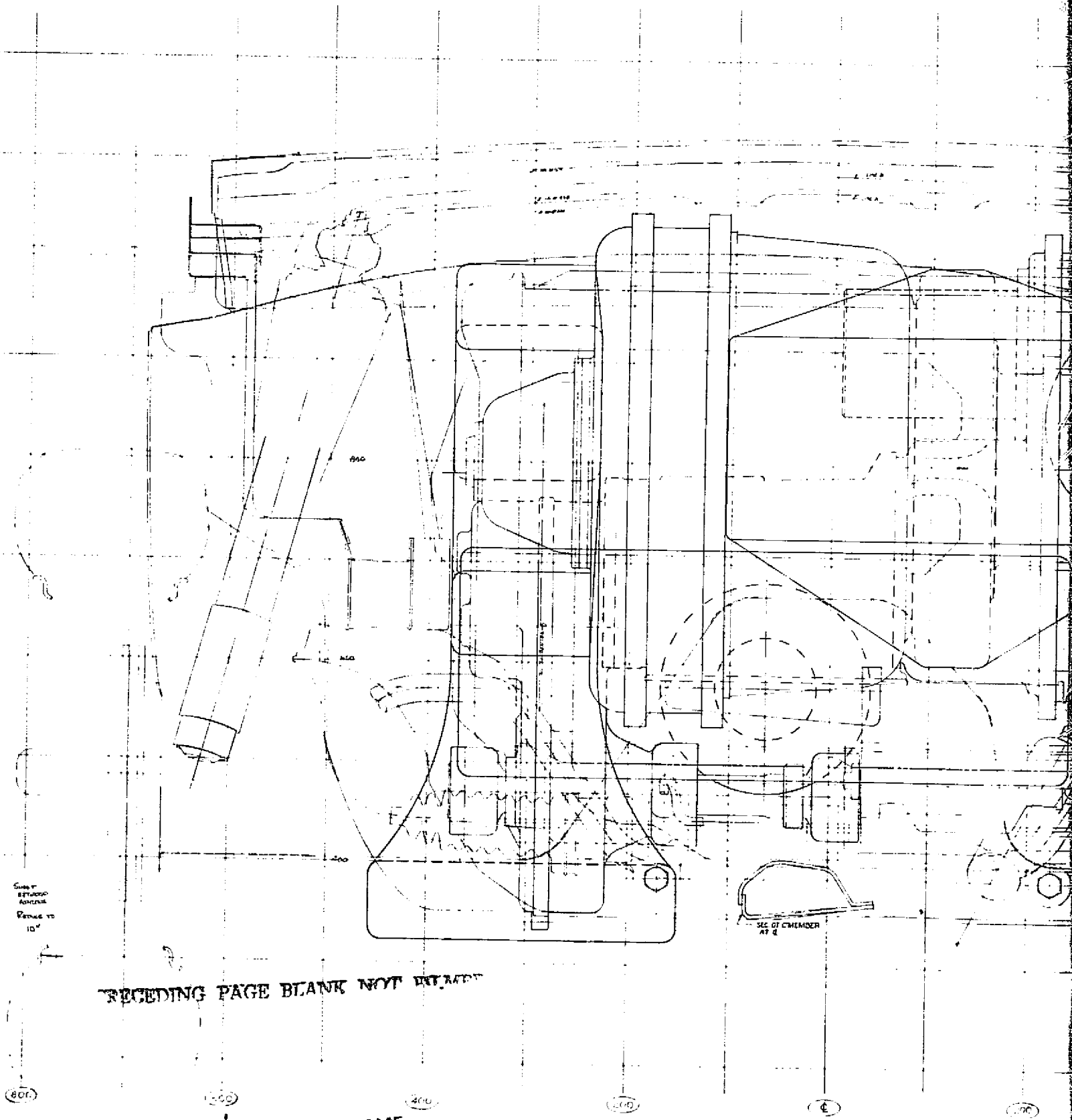


Figure 5.25(a) Front Wheel Drive Installation of Ford IGT Engine (Side View)



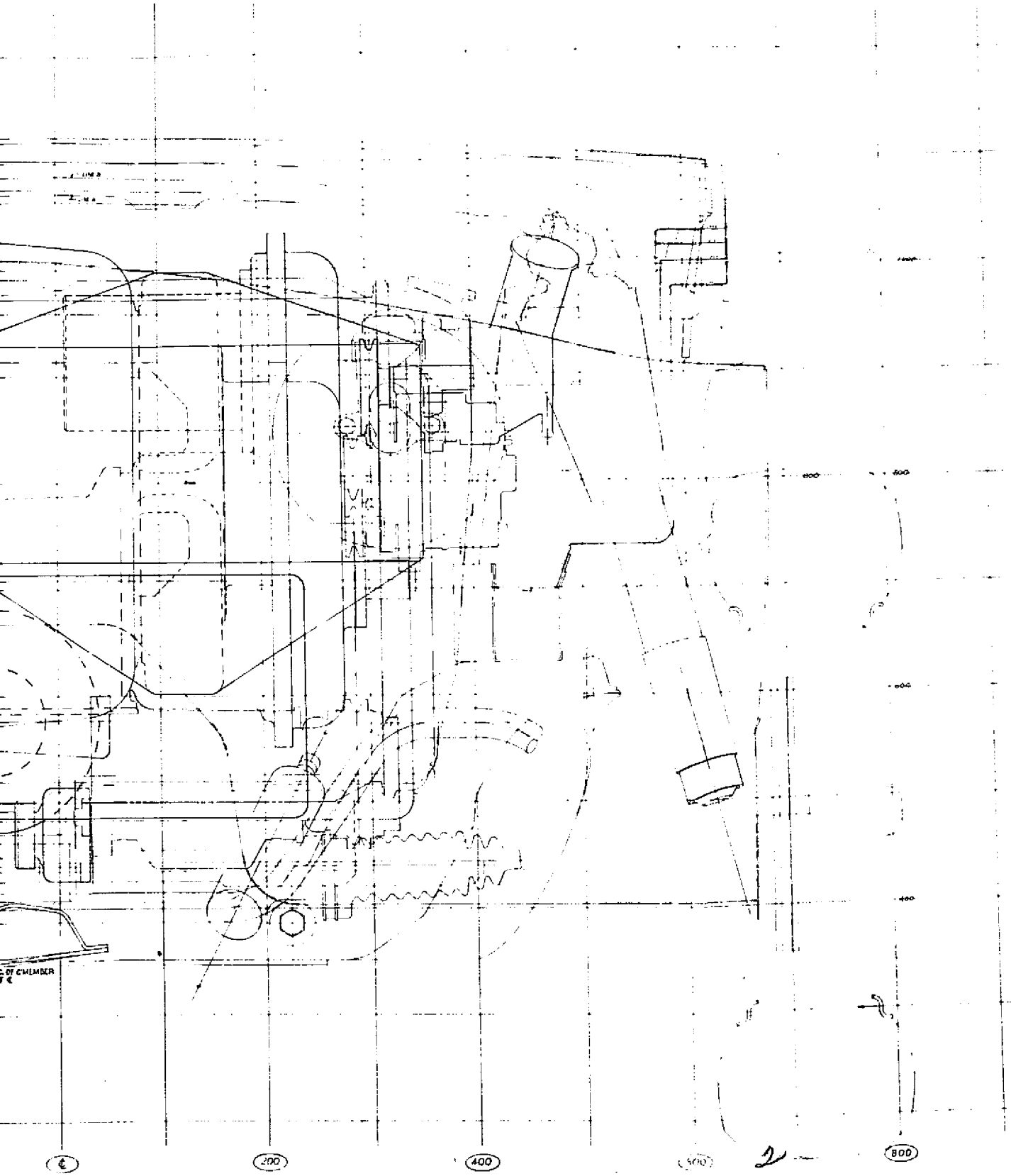
of Ford IGT Engine (Side View)



PRECEDING PAGE BLANK NOT FILMED

FOLDOUT FRAME

Figure 5.25(b) Front Wheel Drive Installation of Ford IGT Engine



Drive Installation of Ford IGT Engine (Front View)

FOLDOUT FRAME

5.7 Sensitivity Analysis

A parametric study has been conducted to determine the sensitivity of powertrain performance to changes in component performance. Seven performance parameters were investigated for each of the four candidate powertrain concepts. A cycle performance computer program was used to determine the base line specific fuel consumption (SFC) for each concept at the 20 percent power point. The same program was then used to calculate the change in engine SFC due to a small increment in each parameter taken individually. The 20 percent power point was chosen for this study because it is representative of the combined federal driving cycle (CFDC).

The SFC derivative is defined as

$$\frac{\partial SFC}{\partial X_i} = \frac{\Delta SFC}{\Delta X_i}$$

where ΔSFC is the change in SFC caused by a change of ΔX of the *i*th performance parameter. The derivatives were used in the risk analysis. The SFC sensitivity was defined as the change in the performance parameter value required to reduce the engine SFC by 1 percent from its baseline. The parameters studied, the baseline values of SFC and engine power, the SFC derivatives and the SFC sensitivities are shown in Table 5.11.

If the performance improvements projected for 1983 did not occur and the technologies did not advance beyond the 1978 levels, the fuel economy projected for 1983 would not be achieved. Table 5.12 shows the percentage change in CFDC fuel economy from the 1983 level which would occur for configuration SS8 if specific improvements did not occur. The estimates of the parameter performance levels at 20 percent power in 1978 and in 1983 are also shown in Table 5.12. These estimates were a summary of information found in Section 3.0, the results of the cycle performance analysis, and the vehicle performance analysis. Two transmission considerations were shown in Table 5.12. The first consideration reflected an improvement in transmission efficiency from 70 to 81 percent. This represents the upgrading in transmission efficiency from the variable stator torque converter and FIOD transmission (concept 3, Section 3.11.2) to the differential split power 4-speed transmission with a variable ratio traction drive unit (concept 13, Section 3.11.2). Secondly, the latter concept involves a start-up clutch which permits the transmission to be declutched at idle and which results in the potential fuel economy improvement changing from 12.2 to 19.5 percent.

PRECEDING PAGE BLANK NOT FILMED

TABLE 5.11

Engine Parameters and Sensitivities

Configuration	Parameter	Sensitivity (1)	Derivative (2)
SS8	Transmission Efficiency, %	+ .870	−.0022
	Turbine Inlet Temperature, °C	+ 34.80	−.000055
Single Shaft Engine	Regenerator Effectiveness, %	+ .245	−.0078
With Radial Turbine	Leakage, %	− 1.566	+.0012
	Pressure Loss, %	− .853	+.0022
	Turbine Efficiency, %	+ 1.044	−.0018
	Compressor Efficiency, %	+ 1.362	−.0014
	SFC, kg/kW-h	.1904	
	Power, kW	20.53	
SS4	Transmission Efficiency, %	+ .880	−.0024
	Turbine Inlet Temperature, °C	+ 27.94	−.000077
Single Shaft Engine	Regenerator Effectiveness, %	+ .259	−.0083
With Radial Turbine	Leakage, %	− 1.354	+.0016
	Pressure Loss, %	− .733	+.0029
	Turbine Efficiency, %	+ .782	−.0027
	Compressor Efficiency, %	+ 1.067	−.0020
	SFC, kg/kW-h	.2140	
	Power, kW	20.14	
SS10	Transmission Efficiency, %	+ .862	−.0023
	Turbine Inlet Temperature, °C	+ 31.93	−.000062
Single Shaft Engine	Regenerator Effectiveness, %	+ .236	−.0085
With Axial Turbine	Leakage, %	− 1.489	+.0013
	Pressure Loss, %	− .728	+.0027
	Turbine Efficiency, %	+ .964	−.0021
	Compressor Efficiency, %	+ 1.394	−.0014
	SFC, kg/kW-h	.1992	
	Power, kW	18.91	
FT4	Transmission Efficiency, %	+ .827	−.0024
	Turbine Inlet Temperature, °C	+ 16.50	−.000120
Free Turbine Engine	Regenerator Effectiveness, %	+ .255	−.0078
	Leakage, %	− 1.485	+.0013
	Pressure Loss, %	− 1.257	+.0016
	Turbine Efficiency-R, %	+ 4.667	−.00043
	Turbine Efficiency-A, %	+ 2.723	−.00073
	Compressor Efficiency, %	+ 1.257	−.0016
	SFC, kg/kW-h	.1936	
	Power, kW	20.14	

(1) Sensitivity: Change in parameter value required to reduce SFC by 1 percent.
(2) Derivative: Change in SFC per change in parameter value.

TABLE 5.12

Effects of Technology Changes on Fuel Economy of Engine Configuration SS8

Parameter	20% Performance 1978	20% Performance 1983	Potential Change In Fuel Economy[1]
Transmission Efficiency[2]	70%	81%	−12.2%
Trans. Eff. w/Declutch	70%	81%	−19.5%
Turbine Inlet Temperature	1052°C	1296°C	− 6.8%
Regenerator Effectivness	96%	97.3%	− 5.1%
Engine Leakage (Total)	7%	5.1%	− 1.2%
Pressure Losses:			
• Turbine Diffuser	3.1%	1.6%	− 1.7%
• Combustor	2.3%	1.2%	− 1.3%
• Inlet and Exhaust	1.7%	1.2%	− 0.7%
• Regenerator	2.5%	3.1%	+ 0.6%
Turbine Efficiency	88%	91%	− 2.7%
Compressor Efficiency	77%	81%	− 2.8%

(1) The potential change is the percent change in fuel economy from the 1983 base that would occur had the parameter performance not improved beyond the 1978 level.

(2) Averaged over the CFDC.

5.8 Risk Analysis

A risk analysis was conducted for each configuration to determine a confidence interval estimate of the overall CFDC fuel economy. The interval estimate reflects the uncertainty in the estimates of 1983 component performances.

Probabilistic methods (References 13 and 14) were used to quantify the performance uncertainty. Three judgmental estimates were obtained for each performance parameter, Table 5.13. These are the optimistic (a), pessimistic (b) and most likely (m) level of performance for each parameter at the 20 percent power level in 1983. Assuming that the forecasts may be modelled by the beta distribution, the expected value, μ_i, of the ith parameter and its variance, σ_i^2, may be obtained as follows:

$$\bar{x}_i = \frac{1}{3}\left[2m + \frac{1}{2}(a+b)\right]$$

$$s_i^2 = \left[\frac{1}{6}(b-a)\right]^2$$

Where x_i and s_i^2 are estimates of μ_i and σ_i^2, respectively. The three estimates, the expected value and the variance of the performance of each parameter are shown in Table 5.13.

A cycle performance computer program was used to calculate a base line specific fuel consumption (SFC*) using base line values of the performance parameters (x_i^*) for each configuration. Assuming that the SFC is a function of seven independent variables and that the linear terms of a Taylor series expansion of the SFC function are reasonably accurate, the expected value of the SFC may be approximated by:

$$\overline{SFC} \cong SFC^* + \sum_{i=1}^{7}\left(\frac{\partial SFC}{\partial x_i}\right)\left(\bar{x}_i - x_i^*\right)$$

The variance of the SFC is

$$\sigma^2_{SFC} \cong \sum_{i=1}^{7} \left(\frac{\partial SFC}{\partial x_i}\right)^2 \sigma_i^2$$

The partial derivatives are calculated in the sensitivity analysis. The coefficient of variation of the SFC estimate is

$$CV_{SFC} = \frac{\sigma_{SFC}}{SFC}$$

The expected value, variance and coefficient of variation of the SFC of each configuration is shown in Table 5.14.

It is assumed that the SFC and the CFDC fuel economy are normally distributed and that the coefficient of variation of the CFDC fuel economy is equal to the coefficient of variation of the SFC. It is also assumed that the values of CFDC fuel economy reported in Section 5.2 are the expected values of CFDC fuel economy. The coefficient of variation and the expected value of the CFDC fuel economy determine the variance of the CFDC fuel economy and confidence intervals may be calculated assuming the normal distribution. Table 5.15 lists the CFDC fuel economy, variance coefficient of variation and 90 percent confidence interval for each configuration. Table 5.16 shows the probability that each configuration will have at least a 20, 40, 45 or 50 percent better fuel economy than the baseline vehicle. It can be seen that, while all of the configurations will certainly meet the specified fuel economy objective of the contract, only configurations SS8 and FT4 have a significant chance for large fuel economy improvements.

The coefficients of variation shown in Table 5.15 are the uncertainty of the fuel economy estimates normalized by the expected economy and may be used to compare the uncertainties of the four configurations.

TABLE 5.13

Estimates of 1983 Component Performance At 20 Percent Power

Parameter	Pessimistic b	Most Likely m	Optimistic a	Expected x_i	Variance s_i^2
Peak Transmission Efficiency, %	87	89.5	90	89.17	.25
Turbine Inlet Temperature (1)	1260	1371	1371	1352.5	342.25
Regenerator Effectiveness, %	96	97.3	98	97.2	.11
Leakage, %	7	5.1	4	5.23	.25
Pressure Loss, %	8.1	7.5	6.6	7.45	.067
Turbine Efficiency, R, % (2)	89	91.5	92	91.17	.25
Turbine Efficiency, R, % (3)	86.7	89.7	90.2	89.3	.34
Turbine Efficiency, A, %	86	88.5	89	88.17	.25
Compressor Efficiency, %	80	81	82	81	.11
Regenerator Inlet Temp., °C Max.	1038	1093	1149	1093	342.25

(1) °C at 100% power
(2) At the optimum rotor tip speed
(3) At 610 m/s rotor tip speed

TABLE 5.14

Specific Fuel Consumption from Cycle Analysis
Units: kg/kW-h

Engine Conf.*	SFC	σ_{SFC}	CV_{SFC}
SS8	.1870	.00326	.0174
SS4	.1818	.00389	.0214
SS10	.1938	.00358	.0185
FT4	.1814	.00375	.0207

TABLE 5.15

CFDC Fuel Economy
Units: km/l

Engine Conf.*	Fuel Economy	Variance	CV_{FE}	90% Conf. Interval
SS8	13.0	.2257	.0174	(12.60, 13.34)
SS4	11.9	.2547	.0214	(11.48, 12.32)
SS10	12.6	.2327	.0185	(12.20, 12.96)
FT4	13.1	.2710	.0207	(12.64, 13.54)

TABLE 5.16

Probability of Obtaining A Specified Minimum Percentage Improvement Over The Baseline Fuel Economy

Engine Conf.*	Percentage Improvement 20%	40%	45%	50%
SS8	100	100	99.996	98.15
SS4	100	82.11	23.69	0.93
SS10	100	99.996	98.37	63.60
FT4	100	100	99.99	98.54

* See Table 5.1 for definition of engine configurations.

5.9 Cost Comparisons

A cost comparison of three single shaft and one two shaft turbine engine concept is shown in Table 5.17.

Due to a lack of complete design material other than schematics for each configuration, these comparisons were made primarily on a judgment basis. Component costs were judged based on a cost of 1 unit for a 6 inch diameter finished cast aluminum impeller.

Configuration numbers in the comparison refer to Section 5.1, Table 5.1 of this report.

TABLE 5.17

Cost Comparisons

Item No.	Description	Material Metal (M) or Ceramic (C)	Relative Mfg. Cost Engine config.*			
			SS6,8	SS2,4	SS9,10	FT2,4
1	Impeller	M	.53	.75	.53	.75
2	Wheel, Turbine	M	3.27	4.63	9.80	4.63
	Wheel, Turbine	C	1.71	2.42	5.13	2.42
3	Shaft, Wheel (M)	M	.05	.10	.15	.10
	Shaft, Wheel (C)	M	.26	.37	.50	.37
4	Inlet Guide Vane Assy.	M	.79	.79	.79	.79
5	Gas Bearing	M	.21	.42	.21	.42
6	Thrust Bearing	M	.10	.12	.12	.12
7	Nozzle Turbine	C	1.37	1.94	4.10	1.94
8	Shroud Turbine	C	1.37	.95	1.37	.95
9	Inlet Turbine	C	.70	1.94	.70	1.94
10	Combustor Assy.	C	2.56	2.56	2.56	2.56
11	Regenerator Core	C	2.56	2.56	2.56	2.56
12	Regenerator Seals	M	1.28	1.28	1.28	1.28
13	Regenerator Drive	M	.96	1.36	.96	1.36
14	Inlet Housing	M	.64	.64	.64	.64
15	Main Housing	M	1.92	2.24	1.92	3.36
16	Regenerator Cover	M	.48	.48	.48	.48
17	Pinion Bearings	M	0	.37	0	.37
18	Reduction Gear	M	.75	.55	.75	.55
19	Gear Coupling	M	0	.10	0	.10
20	Variable P.T.N. Assy.	M	0	0	0	4.63
	Variable P.T.N. Assy.	C	0	0	0	2.42
21	Power Turbine	M	0	0	0	4.63
	Power Turbine	C	0	0	0	2.42
22	Power Turbine Shroud	C	0	0	0	.95
23	Power Turbine Diffuser	C	0	0	0	.30
24	Power Turbine Bearings	M	0	0	0	.37
25	Fixed Stator T.C.	M	0	0	0	.75
26	Variable Stator T.C.	M	1.5	1.5	1.5	0
27	Control Assy.	—	4.5	4.5	4.5	4.5
28	Accessories, Lube, Insul., Etc.	—	3.5	3.5	3.5	4.0
	Total Cost (Ceramic Turbines)		27.69	31.34	34.10	38.67
	Total Cost (Metal Turbines)		29.04	33.28	38.42	45.03

* See Table 5.1 for definition of engine configurations.

Essentially, this cost comparison indicates that a ceramic single shaft turbine engine will be about 40 percent less costly than an all metal two shaft engine. This is consistent with a more complete Ford study in 1973 which indicated about a 50% cost differential between the two engine types.

5.10 Powertrain Selection

The four engine concepts studied in this section, SS6,8; SS2,4; SS9,10 and FT2,4 as defined in Table 5.1, were evaluated and a selection made of a best candidate for the IGT engine using five criteria listed below. The selection criteria were quantified on the basis of either the analytical projections derived in the preceding sections or a judgment and were weighted according to their relative importance as shown:

Selection Criteria	Weighting Factor
1. CFDC Fuel Economy (Section 5.2)	5
2. Relative Manufacturing Cost (Section 5.8)	4
3. Risks (Section 5.7)	3
4. Installation Consideration (Judgment)	2
5. Development and Growth Potential (Judgment)	1

Inputs to criteria 1, 2 and 3 were provided as indicated from the analyses discussed in the preceding sections. The definition of "Risks" as used in the selection criteria is limited to confidence interval estimate of the overall CFDC fuel economy and is expressed as the probability of achieving at least 40% improvement in fuel economy over the baseline vehicle (See Section 5.7).

Criteria 4 and 5 are of purely judgmental nature. In quantifying the "installation consideration" criterion items such as engine weight, engine volume, packageability, installation flexibility and ease, i.e. how adaptable is the powertrain concept to both front and rear wheel drive arrangements?, how extensive engine compartment modifications will these installations require?, etc., were assessed on the basis of comparisons to piston engine installations and the layout studies conducted. Under the "Development and Growth Potential" criterion, the various powertrain concepts were assessed with regards to their adaptability to metallic rotors, fixed boundary heat exchangers (recuperators), variable compressor and turbine geometries and low emission combustor concepts.

The selection criteria quantified for each of the four powertrain configurations were assembled into a selection matrix shown in Table 5.18. The "raw value" which quantify the criteria are the analytical or, as the case may be, judgmental inputs discussed above, they were normalized with corresponding values for the powertrain concept in column 3, designated SS8/T1 i.e., the high rotational speed and high tip speed version of a single spool radial turbine with a ceramic turbine rotor and a variable stator torque converter coupled with a 4-speed Ford FIOD transmission. The product of a normalized value and the weighting factor constitutes the score, with the lowest score indicating the preferred concept. The high tip speed version of a single spool radial turbine, concept SS6,8, having the lowest overall score was selected for detailed study.

TABLE 5.18

Powertrain Selection Matrix

CRITERIA	Weighting Factor	Engine and Transmission Configurations* SS8/T1 Raw Value/ Normalized Value	SS8/T1 Score	SS8/T1 Raw Value/ Normalized Value	SS8/T1 Score	SS10/T1 Raw Value/ Normalized Value	SS10/T1 Score	FT3/T4 Raw Value/ Normalized Value	FT3/T4 Score
CFDC Fuel Economy	5	30.5/ 1.00	5.00	28.0/ 1.09	5.45	29.6/ 1.03	5.15	34.3/ .89	4.45
Relative Manufacturing Cost	4	27.69/ 1.00	4.00	31.34/ 1.132	4.53	34.10/ 1.231	4.93	38.67/ 1.40	5.59
Installation Considerations	2	1.36/ 1.00	2.00	1.50/ 1.30	2.60	1.36/ 1.00	2.00	1.76/ 1.54	3.08
Risks	3	1.000/ 1.00	3.00	.8211/ 1.22	3.65	.99996/ 1.006	3.00	1.000/ .9998	3.00
Development and Growth Potential	1	3.00/ 1.00	1.00	3.70/ 1.23	1.23	5.5/ 1.83	1.83	4.00/ 1.33	1.33
TOTAL			15.00		17.46		16.91		17.45

*See Table 5.1 for definition of engine configurations and Section 5.2 for definition of transmission configurations.

6.0 SELECTED ENGINE DESIGN

The engine selected for continued study was the single shaft machine with a radial turbine. A rotational speed of 12,357 rads/s (118,000 rpm) was selected for optimum specific speed of the compressor and also to minimize the effects of spool inertia as reflected to the driveshaft. Initially the radial turbine rotor would be of metal, to be replaced by a ceramic rotor when the latter is available. Both of the metal and ceramic turbines were designed for maximum efficiency without limitation on the tip speeds. The following sections discuss the preliminary designs and analyses of the engine and its critical components.

6.1 Component Aerothermo Designs

6.1.1 COMPRESSOR

The compressor for the Improved Gas Turbine engine utilizes an aluminum, single-stage, centrifugal impeller. Aluminum was chosen for low cost and ease of manufacturing. An additional advantage of aluminum is its inherent light weight and low polar moment of inertia which aids engine response time. Due to its relatively low strength, however, an aluminum impeller must be limited to pressure ratios of 5:1.

For a pressure ratio of 5, airflow 0.39 kg/s (0.85 pps) and speed 12357 rads/s (118,000 rpm), AiResearch compressor design computer programs provided the preliminary geometric definition of a compressor stage and an estimate of efficiency. Table 6.1 shows the basic preliminary design results and Figure 6.1 shows the approximate meridional view. In Figure 6.2 a preliminary definition of the aerodynamic shape of the compressor diffuser (first stage) is shown.

Figures 6.3 and 6.4 show some of the trends that were observed during the preliminary parametric studies of the compressor. This data was useful in performing design trade-offs considering the mechanical and aerodynamic requirements.

TABLE 6.1

Single Stage Centrifugal Compressor Design

Airflow, Kg/s (pps)	0.39 (0.85)
Rotational speed, rads/s (rpm)	12357 (118000)
Overall pressure ratio	5
Overall stage efficiency, (tot-tot) %	80.5
Specific speed	(67.6)
Blade number	17
Slip factor	0.9
Temp. rise ratio, $\frac{\Delta T}{T}$	0.719
Impeller tip dia., mm (ins)	92.1 (3.626)
Impeller blade angle	40°
Inducer tip dia., mm (ins)	62.5 (2.462)
Inducer hub dia., mm (ins)	30.5 (1.2)
Impeller tot-tot pressure ratio	5.544
Impeller tot-tot efficiency, %	86.7
Inlet temp., °C [°F]	29.4 (85)
Inlet pressure, kPA (psia)	100.31 (14.549)

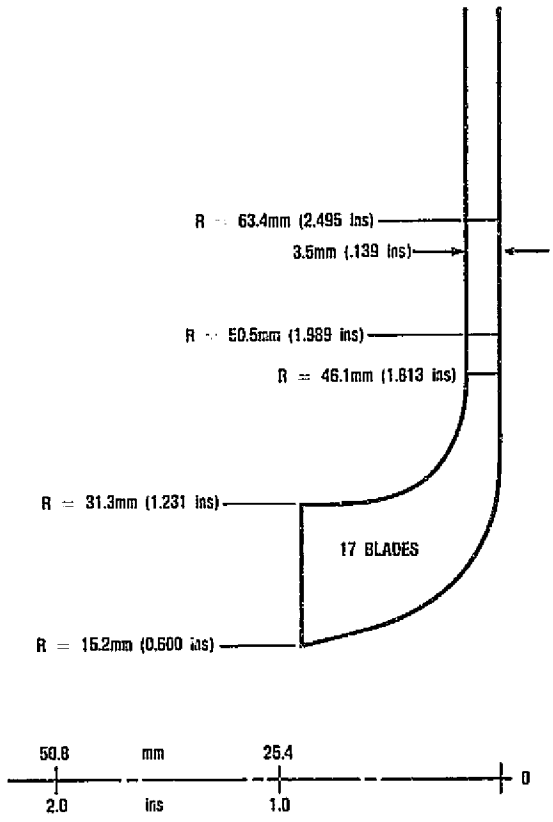


Figure 6.1 Centrifugal Compressor Rotor Meridional Cross-Section

In Figure 6.3 inducer tip relative Mach number is plotted as a function of rotor speed. Compressor losses increase and impeller operating range decreases with increasing Mach number. Previous experience indicates that an inducer tip Mach number of about 1.15 is a practical limit for most Airesearch designs. For an inducer hub dia. of 30.5 mm (1.2 ins) it is seen that the resulting inducer tip relative Mach number is about 1.26, indicating a possible design risk.

Figure 6.4 shows the relationship of rotor speed, hub diameter and compressor stage efficiency based on preliminary loss assumptions. Clearly, this graph shows that a small hub diameter favors high compressor efficiency.

The compressor characteristic maps are shown in Figures 6.5 and 6.6 and are based on actual test data with the flow parameter non-dimensionalized. To match the projected 1983 technology compressor efficiency of 81.3 percent (tot-tot) at design point, the efficiency levels shown in Figure 6.6 were scaled up from 80.5 percent. This improvement in efficiency is assumed to occur during a 5 year R&D program. The same compressor map was used for all the engine off-design analyses which were described in Section 5.1.

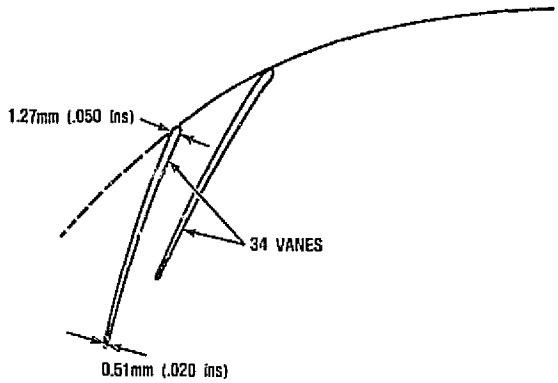


Figure 6.2 Centrifugal Compressor First Stage Diffuser

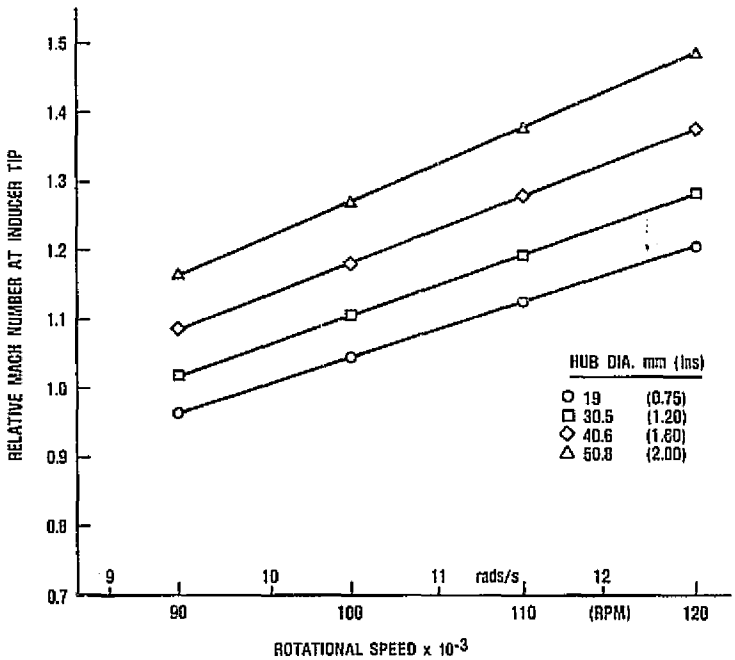


Figure 6.3 Effect of Centrifugal Compressor Speed and Hub Diameter on the Relative Mach Number at Inducer Blade Tip

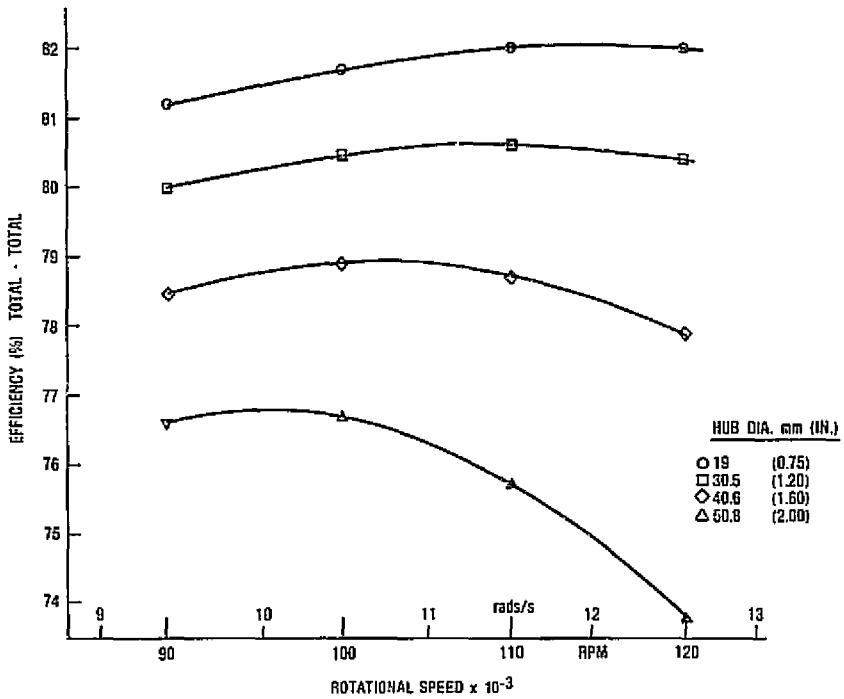


Figure 6.4 Effect of Centrifugal Compressor Speed and Hub Diameter on the Efficiency

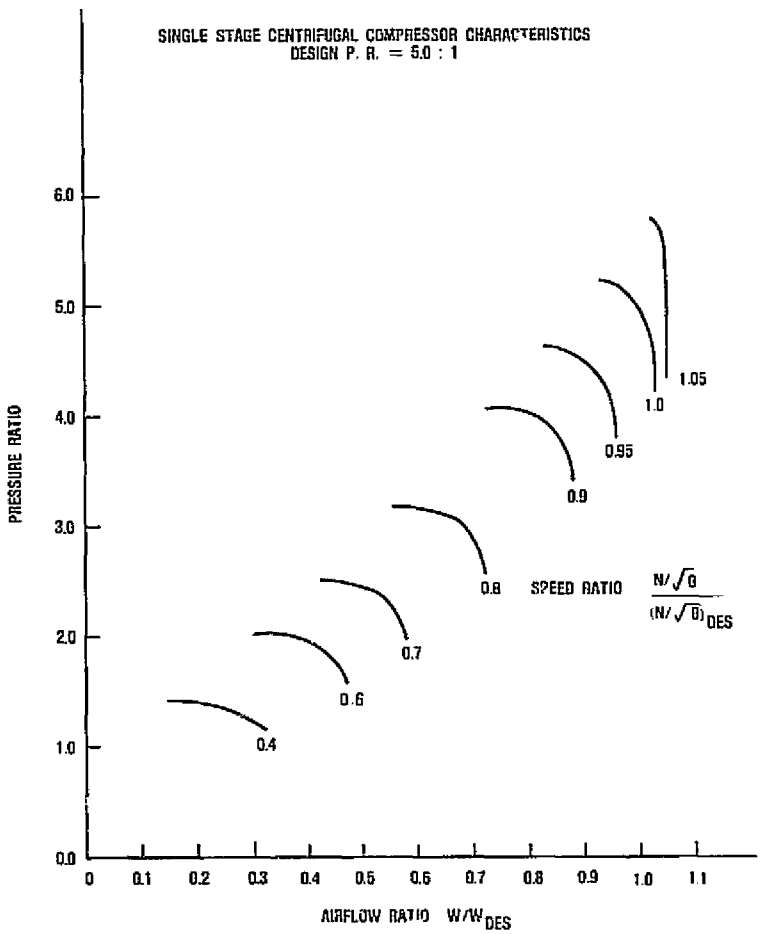


Figure 6.5 Single-Stage Centrifugal Compressor Pressure Ratio and Airflow Characteristic Map

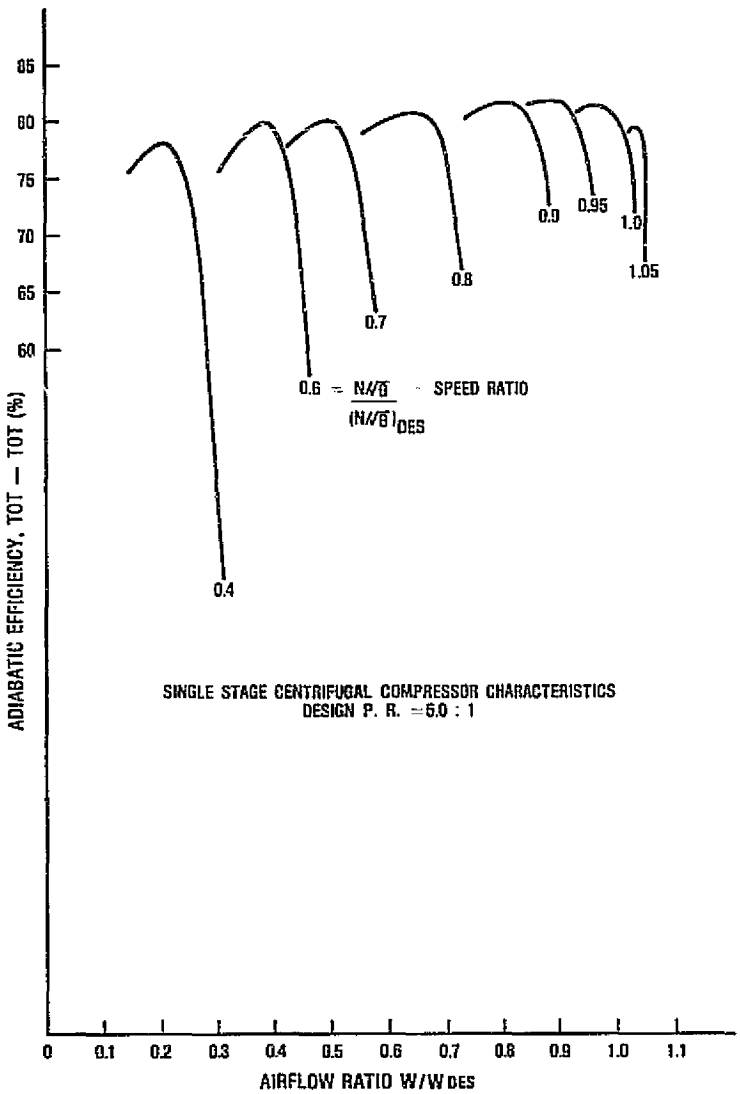


Figure 6.6 Single-Stage Centrifugal Compressor Efficiency Characteristic Map

6.1.2 RADIAL TURBINE

The final cycle analysis performance data was used to define the design point for the metallic and ceramic radial turbines in terms of airflow, pressure ratio, tip speed and rotational speed. A computer program based on a combination of two NASA technical papers, references 15 and 16, was used to generate the basic geometric details of the radial turbine design point. A sketch of the metallic radial turbine flow path is shown in Figure 6.7 and the significant geometric and aerodynamic parameters are shown in Table 6.2. The number of rotor blades were reduced somewhat from optimum aerodynamic conditions based on experience from prior thermal and mechanical stress analysis of other similar metallic rotors. Similar information for the ceramic radial turbine design is shown in Figure 6.8 and also in Table 6.3. Once again somewhat less than optimum number of rotor blades were chosen based on prior thermal and mechanical stress analysis.

The hub and shroud contours and blade thickness distribution are determined iteratively. This process consists of selecting a geometry for a satisfactory determination of hub-to-shroud and blade-to-blade velocity gradients, using computer programs as described in references 17 and 18. Then a blade and rotor stress analysis is completed as described in Section 5.3. This may require some changes to be made to the geometric shape and blade thickness distribution, and consequently the rotor must then be re-analyzed for velocity gradient suitability. Due to time limitations in the study program this complete iteration process was not undertaken for the two radial turbine designs. Instead, the basic rotor

contours were proportioned based on a previously analyzed design that closely resembled the current rotors.

The preliminary stator geometry for both the metallic and ceramic turbines was established based upon previous AiResearch experience. Although the number of vanes shown in Figures 6.7 and 6.8 is about half of the optimum number, as obtained from the design point programs of references 15 and 16, significant improvements in stator performance are expected from the endwall contouring, as shown, in conjunction with a 3-dimensional viscous flow analysis. However, this analysis was beyond the scope of the current program.

The radial turbine off-design results were determined with a computer program as described in reference 19. Performance maps of total-to-total, axial efficiency and airflow vs. pressure ratio were generated and used as input to the engine performance analysis computer program. Total-to-total, axial efficiency considers the turbine rotor exit total pressure to consist of the static pressure at the 'RMS' radius plus the dynamic pressure equivalent of the absolute axial component of discharge velocity. The resulting efficiency and airflow maps for the metallic radial turbine are shown in Figures 6.9 and 6.10. Similar results for the ceramic radial turbine are shown in Figures 6.11 and 6.12. The total-to-total, axial efficiency and the airflow parameters were adjusted, as necessary, to match the engine design point, as derived in section 4.0.

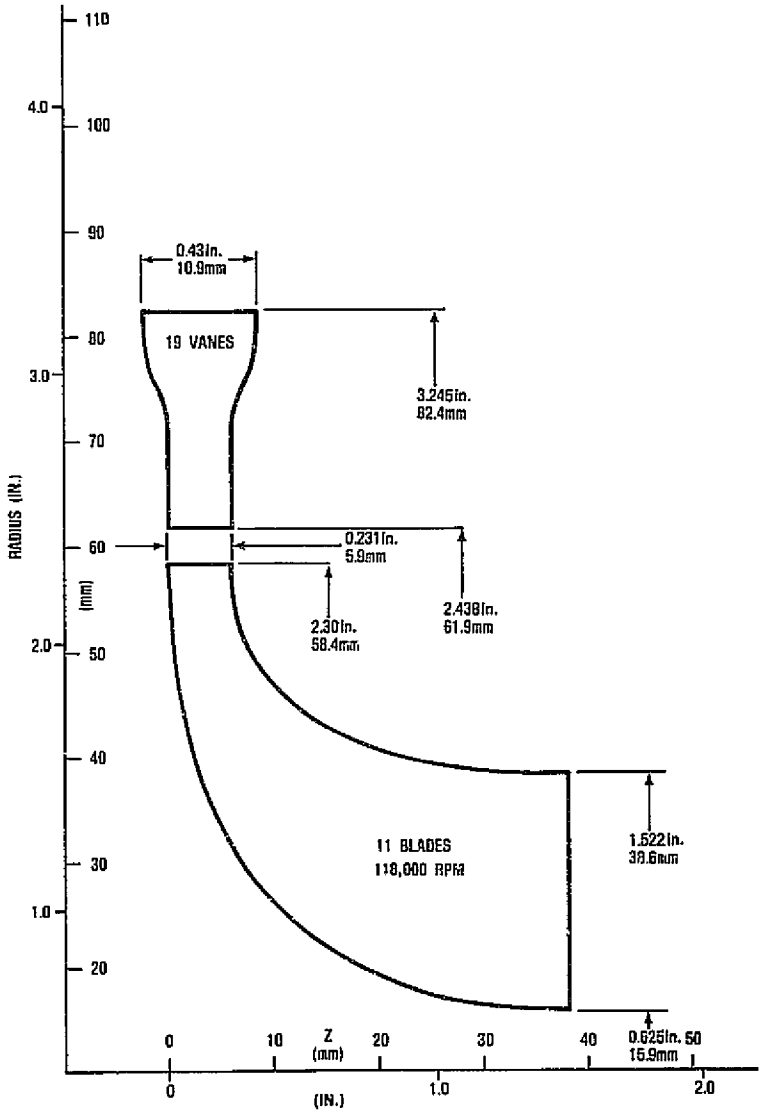


Figure 6.7 Radial Turbine Rotor and Stator Meridional Cross-Section (Metallic Rotor)

TABLE 6.2

Metal Radial Turbine Design Point

General

Inlet Total Pressure	478.0	kPa	69.33	psia
Overall Pressure Ratio (Total-to-Total)	4.15		4.15	
Inlet Total Temperature	1149	°C	2100	°F
Stage Work (ΔH)	439,600	J/kg	189	BTU/lb
Weight Flow	0.37	kg/s	0.81	pps
Rotational Speed	12357	rads/s	118,000	rpm
Specific Speed (Ns)	0.69		89	
Tip Speed	722	m/s	2368	fps
Stage Work Coeff. (λs)	0.84		0.84	
Stage Total-to-Total Efficiency (%)	89.6		89.6	

Rotor

Number of Blades	11		11	
Axial Length	38.1	mm	1.5	ins
Impeller Tip Diam.	116.8	mm	4.60	ins
Exit Shroud Diam.	77.3	mm	3.043	ins
Exit Hub Diam	31.7	mm	1.249	ins
Rotor Exit Meanline Relative Flow Angle	−48.6		−48.6	
Rotor Exit Swirl Angle	− 2.6		− 2.6	

Stator

Number of Vanes	19		19	
Inlet Diam.	164.8	mm	6.49	ins
Exit Diam.	123.9	mm	4.876	ins
Inlet Vane Width	10.9	mm	0.43	ins
Exit Vane Width	5.9	mm	0.231	ins

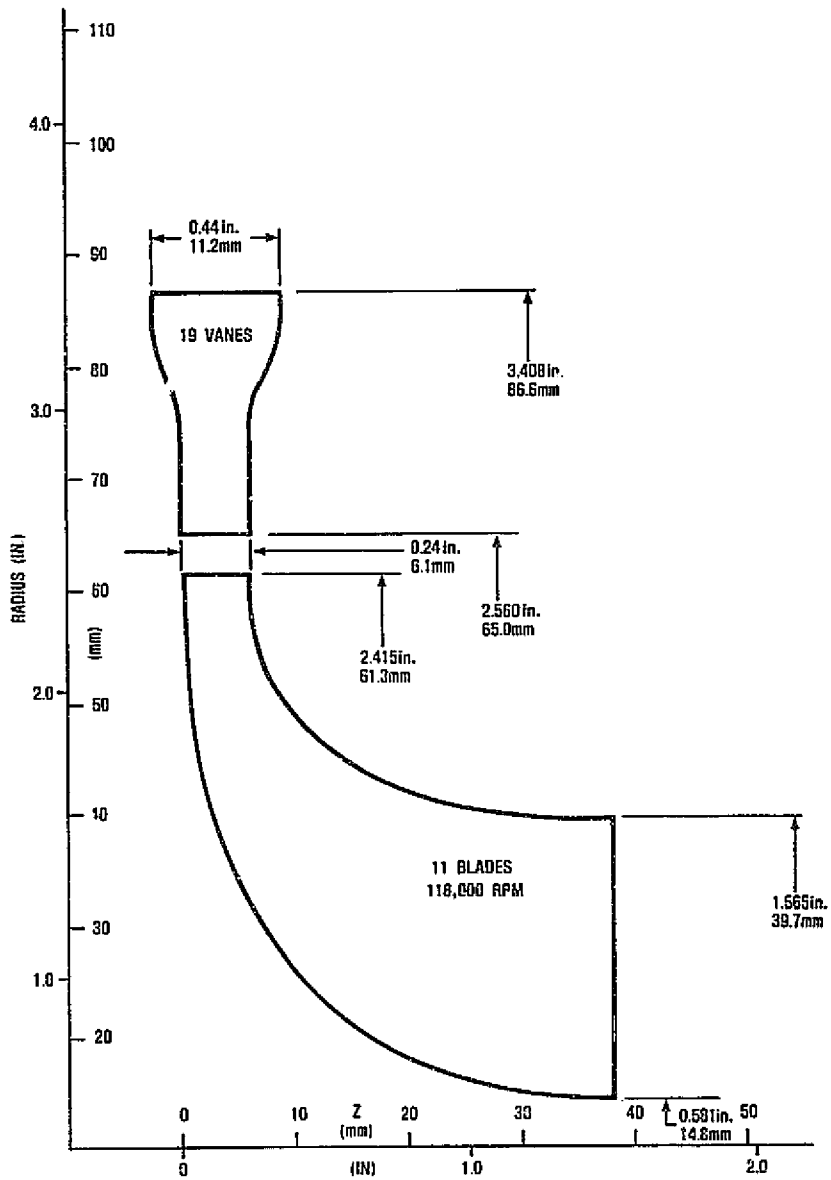


Figure 6.8 Radial Turbine Rotor and Stator Meridional Cross-Section (Ceramic Rotor)

TABLE 6.3

Ceramic Radial Turbine Design Point

General				
Inlet Total Pressure	478.0	kPa	69.33	psia
Overall Pressure Ratio (Total-to-Total)	4.09		4.09	
Inlet Total Temperature	1371	°C	2500	°F
Stage Work (ΔH)	507,000	J/kg	218	BTU/lb
Weight Flow	0.36	kg/s	0.80	pps
Rotational Speed	12357	rads/s	118,000	rpm
Specific Speed (Ns)	0.67		86	
Tip Speed	758	m/s	2487	fps
Stage Work Coeff. (λs)	0.88		0.88	
Stage Total-to-Total Efficiency (%)	89.7		89.7	
Rotor				
Number of Blades	11		11	
Axial Length	38.1	mm	1.5	ins
Impeller Tip Diam.	122.7	mm	4.83	ins
Exit Shroud Diam.	79.5	mm	3.130	ins
Exit Hub Diam.	29.5	mm	1.162	ins
Rotor Exit Meanline Relative Flow Angle	−46.6		−46.6	
Rotor Exit Swirl Angle	− 3.6		− 3.6	
Stator				
Number of Vanes	19		19	
Inlet Diam.	173.1	mm	6.816	ins
Exit Diam.	130.0	mm	5.120	ins
Inlet Vane Width	11.2	mm	0.44	ins
Exit Vane Width	6.1	mm	0.240	ins

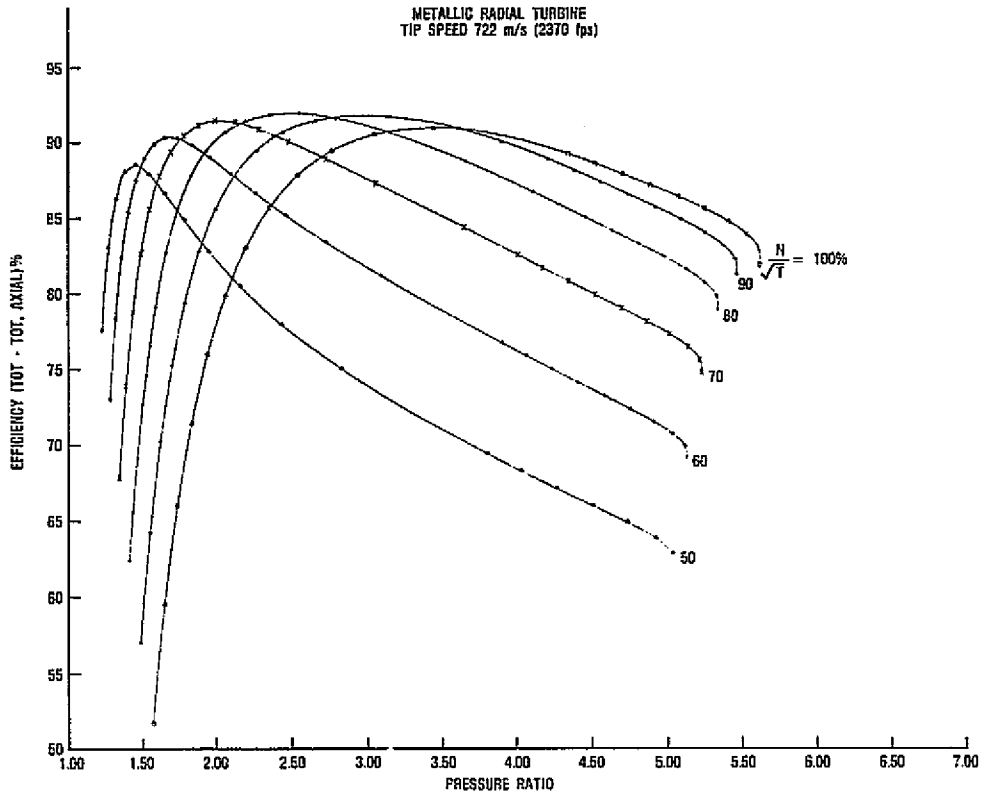


Figure 6.9 Radial Turbine Efficiency Characteristics — Metallic Rotor Tip Speed 722 m/s (2368 fps)

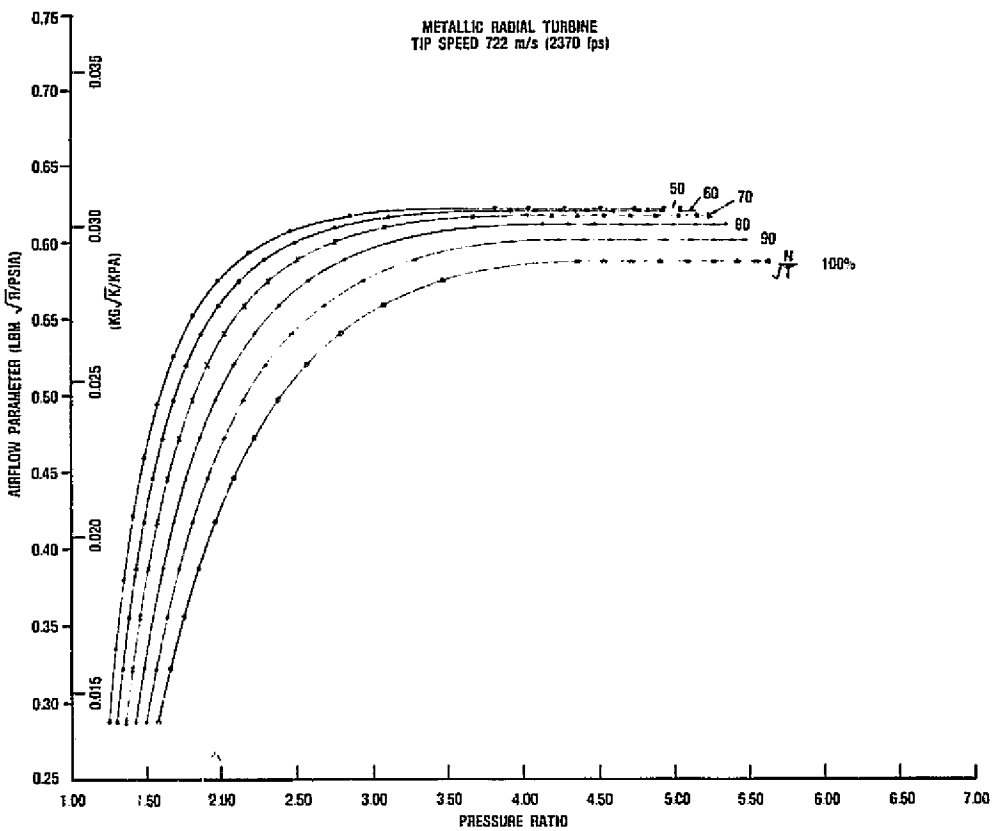


Figure 6.10 Radial Turbine Airflow Characteristics — Metallic Rotor Tip Speed 722 m/s (2368 fps)

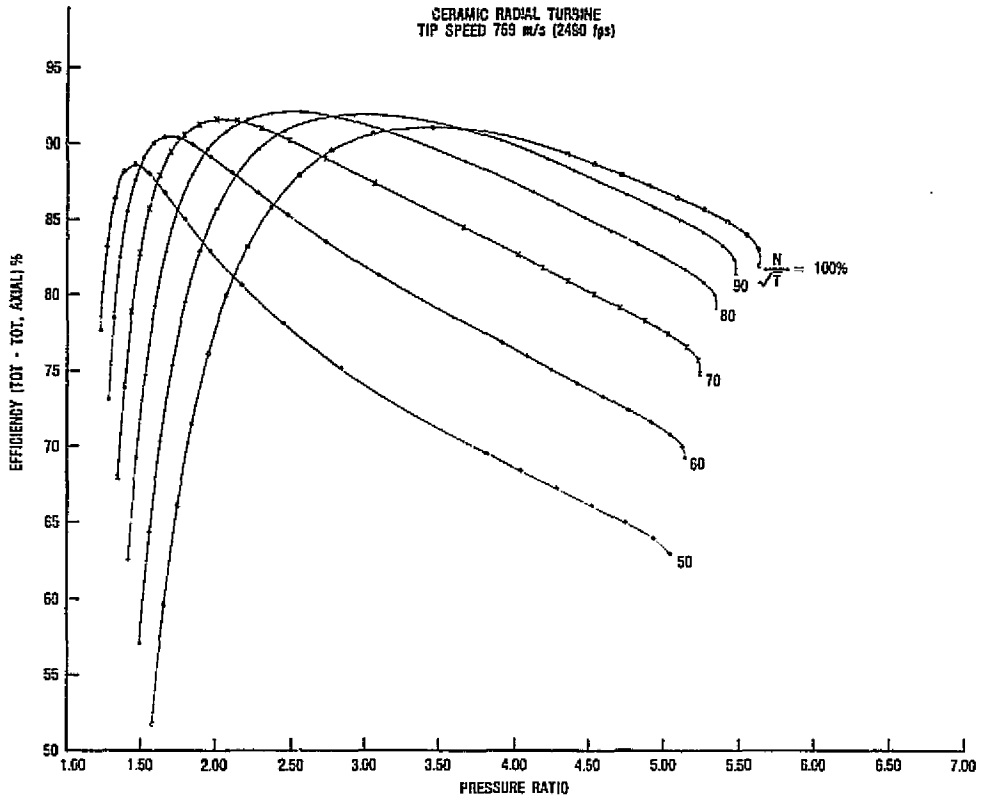


Figure 6.11 Radial Turbine Efficiency Characteristics — Ceramic Rotor Tip Speed 758 m/s (2487 fps)

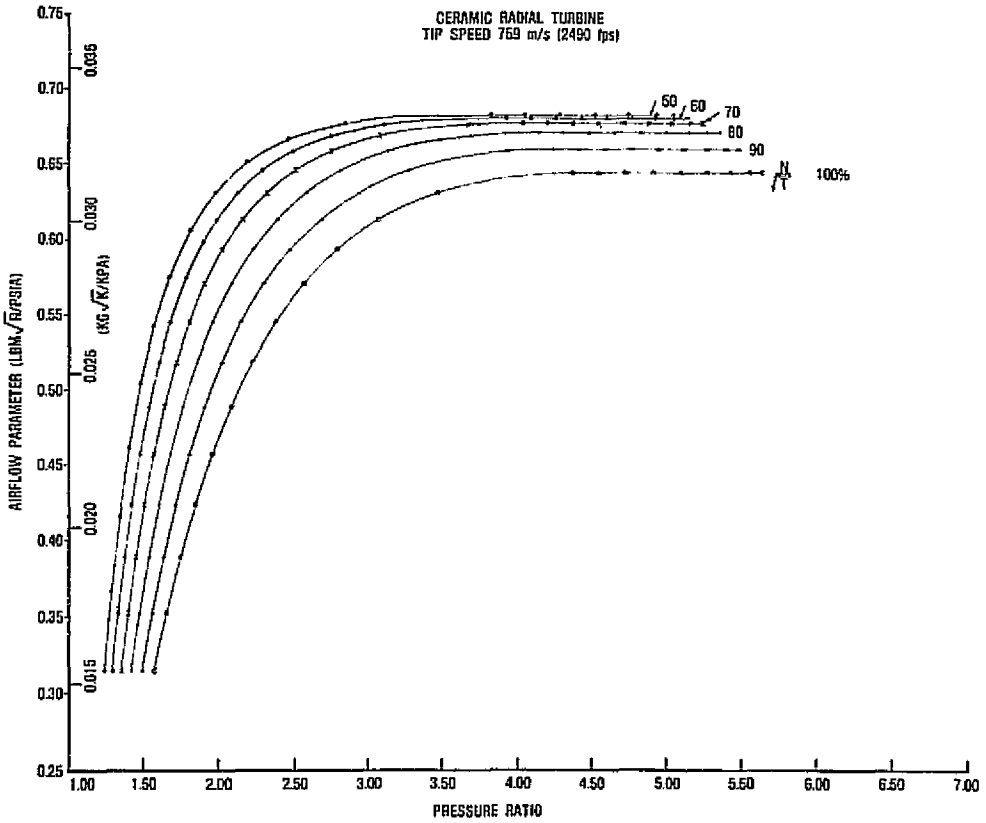


Figure 6.12 Radial Turbine Airflow Characteristics — Ceramic Rotor Tip Speed 758 m/s (2487 fps)

6.1.3 REGENERATOR

The regenerator consists of a ceramic matrix with an effective frontal area equal to that of one of the dual cores of the Ford 820 gas turbine engine, which had approximately twice the airflow of this IGT engine design.

The regenerator core is arranged co-axially around the combustion chamber similar to a configuration which was developed for the Ford Stirling engine, Reference 20. This arrangement resulted in a core with the following dimensions:

effective outer diameter = 0.41 m (16 ins)

effective inner diameter = 0.18 m (7 ins)

thickness of core = 0.07 m (2.8 ins)

design speed = 2.1 rads/sec (20 rpm)

6.1.4 COMBUSTOR

The low emissions combustor was scaled down from a prototype design of an internally vaporizing combustor (premix/prevaporizing type) built for the Ford 820 engine. In prototype form the can combustor was partly ceramic and partly metal. In scaled down form for the IGT engine it was assumed that ceramic parts would replace all of the metal parts. The axial symmetry of the combustor would lend itself to this modification. Emissions results projected from a steady state test rig data on the prototype combustor indicated low levels of emissions could be obtained i.e. 0.1 HC, 1.5 CO, 0.2 NOX gm/mile.

6.2 Mechanical Design

6.2.1 INTRODUCTION

The IGT engine concept selected in Section 5.9 was developed in more detail using aerodynamic components sized to match the engine specifications as discussed in the preceding section. This study concentrated on the analyses and mechanical features considered key to the functional integrity of this particular engine concept. The key areas studied and reported in this chapter are the thermal distortion of engine flowpath and their effect on running clearances, turbine rotor to shaft attachment, turbine diffuser mounting, main shaft dynamics, compressor rotor stresses and deformations, regenerator rotor mounting and the engine-transmission interfaces. In the course of the study it was necessary to repackage the oil cooler matrix to provide additional room around the combustor area for future development. A parametric study was conducted in support of this effort on the oil cooler-fan system and is also reported here.

A detailed design layout of the selected powertrain concept was generated and is shown in Figure 6.13. The details reflect the results of the design studies mentioned above and reported in succeeding Sections. Although two options of radial turbine rotors, a ceramic and a metallic are being considered for the selected engine, rotor attachment studies were limited because of time and funding limitations to the metallic version only which is shown in Figure 6.13 and reported here.

In order to minimize heat soak and emission related problems encountered with oil lubricated bearings operating in high temperature environment, oil lubrication has been eliminated from the engine section of the selected IGT concept. As indicated earlier in Section 5.3 the main shaft bearing, located between the compressor and turbine rotors, is a gas lubricated foil bearing that doubles as a restrictor or a seal for the compressor discharge air which is used to cool the bearing before leaking out into turbine exhaust. To improve its compliance, the foil bearing is supported on a bumper foil. The bearing is a scale-down version of a bumper foil bearing designed by MTI (Mechanical Technology Inc.) for the 820 Ford experimental gas turbine and is similar in concept to the turbine end bearing being developed by the same company for the Upgraded Chrysler Engine under a NASA contract. An alternate concept of a foil bearing, developed by AiResearch is being contemplated for this location. This will be designed and evaluated in the follow-up study.

The gear end of the main shaft was slightly modified to accommodate modifications made to the planetary gear system. The main thrust bearing has been moved forward and was changed to an air lubricated spiral groove thrust-anthithrust bearing eliminating need for an oil-air seal at the compressor inlet. An optional roller bearing location was provided at the end of the shaft in case a need for increased support stiffness in that area was indicated during development stage.

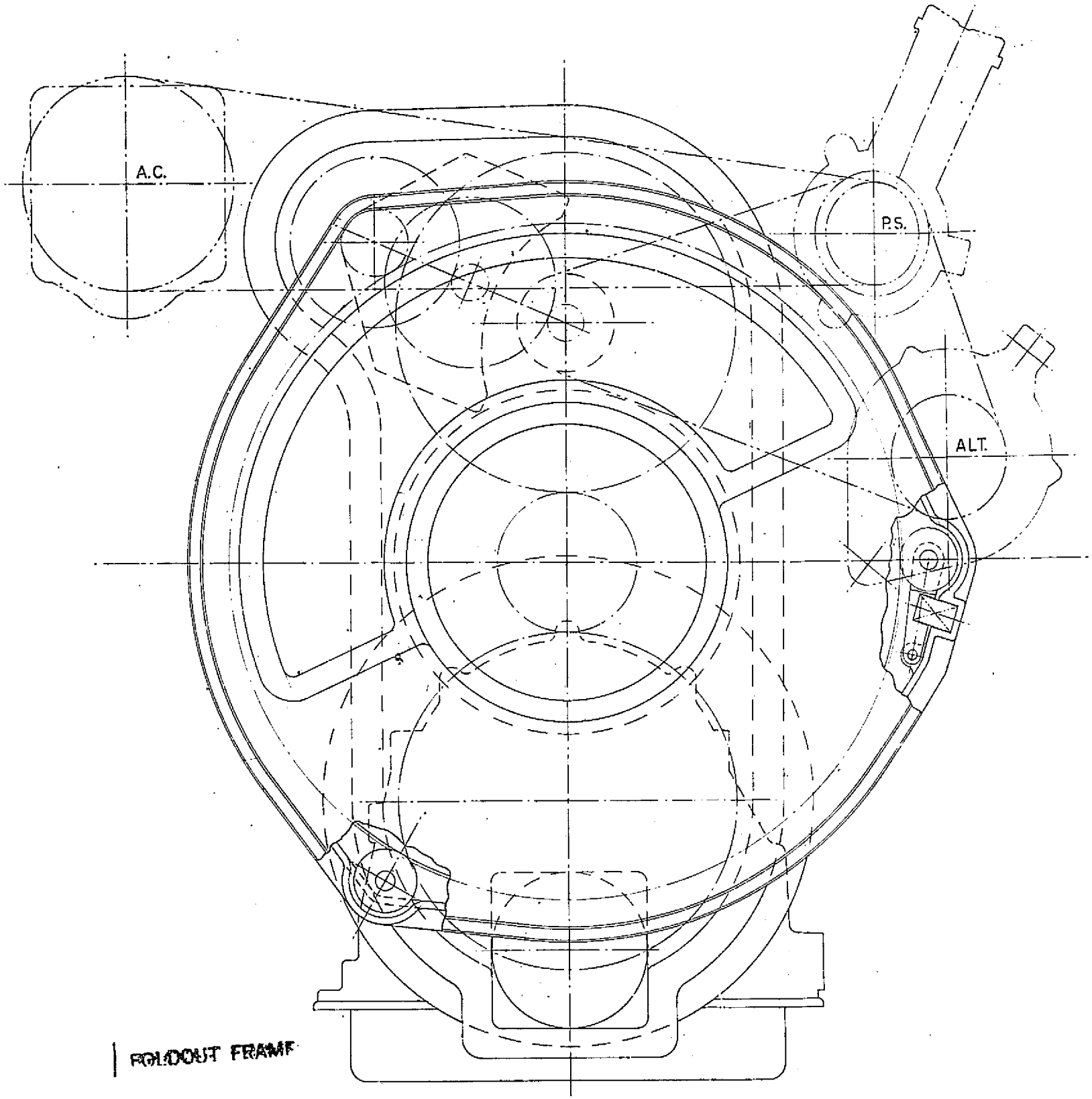
Figure 6.14 shows a proposed bill of materials for the selected engine. Several material options are listed for all key structures. The options would be evaluated during the next Phase of the program. As a rough preliminary guide it is expected that the higher expansion ceramic options will favor the metallic turbine rotor version of the engine. For the ceramic rotor version both low and high expansion ceramics will be evaluated and an optimum selection made following detailed design study.

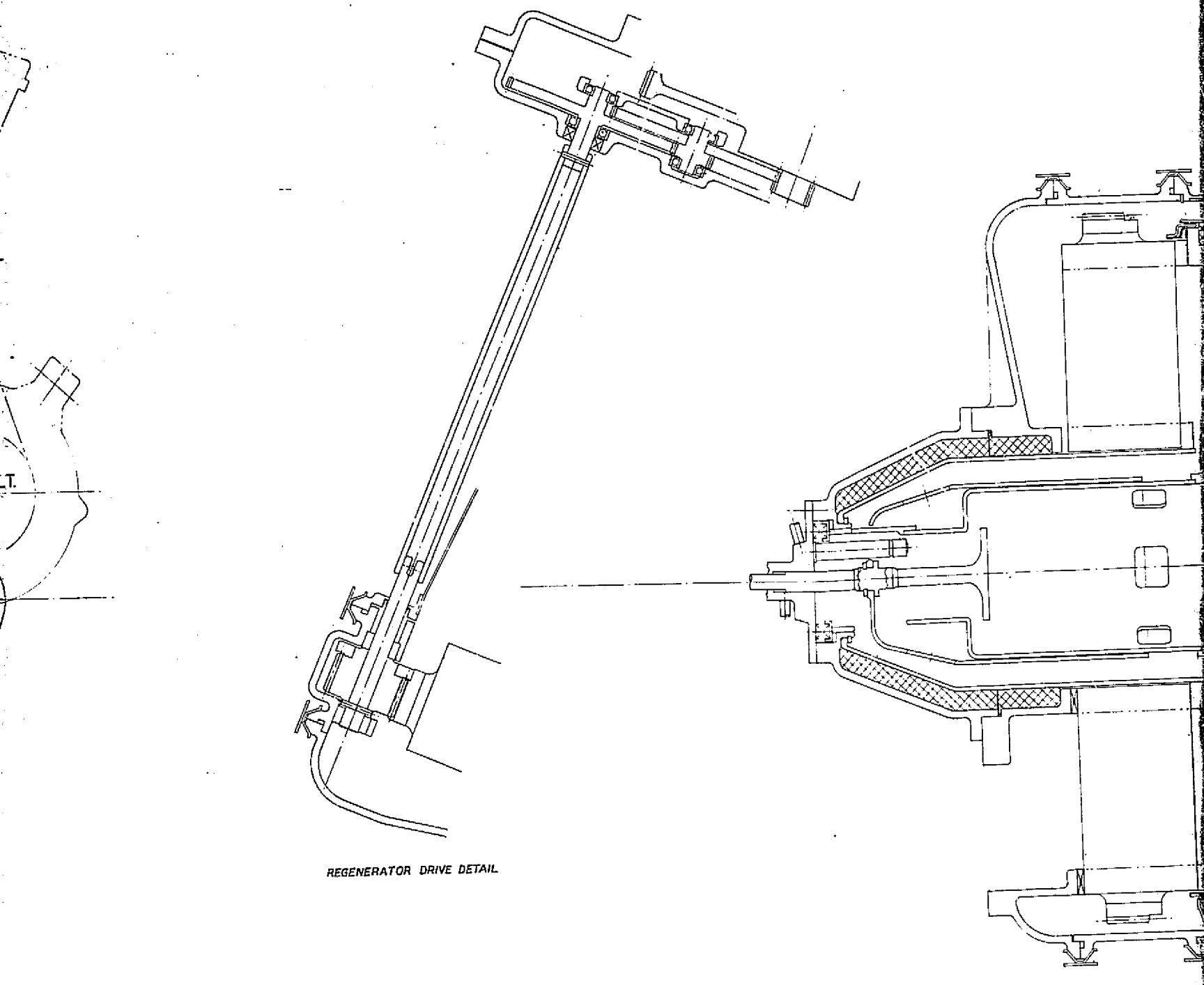
Figure 6.15 identifies individual engine parts which are listed in Table 6.4

TABLE 6.4

Improved Gas Turbine Engine
Part List

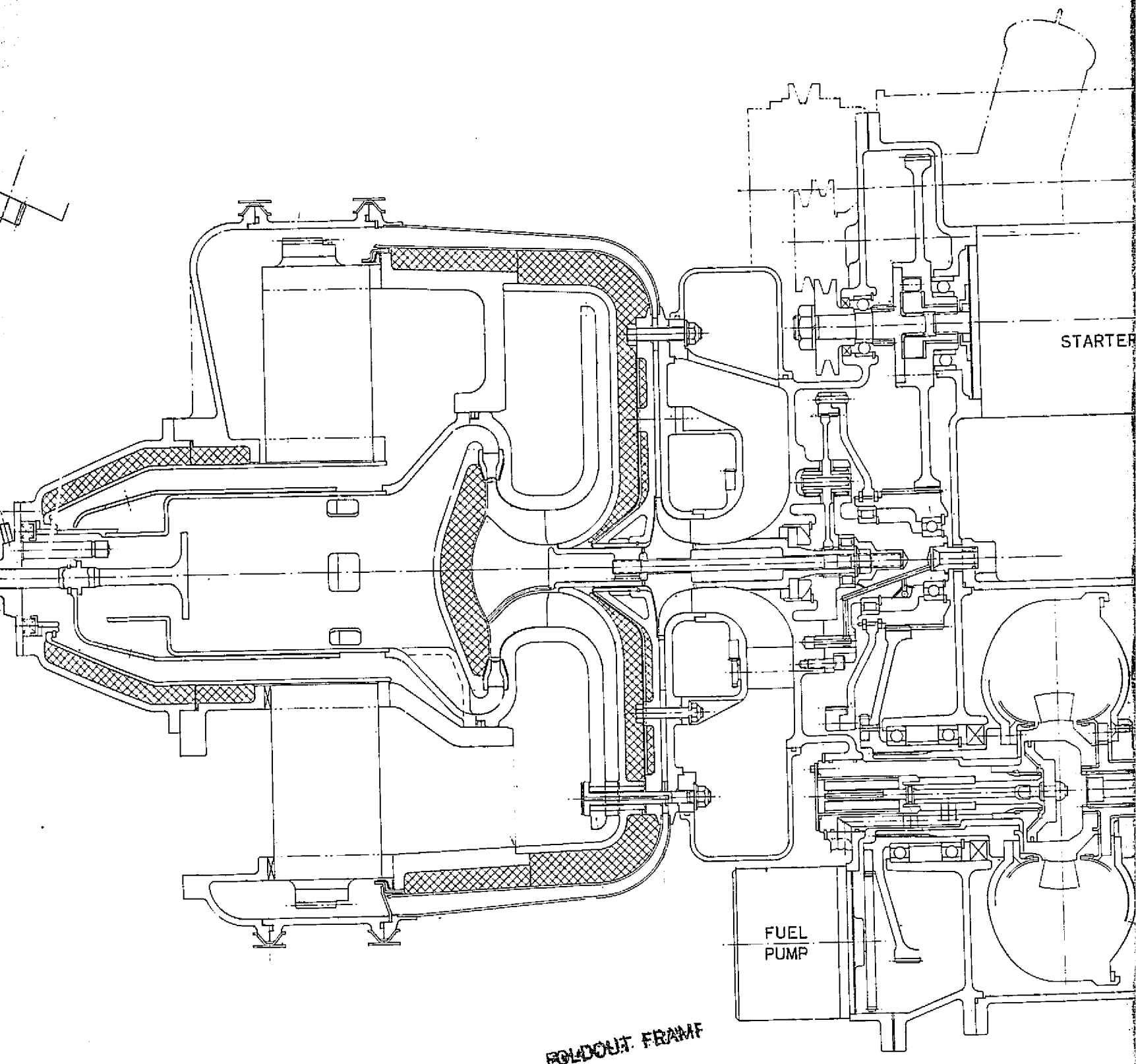
No.	Name	Amt. Req'd.
1.	Gear — Regenerator Drive	1
2.	Bearing — Regenerator Drive Gear	3
3.	Bearing — Regenerator Drive Gear	1
4.	Seal — Regenerator Drive Gear Shaft	1
5.	Pin — 1/8 Dia x 3/4 LG	2
6.	Shaft — Regenerator Drive	2
7.	Shaft — Regenerator Pinion	1
8.	Seal — Regenerator Pinion Shaft	1
9.	Bushing — Regenerator Drive Pinion (Graphite)	2
10.	Pinion — Regenerator Drive	2
11.	Pin — 1/8 Dia x 13/16 LG.	1
12.	Gear Assy — Regenerator Drive Idler	1
13.	Insulation — Fibrous	1
14.	Retainer — Combustor	1
15.	Liner — Combustor Insulation	1
16.	Ring — Split Retainer	1
17.	Retainer — Combustor Loading Spring	1
18.	Spring — Combustor Loading Spring	6
19.	Nozzle Assy — Fuel	1
20.	Centerbody — Combustor	1
21.	Ring — Split Retainer	1
22.	Sleeve — Secondary Air Metering	1
23.	Combustor — Liner	1
24.	Cover — Combustor	1
25.	Retainer — Insulation	1
26.	Cover — Regenerator	1
27.	Seal — Regenerator Cover Outer	1
28.	Seal — O-Ring (Elastomeric)	2
29.	Clamp — Regenerator Housing Cover	2
30.	Core Assy — Regenerator	1
31.	Support — Seal Spring	1
32.	Seal Assy — Compressor Discharge	1
33.	Seal — Regenerator Inner	1
34.	Housing Assy — Diffuser Inner (34 Vanes)	1
35.	Shell Assy — Diffuser Outer	1
36.	Pin — Dowel	2
37.	Screw — Air Cooled	8
	Nut — UBS 5/16 Dia.	8
38.	Insulation — Fibrous	1
39.	Seal — O-Ring	12
40.	Screw — Hex HD 5/16 Dia.	12
	Nut — UBS 5/16 Dia.	12
41.	Housing — Compressor Inlet	1
42.	Gear — Inlet Guide Vane Drive	1
43.	Vane & Gear Assy — Inlet Guide	17
44.	Seal — O-Ring	1
45.	Nut — UBS 3/8 Dia.	1
46.	Bearing — Optional Note: Main Shaft Supported by Planetary Gear	1
47.	Seat — Thrust Bearing	1
48.	Ring — Split Retainer	1
49.	Bearing — Thrust Air	1
50.	Washer — Thrust	1
51.	Bearing — Anti-Thrust Air	1
52.	Shaft — Compressor Mounting	1
53.	Seal — O-Ring	1
54.	Wheel — Compressor	1
55.	Bolt — Compressor & Turbine Retaning	1
56.	Housing — Inlet & Gearbox Support	1
57.	Bolt — Hex 5/16 Dia.	8
	Nut — UBS 5/16 Dia.	8
58.	Plenum — Air Inlet	1
59.	Seal — O-Ring	1
60.	Vanes — Straightener	16
61.	Seal — O-Ring	32
62.	Insulation — Fibrous	1
63.	Ring — Split Retainer	1
64.	Bearing — Foil Air	1
65.	Shell — Exhaust Diffuser Outer	1
66.	Shell — Exhaust Diffuser Inner	1
67.	Insulation — Fibrous	1
68.	Wheel — Turbine	1
69.	Nozzle — (19 Vanes)	1
70.	Ring — Split Seal	2
71.	Housing — Regenerator Support	1
72.	Body — Turbine Inlet Center (Includes Ceramic Foam Insulation)	1
73.	Duct — Combustor Transition	1
74.	Insulation — Fibrous	1
75.	Housing — Regenerator	1


A.C.
P.S.
ALT.
FOLDOUT FRAME



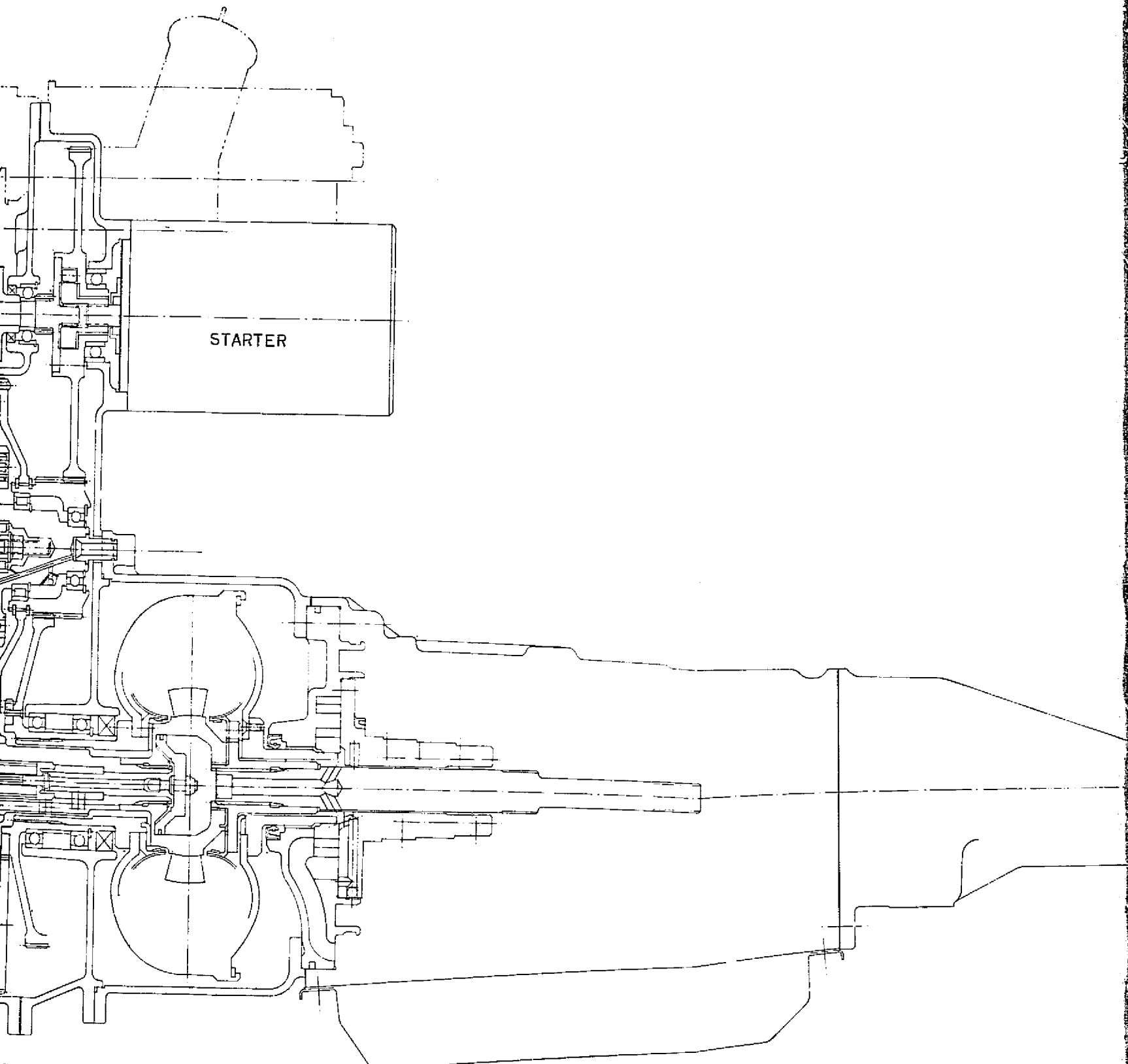
FOLDOUT

Figure 6.13 Detail Design Layout of Ford I

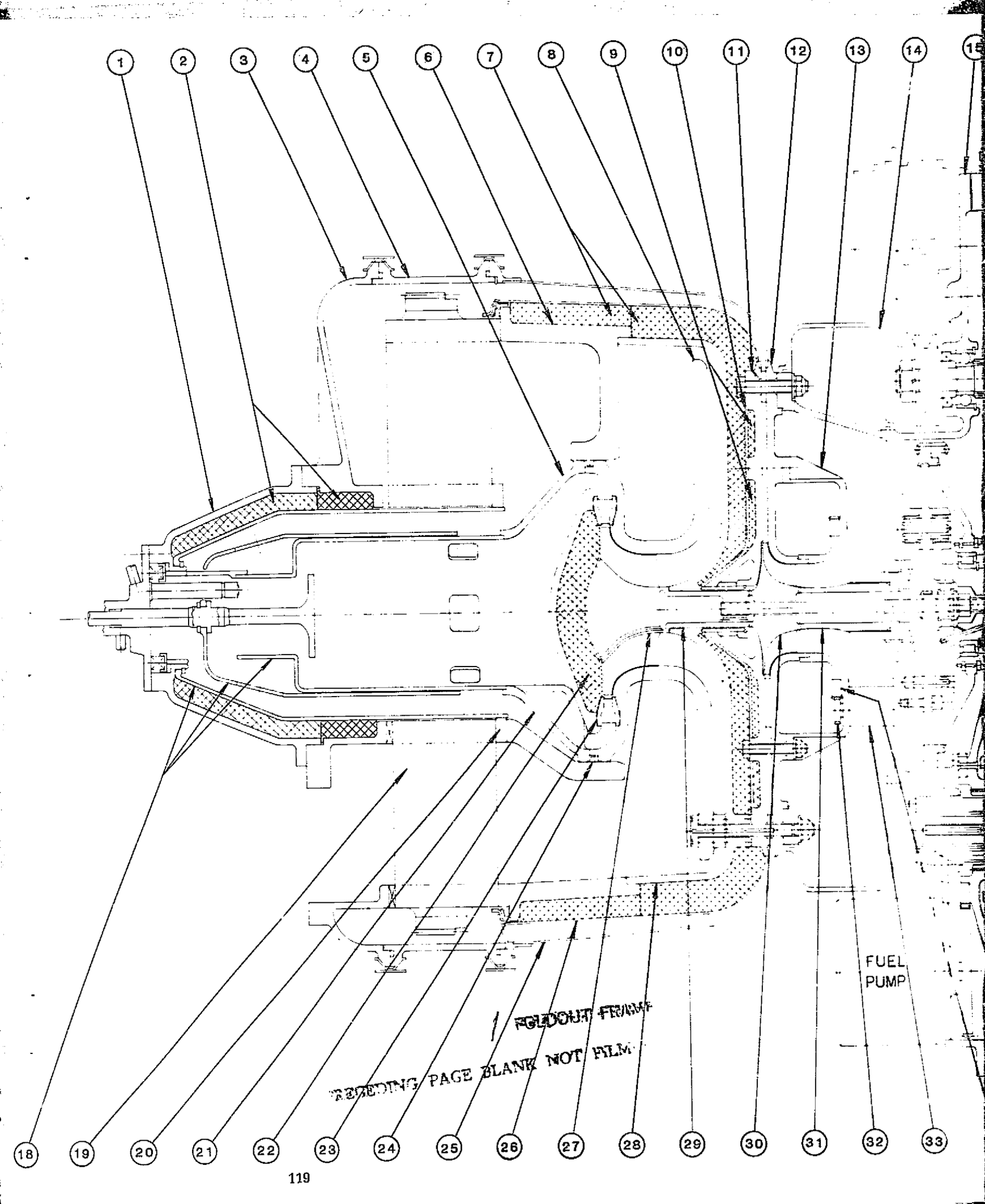


3

Figure 6.13 Detail Design Layout of Ford IGT Engine



4 FOLDOUT FRAME



FOLDOUT FRAME

PRECEDING PAGE BLANK NOT FILMED

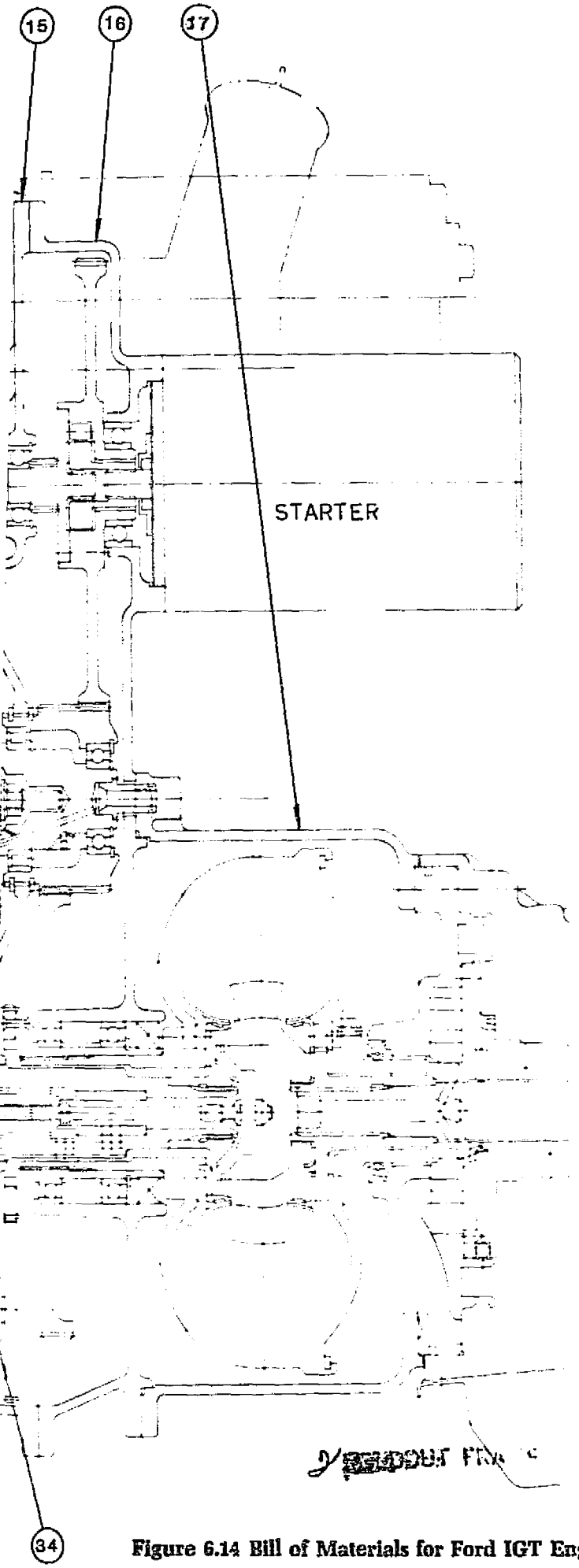


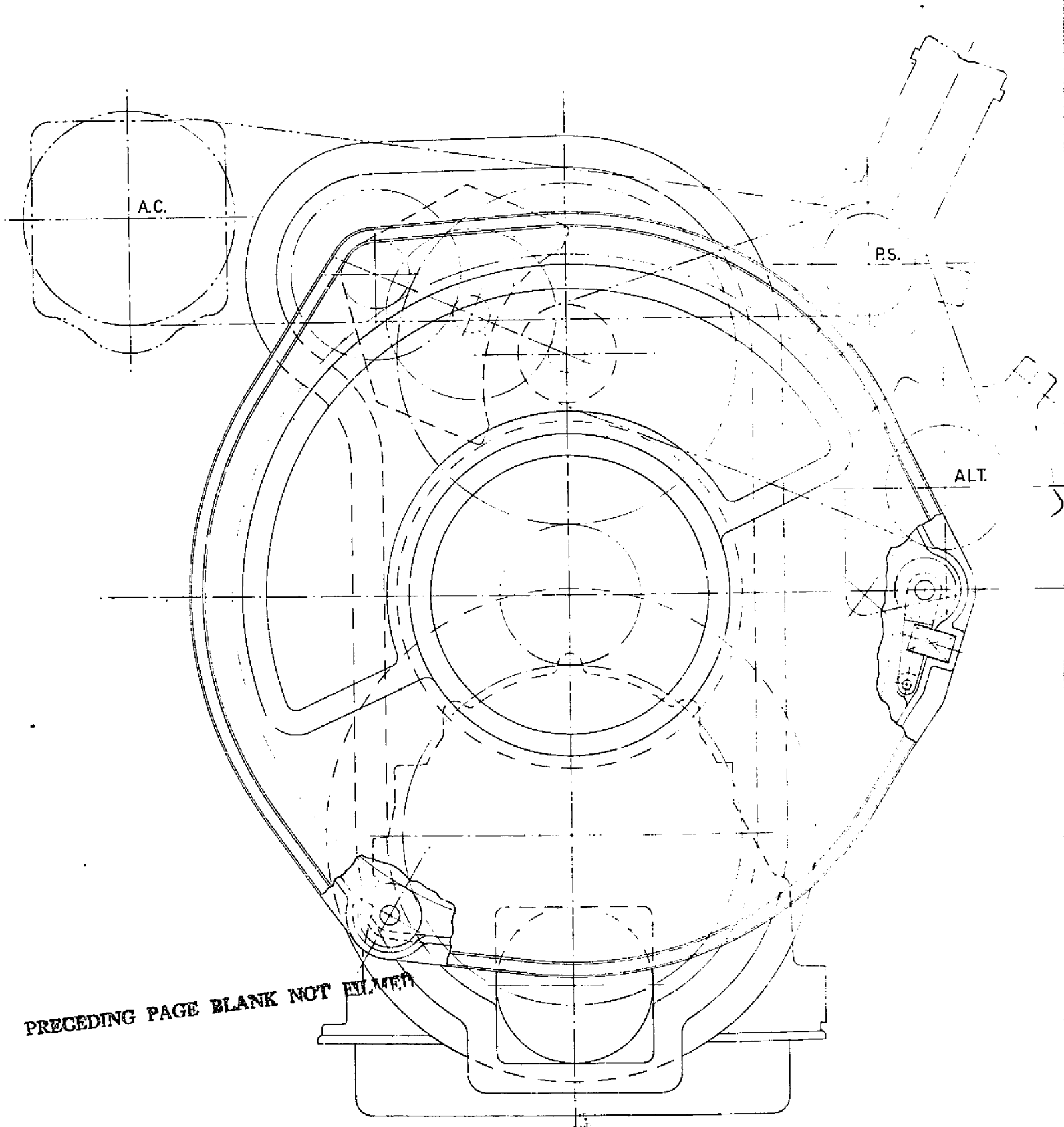
Figure 6.14 Bill of Materials for Ford IGT Engine

MATERIAL

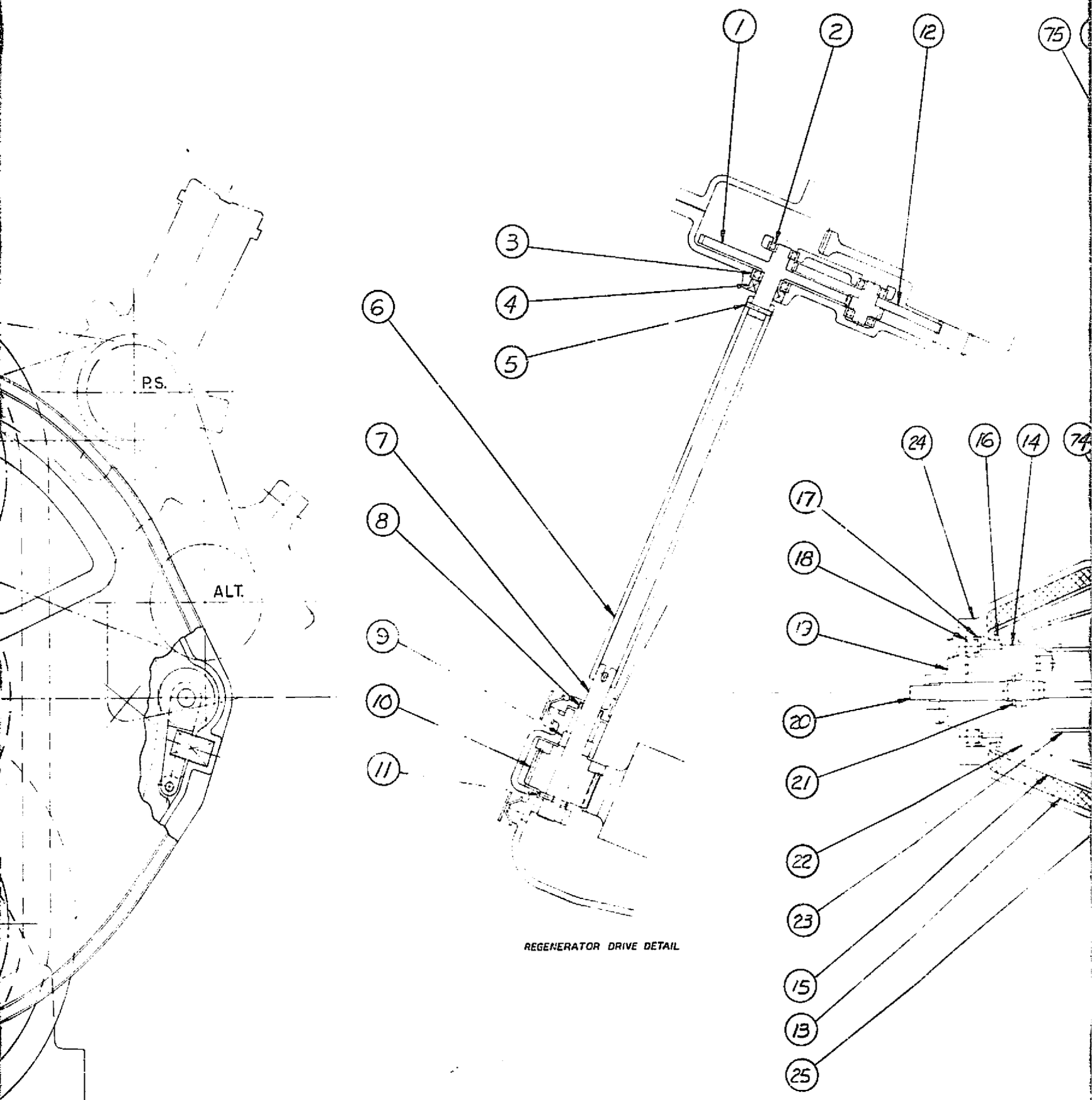
NO.	SHOWN	
1	NI-RESIST	
2	ALUMINUM SILICATE FIBER INSULATION	
3	C-356 DIE CAST	
4	C-356 PERM. MOLD CAST	
5	RB SiC	RS Si
6	LAS	MAS/
7	ALUMINUM SILICATE FIBER INSULATION	
8	RB SiC	RS Si
9	ALUMINUM SILICATE FIBER INSULATION	
10	430 S.S. ALUMINIZED	18 SF
11	NODULAR IRON	
12	NODULAR IRON	C-35
13	NODULAR IRON	
14	FRP	
15	C-356 DIE CAST	
16	C-356 DIE CAST	
17	C-356 DIE CAST	
18	RB SiC	
19	AS	MAS
20	LAS	MAS
21	RB SiC	RS
22	CERAMIC FOAM INSULATION	
23	RB SiC	RS
24	$Si_3 N_4$	AL_2
25	430 S.S	C-3
26	430 S.S.	
27	MAR-M-247	SiC
28	RB SiC	RS
29	SAE 52100 WITH $Cr_2 O_3$ COATING	SiC
30	206-T7 ALLOY	
31	SAE 52100	
32	HIGH TEMP. PLASTIC	
33	HIGH TEMP. PLASTIC	
34	HIGH TEMP. PLASTIC	

MATERIAL

NO.	SHOWN	OPTIONS
1	NI-RESIST	
2	ALUMINUM SILICATE FIBER INSULATION	
3	C-356 DIE CAST	
4	C-356 PERM. MOLD CAST	
5	RB SiC	RS SiC/RB Si_3N_4/RS Si_3N_4
6	LAS	MAS/Si_3N_4
7	ALUMINUM SILICATE FIBER INSULATION	
8	RB SiC	RS SiC/RB Si_3N_4/RS Si_3N_4
9	ALUMINUM SILICATE FIBER INSULATION	
10	430 S.S. ALUMINIZED	18 SR ALLOY
11	NODULAR IRON	
12	NODULAR IRON	C-356 DIE CAST/FIBER REINFORCED PLASTIC (FRP)
13	NODULAR IRON	
14	FRP	
15	C-356 DIE CAST	
16	C-356 DIE CAST	
17	C-356 DIE CAST	
18	RB SiC	
19	AS	MAS
20	LA3	MAS
21	RB SiC	RS SiC/RB Si_3N_4/RS Si_3N_4
22	CERAMIC FOAM INSULATION	
23	RB SiC	RS SiC/RB Si_3N_4/RS Si_3N_4
24	Si_3N_4	AL_2O_3 HIGH DENSITY
25	430 S.S	C-356 DIE CAST/FRP
26	430 S.S.	
27	MAR-M-247	SiC/Si_3N_4 FULLY DENSE
28	RB SiC	RS SiC/RB Si_3N_4/RS Si_3N_4
29	SAE 52100 WITH Cr_2O_3 COATING	SiC/Si_3N_4 FULLY DENSE
30	206-T7 ALLOY	
31	SAE 52100	
32	HIGH TEMP. PLASTIC	3 [illegible] FOAM
33	HIGH TEMP. PLASTIC	
34	HIGH TEMP. PLASTIC	



PRECEDING PAGE BLANK NOT FILMED



REGENERATOR DRIVE DETAIL

Figure 6.
[Sec

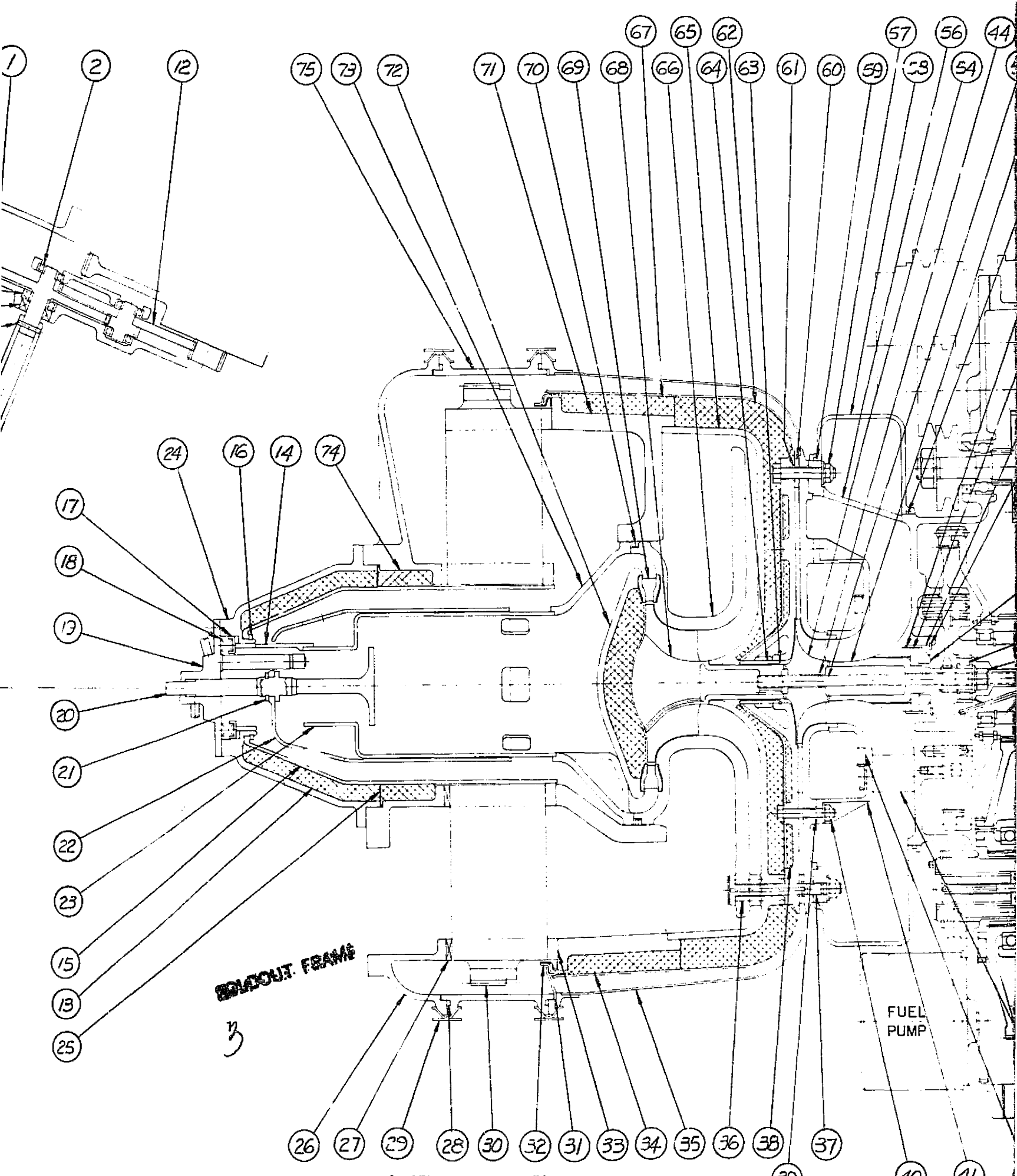
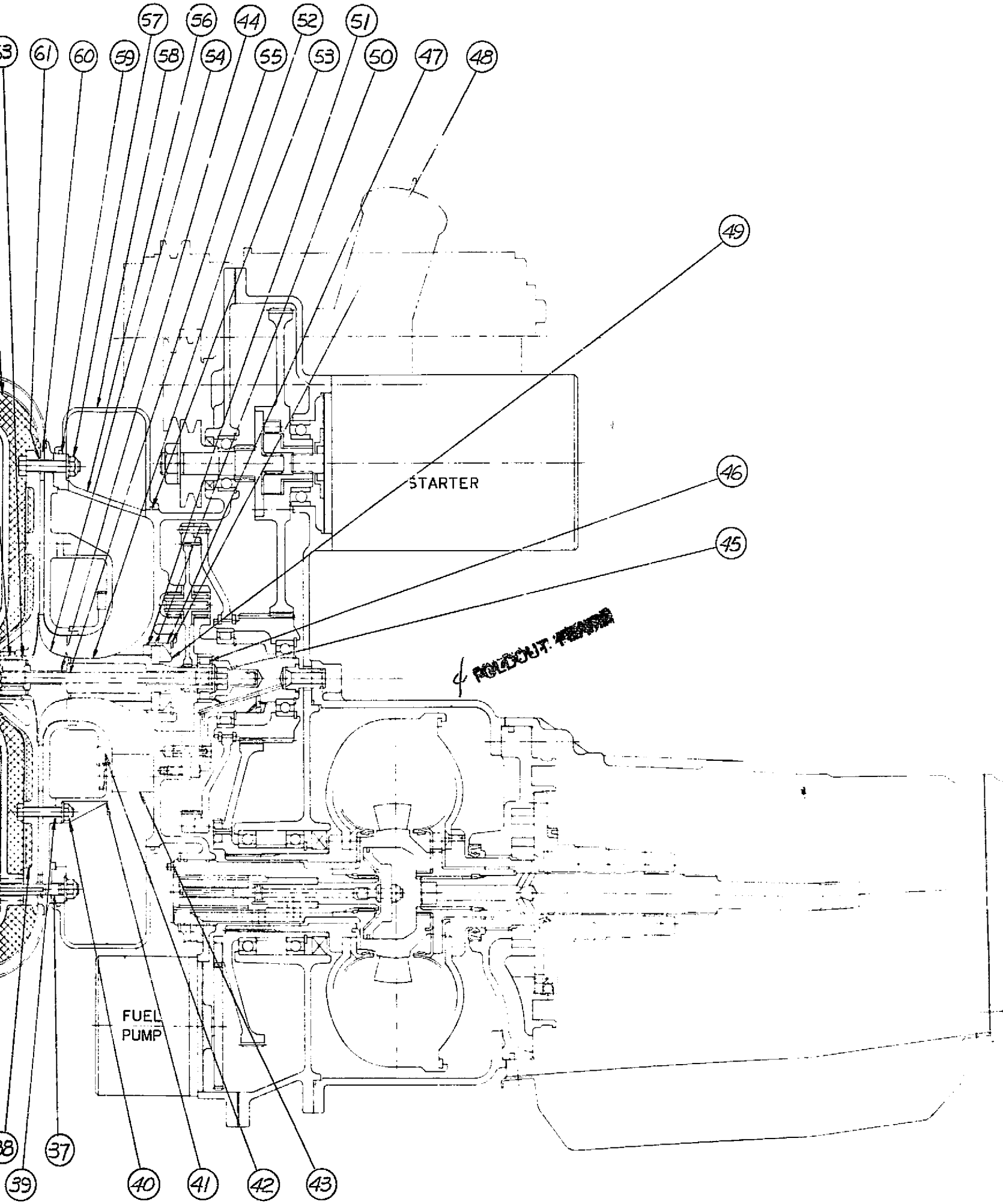
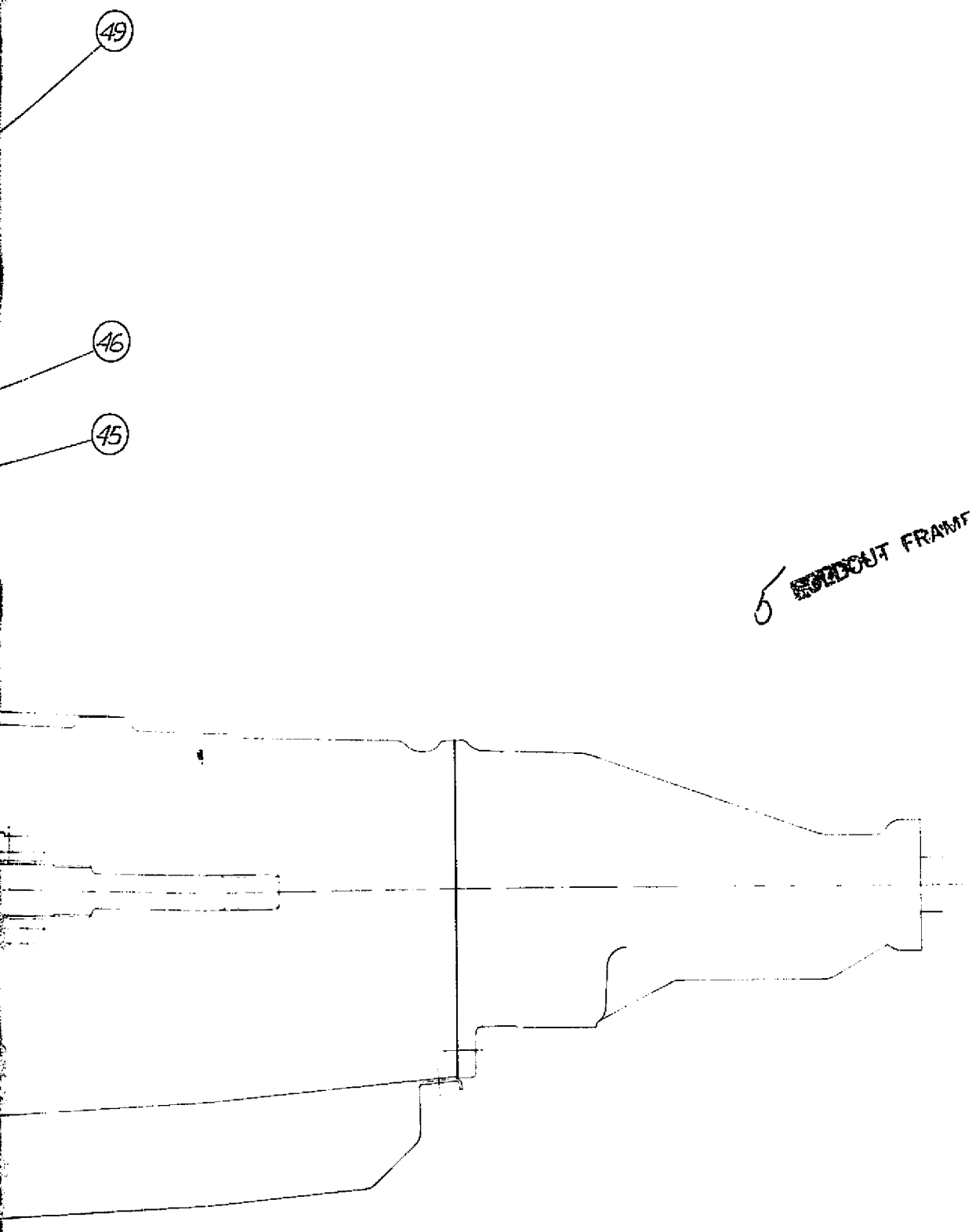


Figure 6.15 Ford IGT Engine Parts List

(See Table 6.4 for Parts List)


57
56
44
52
51
53
61
60
59
58
54
55
53
50
47
48
49
STARTER
46
45
FUEL
PUMP
38
37
39
40
41
42
43


49
46
45
6 BOLDOUT FRAME

6.2.2 TURBINE DIFFUSER MOUNTING

The turbine inner and outer ceramic diffuser shells are mounted to the metallic bearing housing with a curvic coupling face spline, ceramic dowels and cooled metal bolts as shown in Figure 6.13. The curvic coupling is of the type previously developed for ceramic structures and allows relative thermal motions with respect to the bearing housing while maintaining a very accurate control of the concentricity. The split, hollow ceramic dowels align the two diffuser shells. They are located at a radius where the radial thermal deformations of the two shells is matched. The cooled metal bolts provide the clamping load to secure the diffuser shells, the bearing housing and the compressor shroud.

6.2.3 TURBINE ROTOR — SHAFT ATTACHMENT

A metallic bolt is used to secure the three sections of the high speed engine shaft. The shaft is made up of a welded assembly of the radial turbine rotor, the air bearing journal, the compressor and the gear, as shown in Figure 6.13. The tension in the bolt will be high enough to resist the separating forces provided by the torque transmitted through the curvic couplings and to maintain flexural rigidity of the shaft assembly under dynamic loadings induced by the gyroscopic moments and internal loadings generated at the turbine and compressor rotors. The bolt will be tightened with a tensioning device so as to avoid any torsional stress in the bolt. The nominal stress in the bolt is 585 mPa and it will be made of an alloy steel.

6.2.4 DYNAMIC ANALYSIS OF THE MAIN ROTOR SYSTEM

A dynamic analysis was made of the high speed shaft configuration as shown in Figure 6.13 with a ceramic turbine rotor. The proximity of critical speeds to the operating region of the engine and the sensitivity of the dynamic system to the stiffness of the shaft supports were determined. The engine shaft was modelled as an assembly of straight cylinders and disks as shown in Figure 6.16 and the analysis was made with a proprietary Ford vibration computer program to determine the natural frequencies and mode shapes. The gyroscopic and centrifugal effects of the compressor and turbine disks were included in the model.

The shaft was elastically mounted in an air bearing between the compressor and turbine disks. The second elastic mount was at the gear which is the sun gear of a planetary reduction gear set. An analysis was conducted to determine the spring constant for the gear support. It was shown that the spring constant for the planetary system was a function of the square of the rotational speed and had the form

$$k_1 = \beta\omega^2$$

the gear spring rate coefficient, β, being a function of the reflected inertia of the entire drivetrain. It was estimated that the gear spring rate coefficient for the configuration studied was

$$\beta = .0115 \text{ N/cm/(rad/sec)}^2$$

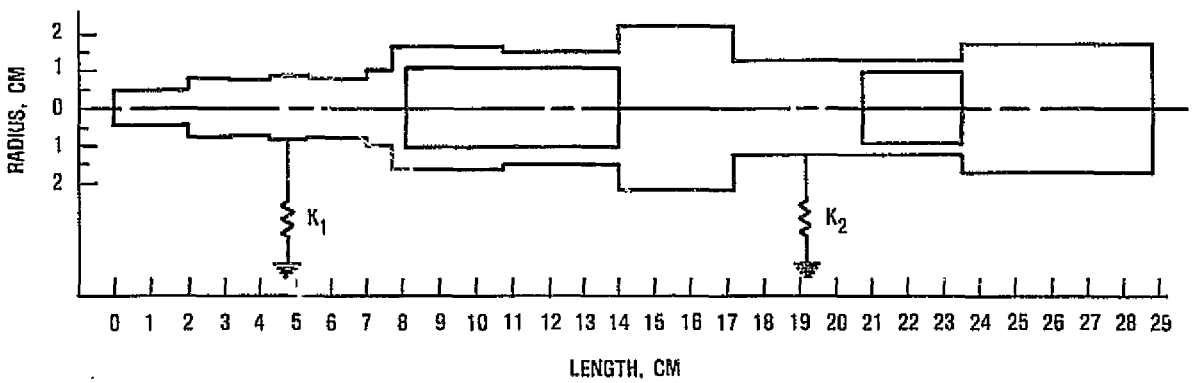


Figure 6.16 Shaft Vibration Model

From previous studies of air bearings, the air bearing spring rate was estimated to be 70050 N/cm. Figures 6.17 and 6.18 show the effect of the air bearing and the gear spring rates, respectively, on the critical speeds of the shaft. It may be seen that, for the estimated spring rates over the operating range of the engine, none of the critical speeds are encountered. The flatness of the frequency curves, particularly of the second mode, indicated that this shaft-bearing system was insensitive to the spring rate of either support. A free-free shaft system with no supports was investigated and it's first flexural mode frequency was found to be nearly identical to the second mode frequency of the shaft-bearing system. It was also shown that the nodal points of the free-free system almost coincide with the bearing locations. This explained the insensitivity of the second mode (first flexural mode) to the support spring rates. The critical mode shapes or the design spring rates are shown in Figure 6.19. The shaft model was modified to include a metallic turbine and, for the design spring rates, no critical speeds occurred near the operating range of the engine.

6.2.5 REGENERATOR SUPPORT

The engine regenerator is supported at three points along its circumference, on the drive pinion, on a fixed roller and on a spring loaded roller as shown by the front view in Figure 6.13. The maximum rotational speed of the regenerator is 20 rpm; the maximum power to overcome frictional losses has been estimated at 0.37 kW. The drive pinion to ring gear ratio is 10:1. An analysis was conducted to determine the loads at each of the support points. The loads at the pinion and at the fixed roller are a function of the power required to drive the regenerator, the angular position of the supports and the force set on the spring loaded roller. The position of the drive pinion was fixed by the gear box geometry and the spring loaded roller was placed on the horizontal centerline. The position of the fixed roller was varied to obtain support reactions which were consistent with the current state of the art. The reaction at the drive pinion was 389 N, at the fixed roller, 1226 N and at the spring loaded roller, the reaction was 136 N. Dry lubricated sleeve bearings were designed to support these loads at the rotational speeds of the rollers and gear.

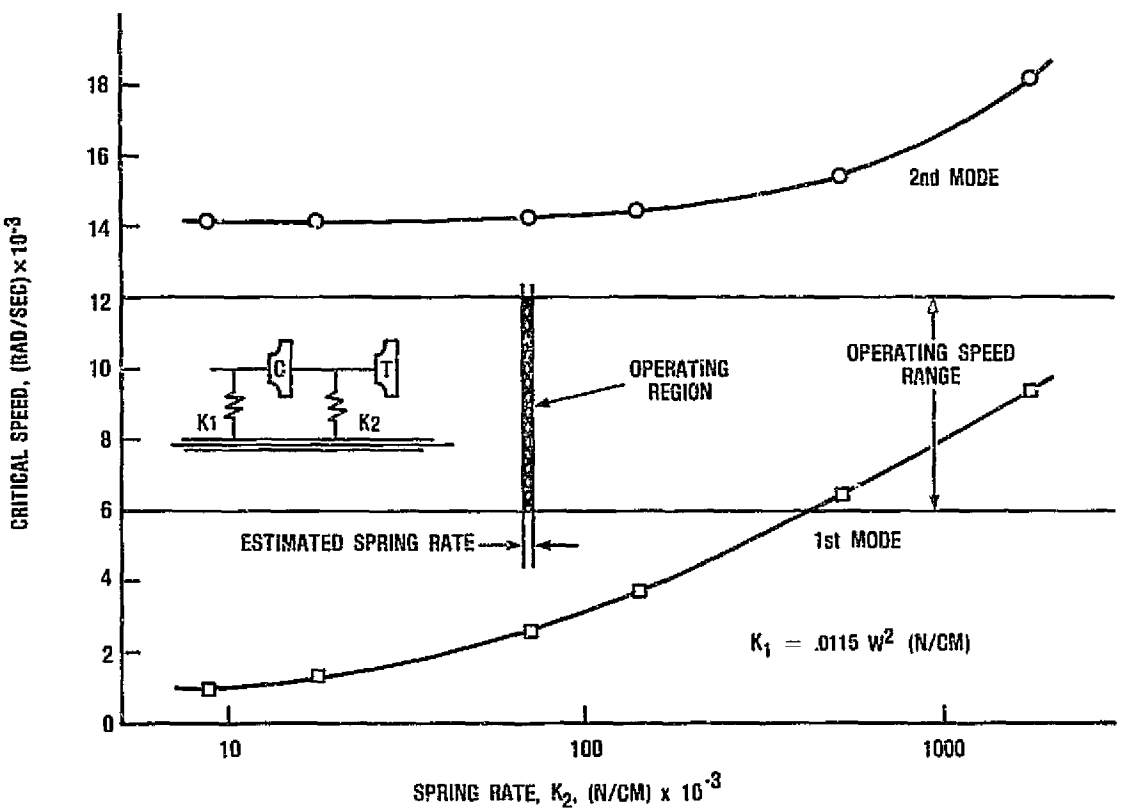


Figure 6.17 Critical Speed vs. Gas Bearing Spring Rate

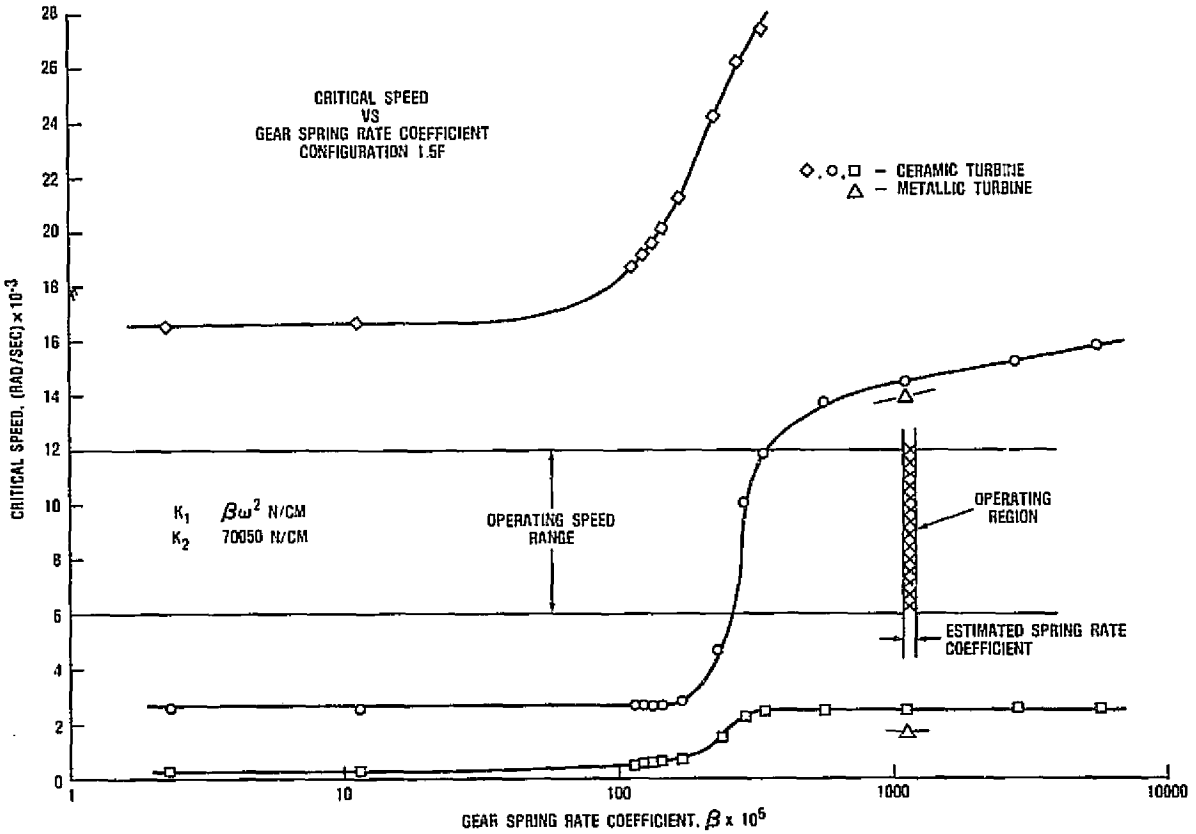


Figure 6.18 Critical Speed vs. Gear Spring Rate Coefficient

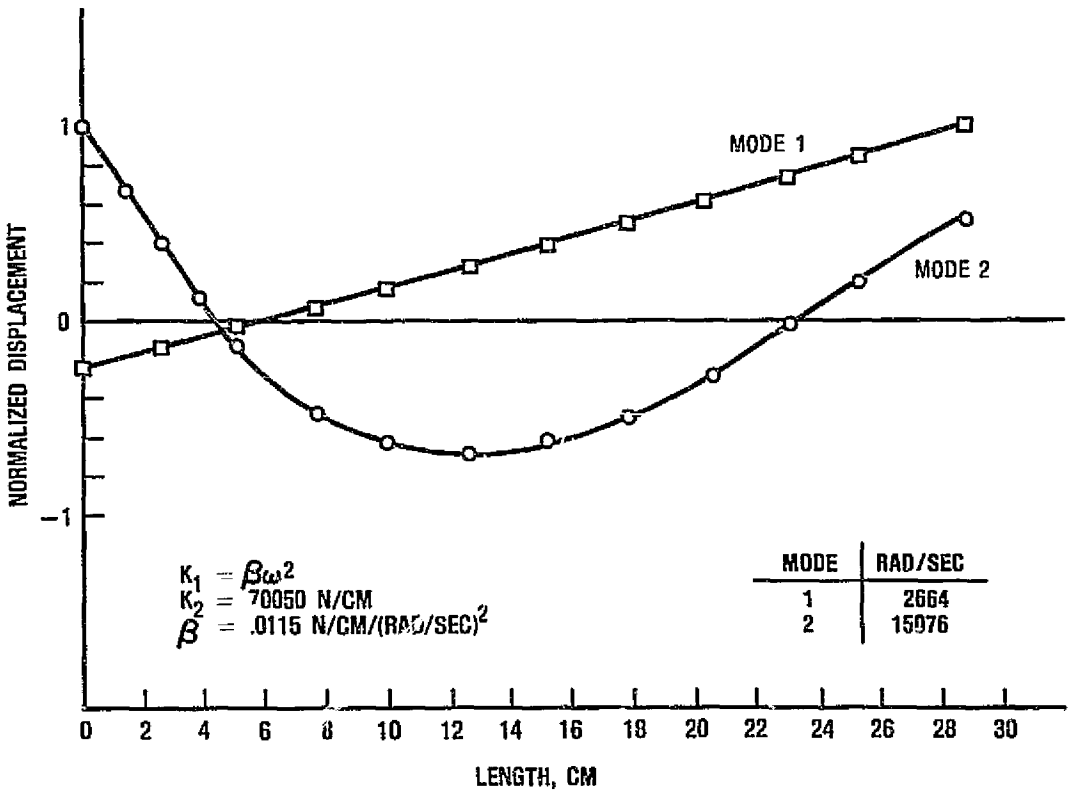


Figure 6.19 Vibration Mode Shapes

6.2.6 REDUCTION GEAR

The reduction gear consists of a high speed star gear arrangement in series with a single reduction gear box.

TABLE 6.5

Reduction Gearing Design Results

Star Gear Data (3 Planets)	
Max. Input Speed	120,000 rpm
Max. Input Power	102.9 kW (138 hp)
Ratio	11:1
Max. Output Speed	10909 rpm
Pitch Line Velocity	112.2 m/s (21893 fpm)
Bending Stress at Fillet	108.8 x 10^6 Pa (15785 psi)
Compressive Stress	845.9 x 10^6 Pa (122687 psi)
PVT Factor	33.6 x 10^6 Nm/m/sec (630,000 lb. ft/in/sec)
Max. Tooth Contact Frequency	40,000 c.p.s.
Max. Planet Speed	24,000 rpm
Max. Planet Bearing Load	307N (60 lbs.)
Single Reduction Gear Data	
Max. Input Speed	10909 rpm
Max. Input Power	102.9 kW (138 hp)
Ratio	2.43:1
Max. Output Speed	4489 rpm
Pitch Line Velocity	52 m/s (10240 fpm)
Bending Stress at Fillet	183.9 x 10^6 Pa (26665 psi)
Compressive Stress	473.4 x 10^6 Pa (68662 psi)
PVT Factor	8.75 x 10^6 Nm/m/sec (164,000 lb. ft./in/sec)
Max. Tooth Contact Frequency	14363 c.p.s.
Involute Contact Ratio	2
Helical Contact Ratio	2

All the design parameters for the gears, including pitch line speed, bending stress, compressive stress, and scoring factor are within the range of previous Ford turbine engineering design practice.

To simplify the star gear arrangement, spur gears will be used to eliminate thrust loads and overturning couples on the planets if helical gears are used. Since the tooth contact frequency, 20,000 cps, at engine idle is outside of the audible range, noise should not be a problem.

The single reduction gear uses an integral helical and involute contact ratio design to minimize load fluctuations and reduce noise.

Rolling element bearings will be used to minimize power losses and present no problem as regards life and reliability.

Use of the star gear eliminates the need for a bearing on the high speed rotor shaft, since the sun gear is floating and is positioned by the planets, otherwise the design is conventional and presents no unique problems not previously encountered in Ford experience.

6.2.7 BEARING HOUSING AND COMPRESSOR SHROUD DEFORMATION ANALYSIS

A two-dimensional finite element analysis was conducted to determine the stresses and deformations of the compressor shroud and bearing housing shown in Figure 6.13. The deformations of these structures affect the critical clearance at the compressor and the diffuser vanes and, as a consequence, the efficiency of these components. Design iterations were performed to minimize the deformations. For this analysis, both structures were assumed to be made of nodular iron. The compressor shroud could have been made of die cast aluminum or fiber reinforced plastic as alternatives to nodular iron. The bearing housing was stiffened with radial ribs on the inside with insulation between the ribs to control the flow of heat to the compressor air. A sheetmetal shield was placed over the ribs and insulation and a small amount of air was introduced under the shield to act as a coolant. These features are called out in the Parts List, Table 6.4 and Figure 6.15. The maximum equivalent stress in the bearing housing and in the compressor shroud were found to be 230.7 MPa and 23.1 MPa, respectively. Plots of the original and deformed structures are shown in Figure 6.20 with critical deformations called out. The axial deformations of the shroud at the compressor were acceptable. The deformations at the compressor diffuser required a shrouded diffuser vane with an elastomeric seal to the bearing housing and compressor shroud.

6.2.8 COMPRESSOR ROTOR ANALYSIS

Preliminary stress analysis of a compressor rotor was conducted. The investigated rotor is of slightly different configuration and different rotational speed than the rotor selected for the IGT engine and shown in Figure 6.1. However, because it operates at the same tip speed as the selected rotor the results of the analysis shown in Figures 6.21 through 6.24 are representative. Figures 6.21, 6.22 and 6.23 show respectively the radial, tangential and the equivalent stress distributions at full power operation assuming K-01 aluminum alloy.

Because of modeling approximations employed in the analysis both the maximum stress levels and deformations, shown in Figure 6.24, should be viewed as conservative. With the temperature of the rotor at the critically stressed bore (265 MPa — Figure 6.23) estimated at between 175° and 200°C, the stresses appear to be within the 1983 technology projections for aluminum alloys.

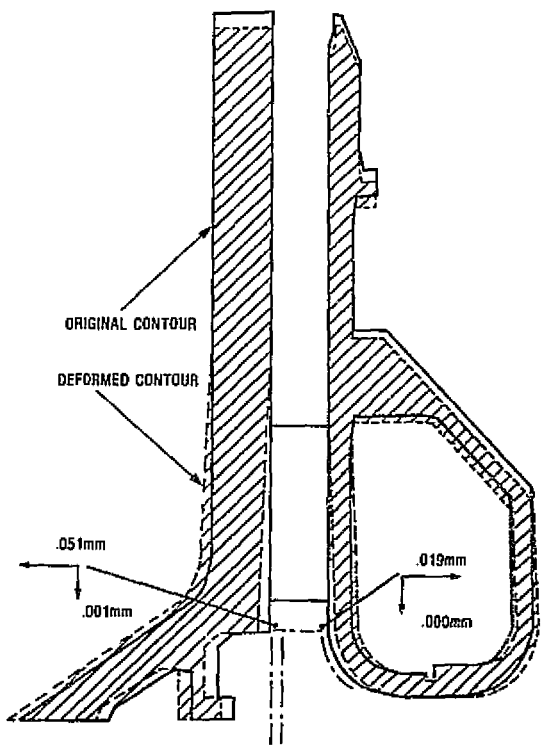


Figure 6.20 Bearing Housing and Compressor Shroud Deformation

The axial deformations at the tip of the impeller are high and may result in an excessive reduction in shroud clearance. As mentioned earlier, these estimates are conservative and it is expected that a more detailed analysis using a 3-dimensional model of the rotor in conjunction with the thermal growth analysis of engine flow path components, discussed in section 6.3, will resolve this problem. As an additional safeguard, use of an abradable shroud will be considered.

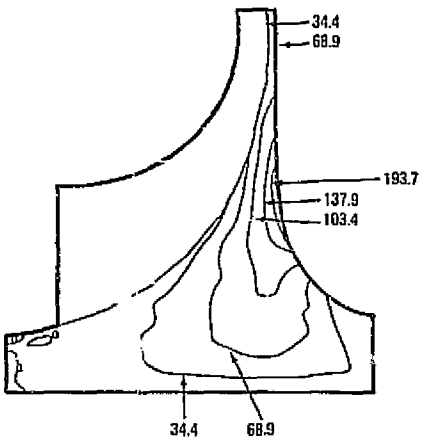


Figure 6.21 Compressor Rotor Radial Stresses (MPa)

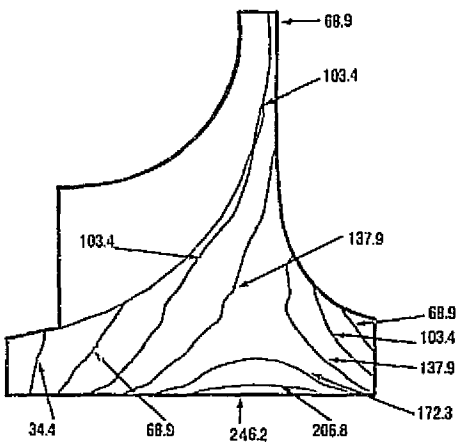


Figure 6.22 Compressor Rotor Tangential Stresses (MPa)

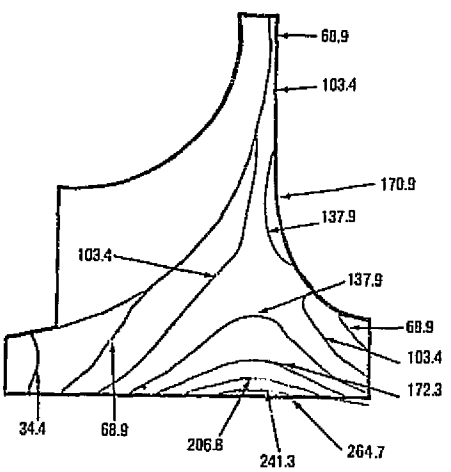


Figure 6.23 Compressor Rotor Equivalent Stresses (MPa)

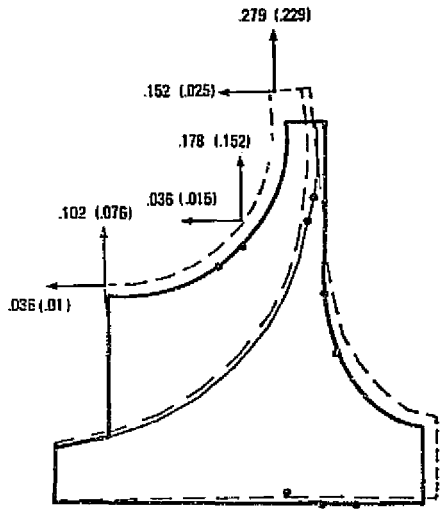


Figure 6.24 Compressor Rotor Thermal and Centrifugal Growths (mm), (Thermal only Growths in Parenthesis)

6.2.9 OIL COOLER

A parametric study was conducted to determine the minimum required heat exchanger volume, pressure drop and air flow for a crossflow oil cooler. The design was based on the assumption that 7.5% of the engine power, i.e. 7.5kw, was rejected to the engine oil as heat. It was assumed that the oil would flow into the cooler at a rate of 4.4 litres per minute at 150°C and leave at 90°C. A commercially available cooling fan was selected and a minimum heat exchanger volume of 4.6 litres was determined. The volume of the cooler shown in the installation drawing, Figure 5.24(a), (b) and (c), was increased to 8.8 litres to provide a factor of safety for the design and to account for higher air temperatures resulting from the position of the air conditioning condenser.

6.3 Thermal Analysis

6.3.1 INTRODUCTION

One of the primary problems to be solved as a prerequisite to establishing mechanical feasibility of a turbine engine is determination and control of flow path component assembly thermal growth. Turbine and compressor efficiencies are both, to a large degree, dictated by tolerances in the blade-to-shroud flow regime gap. Therefore, determination of temperature distribution within the turbine and the resulting thermal growth of its components under various steady state and transient (including soak back) engine conditions constitutes a critical requirement in accurately predicting engine performance over a range of operating conditions (e.g., start-stop, cold-hot, acceleration, etc.). A successful turbine design requires that a prior knowledge of component thermal growth be incorporated into the design and that a measure of passive and active control be exercised over it. Effective thermal control can be exercised through heat shorts, thermal dams (e.g., insulation) and cooling streams (regulated/unregulated) incorporated into the design.

An appropriate tool for studying thermal characteristics (i.e., thermal response under various operating conditions) of the turbine engine is a finite element model. The model developed for analyzing the IGT engine is axi-symmetric. It is composed of 978 nodes, 995 elements, 52 material options, 35 fluid streams and 539 boundary condition elements.

6.3.2 THERMAL MAP APPROACH

The technical approach selected for determining the thermal requirements for the turbine is shown schematically in Figure 6.25. The heart of the analysis consists of the axi-symmetric model and finite element program. All other programs, files and activity were determined as supporting requirements either direct or indirect. The axi-symmetric finite element model is shown in Figure 6.26. A rather detailed model geometry was selected to provide an accurate representation of the various flows, insulation and hardware and their relative thermal interactions.

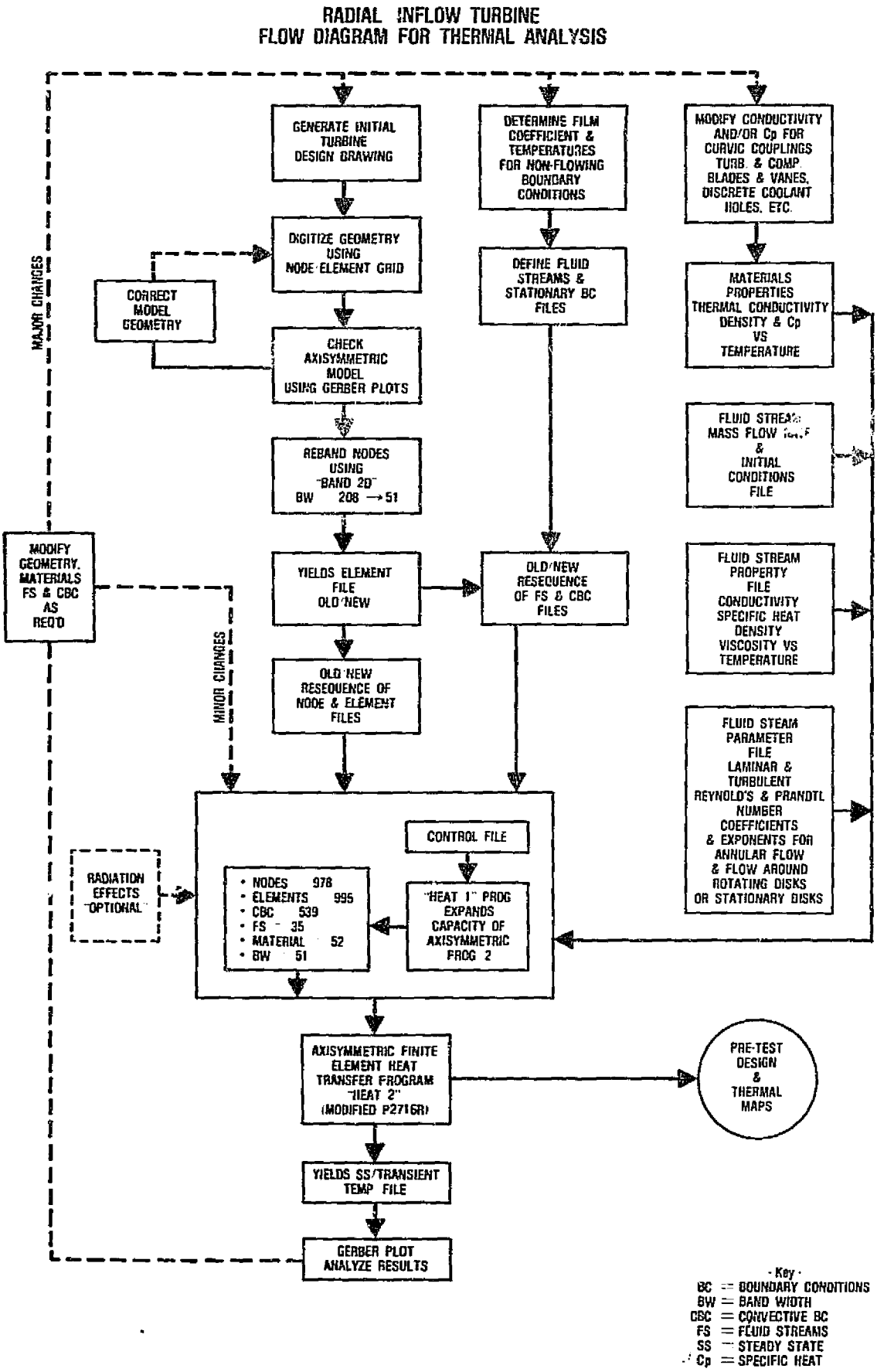


Figure 6.25 Flow Diagram for Thermal Analysis

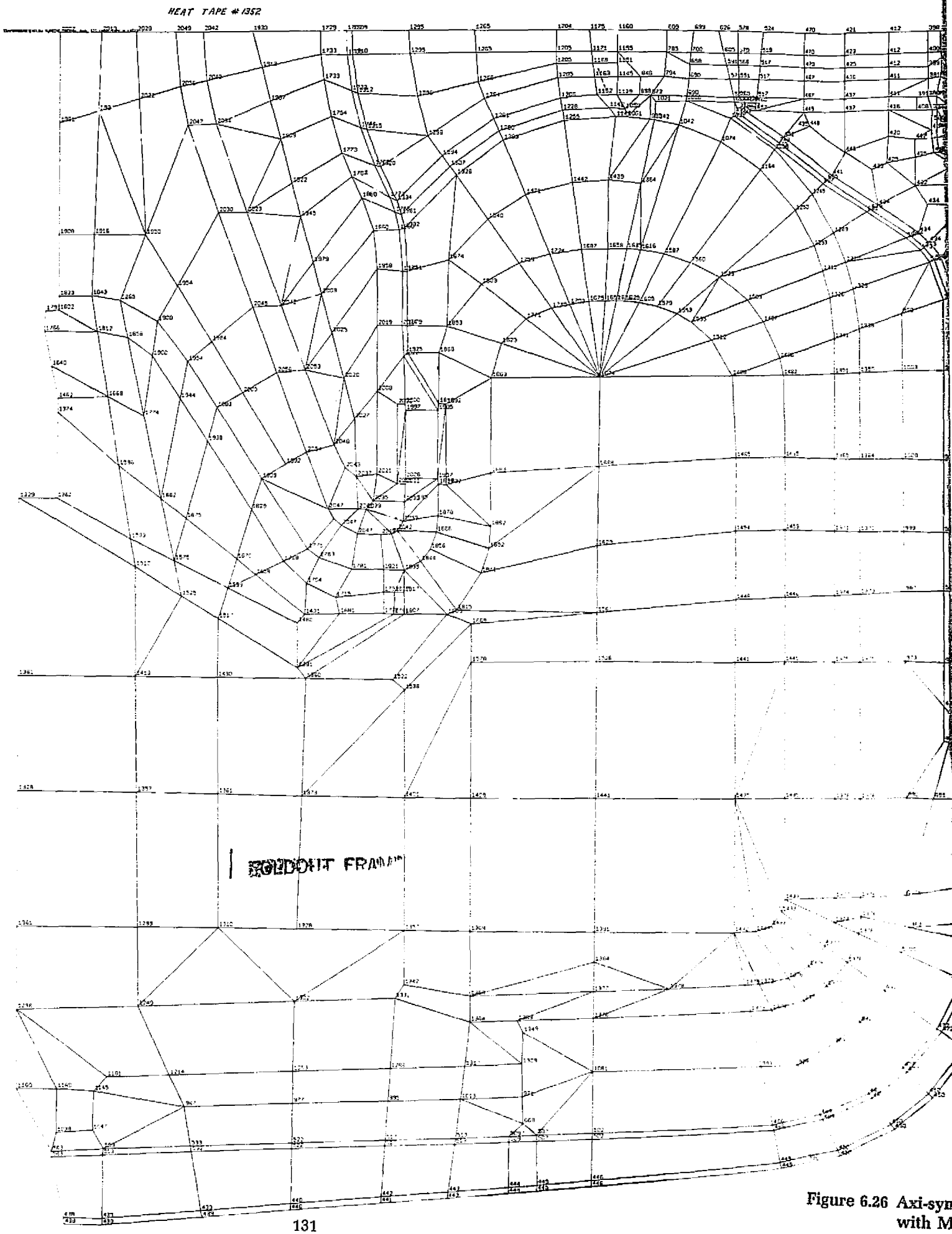


Figure 6.26 Axi-syn
with M

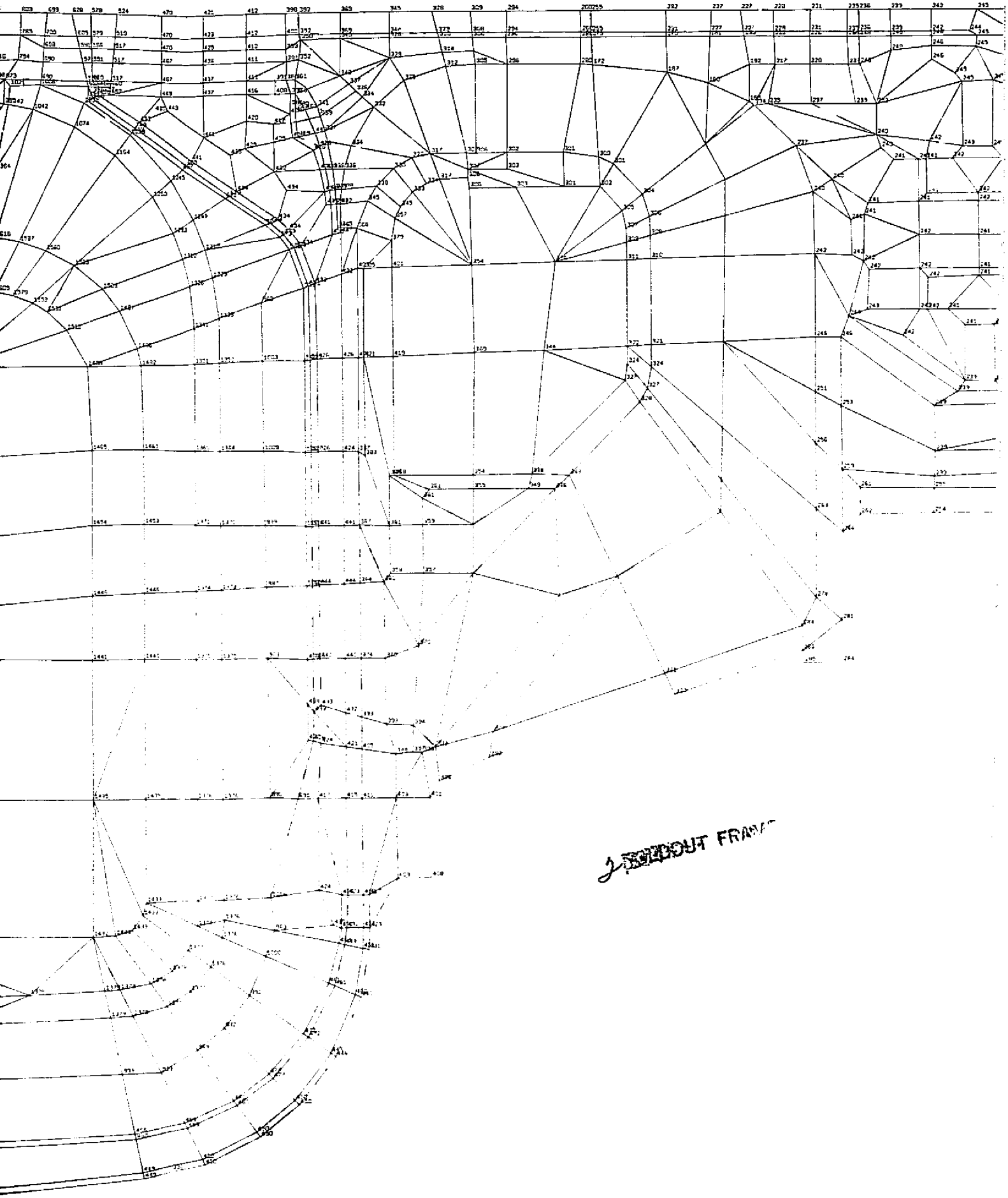
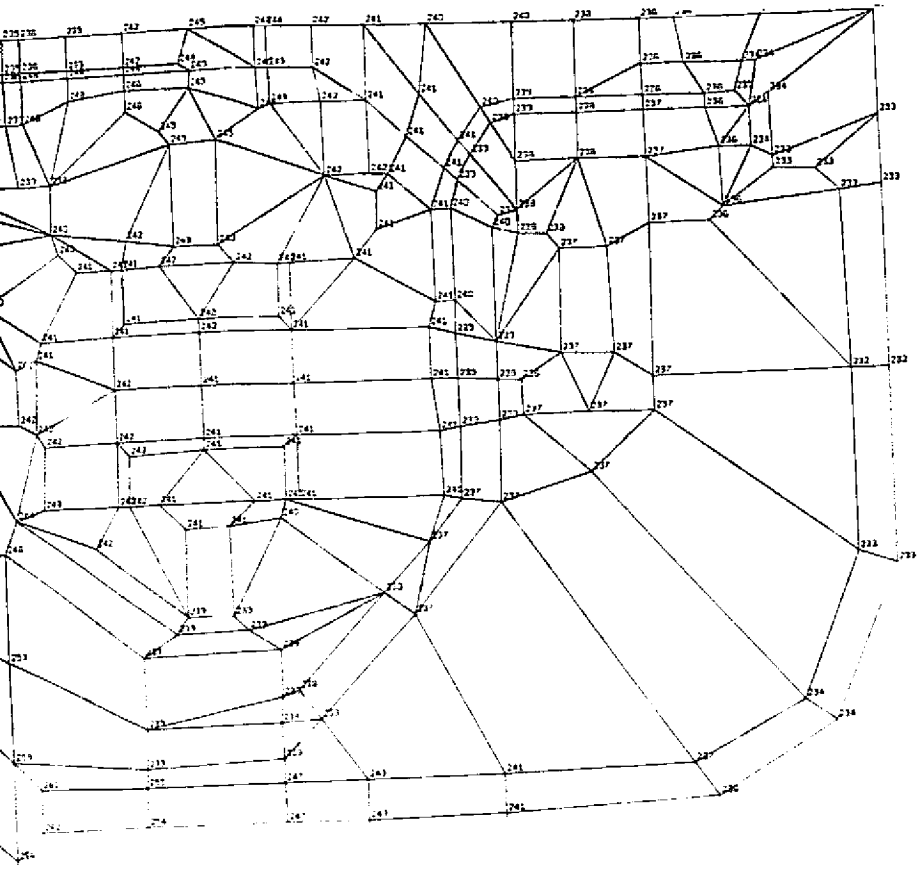


Figure 6.26 Axi-symmetric Finite Element Model Showing Temperature Distribution at Full Power with Metal Turbine Rotor



3 GOLDOUT FEWNR

on at Full Power

The analysis scheme is iterative in nature and was conceived to be utilized as a design and development tool. Design changes (e.g., material, geometry, insulation, etc.) can be input and recomputed to determine their impact on the thermal characteristic of the turbine. The initial input requirements are a design drawing which represents the best estimate of the turbine configuration prior to the detailed thermal analysis. As the design progresses, the required modifications are made. The final result should be a thermal map which reflects the final design modifications and should include transient (start up), acceleration and soak back (shut down) thermal characteristics of the engine. Axial thermal growth and hence resulting changes in critical clearances (i.e., efficiencies) can be determined as a result of these analyses.

6.3.3 DISCUSSION AND RESULTS

The first iteration steady state temperatures derived, using the procedures previously discussed, are shown at the nodal junctions in the finite element model of the engine, Figure 6.26. This particular model uses a MAR-M-247 air-cooled turbine with a ceramic shroud and diffuser. The gear box and compressor inlet volute are primarily aluminum. The compressor diffuser bearing housing structures are composed of nodular iron castings and 430 stainless steel stampings. The turbine stator or nozzle is silicon nitride, and the turbine shroud is reaction bonded silicon carbide. For the regenerator inlet housing LAS (Lithium Aluminum Silicate) was selected because of its excellent insulative characteristics. The shaft is SAE-52100. Steady state working fluid operating temperatures were determined from the IGT design study. The reference point from which all the axial clearance changes were calculated is the engine thrust bearing location, see Figure 6.13.

Calculation of the differential expansions, which result in changes in clearance, between the shroud and blades of the compressor are shown in Table 6.6. These represent free thermal growths and do not include deformations induced by thermal and mechanical stresses.

Calculation of the changes in clearances between the shroud and blades of the cooled metal radial turbine are shown in Table 6.7. The deformations due to bending, centrifugal loading, etc. have not been included in these calculations and have been assumed to be negligible. The changes in clearances were computed from a cold engine state to the 100 percent power, steady state condition.

The thermal model is sensitive to boundary conditions, design geometry, and material assumptions. Therefore, as the turbine design progresses, the approach used in the flow diagram in Figure 6.25 will be to update the model and study improvements in thermal design of the engine with respect to both steady state and transient operation typical of vehicular application.

PRECEDING PAGE BLANK NOT FILMED

TABLE 6.6

Compressor Clearance Changes Due to Thermal Growth

	Axial Direction
Rotor Position Change	0.23 mm (0.009 ins)
Housing Position Change	0.41 mm (0.016 ins)
Differential Expansion	0.18 mm (0.007 ins) — clearance reduced

	Radial Direction	
	Inducer Tip	Impeller Tip
Rotor Expansion	0.08 mm (0.003 ins)	0.13 mm (0.005 ins)
Housing Expansion	0.05 mm (0.002 ins)	0.08 mm (0.003 ins)
Differential Expansion	0.03 mm (0.001 ins)	0.05 mm (0.002 ins) — clearance reduced

TABLE 6.7

Turbine Clearance Changes Due to Thermal Growth

	Axial Direction
Rotor Position Change	0.91 mm (0.036 ins)
Housing Position Change	0.76 mm (0.030 ins)
Differential Expansion	0.15 mm (0.006 ins) — clearance increased

	Radial Direction	
	Expeller Tip	Exducer Tip
Rotor Expansion	0.74 mm (0.029 ins)	0.41 mm (0.016 ins)
Housing Expansion	0.18 mm (0.007 ins)	0.15 mm (0.006 ins)
Differential Expansion	0.56 mm (0.022 ins)	0.25 mm (0.01 ins) — clearance reduced

6.4 Control Systems Concept

The control system concept presented here is directed toward mid-1980 passenger car application of a single shaft, radial compressor gas turbine engine with ceramic regenerator and flow path. Fuel economy and exhaust emissions standards, and the engine design based on these standards, have strongly influenced the choice of a control system. The high turbine inlet temperature required for fuel economy and the flame temperature operating "window" required for minimum exhaust emissions have placed difficult constraints on the control system. The intended use of ceramic flowpath components, the radial compressor and the advent of the microprocessor have enabled a unique control concept to be proposed.

The system utilizes three separate but interrelated major control loops: loop one regulates fuel flow to control engine speed, loop two regulates a variable stator torque converter to control turbine inlet temperature and loop three maintains combustor flame temperature by controlling a variable geometry combustor. Additional control subsystems provide for control of variable inlet guide vanes, automatic start sequencing and error detection/failure mode operation.

The application of this engine to passenger cars means that the control system must be designed with the following factors being of paramount importance:

1) low cost at high production volumes,
2) maintainability/serviceability
3) durability
4) vehicle fuel economy and exhaust emissions standards.

6.4.1 CONTROL SYSTEM OVERVIEW

The rapid growth of onboard computer technology in current production vehicles makes it very probable that microprocessor-based control system will be utilized in any advanced engine control systems. This is evident in the control system functional schematic for a variable inlet guide vane, single-shaft, gas-turbine-powered vehicle shown in Figure 6.27. The engine is coupled to the rear wheels through a variable stator torque converter and a Ford 4-speed transmission.

Driver control and operation is identical to that for existing automatic transmission vehicles powered by a spark-ignition engine. As a result, standard items such as a drive gear selector, a foot-operated accelerator and brake pedal and an ignition switch (with off, run and start positions) are used to control the vehicle.

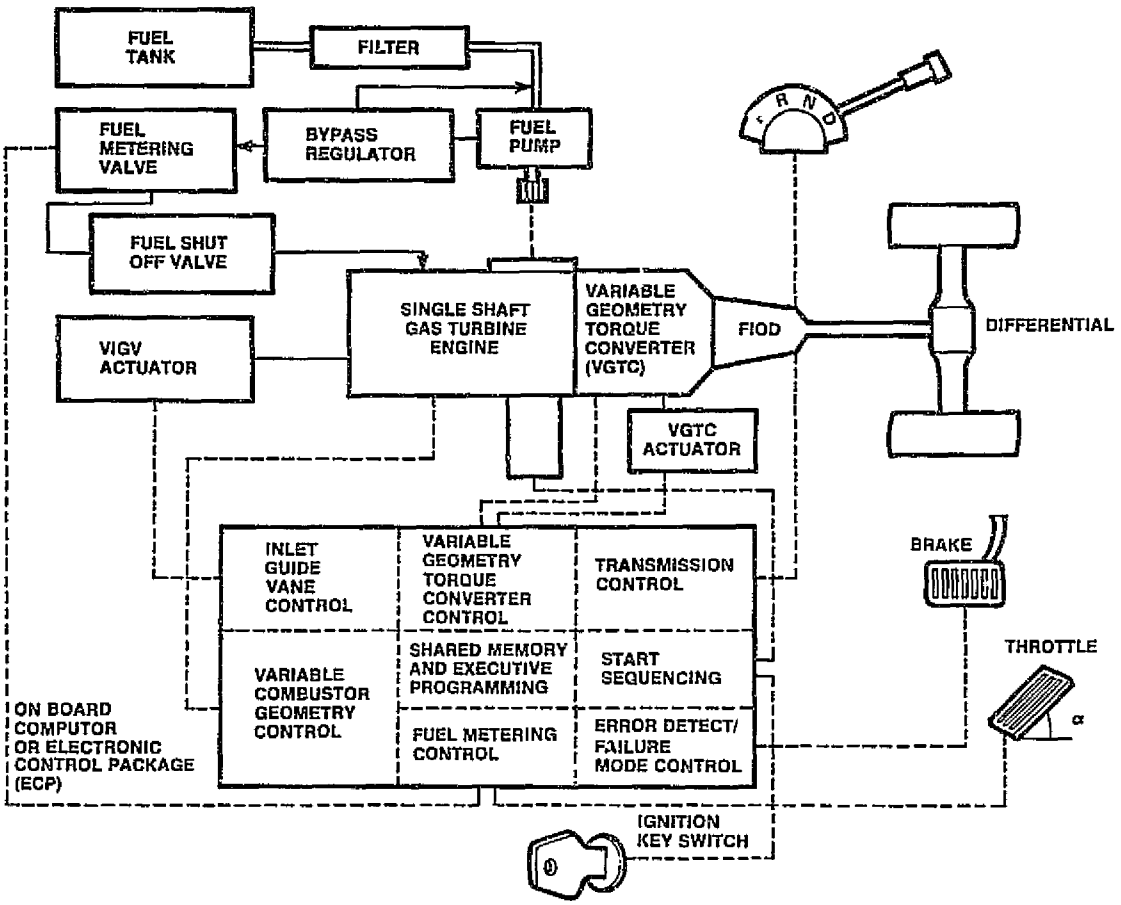


Figure 6.27 Functional Schematic of Control System

All essential control functions are performed under the direction of the various sections of the Electronic Control Package (E.C.P.). This would be a multiprocessor system composed of several sub modules on a common system bus, using shared memory. Each section of the ECP could then be available separately for servicing.

The proposed gas turbine engine control system is designed to accomplish the following objectives:

- Control engine power in response to throttle position
- Maintain engine gas temperature limits: 1) regenerator inlet temperature
  2) combustor flame temperature
  3) turbine inlet temperature
- Protect against engine overspeed
- Prevent combustor blowout during transients
- Maximize fuel economy and minimize exhaust emissions
- Permit automatic starting
- Synchronize operation of engine and transmission
- Provide engine braking
- Provide fuel shutoff for engine shutdown
- Provide fail safe control
- Provide for failure mode vehicle operation ("limp home" capability) wherever possible.

6.4.2 CONTROL SYSTEM COMPONENTS

To accomplish these objectives requires a control system which addresses the unique relationship that exists between the engine, transmission and fuel management system. This control system is comprised of eight major elements (as seen in Figure 6.27):

(a) Fuel metering section

(b) Inlet guide vane control

(c) Automatic start sequencer

(d) Transmission control

(e) Failure detector/failure mode operation control

(f) Combustor geometry control

(g) Variable Geometry Torque Converter control

(h) Sensors/actuators

While a great deal of interaction among these various control subsections occur, the basic operation of each section is described in the following paragraphs.

6.4.3 FUEL METERING SECTION

The fuel metering section consists of a hydromechanical fuel pressure regulator to maintain a fixed differential pressure across a pair of high pressure, electronically actuated fuel injection nozzles. These nozzles (one for low fuel flow, both operated for high fuel flow) are pulse width modulated by the Electronic Control Package (ECP) to provide the fuel required to maintain engine speed.

The Fuel Metering Section of the ECP monitors engine speed and varies the injector pulse width to provide sufficient fuel to maintain the desired speed. This speed setpoint is scheduled by throttle position, as shown in Figure 6.28.

6.4.4 VARIABLE INLET GUIDE VANE CONTROL

The Variable Inlet Guide Vane control schedules inlet guide vane position (in an open loop manner) as a function of turbine inlet temperature (T_7), the rate of speed request change (decel condition) and a brake pedal position switch.

Guide vane regulation (closing) as a function of T_7 is done to improve part throttle fuel economy, while the partial opening of the vanes under decel conditions improves engine "braking feel" prior to actual application of the vehicle service brakes. This scheduled opening of the guide vanes prior to service brake application provides engine braking which is augmented by the variable stator torque converter (to be discussed later).

During rapid acceleration demand or "kick-down" situations (large $\Delta N/N$) the inlet guide vanes are opened past the maximum efficiency zero angle position to provide additional power. This also works in conjunction with the variable stator torque converter control which briefly reduces engine load to permit rapid engine acceleration.

The inlet guide vane control system is shown in Figure 6.29.

6.4.5 START SEQUENCING SYSTEM

This portion of the ECP provides all of the logic to properly sequence a safe start following key switch movement to the 'START' position. The starter can be engaged only if:

1) The engine is not already turning fast enough to damage the starter drive.

2) The transmission is in 'PARK' or 'NEUTRAL'

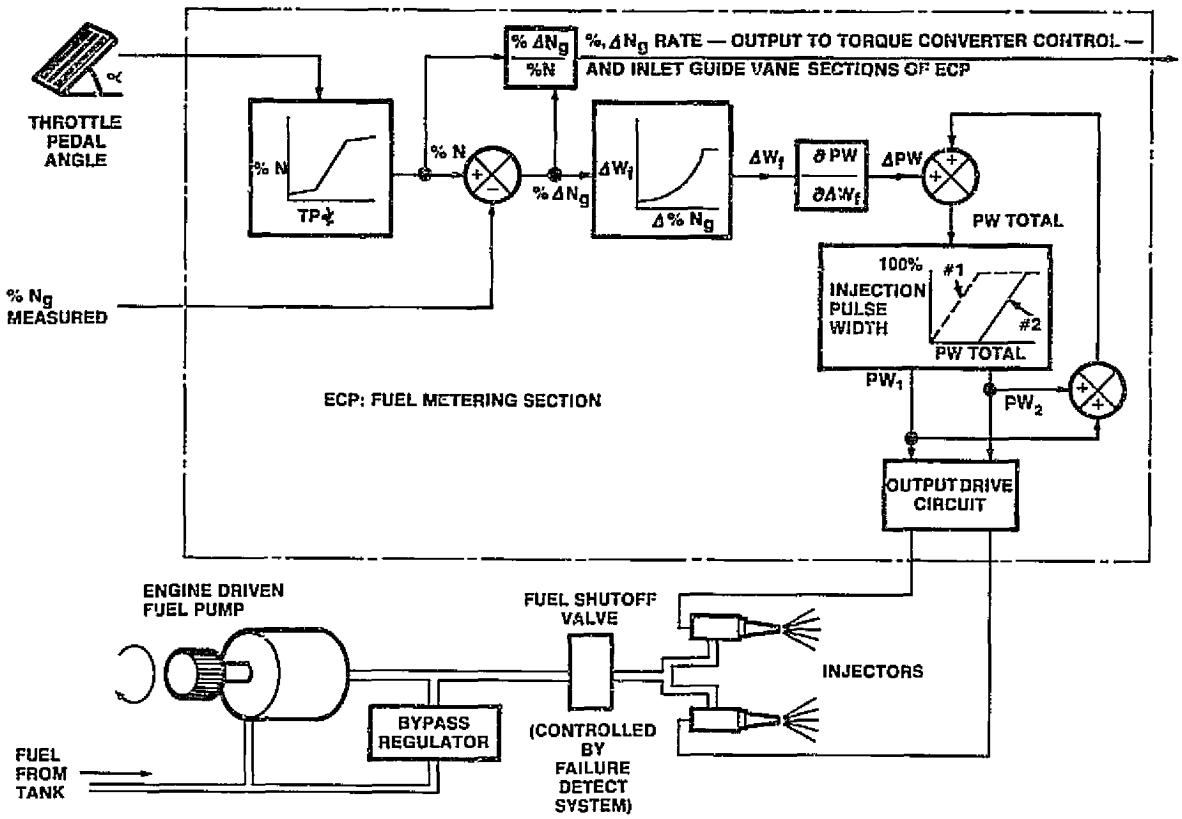


Figure 6.28 Fuel Metering Section

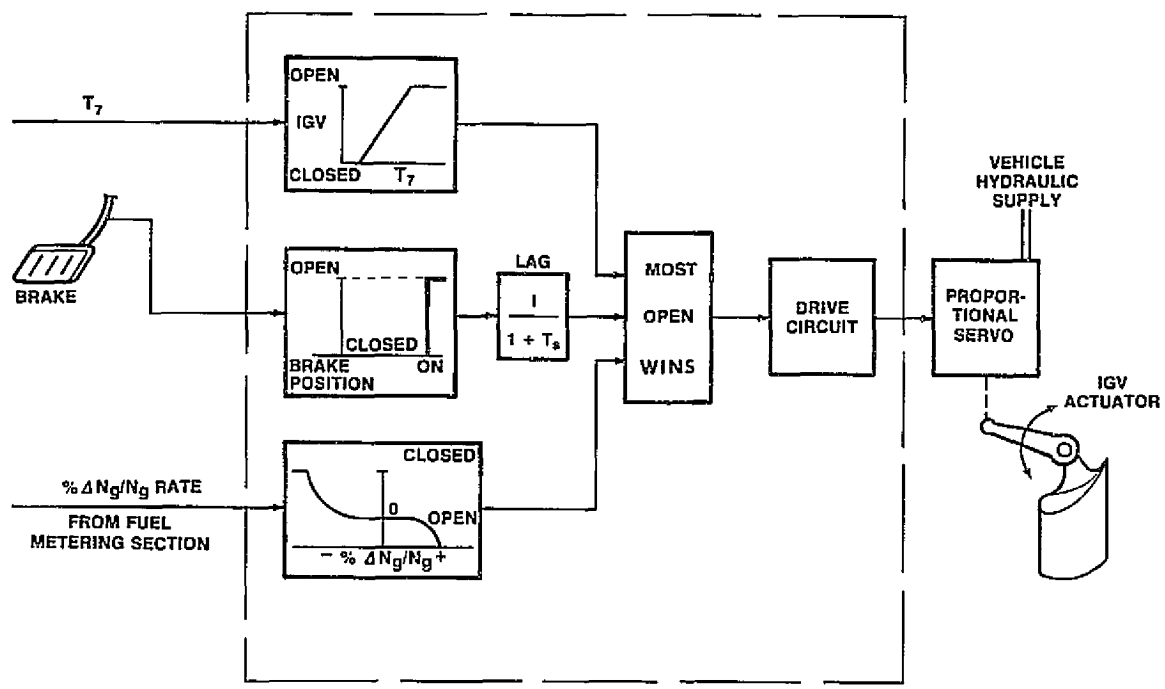


Figure 6.29 Inlet Guide Vane Control

During the start-up process, fuel is turned on, inlet guide vanes are held open. The variable geometry torque converter is placed in the no load condition, and engine parameters are monitored (by the Failure Detector System, discussed later). Logic in the start sequencer will determine if a "hung start" or other start up irregularly occurs. In the event of any out-of-limit parameters, the start will be terminated.

Once engine speed reaches approximately 50%, the starter is disengaged and the start sequence is complete. At this point, the Failure Detector/Failure Mode Control (discussed in the next section) will assume responsibility for detecting and acting upon out-of-limit conditions. The logic for these protection features after start-up differs from that used before starter cut-out. An example of this difference is the treatment of engine oil pressure: This parameter is monitored constantly above 50% engine speed, but during start-up the low oil pressure signal is ignored until after 25% engine speed, allowing time for pressure build up.

6.4.6 FAILURE DETECTOR/FAILURE MODE CONTROL

This portion of the ECP will monitor all vital engine parameters (temperature limits, oil pressure, engine speed, presence of combustor flame, etc.) and determine whether or not operation is within prescribed limits. Out-of-limit conditions fall in three categories: 1) immediate engine shutdown is required, 2) initiate some warning signal to the driver and go to a failure mode operation condition and 3) initiate a warning only. Failure mode operation provides for reduced power operation in order to have a "limp home" capability.

In addition to such engine failures as mentioned above, sensor failure could occur which would have to be detected and acted upon. Such failure would not terminate engine operation, but would fall into category 2 or 3 as outline above.

Engine deterioration indications could be monitored here as well. For example, regenerator system deterioration (which could effect both fuel economy and exhaust emissions) could be detected by detecting turbine exit temperature and combustor inlet temperature variations which fall out of prescribed limits.

6.4.7 COMBUSTOR GEOMETRY CONTROL

The combustor geometry control system varies the split between combustor primary and secondary airflow to maintain combustor flame temperature within prescribed limits. This is required to keep exhaust emissions (of NO_X and CO) within statutory limits. In order to assure accurate position control of the variable geometry, closed loop proportional plus integral position controls are used (Figure 6.30).

During acceleration and deceleration conditions, the combustor control system would likely not respond rapidly enough to prevent undesirable emissions transients, however. This is compensated for by adding an ACCEL/DECEL mode position request to the system output.

Rather than measuring flame temperature (approximately 1649°C (3000°F) directly, it may be synthesized for durability reasons, from airflow, fuel flow and combustor inlet temperature.

6.4.8 TRANSMISSION CONTROL

The transmission control causes gear changes in the 4-speed transmission to occur at points which are optimized for vehicle performance, emission control and fuel economy. These shift points are a function of vehicle speed, power demand (i.e., throttle position) and engine speed. With all of the parameters available to the onboard computer, optimum shift points are calculated and gear changes are accomplished by activating solenoid valves.

A rapid acceleration (or "kickdown") feature is provided whereby a downshift is made in the event of near full throttle angle and a large discrepancy between speed request and actual engine speed.

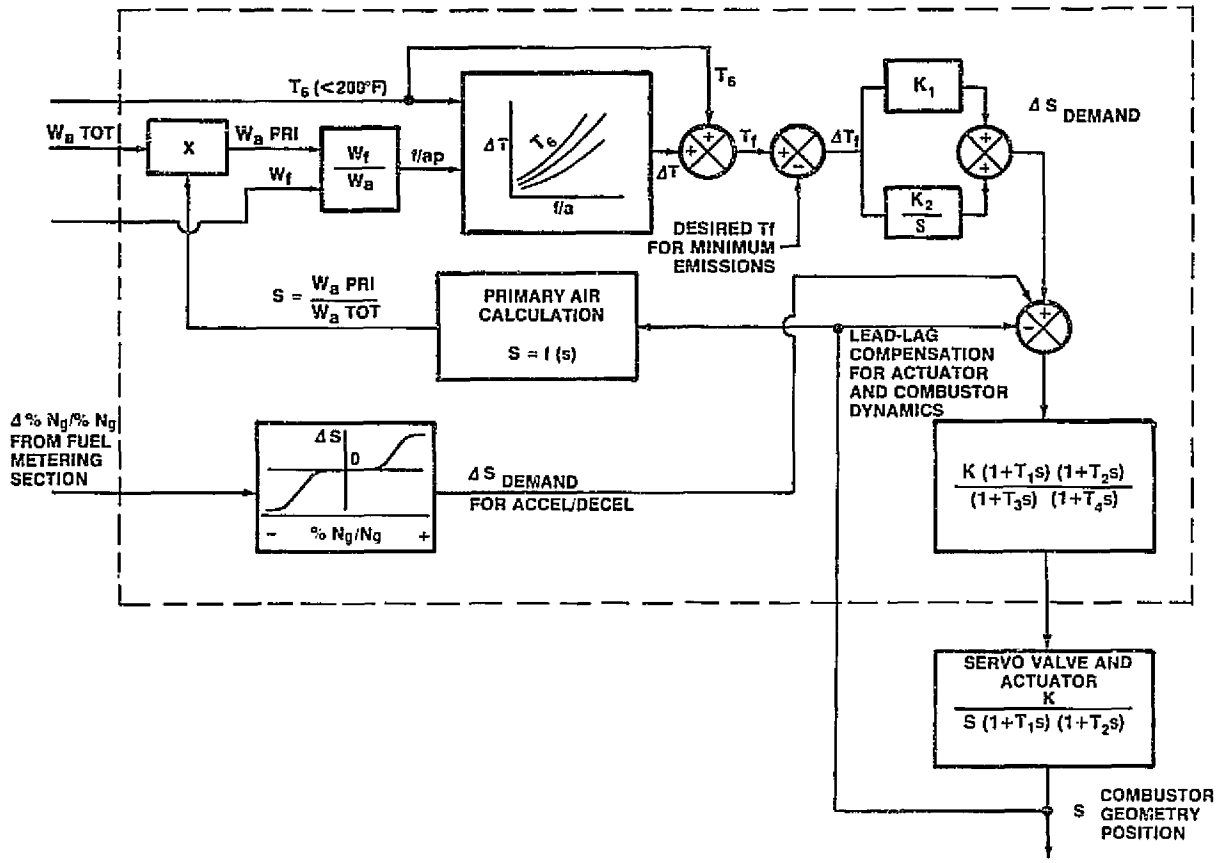


Figure 6.30 Variable Geometry Combustor Control

6.4.9 VARIABLE STATOR TORQUE CONVERTER CONTROL

Inputs of throttle pedal angle (TPA), compressor inlet temperature (T_2) and synthesized turbine inlet temperature (T_7) are used to schedule a $T_7 = f(TPA, T_2)$ and control closed loop to this scheduled T_7 by varying engine load (i.e. torque converter stator vane position). A minor loop provides stator vane position (β) feedback for stability and rapid response. Turbine inlet temperature lead compensation is provided in the electronic stator vane control to produce an instantaneous T_7 signal. Lead-lag compensation is also applied to the electronic stator vane control output signal to compensate for dynamics of the hydromechanical valves required to provide flow to the actuator. In addition to these features shown in the block diagram of Figure 6.31, the following functions are also provided:

1) Acceleration mode positioning of the stator vanes to reduce load on the engine briefly, allowing the main shaft to accelerate more rapidly.

2) Deceleration mode positioning of the stator vanes to load the engine during deceleration, thereby increasing the main shaft deceleration rate.

Both of these features operate in conjunction with the Inlet Guide Vane Control, as previously mentioned.

In the event of future transmission development work on Continuously Variable Transmissions, some reprogramming of this section of the ECP would be required; hardware would be essentially unchanged, however. This should minimize the controls effort required to test new transmission alternatives.

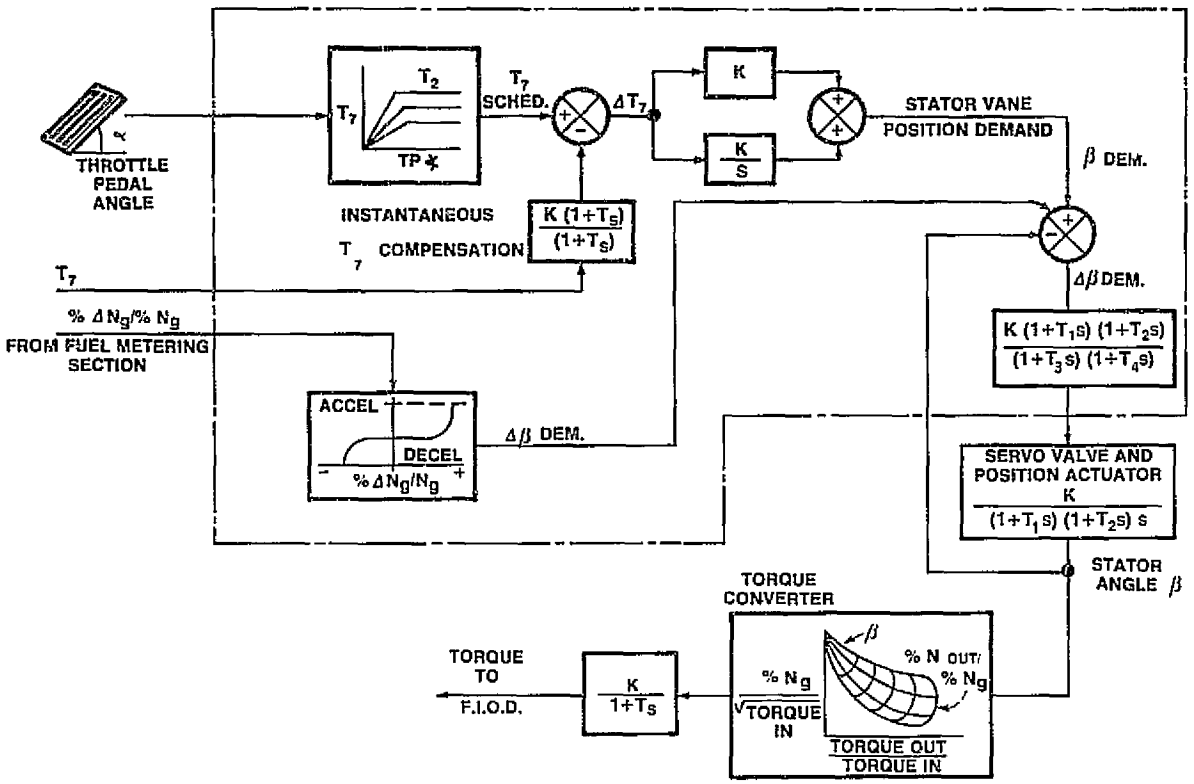


Figure 6.31 Variable Stator Torque Converter Control

6.4.10 SENSORS/ACTUATORS

In order to provide the control functions described in previous paragraphs, sensors (other than the usual automotive equipment) will be required for:

1) engine speed: magnetic or opto-electric probe
2) regenerator gas inlet temperature: Cr-Al thermocouple, thermistor capable of 1095°C (2000°F) operation, acoustic device, or low level radiation measurement.
3) combustor inlet temperature, same as for item 2.
4) torque converter stator position: linear potentiometer, line opto-electric position decoder or LVDT.
5) combustor geometry position: same as above
6) combustor flame detector: ionization probe or opto-electric device
7) airflow: differential pressure, total to static pressure, vortex shedding, acoustic or ionization device
8) compressor inlet temperature, thermistor
9) throttle position: potentiometer, optical encoder or LVDT.

In the above list, no mention is made of a turbine inlet temperature or flame temperature sensor. It is assumed that turbine inlet temperature will be synthesized from airflow, combustor inlet temperature and fuel flow just as flame temperature was calculated in the combustor geometry control.

The alternative to these calculations procedures are to measure two temperatures in excess of 2500°F or rely on open loop fuel scheduling: these items will be discussed later.

In order for the ECP to effect vehicle operation, actuators and servos must be provided. In addition to the fuel metering nozzles, there are:
1) inlet guide vanes: ECP current to mechanical position using the vehicle hydraulic fluid supply.
2) combustor geometry: ECP current to hydraulic fluid flow which is integrated by a piston type actuator.
3) torque converter geometry: as above.

4) fuel shutdown: a 3-way solenoid valve with the third port returning fuel to tank at shutoff. This prevents fuel spillage into the engine after shutdown.
5) transmission shifting: three solenoid valves to convert ECP outputs to hydraulic pressure.

6.4.11 CONTROL SYSTEM DESIGN

From the first three items on the list of factors influencing the control design (see Introduction), it would seem that a fuel scheduling type of control might be ideally suited for passenger car application. The simplicity of such a system would make it inherently less costly and more reliable. Unfortunately, production tolerances of any mass-produced gas turbine engine are likely to preclude the use of any simple scheduling control if fuel economy and exhaust emission requirements are to be met. Even if such a control could perform satisfactorily on a new engine, it is almost certain that long-term engine deterioration would shift engine operating characteristics enough to cause excessive exhaust emissions. Therefore, in spite of its inherent simplicity, a scheduling type control system is felt to be inadequate.

A second alternative approach is to operate closed loop around a measured turbine inlet temperature. For the case of the metal rotor engine, this requires measurement of 1150°C (2100°F) with a probe which has adequate time response and durability. Such probes can probably be made available in large quantities, although thermocouple and acoustic-type sensors may be more expensive than is desirable. Research into providing lower cost thermistors for 1150°C (2100°F) operation should be undertaken in Phase II of this program.

The eventual application of this control system is the ceramic gas turbine, however, and this will require 1370°C (2500°F) temperature measurement. No method of measuring these temperature levels exists for low cost, high-volume production at this time. In order to address this problem, high temperature measurement research is proposed for Phase II. This is obviously a high-risk program, however, and it is felt that the proposed control system should not rely too heavily on the success of this effort.

Since it is believed that closed loop control is required, but T_7 measurement technology may not be adequate, another means of providing a T_7 signal is needed. The prospect of calculating T_7 based on fuel/air ratio and combustor inlet temperature has been considered previously, but there are usually three drawbacks to this approach:
1) the need to measure fuel flow,
2) the need to measure airflow,
3) operation near the surge line requires extreme accuracy in the above measurements and in the calculation process.

For the radial flow compressor design being considered here, operation near surge is not a consideration, however. Maximum efficiency operation places the operating line well away from surge.

If fuel metering were to be done by a proportional solenoid-operated metering valve or by a hydromechanical system, the fuel flow measurement would still be required. The use of the microcomputer and pulse width modulated fuel metering nozzles eliminate this need, however. Since the fuel injector nozzles are solenoid operated valves, the linearity and hysteresis problems associated with a proportional solenoid are eliminated. Fuel flow for a given pulse width is then known with considerable accuracy and the only problem remaining is to measure airflow.

A number of airflow measurement techniques have been developed over the past several years which would appear to have application here. Although Phase II research on airflow measurement will be needed, the changes for success would seem much better than for the high temperature measurement research program.

A similar, but even more difficult, problem arises due to the need to control combustor flame temperature (T_f). The approximately, 1650°C (3000°F) flame temperature must be controlled in order to operate within the "window" of the NO_X and CO emissions curves. Obviously, measurement of T_f is even less likely than the measurement of T_7. Flame temperature is determined by fuel flow and primary airflow; fuel flow is metered to maintain engine speed, leaving primary airflow as the parameter for controlling T_f.

By providing a variable split between combustor primary and secondary airflow, flame temperature can be maintained at the desired value. In order to satisfy accuracy requirements, the variable geometry for this system will have to have a closed loop control around combustor geometry position. The closed loop control system feedback signal can also be used to calculate primary airflow if the total airflow is known:

$$W_{Total} = W_{Pri} + W_{Sec}$$

$$\text{airflow split, } S = \left(\frac{W_{Pri}}{W_{Sec}}\right) = f\left(\frac{A_{Pri}}{A_{Sec}}\right) = g\,[\text{position}]$$

where: A= combustor flow area

This permits T_f to be calculated from total airflow, combustor geometry position, fuel flow and combustor inlet temperature, T_6 (less than 1095°C (2000°F)). The principle source of error in such a system is the possibility of excessive regenerator seal leakage. This condition can be detected by the ECP, however, since it monitors both regenerator hot side temperature (T_{11}) and combustor inlet temperature. If regenerator system leakage is excessive, T_{11} and (T_{11}-T_6) will fall outside prescribed limits and a driver warning can be displayed so that corrective action can be taken. The effect of excessive regenerator seal leakage under the proposed control implementation is to raise both T_7 and T_f. The increase in T_f will cause an increase in exhaust emissions (NO_x) until corrective action is taken. While the increase in T_7 cannot persist for long in the case of the metal rotor engine and a delayed shutdown might be necessary, it will be of little immediate consequence to ceramic rotor durability. Surge margin is sufficient in either case due to the radial compressor characteristics.

The relationship between the various control system sections, the engine, transmission and vehicle are shown in Figure 6.32.

It shall be noted that considerable simplification of the control system and engine could be realized if current NASA research in low emissions combustors is successful. This would eliminate the need for a variable geometry combustor and its associated control system.

Phase II Plan

It is believed that the proposed control system concept will reduce the amount of research and development required to measure the high temperatures that a conventional closed loop control system would require. Emphasis for Phase II research would then focus on the airflow measurement system. Numerous alternatives for airflow measurement are available (see Section 6.4.10) and an airflow measurement research and development program should be a much lower risk venture than a high temperature measurement program.

Early stages of the Phase II program (with metal rotors) could still utilize this control concept, although the temporary addition of T_7 measurement for safety shutdown purposes would be desirable.

Some development work may be required to provide improved electronically actuated fuel nozzles for operation at five atmoshperes combustor pressure, but this would not seem to require a major effort.

The amount of effort expended on the multiprocessor system software will be extensive but, again, no research and development breakthroughs are required for success.

Presently active low emissions combustor research should be continued in Phase II in an effort to eliminate the need for the variable geometry combustor. Success in this effort would considerably reduce the proposed system complexity.

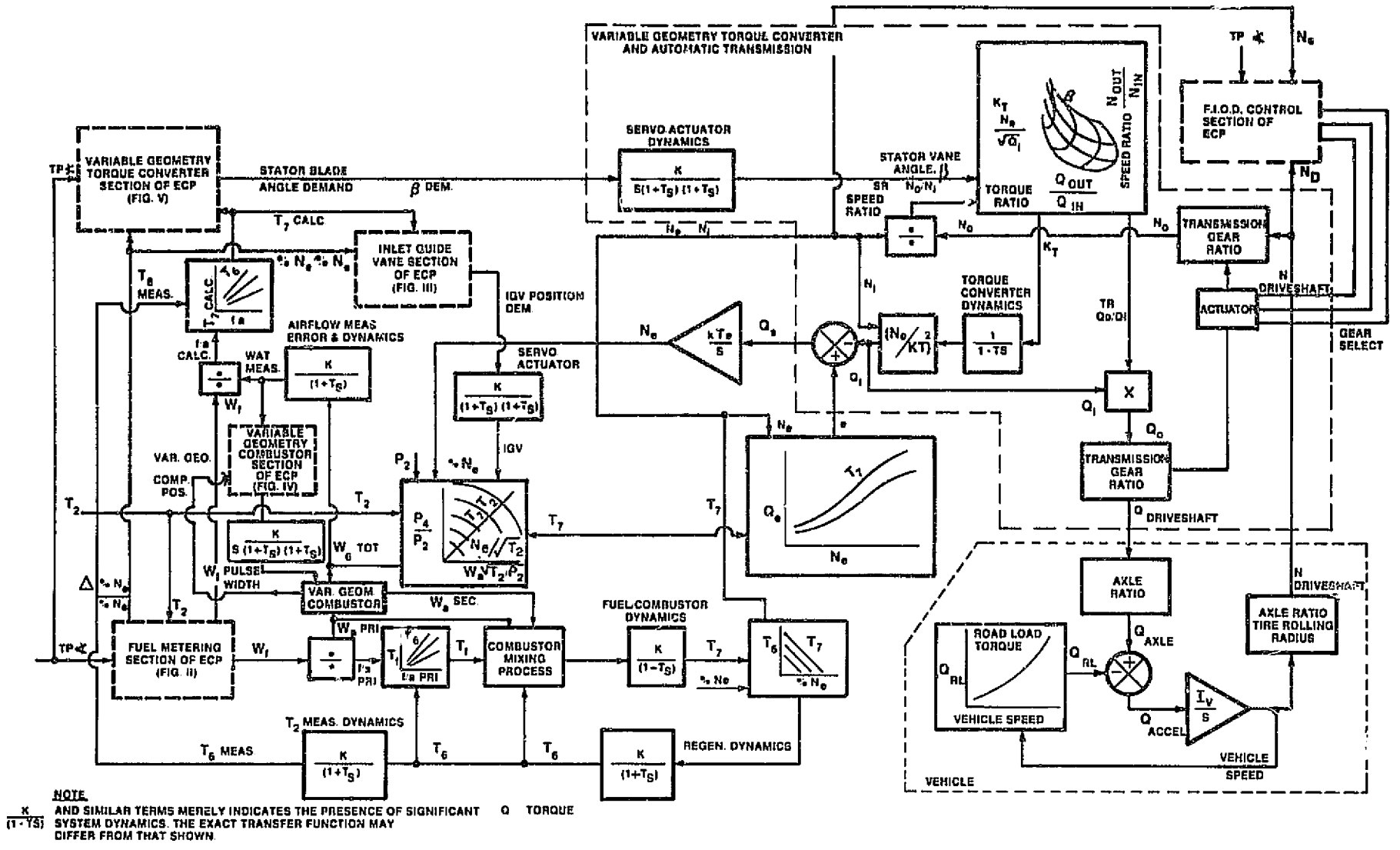


Figure 6.32 Vehicle Control System Block Diagram

All of the concepts presented (except the use of VIGV's for engine braking) have been demonstrated on various advanced engines within Ford Motor Company and this control system concept offers a high probability of meeting the requirements for 1980's passenger car production.

7.0 COST ANALYSIS

An accurate cost analysis, would include a cost of ownership difference comparison between a piston engine vehicle and a turbine engine vehicle for 160934 kilometers. Those items which would be different between a piston engine vehicle and a turbine engine vehicle are initial cost, scheduled maintenance and repairs, and fuel cost.

7.1 Initial Vehicle Cost

To arrive at a reasonably accurate initial cost of a turbine vehicle, it would be necessary to complete detail drawings of all engine parts and unique vehicle parts, complete a manufacturing process plan for each of these parts, and do a comprehensive add and delete cost analysis of the vehicle versus a piston engine vehicle. Such an analysis is beyond the scope of this contract but should be completed in the development program.

However, based on previous cost studies of automotive turbine engines at Ford, which related the variable cost of turbine and piston engines and the retail cost of the complete vehicle, it is possible to make a judgment of the relative cost. While it is expected that the cost of the engine selected in this design study will be more favorable than earlier designs, it has been conservatively assumed for this study that previous experience applies.

Therefore, in the absence of sufficient input to conduct an accurate initial cost study, it is judged that a vehicle with the selected turbine and optimum split power transmission would cost 10% to 20% more to the customer than a comparable 1978 piston engine vehicle ($560 to $1,120). However, more stringent future emission requirements, beyond 1978, for the piston engine could significantly reduce this cost difference.

7.2 Scheduled Maintenance and Repairs

While aircraft experience has shown that time between overhauls is much greater for turbine engines than for piston engines, there is insufficient experience with regenerative turbine engines in automotive service to estimate maintenance and repair costs. While it is believed that repair costs for the turbine will eventually be less than for the piston engine, to avoid speculation, it is assumed for this study that they are equal to those for the piston engine.

7.3 Fuel Cost

Using fuel mileage numbers from Section 5.2 of this report.

Fuel cost for the V8 engine with three speed automatic transmission based on 8.33 km/l (19.6 mpg) over 160,934 kilometers (100,000 miles) at 18.5 cents per litre (70 cents per gallon) is $3571.

Fuel cost for the single shaft turbine engine with a variable stator torque converter and four speed transmission based on 12.9 km/l (30.5 mpg) over 160,939 kilometers (100,000 miles) at 18.5 cents per litre is $2295.

Fuel cost for the single shaft turbine engine with a variable stator torque converter split power transmission based on 14.7 km/l (34.5 mpg) over 160,934 kilometers (100,000 miles) at 18.5 cents per litre is $2029.

Fuel cost for the single shaft turbine engine with a traction drive split power unit plus 4 speed transmission based on 16.1 km/l (37.9 mpg) over 160,934 kilometers (100,000 miles) at 18.5 cents per litre is $1,847.

7.4 Cost of Ownership Difference Comparison

The cost of ownership difference between a piston engine vehicle and a single shaft turbine engine vehicle becomes:

	Initial Vehicle Cost Difference	Difference in 160934 km Fuel Cost	Cost as compared to piston engine
S.S. Turbine with VSTC and 4 speed transmission	+$560 to $1120	−$1276	−$716 to −$156
S.S. Turbine with split power VSTC and 4 speed transmission	+$560 to $1120	−$1542	−$982 to −$422
S.S. Turbine with split power traction drive and 4 speed transmission	+$560 to $1120	--$1742	−$1164 to −$622

8.0 POWERTRAIN DEVELOPMENT PLAN

8.1 Research and Development Program

Since it is understood that the long lead time research and development efforts are to be combined with the engine development program a coordinated plan is submitted (Table 8.1, Figure 8.1 and Figure 8.2) Because of the importance of attaining the goals of each of the component subsystem R&D efforts, each of the 28 sub-projects has been described separately with cost and manning schedules. While the major improvements from these sub-projects will have been attained midway through the total program, iterative improvements are expected and therefore some projects will continue until the end of the development program. Additionally some of the major sub-projects, which result in specific components or subsystems for the engine, have been charged with supplying parts for the various engine builds. These projects are 8.1.7 low emission combustor, 8.1.9 ceramic stationary components, 8.1.12 and 8.1.13 regenerator improvements, 8.1.14 ceramic turbine wheel and 8.1.19 optimum transmission.

Explanation of the need for and timing of some of these projects may be helpful. Because of the continuous improvements being implemented on piston engine systems and other alternative engines it is necessary that the gas turbine contain the most advanced technology that is possible. This overall plan includes an October 1983 demonstration of a metal turbine wheel engine operating at 1150°C (2100°F) or if possible a ceramic wheel engine operating at 1371°C (2500°F). Either engine will require stationary ceramic components. While the 1150°C engine may exhibit adequate fuel economy to meet the contract objectives, there is risk that it may not be sufficiently better than advanced piston engines to warrant a production program. Development of the ceramic wheel is therefore included, conversely, the metal wheel is needed for initial engine development.

- **Engine Design 8.1.1** starts with a substantial effort at the beginning of the program in order to define the component configurations that are needed to commence the subprograms in FY 1980, particularly stationary ceramic components (8.1.9). Iterative results from the sub-programs will be incorporated continuously in the master engine design.
- **Engine Development 8.1.2** commencing in 1981 will incorporate much of the results of subprograms in the first engine build in mid 1981. Because the engineering and supply of some of the parts are provided for in other subprograms, the cost of this project is proportionately low.

- **Ceramic Design Analysis 8.1.5** is a companion project to and concurrent with engine design and utilized the special analysis techniques necessary in design of brittle materials.
- **Ceramic Stationary Components (Process) 8.1.9** encompasses the development of materials refinement and the process of fabrication of each of the specific design of ceramic parts. This is a lengthy effort which works iteratively with ceramic component development.
- **Ceramic Component Development 8.1.10** covers cold and hot rig testing of ceramic parts to develop them to a level of durability needed prior to engine testing. This method is also used to proof test and qualify new parts for each engine build.
- **Ceramic Turbine Wheel Process 8.1.14** includes the development of materials and the turbine wheel fabrication process similar to 8.1.9. Completion time for this project is the least predictable and therefore it must be started early.
- **Control System 8.1.17** is an extensive project because of the many control functions and boundaries involved. In the central philosophy for this single shaft engine, turbine inlet temperatures and HP are essentially single valued function of engine speed, except for certain transient operations, while engine speed is controlled by transmission functions. Variable geometry of the combustor must be controlled to maintain flame temperature within limits, and variable inlet guide vanes must also be controlled. Three versions of the CVT (transmission) must be considered during the control development program.
- **Combustion Temperature Sensor 8.1.18** provides for a means of sensing the flame temperature in the primary zone of the combustion chamber and the turbine inlet temperature. This is the preferred means for control of the low emission combustor. Technology for practical measurement of these high temperature levels does not currently exist and therefore the project is lengthy. Until this sensor is developed, an interim or alternative approach to control logic will be used wherein regenerator inlet temperature, flow and state point conditions at the combustor inlet will be used to infer combustor flame temperature and turbine inlet temperature.
- **Compressor Wheel Fabrication 8.1.25 and 8.1.26 and Non-Metallic Cases 8.1.27** are cost reduction process developments which can be deferred until later in the program when the engine design has solidified.
- **Turbine Wheel Casting Development 8.1.28** covers the development of the casting process for producing the metal turbine wheel with consistent material characteristics, but including internal cooling passages to permit operation at 1150°C (2100°F). A second part of this project in FY 1983 would only be undertaken if the metal wheel engine is determined to be viable, and the ceramic wheel is not available in time. This second part includes a second tooling iteration to insure feasibility of consistent quality in high volume production.
- **Ceramic Recuperator 8.1.29** is considered to be a discretionary "below the line" project. The single shaft engine configuration selected is uniquely suitable for use of a radial flow counterflow configuration of fixed heat exchanger. It would offer potential advantages of reduced leakage resulting in better performance and fuel economy, and completely symmetrical annular flow path from turbine to heat exchanger, thereby reducing thermal distortion and improving heat exchanger effectiveness at significantly reduced cost. However, it is a long and higher risk program than the regenerator, and is therefore considered as a discretionary "below the line" option.

In summary, an integrated engine development plan and technology R&D sub-project plan including 28 projects plus an optional below the line project is proposed. The duration of the program is from FY 1979 through FY 1985 with minimal cost in the first 9 months of FY 1979. A vehicle demonstration of the engine with either metal or ceramic turbine wheel is scheduled for October, 1983. One major redesign of the engine is planned beginning in FY 1982.

The cost of the total program is $65 million exclusive of the "below the line" option. Major annual expenditures of $11 to $13 million occur from FY 1980 through FY 1983. Detail program plans are contained in the following sections 8.1.1 to 8.1.29.

TABLE 8.1

Overall Component Development Program

FISCAL YRS.	79	80	81	82	83	84	85
8.1.1 Engine Design							
8.1.2 Engine Development							
8.1.3 Rad. Turbine Aero. Development							
8.1.4 Compressor Development							
8.1.5 Ceramic Design Analysis							
8.1.6 Low Loss Ducting							
8.1.7 Low Emissions Combustor							
8.1.8 Air Bearing & Shaft Dynamics							
8.1.9 Ceramic Stationary Components (Process)							
8.1.10 Ceramic Component Development							
8.1.11 Regenerator Flow Distribution							
8.1.12 Regenerator Seal Leakage (2.5%)							
8.1.13 Regenerator Temperature (1100°C)							
8.1.14 Ceramic Turbine Wheel (Process)							
8.1.15 Ceramic Wheel Attachment							
8.1.16 Turbine Nozzle Sealing							
8.1.17 Control System							
8.1.18 Combustion Temperature Sensor							
8.1.19 Optimum Transmission Development							
8.1.20 NDE							
8.1.21 Ceramic Material Characterization							
8.1.22 Vehicle Package Design							
8.1.23 Inlet System Ducting							
8.1.24 Exhaust System Ducting							
8.1.25 Powder Metal Compressor Wheel							
8.1.26 Die Cast Compressor Wheel							
8.1.27 Non-Metallic Cases							
8.1.28 Turbine Wheel Casting							
8.1.29 Ceramic Recuperator							
Total — $(000)	2850	10588	12870	11703	11528	7772	7115

Total Development Program Cost $64,426,000

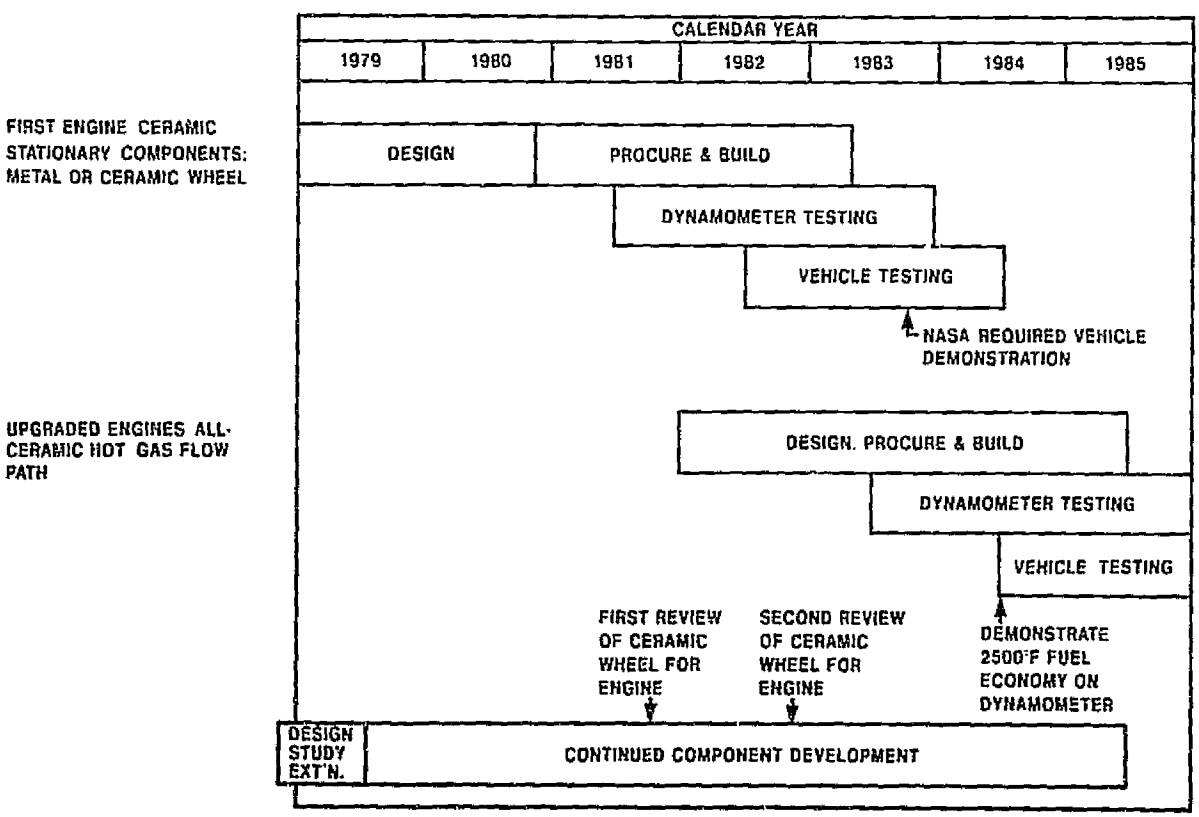


Figure 8.1 DOE/NASA Gas Turbine Engine Program — Timing Chart

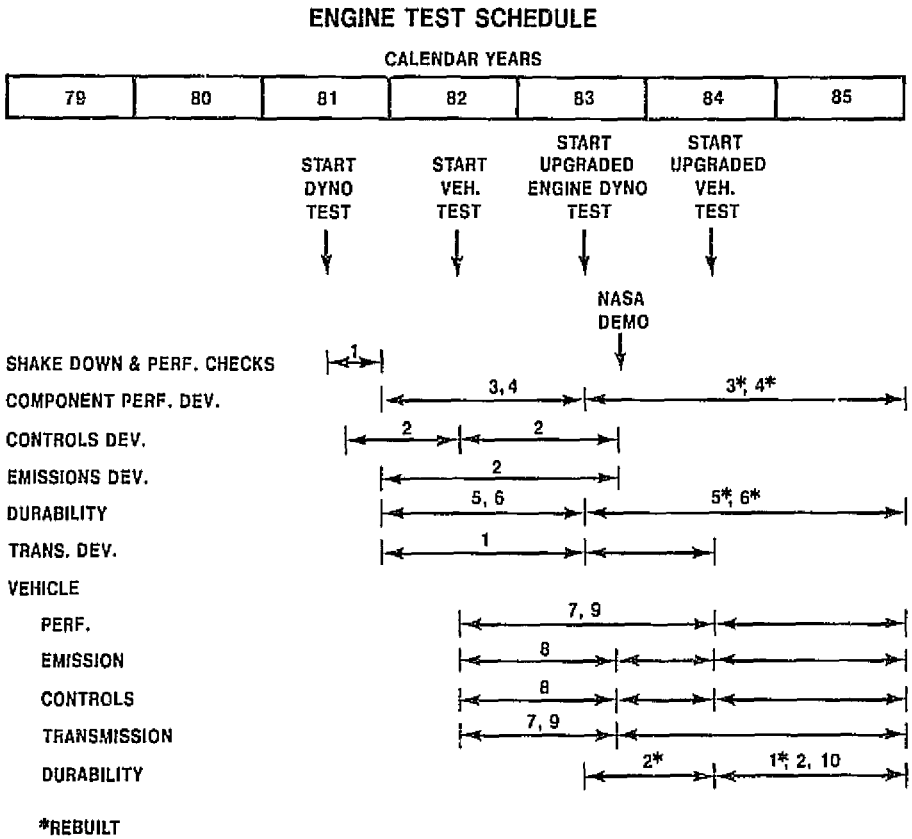


Figure 8.2 Engine Test Schedule — Timing Chart

8.1.1 ENGINE DESIGN

Problem Definition

The various Long Lead Research and Development (LLR&D) programs, which are aimed at resolving the open issues identified in Phase I, need to be designed and executed within the constraints of the selected power system concept. Proper interfacing of the design solutions and/or modifications resulting from the individual programs is, therefore, required to assure the integrity of the overall power system concept and to facilitate an early implementation of these solutions, preferably by the first build of the engine scheduled for early 1981. In line with this schedule, it is planned that the release of engineering drawings for hardware procurement will commence towards the end of Phase I extension. To accomplish this, the detailed design of the power system will need to be completed during that time along with the appropriate analyses and design investigations as deemed necessary for the release of detailed drawings. Since many of the LLR&D programs will continue into the engine development phase of the program, the results of these individual studies would not be implemented into the initial build of the engine. A good example is the ceramic rotor. Engine design is, therefore, going to be an ongoing effort and it is anticipated that second design iteration of the engine will be required halfway through the program to incorporate these modifications. This design iteration will also include results of an extensive cost reduction studies that will be conducted in the meantime.

Development phase of the powerplant and powerplant-vehicle system will be supported for its duration with extensive failure analysis consisting of detailed analyses of failures, design modifications and limited bench tests.

Workplan

1. Coordinate solutions and design modifications resulting from individual component development programs — Continuous effort.

2. Develop detailed power system design, fully supported by aerodynamic, thermal, mechanical and cost analyses and generate detailed engineering drawings for hardware procurement.

First design iteration	End of 1980
Second design iteration	Early 1983

3. Perform and update powertrain performance analyses using results of individual component development programs and the results of engine and engine-vehicle tests — Continuous effort.
4. Develop vehicular installation layouts of the powertrain and generate detailed drawings of engine ducting, oil cooling system and vehicle modifications required to adapt the vehicle system to a gas turbine powerplant.

First design iteration	End of 1981
Second design iteration	Middle of 1983

5. Provide design support and conduct failure analyses in support of engine and rig tests — Continuous effort.

8.1.2 ENGINE DEVELOPMENT

A ten engine development program will be initiated during FY 81. The first of six (6) dynamometer locations will be required on June 1, 1981 with all six locations operational by November 1, 1981 and continuing through 1985 on a two-shift basis as required.

A six vehicle fleet is planned for track and on-road test evaluation and total systems development. The first vehicle tests will be initiated during June 1982 and continuing through December 1985. Complete dynamomter support of the vehicle test program will be provided as required.

The dynamometer and vehicle engine activity is divided by tasks (see also Figure 8.2, Section 8.1) as follows:

Engine No. 1 — Engine functional shakedown tests and performance baseline data: Duration 6 months. Transmission development will be initiated following shakedown testing and continue through June 1984. An updating rebuild of this engine will be installed in a vehicle for track and on-road durability testing through 1985.

Engine No. 2 — Controls development and exhaust emissions evaluation tests will be initiated during September 1981 and continue through August 1983. An updated rebuild of this engine also will be utilized in the vehicle durability fleet.

Engine No. 3 and 4 — A continuous component performance improvement program will be carried out from Jan. 1982 through Dec. 1985. Modified components and sub-assemblies evolved from the on-going R&D and component development programs will be scheduled into engine build for verification tests. Also, candidate designs and design modifications resulting from the NASA sponsored R&D programs will be scheduled for test and evaluation. A major design update is planned for mid-1983 with minor updates and rebuilds occurring as required.

Engine No. 5 and 6 — A dynamometer durability test program will be initiated during Jan. 1982 and continue through December 1985.Test cycles will include simulated track and road durability routes currently used for production vehicles, as well as specialized steady state tests to verify problem solutions on an accelerated basis. A strict parts change procedure will be maintained to provide proper control over the problem-solving procedures and assure no compromise in performance, fuel economy and/or emissions objectives. A major update rebuild is scheduled for mid-1985.

Engine No. 7 and 8 — These engines represent a mid-1982 development level and will be used to evaluate in-vehicle performance, fuel economy, and driveability of the engine-transmission system. Dynamometer calibration and test correlation of dyno SFC and miles per gallon will be compared.

Engine 9 — Engine 9 will be used exclusively in vehicle exhaust emission evaluation and controls development. Vehicle testing will include track and road testing under all environmental conditions. A standard Ford jury evaluation of driveability will also be performed.

Engine 10 — Engine 10 will be built in mid-1984 and incorporate the best available components and design features. Engines 1 and 2 will be rebuilt with updated parts and these three (3) engines will be utilized in a 3 vehicle durability test program at the Arizona Proving Ground. This test program will begin in mid-1984 and end during December 1985, with an objective of accumulating 50,000 miles on each vehicle.

Objectives and Milestones

Major Milestones are as follows:

June 1, 1981	Initiate Dynamometer Testing
June 1, 1982	Initiate Vehicle Testing
June 1, 1983	Initiate Dynamometer Test of engine with a ceramic turbine wheel.
November 1, 1983	Demonstrate Vehicle to NASA that is 20% better than baseline fuel economy at .4 NOX.
June 1, 1984	Initiate vehicle testing of engine incorporating a ceramic turbine wheel.
Dec. 1, 1985	Demonstrate 50,000 miles vehicle durability.
	Demonstrate fuel economy improvement over baseline at 0.4 NOX.

8.1.3 RADIAL TURBINE — AERODYNAMIC DEVELOPMENT

Problem Definition

The increase in fuel economy of a vehicle due to improving the optimum efficiency of a radial turbine from the state-of-the-art level of about 88%, for a nominal 75kW (100 HP) high temperature engine, to 91% is about 3 percent. High efficiency radial turbine designs should be developed for both cooled metal and ceramic rotors.

A radial turbine design which is limited to a tip-speed below the optimum value displays a low efficiency at part load. For an automotive engine which operates most of the time at low levels of power it is essential that the part load efficiency be maximized.

The turbine diffuser system is a component that should be evaluated with the turbine rotor. The turbine test rig should simulate the engine diffuser and the regenerator collector plenum.

A high temperature radial turbine designed for the optimum efficiency will have a considerably larger diameter than that of the associated compressor. It is conceivable that upon starting the engine the radial turbine may successfully oppose the compressor pressure rise which would result in back-flow of the air through the combustor and difficulty in obtaining light-off.

Work Plans

1. Prepare a radial turbine aerodynamic design for the optimum tip speed for both cooled metal and ceramic rotors using the latest 3-D viscous flow computer analysis program. Conduct mechanical and thermal stress analysis on a 3-D finite element model of the rotor, iterating on blade thicknesses and passage contours to obtain an acceptable stress level without detracting from the aerodynamic efficiency.

2. Correlate low temperature aerodynamic test results and LDV measurements with the computer model of the flow and refine as necessary. Repeat the process to develop a highly efficient radial turbine.
3. The turbine diffuser and flow distribution at the regenerator core inlet face will be evaluated and modifications made to optimize the system for the design pressure recovery and good flow distribution over the face of the core.
4. Evaluate the direction of flow between typical radial turbines and compressors for a high temperature engine by a back-to-back tests. Make recommendations as necessary.

8.1.4 COMPRESSOR DEVELOPMENT

Problem Definition

It is anticipated that an improvement in state-of-the-art efficiency of the selected engine configuration compressor from about 77 to 81 percent would improve the vehicle fuel economy by about 2.8 percent. Furthermore, the application of compressor variable inlet guide vanes to maximize the "low load" turbine inlet temperature will improve the vehicle fuel economy by about another 4 percent. To obtain both of these improvements requires a comprehensive research program on compressors.

Work Plan

1. Design an optimum specific speed compressor using the latest 3D-viscous flow computer models. Test compressor in a rig using Laser Doppler Velocimeter (LDV) techniques to determine local velocities in the rotor. Correlate results with the computer model and refine the model.
2. Repeat the process as necessary through 1982.
3. Provide update designs to the engine development program.

8.1.5 CERAMIC DESIGN TECHNOLOGY

Problem Definition

Design technology for ceramic materials is relatively new and still in a development stage. Continuation of this effort is paramount to the success of the IGT engine which is structured around a ceramic hot flow-path. Design tools for ceramics, developed so far, are based on relatively simplistic failure models which are still far from proven. New more sophisticated models are being developed that should improve the predictive capability of the designer and thus enhance the reliability of his concepts. These will require testing and evaluation in realistic applications before their implementation into acceptable design codes.

Ceramics have been shown to follow statistical rules. Statistical tools are, therefore, needed to analyze data and conduct verifications of component reliabilities.

Development of ceramic technology is envisioned to be a continuous effort aimed at improving reliability of ceramic designs and as such needs to be supplemented with design and development studies of reliable, cost effective interfaces for ceramic and ceramic-metallic structures.

Work Plan

1. Continue development of design tools for ceramic structures. Update and modify existing analytical codes as needed to support failure analyses and improve reliability of designs — Continuous effort.
2. Develop statistical tools to analyze material strength data for use in the reliability analysis. Develop statistical methods for the verification of component reliability from test data — Continuous effort.
3. Conduct design studies on metallic-ceramic and ceramic-ceramic interfaces. Develop reliable, cost effective, thermally compliant devices for centering of ceramic structures under load, example, curvic coupling face spline for ceramics. This will be a continuous effort. The coupling optimization

and development will need to be completed prior to first engine test, i.e. end of 1980. Manufacturing studies on curvic coupling will continue till end of 1981.

4. Investigate means of improving reliability of ceramic structures. Conduct design studies and tests in support of this effort — Continuous effort.

8.1.6 LOW LOSS DUCTING

Problem Definition

Pressure losses within the engine flow passages represent cycle efficiency losses which adversely affects the fuel consumption of the gas turbine engine. For example, a one percent loss in pressure translates into about a one percent decrease in route fuel economy. Pressure losses also affect the size of an engine in that larger pressure losses mean a greater air flow will be required for the same power level. The duct from the compressor discharge to the regenerator, the duct from the regenerator to the combustor inlet, the duct from the turbine diffuser to the regenerator hot gas inlet, and the duct from the regenerator to the exhaust system are potential sources of excessive pressure losses.

Work Plan

1. Analyze and modify the flow path to minimize pressure loss and flow distortion using 3D viscous flow computer model as required.
2. Construct a physical model for test simulating the engine flow path.
3. Conduct cold flow tests to measure distribution and pressure losses. Modify the flow path by clay modeling or otherwise to develop improvements iterating between computer modeling and physical test.

8.1.7 LOW EMISSIONS COMBUSTOR

Problem Definition

Extensive investigations, made by Ford and other companies, with conventional gas turbine combustors have shown that the direct spray combustor cannot be modified to satisfy the Federal Emissions Standards of 0.4 gm/mi., 3.4 gm/mi., 0.4 gm/mi., for HC/CO/NOx. Generally, any modifications made to a conventional combustor to reduce NOx results in unacceptable increases in HC and CO emissions.

The combustor inlet and discharge temperatures, in the high temperature engine, are significantly higher than those encountered in today's 1050°C (1900°F) engine. A combustor must, therefore, be developed that is capable of operating in this environment and capable of satisfying the Federal Emissions Standards. Because of the expected combustor inlet temperatures of the order of 1070°C (1950°F), and the need to avoid quenching of the flame, with resultant high CO and HC emissions associated with the cooled wall regions of a metal combustor, a ceramic walled combustor is considered to be essential.

Work Plan

Analyze combustor concepts for the operating environment predicted for the high temperature improved gas turbine, including fuel handling and cold start requirements. Combustor concepts to be considered are:

- Variable geometry premix/prevaporizing
- NASA ceramic multi-element
- Catalytic
- Staged combustion

Select one or more concepts. Prepare designs and build the system for testing and evaluation.

Design combustor test rigs for evaluation of concepts. Test rig will include an air preheater to supply high temperature 1095°C (2000°F) non-vitiated air to the combustor.

8.1.8 AIR BEARINGS AND SHAFT DYNAMICS

Problem Definition

To design, develop, and demonstrate air bearing system (main support bearing and thrust/antithrust bearing) for the main spool of the IGT engine including shaft dynamics.

Work Plan

1. Design engine simulator test rig.
2. Design and Fabricate spiral groove thrust/antithrust bearing.
3. Design and Fabrication of main support foil bearing.
4. Procure and build engine simulator rig.
5. Shakedown test the rig and conduct cold test development of the air bearing system in engine simulator rig.
6. Conduct hot test development and demonstrate air bearing system under simulated engine conditions.

8.1.9 CERAMIC STATIONARY COMPONENTS (PROCESS)

Problem Definition

In order to meet the minimum fuel economy objectives of the program it is necessary that the engine be designed to operate at at least 2100°F (1150°C) turbine inlet temperature. While it is expected that a metal radial turbine wheel will be acceptable at this temperature it is necessary that the stationary hot flow path components be made of ceramic.

Work Statement

1. Develop ceramic materials and fabrication processes capable of producing radial turbine stationary components meeting design requirements.
2. Establish tooling and fabrication processes and supply prototype components for rig testing.
3. Fabricate and supply components for engine testing which incorporate the results of rig testing, aerodynamic testing, and continued material and process development.

The stationary components that are to be fabricated from slip cast reaction bonded silicon nitride are the outer and inner turbine inlet body, turbine diffuser and diffuser shroud.

The turbine nozzle or stator will be made from injection molded silicon nitride and/or silicon carbide.

The inner liner or main case will be subcontracted to a low expansion glass ceramic supplier.

Work Plan

Slip Cast Components

1. Commence material and process development and order molds, FY79
2. Supply parts for hot rig testing late FY80.
3. Incorporate improvements dictated by rig testing, establish process and commence fabrication of engine parts by mid FY81.

4. Continue to supply parts for rig and engine test with iterative improvements FY82 to FY85.

Turbine Stator

1. Order injection molding tooling and experiment with existing axial stator tooling (FY79) until radial tooling is received early in FY80.
2. Continue iterative process development of silicon nitride parts in conjunction with hot rig testing and commence fabrication of parts for engine test (FY81).
3. Commence development of RBSC and higher density RBSN second quarter of FY81.
4. Select best material and process and continue to supply test parts (FY82 to FY85).

Inner Liner

1. Subcontract material and process development ($250K/year) to glass ceramic supplier and commence physical property testing (FY79).
2. Establish adequate physical properties (early FY80) and initiate hot rig testing of part (late FY80).
3. Approve fabrication process and commence fabrication of parts for engine test (mid FY81).
4. Continue to supply test parts with development changes as required (FY82 to FY85).

8.1.10 CERAMIC COMPONENT DEVELOPMENT (TEST)

Problem Definition

Each of the ceramic components produced under process development projects must be developed by hot testing in rigs prior to the first engine build. Subsequent parts must be qualified for each engine build. This is an iterative development program between 8.1.9 Ceramic Stationary Components (process), 8.1.14 Ceramic Turbine Wheel (process) and 8.1.2 Engine Development projects.

Work Plan

The planned effort is broken down into two major categories: stationary flowpath components and structures and the radial turbine rotor. (See attached task timing chart Figure 8.3) For both categories, test rigs are to be designed and built for use in testing the required components. Where possible, existing rigs and/or hardware will be utilized.

Stationary component test and development will be conducted in two test rigs, one for transient evaluation and one for steady state evaluation.

Radial turbine rotor test and development will be conducted in a hot spin test rig and in a cold spin pit used to screen candidate rotors.

8.1.11 REGENERATOR FLOW DISTRIBUTION

Problem Definition

Because of the restricted space allowed for ducting in automotive gas turbines, distortion of the flow at the inlet to the high and low pressure sides of a regenerator is a common occurrence. Consequently, the full flow area of a regenerator is not utilized effectively, which can result in a loss of as much as 5% in effectiveness if not corrected. This development should be initiated early in the program in order to incorporate necessary changes to the flow path ducting components before tooling commitments are made.

Work Plan

1. Investigate flow distortion in a laboratory model that simulates the I.G.T. Ford automotive engine regenerator flow path.

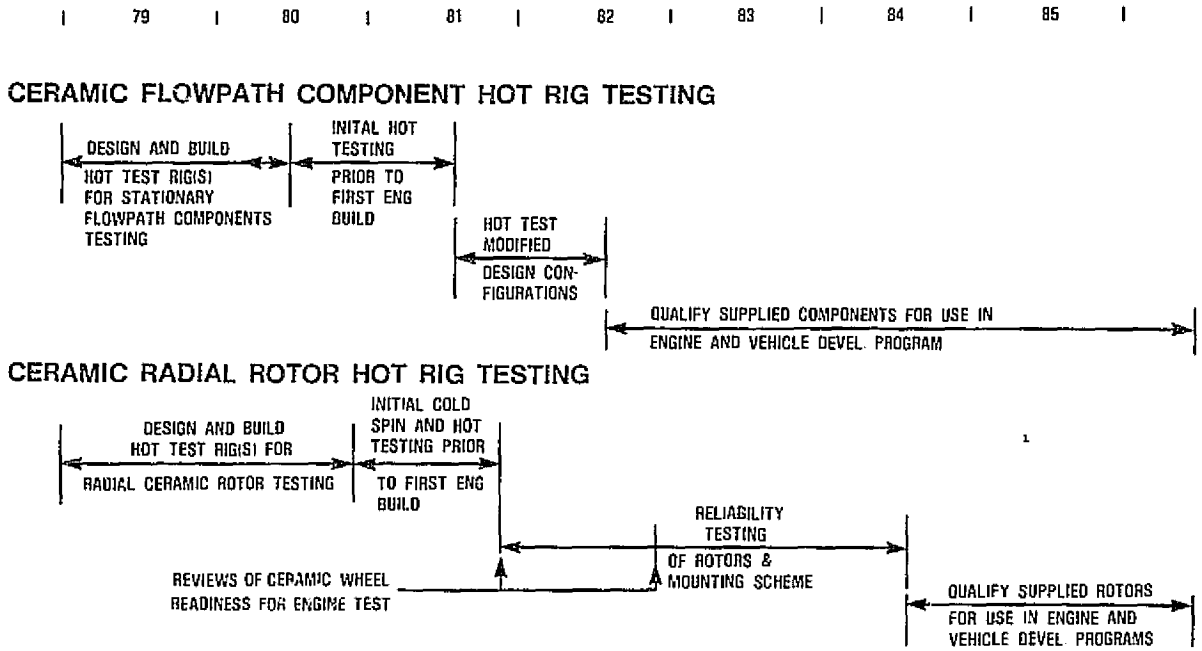


Figure 8.3 Ceramic Components Development — Timing Chart

2. Evaluate corrective actions to the test model to eliminate the distortion with minimum increase in engine package dimensions.

8.1.12 REGENERATOR SEAL LEAKAGE (2.5%)

Problem Definition

The current regenerator seal system used in the Ford 707 gas turbine engine has a leakage that is in the 4 to 5% range. The long-range objective for the improved gas turbine engine is a leakage that is 2.5% of engine air flow.

Work Plan

1. Fabricate an improved static seal test rig to evaluate regenerator seal designs at room temperature.
2. Fabricate a regenerator test rig to evaluate regenerator seal designs at simulated engine flow conditions.
3. Evaluate improvements in seal design and manufacturing processes for reduced system leakage.

8.1.13 REGENERATOR TEMPERATURE – 1100°C (2000°F)

Problem Definition

The present generation of ceramic regenerators appear to be limited to temperatures of 1000°C (1832°F). The temperature limitation of the present seal coatings is unknown, but may also be limited to this same temperature. The objective of this program is to develop ceramic regenerators, seal coatings and seal diaphragm systems with temperature capability of 1100°C (2000°F) in order to improve part load fuel economy by 3%.

Work Plan

1. Fabricate a regenerator test rig with temperature capability of 1100°C (2000°F).

2. Update existing seal wear test rigs for 1100°C (2000°F) temperature capability.
3. Screen new seal coatings and core materials in the seal wear test rig.
4. Fabricate acceptable automotive sized seal or core designs for evaluation in the high temperature regenerator test rig.
5. Utilize additional laboratory tests and analysis pertaining to regenerator aerothermodynamic, heat transfer, thermal and mechanical stress in addition to matrix and seal coating material evaluations.

8.1.14 CERAMIC RADIAL TURBINE WHEEL (PROCESS)

Problem Definition

To insure adequate fuel economy, performance and engine response time, at low cost a ceramic radial turbine wheel is needed. A process for fabrication of a radial wheel with adequate material properties must be developed.

Work Statement

(a) Develop ceramic materials and fabrication processes capable of producing monolithic radial turbine rotors meeting design requirements (minimum values assumed to be an RT strength of 90 Ksi with a Weibull slope (m) of 13).

(b) Establish tooling and fabrication processes and supply prototype rotors for spin and rig testing.

(c) Fabricate and supply rotors for engine testing which incorporate the results of rig testing, aerodynamic testing, and continued material and process development.

Work Plan

1. Commence development of material properties in reaction bonded silicon nitride, sintered silicon nitride and sintered carbide. (FY79)
2. Achieve material properties in test bars, procure tooling and supply parts for hot test rig. (FY80)
3. Achieve material properties in samples from rotors, select best material, and supply rotors for engine test. (FY81)
4. Continue material, process and tooling refinement and supply parts for rig and engine test (FY82 to FY85).

8.1.15 CERAMIC WHEEL ATTACHMENT

Problem Definition

A ceramic radial turbine wheel can not be attached to the shaft by use of a through bolt without incurring undesirable stress levels. Therefore, a means of attaching a boreless wheel to a metallic shaft is required which maintains concentricity and minimizes thermal stress despite differential thermal expansions.

Work Plan

1. Design and analyze rotor attachment concepts. Select two and design static test fixtures. (FY80)
2. Procure attachment and test fixture hardware. (FY80)
3. Build test rigs and conduct static tests and development. (FY81)
4. Build dynamic simulator hardware and conduct cold and hot dynamic testing and development in the main shaft (air bearing) simulator rig. (FY81)

8.1.16 TURBINE NOZZLE SEALING

Problem Definition

In order to facilitate low cost accurate fabrication of a ceramic nozzle assembly for a radial turbine, an integral sandwich construction is proposed where the nozzle vanes are molded integrally between two thin-walled shrouds. The nozzle assembly is in turn sandwiched between two load bearing structures that form the turbine inlet passage and the rotor cavity. Bypass leakage of gases over the two shroud surfaces will seriously affect turbine efficiency and therefore a sealing means must be developed.

Work Plan

Build the rig and conduct test and development.

8.1.17 CONTROL SYSTEM DEVELOPMENT

Problem Definition

The task is to define and implement the best compromise control system for automotive application of a single-shaft, regenerative gas turbine engine. Considerable computer simulation of the dynamics of the vehicle, engine, transmission and control system will be required to arrive at the best compromise among performance, fuel economy and exhaust emissions objectives.A principal area of concern is the method of measurement or synthesis of Turbine Inlet or Combustor Flame Temperature. This must receive considerable emphasis due to the impact the selected method will have on vehicle cost and reliability.

Work Plan

The first year's effort involves four major areas of activity. First, two computer programs are written to dynamically model the entire engine/vehicle/control system and to exercise this model over various driving cycles to optimize performance, fuel economy and emissions. Second, a study is made of methods of measuring or synthesizing turbine inlet and combustor flame temperature and the best two candidates are tested. The third activity is to define the control strategy in detail. The fourth activity is the start of procurement and test of control system hardware. (FY80)

At the start of the second year, optimization studies are made while the control system microcomputer software design begins. Durability testing of the selected temperature measurement method is completed as is dynamic testing of both engine and transmission. All of this testing is used to refine the modeling and optimizing programs in order to improve the control system. (FY 81)

Year three begins with programmed dynamometer testing of the entire vehicle system prior to actual road tests. This data is used to further improve the control system software. (FY82)

In the year the ceramic engine is available for test, its early running will be used to update the computer models. The newly optimized model will permit the final control algorithms to be developed and demonstrated in both programmed dynamometer and road testing.

8.1.18 COMBUSTION TEMPERATURE SENSOR DEVELOPMENT

Problem Definition

Measurement of turbine inlet temperature and/or combustor flame temperature requires temperature probe operation in the 1370-1650°C (2500-3000°F) range. If such measurements are to be used for control purposes, these probes must have quick response, a long maintenance-free life, give repeatable readings and, for production automotive application, they must be as inexpensive as possible.

These difficult and conflicting requirements are not met by present technology temperature measurement techniques. A concerted research and development effort will be required to provide this new technology.

A partial list of candidates for consideration are optical pyrometer, low level radiation methods, fluidic or ultrasonic probes and new technology, high temperature thermistors.

Work Plan

During the first year, efforts are concentrated in three major areas. First, current technology temperature measurement methods are analyzed and the three most promising are tested. Secondly, computer programs are written for dynamic and stress/durability modeling. These will be utilized for design improvements to be made in later portions of the program. The third major activity of the first year is the study of possible ceramic temperature probe materials and methods. (FY80)

During the second year, the best of the current techr ology candidates are redesigned for improved performance, durability and cost. Design begins on temperature measurement devices using new ceramic technology. (FY81)

In the third year, both the redesigned current technology probes and the ceramic probes are tested. First these will be tested in performance and durability rigs, and then in the metal engine. (FY82)

The fourth year of the program concentrates on the final redesign and evaluation of those measurement systems that have proved best. Rig testing is followed by testing in the ceramic engine and a vehicle test/demonstration program. (FY83)

8.1.19 OPTIMUM TRANSMISSION DEVELOPMENT

Problem Definition

Feasibility studies indicate that transmission concepts, other than using a variable stator torque converter in series with an automatic transmission, exist which minimize the amount of power going through the variable speed device, resulting in 20% improvement in vehicle acceleration and 24% in vehicle fuel economy if the variable speed device is a traction drive (concept 13, Section 3.11.2). Alternately a differential split power arrangement (concept 6, Section 3.11.2) using the variable stator torque converter yields 10% improvement in acceleration and 13% improvement in fuel economy. The traction drive represents a much higher program risk than the variable stator torque converter. A comprehensive program is, therefore, needed.

Work Plan

The development plan consists of four phases with phases 1 through 3 commencing concurrently, and phase 4 overlapping phase 3 in the second year. Phases 1 and 2 cover development of the variable stator torque converter and the traction unit. Phase 3 provides the optimum ratio 4 speed gear box which is part of the system. Phase 4 covers development of the control system and vehicle testing.

Phase 1— Split power to a variable stator torque converter by means of a differential compound planetary gear and couple to a production four-speed automatic gear box. This will establish, differential, slip clutch, and shift capability, while providing a midalternate transmission if phases 2 and 3 cannot be completed or do not meet objectives.

Tasks

- Design differential variable stator torque converter unit.
- Specify and design engineering changes to 4-speed automatic, including control and slip clutch.
- Procure and assemble hardware.
- Design test rig and specify tests.

- Procure and assemble test rig.
- Test to establish steady state efficiency of differential variable speed unit with and without transmission.
- Simulate and determine shift feasibility and slip clutch performance on test rig.

Phase 2— Combine the differential compound planetary with a variable speed traction drive capable of transmitting one-third of the engine power, and continue use of the modified production four-speed automatic gear box. This will establish feasibility of the traction drive portion of the transmission and although a toroidal traction unit is preferred, the adaptation of other types of traction units can be investigated.

Tasks

- Design differential traction drive unit.
- Specify and design engineering changes to 4 speed automatic including control and slip clutch.
- Procure and assemble hardware.
- Design test rig and specify tests.
- Modify Phase 1 test rig.
- Test to establish steady state efficiency of the differential variable speed unit with and without transmission.
- Simulate and determine shift feasibility and slip clutch performance on test rig.

Phase 3— Following development of the differential traction unit in phase 2, then develop a new optimum ratio multiple speed transmission with integrated slip clutch.

This will be the optimum transmission which can be vehicle tested to verify performance projections.

Tasks

- Design optimum four speed automatic transmission.
- Procure and assemble hardware.
- Specify test and design changes to phase 2 test rig.
- Modify test rig.
- Test to establish steady state efficiency of complete transmission system.
- Simulate and determine shift feasibility and slip clutch performance on test rig.
- Combine with turbine engine for vehicle testing.

Phase 4—

Tasks

- Transmission Control — Determine, define, develop and proveout the control parameters required to automatically operate the transmission and integrate the engine and transmission control system.

- Production Prototype Transmission — Redesign the feasibility study transmission to correct any development problems and incorporate control system refinements. Build four production prototype transmissions for vehicle testing with a turbine engine.

- Vehicle Testing — Conduct an intensive vehicle testing program of the transmission to verify fuel economy, transient response, and durability.

8.1.20 NON-DESTRUCTIVE EVALUATION

Definition of Problem

In order to insure adequate reliability of ceramic components during development and at reasonable cost in production, accurate and rapid N.D.E techniques must be developed.

Work Plan

- Inspect all test specimens and components fabricated during the program using existing N.D.E. techniques such as visual inspection, X-ray radiography and dye penetrants. (continuous)
- Develop transducers and transducer coupling techniques that permit ultrasonic inspection of complex gas turbine parts such as the air foil of a rotor. (FY79 to FY81)
- Assess the feasibility of emerging N.D.E. techniques. (continuous)
- Develop N.D.E. programs and conduct research on the above N.D.E. techniques as warranted based on the results of feasibility studies. (continuous)

8.1.21 CERAMIC MATERIALS CHARACTERIZATION

Problem Definition

Designers of components for ceramic gas turbine engines must be supplied data defining the engineering property characteristics of ceramic materials of interest. In many instances, the ceramic materials required are experimental and not commercially available and, therefore, a well developed data base is not presented in the literature. This requires that techniques and equipment for measuring ceramic material strengths, thermal properties, and microstructural properties of experimental ceramic materials be available, and that extensive data compilation on candidate ceramic materials be carried out in support of ceramic design and component part fabrication activity.

Work Plan

1. Measure and compile data required to adequately define candidate ceramic gas turbine material properties. Time and temperature dependence of mechancial and thermal properties will be measured and interpreted with respect to microstructure, flaws, inclusions, purity, and processing variables. Property results will be related to pre-test NDE characterization and post-test fracture mode analysis. Data compilation and presentation methods will utilize statistical analysis techniques. Per batch and batch-to-batch property variations will be monitored to provide a broad data base. Environment efforts such as oxidation and hot gas exposure will be evaluated and effects of cyclic loading will be determined.

2. Correlation of material property data obtained from test samples cut from representative fabricated components will be made to determine size effects and part fabrication effects on based material characteristics.

8.1.22 VEHICLE PACKAGE DESIGN

Problem Definition

A design of the installation of the gas turbine powertrain in a selected vehicle must be accomplished and the adapting parts and vehicle modification must be designed and detailed to permit construction of test and demonstration vehicles.

Work Plan

1. Design the gas turbine vehicle package and detail the engine parts for the Phase I vehicle builds.

2. Modify the design to accommodate changes to the powertrain vehicle which affect the package.

3. Repeat for the Phase II vehicle builds.

8.1.23 INLET SYSTEM DUCTING

Problem Definition

The inlet system consists of the inlet filter and inlet duct for uniform flow distributor at the entrance to inlet guide vanes (IGV).

Deviations from the design IGV inlet flow condition generally have a detrimental effect on the performance of a radial compressor in terms of flow capacity, pressure ratio, and surge line. A horseshoe type inlet is especially prone to potential distortions because the air enters from one direction in a radial fashion. Therefore, the entire inlet system, including the air filter must be designed to minimize the pressure loss and flow distortions at the compressor IGV inlet. Both an analytical and experimental approach will be necessary to achieve these objectives.

Work Plan

1. During the engine design plan, an analytical study will be made. Known empirical relationships will be used to size duct flow areas and area transition regions. The air and mist filters will be designed with vendor assistance according to relationships between air flow, filtration effectiveness, and pressure loss characteristics. Where a critical flow problem exists, such as just upstream of the IGV's, a 3D viscous flow computer model will be used to study the flow pattern and dictate revisions.
2. After the design phase, an experimental investigation of the inlet system will take place. The flow condition at the IGV entrance will be studied for pressure loss and uniformity. If excessive pressure losses or flow distortions do occur, the source of the problem will be investigated. Modifications to the flow path model, e.g., with clay, will be made to correct the problem. These modifications will then be factored into the flow path design.

8.1.24 EXHAUST SYSTEM DUCTING

Problem Definition

An automotive exhaust system usually involves a tortuous path through the underside of the car where adequate room for a large cross-sectional area duct, thermally and acoustically insulated, is difficult to obtain. A pressure loss of one percent (4" H_2O) translates into approximately one percent loss in fuel economy. Pressure losses also affect the size of an engine in that larger pressure losses mean a greater air flow and correspondingly greater duct sizes are required.

Work Plan

During the engine installation phase, an analytical study will be made on various alternate configurations. Empirical loss relationships will be used to optimize the design. The effect of different approaches to provide adequate thermal and acoustic insulation will be assessed. Where it is judged practical 3D-viscous flow analytical models will be constructed to optimize the losses.

On completion of the design phase of the exhaust system, flow models consisting of actual engine hardware will be constructed for testing. Where excessive losses are measured modifications will be made to minimize the losses. These modifications will then be factored into the engine design.

8.1.25 POWDER METAL COMPRESSOR WHEEL

Problem Definition

Current methods of casting aluminum compressor wheels do not produce the dimensional accuracy or surface finish necessary to obtain the highest aerodynamic efficiency. Powder metallurgy and die casting offer the potential of resolving this problem for high volume production, but each requires development to assure that the necessary physical properties are obtained consistently and uniformly throughout the part.

Work Plan

Laboratory Process Development and Support	1983-1985
Prototype Fabrication Process Development	1983-1985
Final Component Fabrication & Qualification Testing	1984-1985

8.1.26 DIE-CAST COMPRESSOR WHEEL

Problem Definition

Current methods of casting aluminum compressor wheels do not produce the dimensional accuracy or surface finish necessary to attain the highest aerodynamic efficiency. Powder metallurgy and die casting offer the potential of resolving this problem for high volume production, but each requires development to assure that the necessary physical properties are attained consistently and uniformly throughout the part.

Work Plan

Laboratory Die Casting Process Development & Support	1983-1985
Prototype Component Die Casting Process Development	1983-1985
Final Component Die-Casting Process-Component Qualification Testing	1984-1985

8.1.27 NON-METALLIC CASES

Problem Definition

The engine outer case and related components listed below are machined castings or parts fabricated from sheet metal. In addition to being inherently expensive, they contribute significantly to the weight of the engine and require sound and thermal insulation to reduce the noise and minimize heat losses. The objective of this program is to develop materials and process to fabricate these components from low cost, lightweight fiber reinforced composite materials, adapting injection molding and thermoforming.

Work Plan

The candidate plastic materials include silicones, polyimides, high temperature polyesters, polystyrenes, polycarbonates, cycloaliphatic epoxies and polyaryl sulphones. The reinforcement materials to be considered are graphite, S-glass, E-glass, the aluminum silicate, nylon and possibly polyester in chopped as well as woven fabric form. The initial phase of the program will be optimization of the composition on the basis of formability in processing and stress capability at the maximum operating temperature. The subsequent phases will involve (a) design of tooling and fabrication of components and (b) the evaluation of the components in actual or simulated engine environment. The components to being considered are: (1) engine outer case (2) compressor diffuser (3) compressor inlet shroud (4) air inlet plenum (5) exhaust duct (6) inlet-reduction gear box structure.

8.1.28 TURBINE WHEEL CASTING

Problem Definition

A metal radial turbine wheel is needed for initial engine development. Preliminary design studies conducted on a high efficiency metallic, inflow radial turbine rotor indicate that in order to operate at a 1150°C (2100°F) turbine inlet temperature with presently available superalloys, the rotor hub must be cooled. Cooling will allow the rotor to meet the durability requirements of 100 hours at full power and of the transient operation of a vehicular turbine engine. Designs and processes must be developed to provide the prototype hardware. If the ceramic wheel is not available in time and the metal wheel

engine is determined to be viable, the manufacturing processes will be developed to provide casting quality which is suitable for production.

Work Plan

- Conduct design studies of convective cooling concepts that can be used with casting techniques.
- Optimize the geometry and location of cooling passages.
- Conduct manufacturing studies to develop and verify the casting methods for prototype turbine wheels.
- Following the completion of the initial engine development, prepare iterations of the casting tooling and develop the manufacturing quality control for production quantities of turbine rotors.

8.1.29 CERAMIC RECUPERATOR

Problem Definition

The state-of-the-art heat exchanger systems for the automotive gas turbine engine are of regenerative type. Although these systems have demonstrated capability to 1000-1100°C (1850°-2000°F), the sealing requirements for higher temperature applications can add to the component cost significantly. It is therefore desirable to develop a compact stationary heat exchanger capable of performance equivalent or better than that of a regenerative heat exchanger and suitable for temperatures up to 1100°C (2000°F). Such a design can significantly reduce cost, provide aerodynamic and thermal symmetry and reduce leakage.

Work Plan

Configuration Analysis and Optimization	
— Phase I Preliminary Analysis	1980-1981
— Phase II System Optimization	1981-1984
Laboratory Material & Process Development	
— Phase I Preliminary Development	1980-1981
— Phase II Advanced Fabrication Support	1981-1984
Prototype Component Development	1981-1984
Final Component Development and Manufacturing Process Specification	1982-1984

8.2 Estimated Production Program Costs & Schedule

The program preparation for production required to launch the 100 HP passenger car turbine engine is estimated to take 4 years. At the end of four (4) years the first production engines will be delivered for installation into production vehicles.

No high volume turbine production experience exists from which to support these estimates, however, the Ford Motor Company did launch a low volume production truck turbine powerplant in the early 1970's and this experience plus the background of high volume piston engine lines are used to develop and support cost estimates.

The program of preparation for production includes, continuing Product Engineering, Process Engineering, facilitization and launching of production. This analysis assumes conversion of an existing plant and therefore does not include cost for site preparation or construction of a building.

Product Engineering

Product Engineering tasks that must be completed in order to successfully launch a volume production program after concept feasibility has been established in Research are:

1. Develop and optimize the product design.

   This involves the following sub-tasks:

   - Production prototype build-up
   - Materials selections
   - Product reliability determination
   - Unit cost minimization
   - Dimensional tolerance determination
   - Specification determination:
     - surface finishes
     - heat treatments
     - geometry specs.
     - surface treatments
   - Manufacturing feasibility (partial)
   - Q. C. and test requirements

2. Product manufacturing feasibility assurance determination:

   Involvement in:

   - Pilot quantity production run
   - Pilot production field test program

   Evaluate feedback from pilot production run and field test program and effect design changes as indicated:

   - Retesting as required.

3. Final product design approval and release.

4. Concurrent to above, aid and coordinate the efforts of selected suppliers in the development of the design and acceptance of purchased, non-standard components and raw materials.

5. Supply aid to the manufacturing divison through the production launch period. (This will extend beyond the four-year period.)

Facilitization, Process Engineering and Launching

The production facilitization of the 100 HP turbine is estimated at $1.147 billion and assumes a plant conversion cost estimated at $10.00 per square foot. Table 8.2 indicates the cost elements making up the total cost. Process engineering costs are included in these figures.

TABLE 8.2

Production Facilitization Costs, $(Millions)

Building Rearrangement at $10/ft^2 (2.25 mft^2)	23
Machines (includes investment requirements at prime supplier plants)	420
Special durable tooling	180
Gages	30
Automation	30
Material Handling	15
Waste disposal	10
Plant Engineering	75
Subtotal	783
Launching (20% + Contingency (10%)	235
Product Engineering	129
Total	$1,147

The estimate includes the following assumptions:

- Annual facility capacity of 500,000 units,
- All major ceramic components will be produced in plant except for the ceramic inner housing and the regenerator core,
- Engines will be 100% heat tested,
- Engines will be dynamometer tested at a rate of 2 per shift,
- Existing facilities will be used for the torque converter and transmission requirements,
- Plant will operate on 3 shifts (123 hours per week).

The estimates are based on previous piston engine experience and the known difference between turbine and piston powerplants. Table 8.3 illustrates the factors considered to support the cost estimates which are higher than a piston engine by a factor of 2.

TABLE 8.3

Major Differences Between Turbine and Piston Engines Relative to Facility Cost Estimates.

FEATURE	PISTON ENGINE	TURBINE ENGINE
Basic engine	conventional	revolutionary
Product design basis	similar to existing engines	all new
Volume Mfg. Facilities	bulk on hand to use as is or retool	all new many must be developed
Volume Mfg. processes	primarily conventional	revolutionary
Raw Materials	common and available	facilities and processes for volume production must be developed for some components
Project launching	few new skills and processes to develop and for volume production	many new skills, process and facilities to be developed and debugged

DISCUSSION OF RESULTS

Initially, twenty-two configurations of gas turbine engines were considered. These were examined judgmentally, based on previous experience of both contracting companies, and were ranked for fuel economy, cost, packageability, risk of a long development program, and driveability feel. Double weight was assigned to cost and fuel economy. A single-shaft regenerative engine with a centrifugal compressor and variable inlet guide vanes ranked first with a radial turbine and second with an axial turbine (Section 2.). The two-shaft (i.e., free-power turbine) engines were not ranked near the top principally due to the higher cost and development risk associated with variable geometry ceramic nozzles. However, because of industry interest in this configuration, a two-shaft arrangement with centrifugal compressor, variable inlet guide vanes, radial gasifier turbine, axial power turbine with variable nozzles, and single regenerator was selected together with the two single-shaft engines for further study.

While current day technology was well defined with a body of data, it was necessary to make projections of the level of component technology that could be developed within the 5-year period (Section 3.0). Performance of the aerodynamic components and heat exchanger were projected based on demonstrated laboratory data and/or successes in other applications. Pressure losses, leakages, and mechanical losses projections were assumed to be a matter of normal development.

Material properties used in the projections for metallic turbine wheels were based upon the technology expected to be available in 1983. It is projected that casting of the particular wheel can be developed to yield consistent nominal values (Section 3.10.1). Properties of ceramic materials also were based upon the technology expected to be available in 1983 (see Section 3.10.2 and Figure 5.18).

A preliminary study of vehicle power requirements with the turbine engine indicated that 75 kW (100 HP) was adequate to meet vehicle acceleration of 0 to 96.5 km/hr. (0 to 60 mph) in 15 seconds. Cycle analysis of the 75 kW (100 HP) engine showed that a design point pressure ratio of 5:1 yielded

near optimum specific power at full load and near optimum specific fuel consumption at 20% load. Since much of the Contractors previous experience existed in the development of regenerators and aluminum compressors near to this pressure ratio, 5:1 was selected for the more detailed comparative study.

Initially, in order to be conservative, single-shaft engine designs with limited turbine tip speeds and rotational speeds were studied. For the metal radial turbines, an inlet temperature of 1205°C (2200°F) and a tip speed of 610 m/s (2000 fps) were considered. For ceramic radial turbines at 1370°C (2500°F) inlet temperatures the tip speed was also limited to 610 m/s (2000 fps). In both cases a rotational speed of 9425 rads/s (90,000 rpm) was considered. In order to improve performance and fuel economy, subsequent studies were made at the optimum tip speeds; 722 m/s (2370 fps) for the metal radial turbines at an inlet temperature of 1150°C (2100°F) and 759 m/s (2490 fps) for the ceramic radial turbines at inlet temperatures of 1370°C (2500°F). Also, the speed was raised to 12357 rads/s (118,000 rpm) to optimize the compressor specific speed and to improve the engine response time. Preliminary studies have indicated that some intermediate tip speeds favoring lower strength requirements may not have a significant effect on fuel economy and performance. These would have to be investigated for any future development program. Since a lower tip speed provided optimum performance for the free turbine engine, additional studies are not needed to establish a trade-off between performance and turbine wheel strength requirements.

The metal axial turbine wheel version of the single-shaft engine was limited to 1065°C (1950°F) T.I.T. because of higher relative temperatures and impracticality of cooling. Ceramic wheel versions of the axial and free turbine engines were also studied at 1370°C (2500°F) T.I.T.

For the purpose of narrowing the selection of the best engine, detailed studies were made including engine design layouts, vehicle installation layouts, manufacturing costs, vehicle acceleration performance and fuel economy, sensitivity of fuel economy to component efficiency and statistical risk or probability of attaining the projected fuel economy.

Studies of vehicle acceleration performance and fuel economy over the Combined Federal Driving Cycle (CFDC) were made (see Section 5.2). Objectives included acceleration from 0 to 96.5 km/hr. (0 to 60 mph) in 15 seconds, and fuel economy improvements of 30 percent to 50 percent over the 8.3 km/l (19.6 mpg) of the baseline vehicle. In addition, although not a contract objective, the initial start-up time as measured by the distance traveled in the first 4 seconds was also examined. A comparable piston engine of 15 second, 0 to 96.5 km/hr (0 to 60 mph) capability would have a 4 second start-up distance of 19.5 m (64 feet). This was considered a desirable criteria.

While the two-shaft engine was assumed to use a conventional torque converter with automatic transmission, (concept 19, Section 3.11.2) the single-shaft engine requires a continuously variable transmission, and Ford has conducted a prototype development of such a transmission which consists of a variable stator torque converter in conjunction with a conventional 3-speed gear changing automatic transmission (similar to concept 2, Section 3.11.2). However, because of the potential beneficial effect on fuel economy, a study of 15 other transmission concepts for single-shaft engines was made, from which two were selected for further study (Section 5.4). Both of these concepts consisted of a differential split power arrangement, in conjunction with a 4-speed gear changing automatic transmission, in which not more than one-third of the power passes through the continuously variable unit. In the optimum case, (concept 13, Section 3.11.2) the variable unit is a traction drive; in the second concept, which was recommended as the prime candidate (concept 6, Section 3.11.2) a variable stator torque converter is the variable unit. In comparison to the existing non-split path variable stator torque converter with a 4-speed transmission, (concept 3, Section 3.11.2) these new split path concepts were shown to yield improvements in vehicle fuel economy of 24 percent (traction drive) and 13 percent (variable stator torque converter) including 5 percent due to declutching at idle to eliminate torque converter drag.

All of the optimized 1370°C (2500°F) ceramic engines (single-shaft and free turbine) were found to equal or exceed the objectives with any transmission. The metal free turbine engines could not meet the objectives. The single-shaft metal engine required the optimum transmission, concept 13, Section 3.11.2. to be viable.

Conclusions that may be drawn from Section 5.2 and which are summarized below and in Table 9.1 are:

1. Variable inlet guide vanes (VIGV) on the compressor improved fuel economy of the better configurations by 4 percent. All the following conclusions are with VIGV.
2. The optimum transmission, concept 13, improved fuel economy by 24 percent and vehicle acceleration by 20 to 30 percent.
3. The optimum compressor specific speed and turbine wheel tip speed single-shaft engine produced 20 percent better fuel economy than the limited tip speed 610 m/s (2000 ft/sec) engine, when idle speed of the limited tip speed engine was adjusted to give comparable 4 second start-up distance.
4. The single-shaft engine with optimum split power transmission, concept 13, gave 47 percent and 23 percent better fuel economy with metal wheel and ceramic wheel respectively, than the equivalent two-shaft engine adjusted for comparable 4 second and 0 to 96.5 km/hr. (0 to 60 mph) accelerating ability.
5. The single-shaft axial turbine engine produced fuel economy and 0 to 96.5 km/hr. (0 to 60 mph) acceleration comparable to the optimum tip speed single-shaft radial turbine engine, but somewhat better 4 second start-up distance in both metal and ceramic versions.
6. The two-shaft free power turbine engine with metal turbine wheels could not be adjusted to give both acceptable fuel economy and 4 second start-up distance.
7. The single-shaft metal wheel engine requires the optimum split power transmission, concept 13, to attain an acceptable 4 second start-up distance and 0 to 96.5 km/hr. (0 to 60 mph) acceleration time.

TABLE 9.1

CONCLUSIONS – PERFORMANCE AND FUEL ECONOMY

CONCLUSION	ENGINE*	TRANSMISSION†	TURBINE INLET TEMPERATURE °C (°F)	IDLE SPEED %	4 SECOND DISTANCE m (ft)	ACCEL TIME 0 96.5 km/hr (0 60 mph) Secs	CFDC FUEL ECONOMY km/l (mpg)		% OVER BASELINE	VARIABLE BEING COMPARED
1	SS5	T1	1150 (2100)	50	7.6 (25)	15.2	11.7	(27.5)	40	Without IGV
	SS6	T1	1150 (2100)	50	7.6 (25)	15.2	12.0	(28.3) 3%	44	With IGV
1	SS7	T1	1370 (2500)	50	19.5 (64)	11.6	12.4	(29.2)	49	Without IGV
	SS8	T1	1370 (2500)	50	19.5 (64)	11.6	13.0	(30.5) 4.5%	56	With IGV
2	SS8	T1	1370 (2500)	50	19.5 (64)	11.6	13.0	(30.5)	56	Available VSTC Transmission
	SS8	T3	1370 (2500)	50	25.6 (84)	9.1	16.1	(37.9) 24%	93	Diff. Split Power, 4 Spd + Traction Drive
3	SS2	T1	1205 (2200)	60	7.9 (26)	14.2	10.0	(23.6)	20	Limited — Compressor Specific Speed and Turbine Tip Speed
	SS6	T1	1150 (2100)	50	7.6 (25)	15.2	12.0	(28.3) 20%	44	Optimum — Compressor Specific Speed and Turbine Tip Speed
4	SS8	T3	1370 (2500)	50	25.6 (84)	9.1	16.1	(37.9)	93	Single Shaft Engine
	FT4	T4	1370 (2500)	60	25.6 (84)	9.1	13.1	(30.8) 23%	57	Free Turbine Engine
4	SS6	T3	1150 (2100)	50	16.2 (53)	12.6	14.8	(34.9)	78	Single Shaft Engine
	FT2	T4	1205 (2200)	60	15.2 (50)	12.7	10.1	(23.7) 47%	21	Free Turbine Engine
5	SS6	T1	1150 (2100)	50	7.6 (25)	15.2	12.0	(28.3)	44	Radial Turbine
	SS9	T1	1065 (1950)	50	12.2 (40)	15.5	12.1	(28.5)	45	3 Stage Axial Turbine
5	SS8	T1	1370 (2500)	50	19.5 (64)	11.6	13.0	(30.5)	56	Radial Turbine
	SS10	T1	1370 (2500)	50	21.9 (72)	11.6	12.6	(29.6)	51	3 Stage Axial Turbine
6	FT1	T4	1205 (2200)	49	7.9 (26)	14.4	11.9	(27.9)	42	Idle Speed 48%
	FT2	T4	1205 (2200)	60	15.2 (50)	12.7	10.1	(23.7)	21	Idle Speed 60%
7	SS6	T1	1150 (2100)	50	7.6 (25)	15.2	12.0	(28.3)	44	Available VSTC Transmission
	SS6	T3	1150 (2100)	50	16.2 (53)	12.6	14.8	(34.9)	78	Diff. Split Power, 4 Spd + Traction Drive

*See Table 5.1 for definition of engine configurations
†See Tables 5.5 and 5.7 for definition of transmission configurations

A sensitivity analysis of the effect of variation of component efficiencies and losses on the specific fuel consumption was done at the 20 percent power point. An estimate of the most pessimistic and most optimistic divergence from the projected values of component efficiency and losses, combined with the sensitivity in a risk analysis indicated that, with 90 percent confidence, the projected values of specific fuel consumption should be met within 5 percent.

An alternative approach to risk analysis assessed the probability of not attaining a 40 percent fuel economy advantage versus the baseline 8.3 km/l (19.6 mpg) with the ceramic 1371°C (2500°F) T.I.T. engines using the existing transmission, concept 3, (i.e., without the optimum transmission). On this basis there was insignificant risk for any of the three configurations.

The sensitivity analysis together with the detailed engine and vehicle performance analysis was used to approximate the decrease from projected fuel economy that would occur if one or more important losses or efficiencies did not progress from current technology to 1983 technology. Table 9.2 was based essentially on the results from Section 5.6, Table 5.12, for the ceramic rotor, single-shaft engine.

TABLE 9.2

Effect on Ceramic Engine Fuel Economy — Current Versus 1983 Technology

Component Factor	Decrease in Projected Fuel Economy — Percent	
Compressor Efficiency	2.8	
Turbine Efficiency	2.7	
Regenerator Effectiveness	5.1	
Regenerator Temperature (1100°C vs. 1000°C)	2.9	3/
Regenerator Leakage	1.2	
Pressure Losses — Turbine Diffuser	1.7	
— Combustor	1.3	
— Inlet and Exhaust	0.7	
Ceramic Turbine Wheel (1150°C vs. 1370°C)	12	1/ 3/
Optimum Split Power Transmission (With Traction Drive)	19.5	2/

1/ Assumes downsizing of 1370°C engine to HP of 1150°C engine.
2/ From vehicle performance analysis with declutch at idle.
3/ From cycle analysis.

This analysis would indicate that the potentially most fruitful developments are the ceramic radial turbine wheel and the optimum transmission together with the stationary ceramic components which are needed for both the 1150°C (2100°F) and 1370°C (2500°F) engine.

The manufacturing cost analysis consisting of an approximate relative cost estimate, based on the size and complexity of each of 25 sub-assemblies and components, indicated the single-shaft ceramic radial turbine engine as least expensive. The single-shaft axial turbine cost was 23 percent greater and the two-shaft cost was 39 percent greater. Metallic wheel engines were indicated as more expensive

than the same ceramic wheel engines; 5 percent greater for the single-shaft radial, 13 percent greater for single-shaft axial and 16 percent greater for two-shaft. This analysis included the cost of the variable stator torque converter for the single-shaft engine. The incremental cost of the split power transmission concepts would reduce the cost disadvantage of the two-shaft engine to 33 percent.

A formalized, weighted selection criteria, discussed in Section 5.10, was used to compare the relative advantages of the three engine types. By this means of comparison the single-shaft radial engine was shown to be more desirable than the single-shaft axial engine and more desirable than the two-shaft engine, even though the fuel economy advantage of the split power transmission for the single-shaft engine was not included. While this analysis leads to the choice of the single-shaft radial turbine engine there are considerations which should be emphasized.

- The radial turbine wheel will operate at considerably lower material temperatures in the high stress regions than the axial wheels. In the case of ceramics these temperatures are below the level at which time dependent strengths must be considered, but this is not true for the axial wheel. Therefore, the strength requirements of the axial wheel are 20 percent higher than for the radial wheel. Current properties of hot pressed silicon nitride appear adequate for the radial wheel, and moldable grades of silicon nitride and silicon carbide with adequate strength appear within reach (see Figure 5.18 in Section 5.3). Adequate materials for axial wheels may come much later.
- The radial ceramic wheel single-shaft engine is significantly less expensive to manufacture than the axial wheel single-shaft engine, or the two-shaft ceramic wheel engine. If metal wheels are considered, the cost advantage increases (see Table 5.17 in Section 5.8).
- With the optimum transmission the single-shaft ceramic engine shows a fuel economy advantage over the two-shaft ceramic engine of 23 percent when adjusted to comparable acceleration capability (see Table 9.1).
- The two-shaft metal wheel engine is not acceptable for performance and fuel economy at 1205°C (2200°F) operating temperatures.

There are, of course, certain risks in choosing the single-shaft radial wheel engine.

- To date greater effort has been concentrated on development of a process for fabricating ceramic axial turbine wheels and although adequate materials are not yet available, a breakthrough in material properties or development of a viable boreless design could bring in the axial wheel sooner.
- If it is possible to develop a variable turbine nozzle of ceramic, for the two-shaft engine, and if neither of the split power transmissions for the single-shaft engine is successful, then the single-shaft engine will show fuel economy 12 percent less than the two-shaft engine. This is seen from a comparison of engine configurations SS8 and FT3 in Section 5.2.

Following selection of the single-shaft radial turbine wheel engine, a more detailed design and analysis of the engine including aerodynamics, thermal expansions and stresses, mechanical loads and shaft dynamics, confirmed the potential viability of the design (Section 6.0).

A cost of ownership difference comparison assumes those items which would be different between a piston engine vehicle and a turbine engine vehicle are initial cost, scheduled maintenance and repairs, and fuel cost.

To arrive at a reasonably accurate initial cost of a turbine vehicle, it would be necessary to complete detail drawings of all engine parts and unique vehicle parts, complete a process plan for each of these parts, and do an "add and delete" cost analysis of the vehicle versus the piston engine vehicle. Such an analysis is beyond the scope of this contract but should be completed in the development program. However, it is judged that a vehicle with the selected turbine and optimum split power transmission would cost 10 to 20 percent more to the customer than a comparable 1978 piston engine vehicle ($560 to $1,120). However, more stringent future emission requirements for the piston engine could significantly reduce this cost difference.

While aircraft experience has shown that time between overhauls is much greater for turbine engines than for piston engines, there is insufficient experience with regenerative turbine engines in

C-3

the turbine will eventually be less than for the piston engine it is assumed for this study that they are equal to those for the piston engine.

Fuel costs for the ceramic engine with optimum transmission at 70 cents per gallon are $1,850 for 100,000 miles compared to $3,571 for the 19.6 mpg piston engine. The cost of ownership in 1978 dollars for 100,000 miles would, therefore, be $600 to $1,160 less for the turbine engine than for the piston engine.

A powertrain development plan (Section 8.0) has been constructed in which 27 R&D projects have been integrated into the engine development plan (see Table 8.1). Total cost of the program through FY85 is estimated at $65 million. The program, starting in FY1979, provides for demonstration of the engine in a vehicle by October, 1983, at which time the potential for a production program could be reviewed (see Figure 8.1). It is projected that this engine with a metal turbine rotor would meet contract fuel economy and acceleration objectives at this point in time. Decision dates on whether the ceramic turbine wheel is ready for testing in the engine will occur in late 1981 and late 1982. An updated design of the engine will commence dynamometer tests in mid-1983. Engine and vehicle development would continue to point of decision for a production program at the end of 1985. The engine development program includes build of 10 test engines progressively from 1981 through 1984 according to the test schedule shown in Figure 8.2.

A four year production program where an existing plant is converted for turbine manufacture is estimated to cost $760 million for production facilities, $23 million for plant conversion, $235 million for launching and contingency funds, and $129 million for product engineering effort, or $1.15 billion total.

CONCLUSIONS

Results of the Ford/AiResearch Improved Gas Turbine Design Study indicate that the single-shaft ceramic engine with a radial inflow turbine should be selected for development over the single-shaft engine with an axial turbine or the free turbine engine, because projections indicate that:

- The free turbine engine does not meet the fuel economy improvement objectives. It is projected capable of only a 21 percent improvement in fuel economy since it is judged unlikely that ceramic variable power turbine nozzles can be developed within the time frame and the turbine inlet temperature will be limited to 1205°C (2200°F) with metal nozzles.
- Compared to the single-shaft ceramic radial engine, the manufacturing cost of the free turbine engine is 33 percent to 39 percent higher, and that of the single-shaft axial is 23 percent higher. With the metal wheel engines, the advantage of the single-shaft radial is still greater.
- For the configuration studied, the material strength requirements for the ceramic radial wheel are 20 percent less than for ceramic axial wheels.

The single-shaft ceramic engine can meet or exceed all of the objectives with any of the following three continuously variable transmissions, presented in order of recommendation:

- If the low risk and the prime candidate transmission, consisting of a differential split power arrangement with a variable stator torque converter, is considered the projected fuel economy advantage is 76 percent, the 0 to 96.5 km/hr. (0 to 60 mph) acceleration time is 10.1 seconds and the 4 second start-up distance is 21.0 m (69 ft.).
- If the variable stator torque converter in the above differential split-power transmission is replaced by a traction drive unit, then the fuel economy opportunity increases to 93 percent over the baseline, the 0 to 96.5 km/hr. (0 to 60 mph) acceleration time is reduced to 9.1 seconds and the 4 second start-up distance increases to 25.6 m (84 ft.).
- Using, as a back-up position, the available in-line variable stator torque converter and 4-speed Ford FIOD gearbox, the single-shaft ceramic engine is projected to be capable of a 56 percent improvement in fuel economy over the baseline, a 0 to 96.5 km/hr. (0 to 60 mph) acceleration time of 11.6 seconds and the 4 second start-up distance becomes 19.5 m (64 ft.).

If neither the split path transmissions nor the ceramic radial inflow turbine are successfully developed, then the single-shaft engine with a metal wheel and variable stator torque converter plus 4-speed gearbox is projected to provide a 44 percent improvement in fuel economy and acceptable 0 to 96.5 km/hr. (0 to 60 mph) acceleration, although the 4 second start-up distance will not be fully acceptable.

APPENDIX I

RANKING CRITERIA FOR ENGINE CONCEPTS ASSESSMENT

It is assumed that the system will be designed to meet vehicle acceleration requirements, emission requirements, reliability/durability of 100 hours at full power, and noise requirements. Therefore, these factors will not be included in ranking criteria. Each engine will be rated on the following five criteria using a scale of 1 to 10 between the "No-Go" condition and the maximum value. Where the "No-Go" condition is exceeded, the engine is disqualified. The maximum value is not likely to be exceeded, but potential any higher is of declining value.

Criteria	Rating Factor	"No-Go"	Maximum Rating
Fuel Economy (vs. baseline vehicle i.e., 8.3 km/l, 19.6 mpg)	2	30%	+60%
Cost	2	$500 more than piston engine @ 0.4 NO_x	Less than piston
Packageability	1	15.24 cm (6 in.) Interference	7.62 cm (3 in.) Clearance all around
Risk of Longer Development Program	1	10 Years	4 Years
Driveability	1		
Response Time		2.5 Seconds	0.5 Seconds
Transmission Shift Quality		—	=3-Speed Auto.
Starting Time		30 Seconds	5 Seconds
Idle Creep (driveshaft torque)		813 N-M	41 N-M
BTU for Heater		*	8790 W (30,000 BTU/Hr. −17.8°C to 37.8°C (0 — 100°F)

* Use gas heater below 2930 W (10,000 BTU/Hr.).

Fuel Economy is the Combined Federal Driving Cycle Standard or if CFDC is not available, the 20 percent power point.

Cost is the net incremental cost of the vehicle over a comparable performance piston engine vehicle.

Packageability is the ability of the engine transmission accessories and ducting to fit within the prescribed engine compartment without major modification to the vehicle.

The Development Program is complete when all design objectives are met, and the 4-year tooling program, can be authorized.

Driveability is composed of several effects. The transmission related effects cannot be quantified in Task I. Response time and starting time should be of equal weight.

APPENDIX II

TRANSMISSION CONCEPTS RANKING CRITERIA

It is assumed that all the transmissions when coupled with an engine will meet vehicle acceleration requirements, reliability/durability of 100 hours at full power and are feasible in concept. Therefore, these factors will not be included in the ranking criteria.

Each transmission will be rated on the following criteria using a scale of 1 to 10 between the "NO-GO" condition and the maximum value. Where the "NO-GO" condition is exceeded, the transmission is disqualified. The maximum value is not likely to be exceeded, but potential any higher is of declining value.

Criteria	Rating Factor	"No-Go"	Maximum Rating
Efficiency	2	Average	Average 100%
Cost	2	Three times more than Ford C4	Less than Ford C4
Two Second Distance Traveled	2	Om	3.35 m (11 ft.)
Packageability	1	15.24 cm Interference	7.62 cm Clearance all around
Risk of Longer Development Program	1	10 Years	4 Years
Noise at Driver's Ear	1	81 dbA at any lower point	60 dbA at any point
Driveability	1		
No. of Shifts	(1)	10	3
Shift Quality	(2)	Open	Equal to Ford C4
Idle Creep Speed	(2)	29 km/h (18 mph)	3.2 km/h (2 mph)

Efficiency is the average efficiency of 10 increments across the transmission speed range at 100 percent power.

Cost is based on a judgmental comparison with the Ford C4 and is a ratio not an incremental value.

Two Second is the distance in metres that the vehicle travels in two seconds, and is intended as a measure of system lag.

Packageability is the ability of the transmission to be packaged in the prescribed vehicle without major vehicle modification.

Development Program is complete when all design objectives are met and the four year tooling program can be authorized.

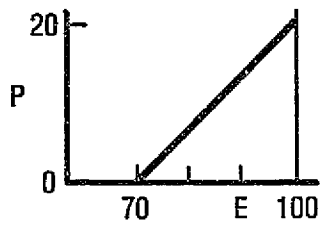
Noise is measured at the driver's ear, windows closed, throughout the vehicle operating range.

Driveability is composed of several effects, the most important of which is shift quality which is a judgmental measure. Number of shifts is less important if shift quality is good and time to shift is less than .5 seconds. Idle creep speed is an indirect measure of idle fuel consumption and is considered to be as significant as shift quality.

APPENDIX III

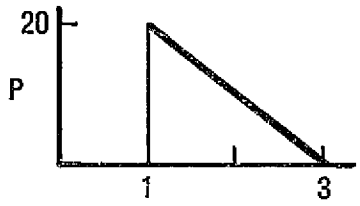
TRANSMISSION CONCEPTS, RATING DETERMINATION

EFFICIENCY



$$P = 2/3E - 46.6$$

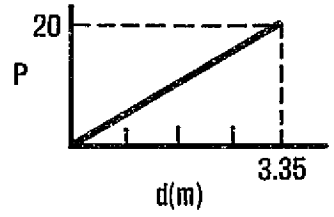
COST



$$P = -10C + 30$$

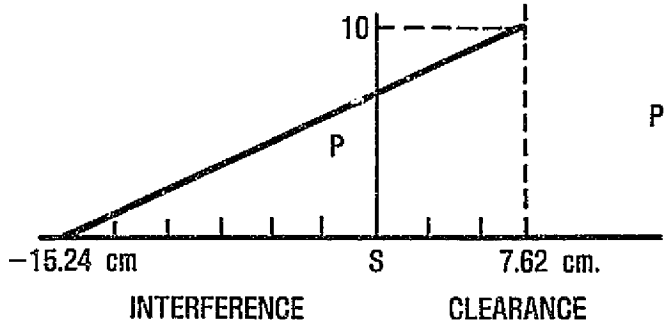
$$C = \frac{\text{COST}}{\text{COST OF 3SP AUTO.}}$$

TWO SECOND DISTANCE



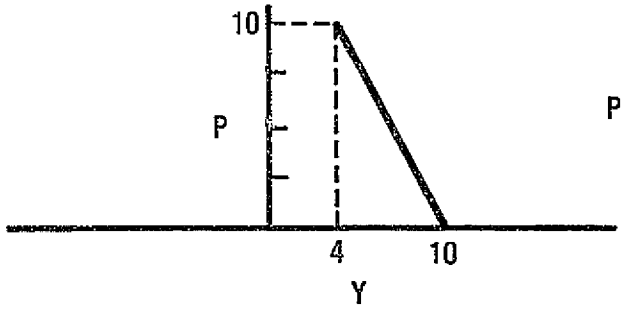
$$P = \frac{20}{3.35}\,d$$

PACKAGEABILITY



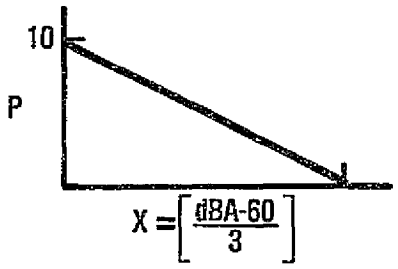
$$P = \frac{10}{9}\,S + \frac{20}{3}$$

DEVELOPMENT RISK



$$P = -\frac{5}{3}\,y + \frac{50}{3}$$

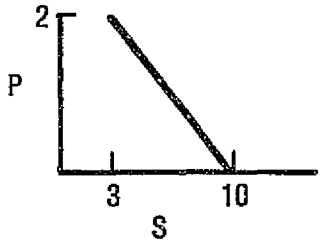
NOISE AT DRIVERS EAR



$$P = -\frac{5}{8} X + 10$$

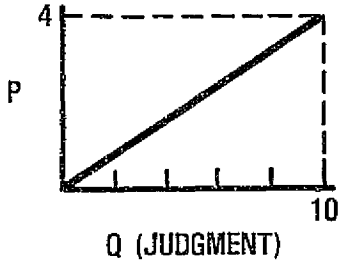
DRIVEABILITY

Nº OF SHIFTS



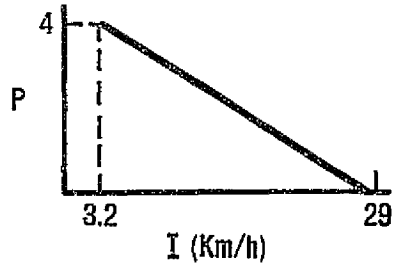
$$P = -\frac{2}{7} S + \frac{20}{7}$$

SHIFT QUALITY



$$P = \frac{4}{10} Q$$

IDLE CREEP SPEED



$$P = -.15 I + 4.35$$

APPENDIX IV

LIST OF ACRONYMS

ACC	Accessories
A/C	Air Conditioner
AX	Axial (Turbine)
CEN	Centrifugal (Compressor)
CFDC	Combined Federal Driving Cycle
CV	Coefficient of Variation
CVT	Continuously Variable Transmission
ECP	Electronic Control Package
EL	Elongation
FIOD	Ford Integral Overdrive
FT	Free Turbine
FY	Fiscal Year
GGT	Gas Generator Turbine
HDC	Highway Driving Cycle
HIP	Hot Isostatic Pressing
H.P.	High Pressure
HP	Horsepower
HPSN	Hot Pressed Silicon Nitride
I/C	Intercooling
IGT	Improved Gas Turbine
LART	Low Aspect Ratio Turbine
LCF	Low Cycle Fatigue
L.P.	Low Pressure
LVDT	Linear Variable Differential Transformer
MOR	Modulus of Rupture
MPG	Miles per Gallon
MPH	Miles per Hour
NDE	Non Destructive Evaluation
PM	Powdered Metal
PR	Pressure Ratio
PSSN	Pressureless Sintered Silicon Nitride
RAD	Radial (Turbine)
RBSC	Reaction Bonded Silicon Carbide
RBSN	Reaction Bonded Silicon Nitride
RECUP	Recuperator
REGEN	Regenerator
R/H	Reheat
RMS	Root Mean Square
RT	Room Temperature
SFC	Specific Fuel Consumption
SHP	Shaft Horsepower
SS	Single-Shaft
SSC	Sintered Silicon Carbide
T.I.T.	Turbine Inlet Temperature
TPA	Throttle Pedal Angle
UDC	Urban Driving Cycle
VIGV	Variable Inlet Guide Vanes
VPTN	Variable Power Turbine Nozzles
VSTC	Variable Stator Torque Converter

APPENDIX V

LIST OF SYMBOLS

A	Amperes or Combustor flow area
a	Optimistic value parameter
b	Impeller tip, blade height or pessimistic value parameter
C_1	Fanning friction factor constant
C_2	Colburn number constant
C_d	Drag coefficient
c	Clearance
EL	Elongation
F	Fanning friction factor $=C_1 R_e^{X_1}$
g	gravitational constant
h	blade height
H_{act}	actual head
ΔH	anthalpy change
HP_i	Horsepower input to transmission
HP_V	Horsepower through variable speed unit
J	Colburn number $=C_2 R_e^{X_2}$ or Joule's equivalent
K	spring rate
K_I	Torque converter input size factor
k	constant
M	Mach number
m	Weibull slope parameter or most likely value parameter
N	Speed
Ng	Gasifier speed
N_o	Transmission output speed
N_i	Transmission input speed
N_S	Specific speed
P	Total pressure
P_{amb}	Ambient pressure
ΔP	Pressure loss
PVT	Gear Tooth Scoring Factor
Q	Volumetric Flow Rate or Torque
R	Pressure ratio
Re	Reynold's number
Re_{REF}	Reference Reynold's number
Rm	Blade mean radius
R_t	Blade tip radius
S_r	Stress rupture strength
S_u	Ultimate strength
S_y	0.2 percent offset yield strength
S_θ	Characteristic strength
T	Total temperature
T_{amb}	Ambient Temperature
U_m	Mean blade speed
U_T	Blade tip speed
W	Airflow rate
W_L	Leakage airflow rate
X_1	Reynold's number exponent for Fanning friction factor
X_2	Reynold's no. exponent for Colburn no.
Z	Number of turbine stages

GREEK LETTERS

β	gear spring rate coefficient or VIGV angle
δ	normalized pressure, P/P_{amb}
ϵ	total strain (elastic plus plastic) or efficiency of variable speed unit
η	efficiency
η_β	compressor efficiency at VIGV angle β
η_{β_o}	compressor efficiency at VIGV angle 0°
η_T	turbine efficiency
η_{To}	turbine efficiency at zero clearance
θ	normalized temperature, T/T_{amb}
λ_m	mean stage work coefficient
λ_s	stage work coefficient
μ	dynamic viscosity or expected value of parameter
ρ	density
σ	stress or variance parameter
ω_i	input speed of variable speed unit
ω_o	output speed of variable speed unit

LIST OF REFERENCES

1. Automobile Gas Turbine Optimization Study. EPA Contract 68-04-0012. AiResearch Manufacturing Company of Arizona. 14 July, 1972, PB 213 389.
2. EPA Urban Dynamometer Driving Schedule. Federal Register, Vol. 42, No. 124, June 28, 1977.
3. EPA Highway Fuel Economy Driving Cycle. Federal Register, Vol. 39, No. 200, October 15, 1974.
4. Low-Aspect-Ratio Turbine Technology Program. AiResearch Manufacturing Company of Arizona. March 31, 1977 Report 75-211701 (2).
5. Smith, S. F., A Simple Correlation of Turbine Efficiency. Jl. Roy. Aero. Soc. Vol. 69, 1965.
6. Christenson, D. C., Frank, A. A., Beachly, N. H.; The Fuel-Saving Potential of Cars with Continuously Variable Transmissions and an Optimal Control Algorithm., ASME 75 WA Aut 20.
7. Cordner, M. A., Grimm, D. H.; Transmission Study for Turbine and Rankine Cycle Engines. U.S. Environmental Protection Agency. APTD-1558, Dec. 1972.
8. Upgrading Automotive Gas Turbine Technology. SAE Paper No. 760280.
9. Ninth Summary Report, Highway Vehicle Contractors Coodination Meeting, ERDA 76-61. Vehicle Systems, Hydromechanical Continuously Variable Transmission. Orshansky Transmission Corporation.
10. Paluszny, A., Wu. W.; Probabilistic Aspects of Designing with Ceramics. ASME Paper No. 77-GT-41, Dec. 1976.
11. McLean, A. F., Fisher, E. A., and Bratton, R. J.; "Brittle Materials Design, High Temperature Gas Turbine." Interim Report, AMMRC CTR 73-32, September, 1973.
12. McLean, A. F., Fisher, E. A., and Bratton, R.J.; "Brittle Materials Design, High Temperature Gas Turbine." Interim Report, AMMRC CTR 75-28, October, 1975.
13. Buffa, E. S.; Modern Production Management. John Wiley and Sons, 1977.
14. Miller, R. W.; Schedule, Cost and Profit Control with PERT. McGraw-Hill Book Company, 1963.
15. Rohlik, Harold E.; Analytical Determination of Radial Inflow Turbine Design Geometry for Maximum Efficiency. NASA TN D-48384, 1968.
16. Glassman, Arthur J.; Computer Program for Design Analysis of Radial-Inflow Turbines. NASA TN D-8164, 1976.
17. Katsanis, T.; Computer Program for Calculating Flow Distribution in a Radial-Inflow Turbine. NASA TM X-52161, 1965.
18. Katsanis, T.; Fortran Program for Calculating Transonic Velocities on a Blade-to-Blade Stream Surface of a Turbomachine. NASA TN D-5427, 1969.
19. Wasserbauer, Charles, A., and Glassman, Arthur, J.; Fortran Program for Predicting Off-Design Performance of Radial-Inflow Turbines. NASA TN D-8063, 1975.
20. Ford Motor Company, Automotive Stirling Engine Development Program. Final Report, to be published. DOE Contract No. EC-77-C-02-4396.

1. Report No.	2. Government Accession No.	3. Recipient's Catalog No.
NASA CR-159580		

4. Title and Subtitle	5. Report Date
Conceptual Design Study of Improved Automotive Gas Turbine Powertrain — Final Report	May, 1979
	6. Performing Organization Code
7. Author(s)	8. Performing Organization Report No.
	10. Work Unit No.
9. Performing Organization Name and Address Research Staff Ford Motor Co. Dearborn, Michigan 48121	11. Contract or Grant No. DEN 3-37
	13. Type of Report and Period Covered Contractor Final Report
12. Sponsoring Agency Name and Address Department of Energy Division of Transportation Energy Conservation Washington, D.C. 20545	14. Sponsoring Agency Report No. DOE/NASA/0037-79/1

15. Supplementary Notes Interim Report. Prepared under Interagency Agreement EC-77-A-31-1040

Final Report Prepared under Interagency Agreement EC-77-A-31-1040 Project Manager, R. P. Geye, Transportation Propulsion Division NASA Lewis Research Center, Cleveland, Ohio 44135.

16. Abstract

A conceptual design study for an improved automotive gas turbine powertrain, at the projected 1983 level of technology, was conducted jointly by Ford Motor Company and AiResearch Manufacturing Company. The investigation identified twenty-two candidate engine concepts and nineteen transmission concepts. Screening of these concepts, predominantly for fuel economy, cost and technical risk, resulted in a recommended powertrain consisting of a single-shaft engine, with a ceramic radial turbine rotor, connected through a differential split-power transmission utilizing a variable stator torque converter and a four speed automatic gearbox. Vehicle fuel economy and performance projections, preliminary design analyses and installation studies in a Ford Fairmont were completed. A cost comparison with the conventional spark ignited gasoline engine showed that the turbine engine would be more expensive initially, however, lifetime cost of ownership is in favor of the gas turbine. A powertrain research and development plan was constructed to gain information on timing and costs to achieve the required level of technology and demonstrate the engine in a vehicle by the year 1983.

17. Key Words (Suggested by Author(s))	18. Distribution Statement
Automotive Gas Turbine Single Shaft Turbine Ceramic Turbine Turbine Transmission	Unclassified — unlimited STAR Category 85 DOE Category UC-96

19. Security Classif. (of this report)	20. Security Classif. (of this page)	21. No. of Pages	22. Price*
Unclassified	Unclassified	180	—

*For sale by the National Technical Information Service, Springfield, Virginia 22161

NASA-C-168 (Rev. 10-75)